

**Texas Water Development Board
Contract Number # 1648302063**

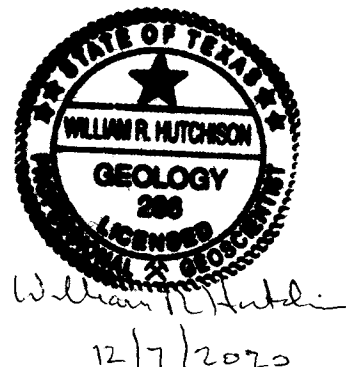
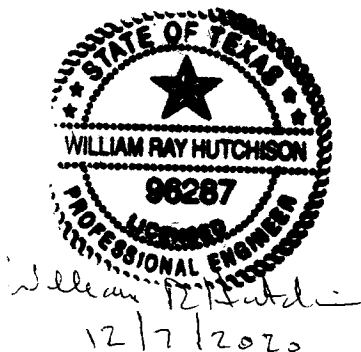
**Numerical Model Report:
Groundwater Availability Model for the Northern
Portion of the Queen City, Sparta, and Carrizo-Wilcox
Aquifers**

by:

Sorab Panday, GSI Environmental Inc.
James Rumbaugh, Environmental Simulations, Inc.
William R. Hutchison, Independent Groundwater Consultant
Staffan Schorr, Montgomery & Associates

PROFESSIONAL SEAL

This document is released under the authority of William Hutchison, P.E. 96287, P.G. 286



This page is intentionally blank.

Table of Contents

Executive Summary.....	xi
1.0 Introduction and Purpose of the Model.....	15
2.0 Model Overview and Packages	15
2.1 MODFLOW 6 Overview	20
2.2 NAME File.....	23
2.3 Initial Conditions Package	23
2.4 Discretization Packages	23
2.5 Node Property Flow Package	58
2.6 Storage Package.....	66
2.7 Well Package.....	66
2.8 General Head Boundary Package	70
2.9 River Package	83
2.10 Recharge Package.....	83
2.11 Evapotranspiration Package	91
2.12 Output Control Package	91
2.13 Iterative Matrix Solver Package	91
3.0 Model Calibration and Results.....	96
3.1 Calibration Procedures	97
3.2 Model Simulated Versus Measured Heads.....	112
3.3 Model Simulated Versus Measured Baseflow	171
3.4 Model Simulated Water Budgets.....	174
4.0 Sensitivity Analyses.....	178
4.1 Procedure of Sensitivity Analysis	178
4.2 Results of Sensitivity Analysis.....	179
5.0 Modeling Limitations.....	196
6.0 Summary and Conclusions.....	197
7.0 Future Improvements	198
8.0 Acknowledgements	199
9.0 References	200

List of Figures

- Figure 1.0-1 Site Location Map
- Figure 2.0-1 Aquifer Outcrops Simulated in the Groundwater Model
- Figure 2.0-2 Conceptual Block Diagram
- Figure 2.4-1 Geologic Units and Model Layers
- Figure 2.4-2 Modeled Top Elevation for Quaternary Alluvium (Model Layer 1)
- Figure 2.4-3 Modeled Bottom Elevation for Quaternary Alluvium (Model Layer 1)
- Figure 2.4-4 Modeled Thickness of Quaternary Alluvium (Model Layer 1)
- Figure 2.4-5 Modeled Top Elevation for Sparta Aquifer (Model Layer 2)
- Figure 2.4-6 Modeled Bottom Elevation for Sparta Aquifer (Model Layer 2)
- Figure 2.4-7 Modeled Thickness for Sparta Aquifer (Model Layer 2)
- Figure 2.4-8 Modeled Bottom Elevation for Weches Formation (Model Layer 3)
- Figure 2.4-9 Modeled Thickness for Weches Formation (Model Layer 3)
- Figure 2.4-10 Modeled Bottom Elevation for Queen City Aquifer (Model Layer 4)
- Figure 2.4-11 Modeled Thickness for Queen City Aquifer (Model Layer 4)
- Figure 2.4-12 Modeled Bottom Elevation for Reklaw Formation (Model Layer 5)
- Figure 2.4-13 Modeled Thickness for Reklaw Formation (Model Layer 5)
- Figure 2.4-14 Modeled Bottom Elevation for Carrizo Aquifer (Model Layer 6)
- Figure 2.4-15 Modeled Thickness for Carrizo Aquifer (Model Layer 6)
- Figure 2.4-16 Modeled Bottom Elevation for Upper Wilcox (Model Layer 7)
- Figure 2.4-17 Modeled Thickness for Upper Wilcox (Model Layer 7)
- Figure 2.4-18 Modeled Bottom Elevation for Middle Wilcox (Model Layer 8)
- Figure 2.4-19 Modeled Thickness for Middle Wilcox (Model Layer 8)
- Figure 2.4-20 Modeled Bottom Elevation for Lower Wilcox (Model Layer 9)
- Figure 2.4-21 Modeled Thickness for Lower Wilcox (Model Layer 9)
- Figure 2.4-22 General Structural Setting
- Figure 2.4-23 Groundwater Model Domain Discretization for Quaternary Alluvium (Model Layer 1)
- Figure 2.4-24 Groundwater Model Domain Discretization for Sparta Aquifer (Model Layer 2)
- Figure 2.4-25 Groundwater Model Domain Discretization for Weches Formation (Model Layer 3)
- Figure 2.4-26 Groundwater Model Domain Discretization for Queen City Aquifer (Model Layer 4)
- Figure 2.4-27 Groundwater Model Domain Discretization for Reklaw Formation (Model Layer 5)
- Figure 2.4-28 Groundwater Model Domain Discretization for Carrizo Aquifer (Model Layer 6)
- Figure 2.4-29 Groundwater Model Domain Discretization for Upper Wilcox (Model Layer 7)
- Figure 2.4-30 Groundwater Model Domain Discretization for Middle Wilcox (Model Layer 8)
- Figure 2.4-31 Groundwater Model Domain Discretization for Lower Wilcox (Model Layer 9)
- Figure 2.4-32 Cross Sections of Gridded Model Layers in the Groundwater Flow Model

Figure 2.5-1	Estimated Sand Fraction Distribution for Sparta Aquifer (Model Layer 2)
Figure 2.5-2	Estimated Sand Fraction Distribution for Queen City Aquifer (Model Layer 4)
Figure 2.5-3	Estimated Sand Fraction Distribution for Upper Wilcox (Model Layer 7)
Figure 2.5-4	Estimated Sand Fraction Distribution for Middle Wilcox (Model Layer 8)
Figure 2.5-5	Estimated Sand Fraction Distribution for Lower Wilcox (Model Layer 9)
Figure 2.7-1	Model Pumping Comparison
Figure 2.7-2	Pumping Well Total Pumping Volume in Sparta Aquifer (Layer 2)
Figure 2.7-3	Pumping Well Total Pumping Volume in Queen City Aquifer (Layer 4)
Figure 2.7-4	Pumping Well Total Pumping Volume in Carrizo Aquifer (Layer 6)
Figure 2.7-5	Pumping Well Total Pumping Volume in Upper Wilcox (Layer 7)
Figure 2.7-6	Pumping Well Total Pumping Volume in Middle Wilcox (Layer 8)
Figure 2.7-7	Pumping Well Total Pumping Volume in Lower Wilcox (Layer 9)
Figure 2.7-8a	Pumping per County
Figure 2.7-8b	Pumping per County
Figure 2.7-8c	Pumping per County
Figure 2.7-8d	Pumping per County
Figure 2.7-8e	Pumping per County
Figure 2.8-1	Modeled General Head Boundary Conditions
Figure 2.9-1	Estimated Annual Streamflows for Trinity River
Figure 2.9-2	Estimated Annual Streamflows for Neches River
Figure 2.9-3	Estimated Annual Streamflows for Sabine River
Figure 2.9-4	Estimated Annual Streamflows for Big Cypress Creek
Figure 2.9-5	Estimated Annual Streamflows for Sulphur River
Figure 2.9-6	Simulated River Boundary Conditions
Figure 2.10-1	Distribution of Average Estimated Annual Recharge Rates for 1980
Figure 2.10-2	Model Recharge Multipliers 1980 to 2013
Figure 2.11-1	Distribution of Modeled Maximum Evapotranspiration Rates
Figure 3.1-1	Calculated Horizontal Hydraulic Conductivity for Sparta Aquifer (Model Layer 2)
Figure 3.1-2	Calculated Horizontal Hydraulic Conductivity for Queen City Aquifer (Model Layer 4)
Figure 3.1-3	Calculated Horizontal Hydraulic Conductivity for Upper Wilcox (Model Layer 7)
Figure 3.1-4	Calculated Horizontal Hydraulic Conductivity for Middle Wilcox (Model Layer 8)
Figure 3.1-5	Calculated Horizontal Hydraulic Conductivity for Lower Wilcox (Model Layer 9)
Figure 3.1-6	Calculated Vertical Hydraulic Conductivity for Sparta Aquifer (Model Layer 2)
Figure 3.1-7	Calculated Vertical Hydraulic Conductivity for Queen City Aquifer (Model Layer 4)
Figure 3.1-8	Calculated Vertical Hydraulic Conductivity for Upper Wilcox (Model Layer 7)
Figure 3.1-9	Calculated Vertical Hydraulic Conductivity for Middle Wilcox (Model Layer 8)

- Figure 3.1-10 Calculated Vertical Hydraulic Conductivity for Lower Wilcox (Model Layer 9)
- Figure 3.2-1 Location of Groundwater Observation Wells and Available Water Level Elevation Data – Quaternary Alluvium (Layer 1)
- Figure 3.2-2 Location of Groundwater Observation Wells and Available Water Level Elevation Data – Sparta Aquifer (Layer 2)
- Figure 3.2-3 Location of Groundwater Observation Wells and Available Water Level Elevation Data – Queen City Aquifer (Layer 4)
- Figure 3.2-4 Location of Groundwater Observation Wells and Available Water Level Elevation Data – Carrizo Aquifer (Layer 6)
- Figure 3.2-5 Location of Groundwater Observation Wells and Available Water Level Elevation Data – Upper Wilcox (Layer 7)
- Figure 3.2-6 Location of Groundwater Observation Wells and Available Water Level Elevation Data – Middle Wilcox (Layer 8)
- Figure 3.2-7 Location of Groundwater Observation Wells and Available Water Level Elevation Data – Lower Wilcox (Layer 9)
- Figure 3.2-8 Observed vs. Simulated Water Level Elevations for Calibrated 1980 and 2013 Conditions
- Figure 3.2-9 Observed vs. Simulated Confined Water Level Elevations for Calibrated 1980 and 2013 Conditions
- Figure 3.2-10 Observed vs. Simulated Unconfined Water Level Elevations for Calibrated 1980 and 2013 Conditions
- Figure 3.2-11 Observed vs. Simulated Water Level Elevations for Calibrated 1980 to 2013 Simulation
- Figure 3.2-12 Observed vs. Simulated Confined Water Level Elevations for Calibrated 1980 to 2013 Simulation
- Figure 3.2-13 Observed vs. Simulated Unconfined Water Level Elevations for Calibrated 1980 to 2013 Simulation
- Figure 3.2-14 Observed vs. Simulated Unconfined Water Level Elevations for Calibrated 1980 to 2013 Simulation showing Wells Overlain by Layer 1
- Figure 3.2-15a Observed vs. Simulated Water Level Elevations for Calibrated 1980 to 2013 Simulation by Layer
- Figure 3.2-15b Observed vs. Simulated Water Level Elevations for Calibrated 1980 to 2013 Simulation by Layer
- Figure 3.2-15c Observed vs. Simulated Water Level Elevations for Calibrated 1980 to 2013 Simulation by Layer
- Figure 3.2-16 Distribution of Water Level Elevation Errors for Calibrated 1980 to 2013 Simulation at Weight = 1
- Figure 3.2-17a Histograms of Water Level Elevation Residuals by Layer
- Figure 3.2-17b Histograms of Water Level Elevation Residuals by Layer
- Figure 3.2-18 Measured and Simulated Water Level Elevation Hydrographs for Select Wells – Quaternary Alluvium (Layer 1)
- Figure 3.2-19 Measured and Simulated Water Level Elevation Hydrographs for Select Wells – Sparta Aquifer (Layer 2)
- Figure 3.2-20 Measured and Simulated Water Level Elevation Hydrographs for Select Wells – Queen City Aquifer (Layer 4)

- Figure 3.2-21 Measured and Simulated Water Level Elevation Hydrographs for Select Wells – Carrizo Aquifer (Layer 6)
- Figure 3.2-22 Measured and Simulated Water Level Elevation Hydrographs for Select Wells – Upper Wilcox (Layer 7)
- Figure 3.2-23 Measured and Simulated Water Level Elevation Hydrographs for Select Wells – Middle Wilcox (Layer 8)
- Figure 3.2-24 Measured and Simulated Water Level Elevation Hydrographs for Select Wells – Lower Wilcox (Layer 9)
- Figure 3.2-25 Simulated Water Level Elevations in Quaternary Alluvium (Layer 1) for 2013
- Figure 3.2-26 Simulated Water Level Elevation Contours in Sparta Aquifer (Layer 2) for 2013
- Figure 3.2-27 Simulated Water Level Elevation Contours in Weches Formation (Layer 3) for 2013
- Figure 3.2-28 Simulated Water Level Elevation Contours in Queen City Aquifer (Layer 4) for 2013
- Figure 3.2-29 Simulated Water Level Elevation Contours in Reklaw Formation (Layer 5) for 2013
- Figure 3.2-30 Simulated Water Level Elevation Contours in Carrizo Aquifer (Layer 6) for 2013
- Figure 3.2-31 Simulated Water Level Elevation Contours in Upper Wilcox (Layer 7) for 2013
- Figure 3.2-32 Simulated Water Level Elevation Contours in Middle Wilcox (Layer 8) for 2013
- Figure 3.2-33 Simulated Water Level Elevation Contours in Lower Wilcox (Layer 9) for 2013
- Figure 3.2-34 Change in Water Level Elevations between 1980 and 2013 in Quaternary Alluvium (Layer 1)
- Figure 3.2-35 Change in Water Level Elevations between 1980 and 2013 in Sparta Aquifer (Layer 2)
- Figure 3.2-36 Change in Water Level Elevations between 1980 and 2013 in Weches Formation (Layer 3)
- Figure 3.2-37 Change in Water Level Elevations between 1980 and 2013 in Queen City Aquifer (Layer 4)
- Figure 3.2-38 Change in Water Level Elevations between 1980 and 2013 in Reklaw Formation (Layer 5)
- Figure 3.2-39 Change in Water Level Elevations between 1980 and 2013 in Carrizo Aquifer (Layer 6)
- Figure 3.2-40 Change in Water Level Elevations between 1980 and 2013 in Upper Wilcox (Layer 7)
- Figure 3.2-41 Change in Water Level Elevations between 1980 and 2013 in Middle Wilcox (Layer 8)
- Figure 3.2-42 Change in Water Level Elevations between 1980 and 2013 in Lower Wilcox (Layer 9)
- Figure 3.2-43 Observed and Modeled Groundwater Level Elevation Contours for Sparta Aquifer (Layer 2)

Figure 3.2-44	Observed and Modeled Groundwater Level Elevation Contours for Queen City Aquifer (Layer 4)
Figure 3.2-45	Observed and Modeled Groundwater Level Elevation Contours for Carrizo Aquifer (Layer 6)
Figure 3.2-46	Observed and Modeled Groundwater Level Elevation Contours for Upper Wilcox (Layer 7)
Figure 3.2-47	Observed and Modeled Groundwater Level Elevation Contours for Middle Wilcox (Layer 8)
Figure 3.2-48	Observed and Modeled Groundwater Level Elevation Contours for Lower Wilcox (Layer 9)
Figure 3.3-1	Simulated Groundwater Interaction Fluxes for 2013 Rivers
Figure 3.3-2	Groundwater Budget for River Flux for the 1980 to 2013 Calibration Simulation
Figure 3.4-1	Water Budget for the 1980 to 2013 Calibration Simulation
Figure 4.2-1	Sensitivity of Weighted Mean Head Error to the Sand Hydraulic Conductivity Value for the Various Geologic Units
Figure 4.2-2	Sensitivity of Weighted Mean Head Error to the Clay Hydraulic Conductivity Value for the Various Geologic Units
Figure 4.2-3	Sensitivity of Weighted RMS Head Error to the Sand Hydraulic Conductivity Value for the Various Geologic Units
Figure 4.2-4	Sensitivity of Weighted RMS Head Error to the Clay Hydraulic Conductivity Value for the Various Geologic Units
Figure 4.2-5	Weighted Mean Error Sensitivity Graph for Model Parameters
Figure 4.2-6	Weighted Root Mean Squared Head Error Sensitivity Graph for Model Parameters
Figure 4.2-7	Measured and Simulated Hydrographs at Select Wells Showing Model Sensitivity – Quaternary Alluvium (Layer 1)
Figure 4.2-8	Measured and Simulated Hydrographs at Select Wells Showing Model Sensitivity – Sparta Aquifer (Layer 2)
Figure 4.2-9	Measured and Simulated Hydrographs at Select Wells Showing Model Sensitivity – Queen City Aquifer (Layer 4)
Figure 4.2-10	Measured and Simulated Hydrographs at Select Wells Showing Model Sensitivity – Carrizo Aquifer (Layer 6)
Figure 4.2-11	Measured and Simulated Hydrographs at Select Wells Showing Model Sensitivity – Upper Wilcox (Layer 7)
Figure 4.2-12	Measured and Simulated Hydrographs at Select Wells Showing Model Sensitivity – Middle Wilcox (Layer 8)
Figure 4.2-13	Measured and Simulated Hydrographs at Select Wells Showing Model Sensitivity – Lower Wilcox (Layer 9)

List of Tables

Table 2.1-1	Summary of Model Input Packages
Table 2.1-2	Summary of Model Output Packages
Table 2.4-1	Stress Period Setup
Table 2.4-2	Summary of Model Domain Discretization

Table 2.5-1	Sand Fraction Range for Each Layer
Table 2.7-1	Pumping Dataset Comparison
Table 2.8-1	General Head Boundary Conditions
Table 2.10-1	Recharge Multiplication Factors
Table 3.1-1	Calibration of Recharge Multiplication Factors
Table 3.1-2	Calibrated Hydraulic Conductivity for Modeled Geologic Units
Table 3.2-1	Weighted Calibration Statistics for the Steady-State 1980 and 2013 Simulation
Table 3.2-2	Weighted Calibration Statistics for the Transient 1980 to 2013 Simulation
Table 3.2-3	Weighted Calibration Statistics by Layer for the Transient 1980 to 2013 Simulation
Table 3.4-1	Water Budget by Layer for the Steady-State 1980 Simulation
Table 3.4-2	Water Budget by Layer at the End of the Transient 1980 to 2013 Simulation
Table 4.2-1	Model Parameter Sensitivity Type

Appendices

Appendix A	Simulated Water Budget and Model Pumping
Appendix B	Model Targets and Residuals
Appendix C	Draft Groundwater Model
Appendix D	Technical Memorandum 1: Pumping Sensitivity
Appendix E	Technical Memorandum 2: Recharge Sensitivity
Appendix F	Technical Memorandum 3: Calculation of Drawdown from Existing Modeled Available Groundwater Using Updated Groundwater Availability Model
Appendix G	Technical Memorandum 4: Comparison of Input and Output Pumping: Previous Groundwater Availability Model and Updated Groundwater Availability Model
Appendix H	Response to Comments

This page is intentionally blank.

Executive Summary

The Texas Water Development Board (TWDB) Groundwater Availability Modeling program intends that numerical models be used as living tools that are updated as data and modeling technology improves. Groundwater is a vital resource in the northern portions of the Queen City Aquifer, Sparta Aquifer, and Carrizo-Wilcox Aquifer System and groundwater pumping is expected to increase in response to growing municipal demands. The primary objective of the project is to update the existing groundwater availability model for the northern portion of the Queen City, Sparta, and Carrizo-Wilcox aquifers to simulate impacts of groundwater pumping on groundwater resources in northeast Texas.

Challenges to the modeling effort contributed a considerable computational effort and uncertainty, and included the following.

- A large domain (greater than 38,000 square miles);
- Complex geology (deep, multi-layered system with outcrops and pinch-outs);
- Fine resolution to effectively handle groundwater to surface water interaction;
- Inconsistent pumping data;
- Inconsistent water level elevation data;
- Lack of well construction data and difficulty assigning water level elevations to appropriate hydrostratigraphic layers; and
- A long 34-year model time-frame (1980 to the end of 2013).

Modeling challenges were addressed by selecting a robust and flexible software to best alleviate the computational burdens and still provide results at the scale of the modeling objectives. The MODFLOW 6 groundwater flow model was used for the simulations with the Groundwater Vistas graphic user interface. The numerical model was built in accordance with the conceptual model and consisted of 9 model layers to represent the 9 hydrostratigraphic units of interest, consisting of the Quaternary Alluvium, Sparta Aquifer, Weches Formation, Queen City Aquifer, Reklaw Formation, Carrizo Aquifer, and Wilcox Aquifer (Upper, Middle, and Lower). These layers have structural features such as pinch-outs and vertical displacements which were successfully represented using MODFLOW 6.

A model grid measuring 193 miles by 201 miles with a base cell size of one square mile (5,280 feet on a side) was used to discretize the domain. Oct-patch refinement was then applied to reduce the cell size to a level of 4, resulting in square cells of 660 feet wide. This refinement was done in the Quaternary Alluvium hydrostratigraphic unit and provided a higher resolution for modeling surface water to groundwater interaction. With the oct-patch refinement, the grid coarsens for deeper layers, with a coarsening of one level for every active layer found beneath the alluvium cells.

Model boundary conditions were constructed in model layer 2 (Sparta Aquifer) to represent the Younger Units hydrostratigraphic unit which was not explicitly modeled and in deeper layers to represent a southern boundary for flow within the lower aquifers (Queen City Aquifer, Carrizo Aquifer, and Wilcox Aquifers). Aquifer and hydrogeologic

properties such as hydraulic conductivity, aquifer storage, rivers, recharge, and evapotranspiration were simulated using various MODFLOW 6 packages. Specifically, hydraulic conductivity of each unit was parameterized using correlation with available sand fraction estimates.

Simulation of groundwater extraction was initially attempted as individual analytic element wells using conceptual model data. However, due to domain-wide data discrepancies, the conceptual extraction data was replaced with pumping from previous modeling and extrapolated through 2013.

The model simulation consisted of a steady-state period representing 1980 conditions followed by transient conditions from 1981 through 2013 using annual stress periods for recharge and pumping. The steady-state 1980 period was simulated using average aquifer conditions.

The model calibration was guided by available data and reflects comments provided by TWDB in their Draft Report Comment Letter dated November 4, 2020. Quantitative and qualitative metrics were implemented in evaluating representativeness of the model. Observed water level elevations in wells and groundwater to surface water flow estimates of gaining and losing reaches were used to constrain the model. Calibration statistics show the model was well calibrated for the spatial and temporal scales of investigation. Mass balance errors were negligible and water fluxes at the various boundaries into and out of the domain were reasonable and consistent with the conceptual model. Qualitative comparison of estimated conceptual groundwater elevation contours to simulated contours confirm that the calibration matched observed conditions across the model domain.

The final model represents the conceptual model. However, the final model and a draft model were similar in calibration statistics, water level elevations measurements, and water budgets, with the only significant difference being calibration statistics in the Queen City Aquifer (model layer 4). Because of this, the sensitivity analyses and predictive sensitivities presented in this report are based on the draft model submitted July 16, 2020 (draft model included as Appendix C).

Sensitivity analyses evaluate the impact of parameter uncertainties and variations in boundary fluxes. Parameters evaluated quantitatively were hydraulic conductivity, recharge, evapotranspiration, and groundwater pumping. Medium to high changes in calibration statistics were noted for changes in the recharge and pumping values and noted for hydraulic conductivity within the Queen City Aquifer, the Middle Wilcox, and Lower Wilcox. Parameters evaluated qualitatively included scenarios of no pumping, constant recharge, and increased storage. Increased storage results showed that storage is not significant to the model calibration. Simulation of no-pumping and constant recharge both affected the model results, causing a decrease in water level elevation fluctuations across the model domain. A better estimation of pumping changes through time will provide better transient calibration to water level elevations changes. As data collection continues and the conceptual model is improved, the uncertainties associated with the model can be reduced.

A predictive model, based on the draft model, was developed for the period 2014 through 2080. Predictive simulations were conducted to evaluate the impact of future pumping and recharge on the aquifers. Four pumping simulations were conducted, simulating future pumping at baseline constant rates corresponding to pumping from the calibrated model for years 2010, 2011, 2012, and 2013. Four recharge simulations were conducted with future recharge modeled as 80 percent, 90 percent, 110 percent, and 120 percent of the calibrated model steady-state period (1980). The predictive simulations found that the groundwater model does not simulate unrealistic increases in water level elevations as the previous groundwater availability model had done. Additionally, a comparison of pumping input to simulated pumping was performed for the existing groundwater availability model and the updated groundwater availability model. The evaluation shows that dry cells in the existing groundwater availability model effectively reduced pumping in that model compared to the updated groundwater availability model. The updated groundwater availability model also showed some reduction in simulated pumping compared to input rates due to supply and demand conditions. However, output pumping from both groundwater availability models are similar.

Since the predictive pumping and recharge values were held constant across the model for all counties, local variabilities in pumping were not evaluated; neither was variability in other model parameters which were also held constant through 2080. Predictive modeling from 2014 to 2080 showed that drawdown at Groundwater Management Area 11 counties may be significantly affected by baseline pumping rates or average recharge conditions. Despite the constant parameters used, the predictive drawdown charts for counties by aquifer may still be useful in guiding the Joint Planning Process and development of desired future conditions.

This page is intentionally blank

1.0 Introduction and Purpose of the Model

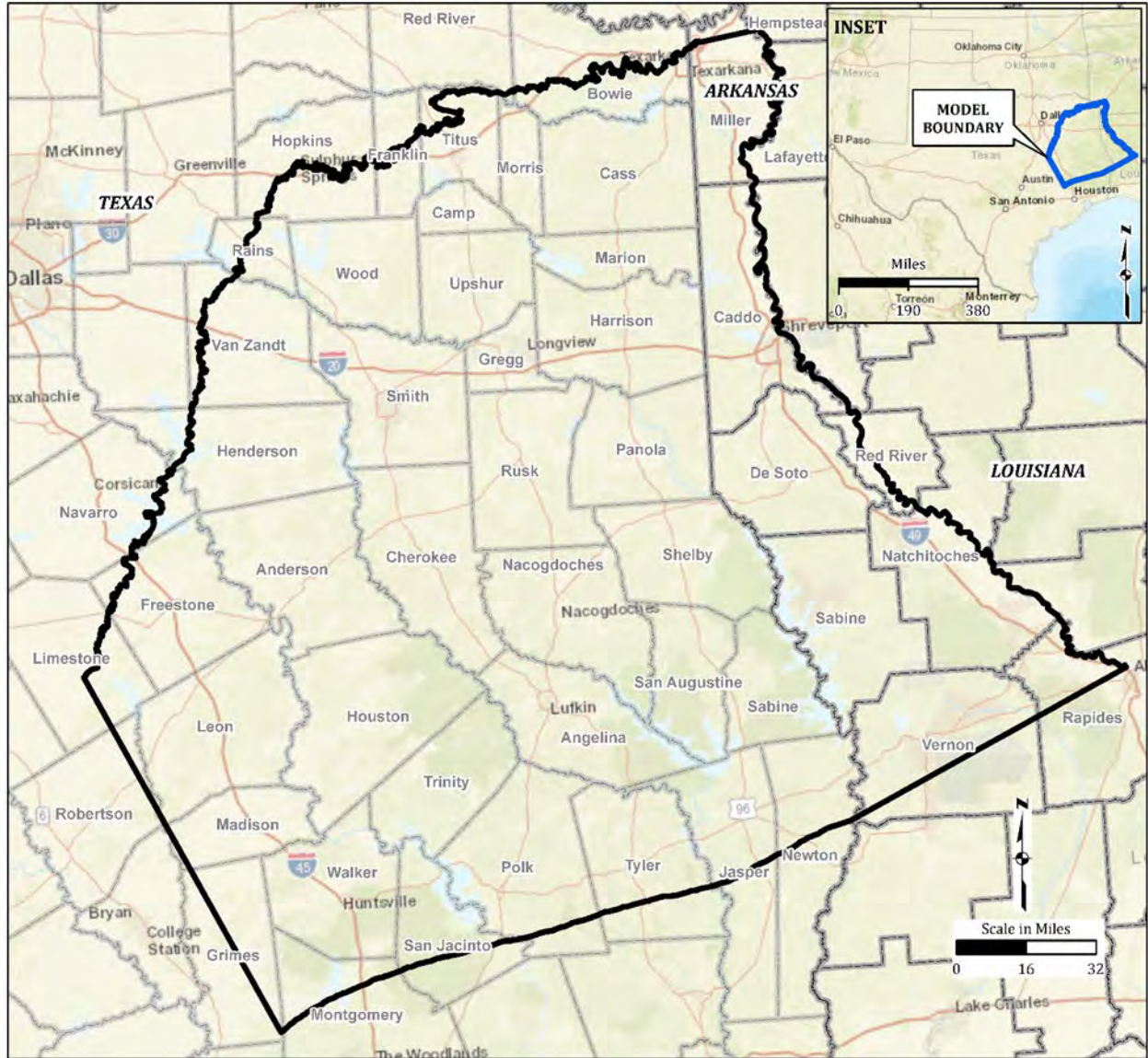
The Texas Water Development Board (TWDB) Groundwater Availability Modeling program intends that numerical models be used as living tools that are updated as data and modeling technology improves. Given this directive, the primary objective of the project is to update the existing groundwater availability model for the northern portions of the Queen City Aquifer, Sparta Aquifer, and Carrizo-Wilcox Aquifer System to simulate impacts of groundwater pumping on groundwater resources in northeast Texas. This model, referred to as the groundwater availability model for the northern portion of the Queen City, Sparta, and Carrizo-Wilcox aquifers, will update the existing groundwater availability model for the northern Carrizo-Wilcox Aquifer (Fryar and others, 2003) and the existing groundwater availability models for the Queen City and Sparta Aquifers (Kelley and others, 2004). The groundwater availability model for the northern portion of the Queen City, Sparta, and Carrizo-Wilcox aquifers is based on the conceptual hydrogeologic model, which is summarized in the Conceptual Model Report (Montgomery and Associates, 2020). The study area is shown on Figure 1.0-1.

The groundwater availability model for the northern portion of the Queen City, Sparta, and Carrizo-Wilcox aquifers will be used to assess future regional impacts from current pumping and projected future pumping. Model results will be used to evaluate long-term groundwater pumping impacts on surface water and groundwater. In addition, the model may be used to assist groundwater conservation districts in Groundwater Management Area 11 with groundwater planning and management.

2.0 Model Overview and Packages

A conceptual model of the hydrogeologic system of the area of interest in the northern portion of the Queen City Aquifer, Sparta Aquifer, and Carrizo-Wilcox aquifers was developed by Montgomery and Associates (2020). The conceptual model, the existing groundwater availability model for the northern Carrizo-Wilcox Aquifer (Fryar and others, 2003), and the existing groundwater availability model for the Queen City and Sparta Aquifers (Kelley and others, 2004) were the basis of the numerical model described in this report.

The groundwater system comprises Quaternary Alluvium and eight southward-dipping aquifers including (from top to bottom) the Sparta Aquifer, Weches Formation, Queen City Aquifer, Reklaw Formation, Carrizo Aquifer, Upper Wilcox, Middle Wilcox, and Lower Wilcox. The Queen City and Sparta Aquifers are classified as minor aquifers in Texas and extend from the Frio River region in south Texas to east Texas with the Sparta Aquifer extending into Louisiana and Arkansas. The Carrizo-Wilcox Aquifer is classified as a major aquifer in Texas and extends from the Rio Grande region in south Texas to northeast Texas and into Louisiana and Arkansas. The Sparta Aquifer is overlain by Younger Units which are not actively simulated in the numerical model.





LEGEND	
	Model Boundary
	County or Parish Boundary
<u>Notes:</u>	
1. Basemap is World Street Map provided by ESRI.	
2. Projected Coordinate System Datum: GAM	

Figure 1.0-1. Site Location Map

The three-dimensional modular groundwater-flow model code MODFLOW 6 (Langevin and others, 2017) was used for the simulations with the Groundwater Vistas, Version 7 (Rumbaugh and Rumbaugh, 2017), graphic user interface. Construction of the numerical model generally required evaluating the area hydrostratigraphy, identifying flows in and out of the model domain, establishing the time period of the simulation, and designing the spatial resolution necessary to perform the simulation.

The numerical model honors the conceptual model layering including pinch-outs and outcrop of the geologic units, discussed further in Section 2.4. Figure 2.0-1 shows the aquifer outcrops simulated in the groundwater model.

Flows in and out of the model domain were discussed in the conceptual model sections related to pumping, exchange with the Younger Units, recharge, rivers, and evapotranspiration. The conceptual block model, shown in Figure 2.0-2, illustrates the groundwater flux between hydrostratigraphic units. These flows were translated into model boundary conditions using the boundary condition packages of MODFLOW 6. Boundary condition packages simulate interaction of the model with the “outside world” and allow water to flow into or out of the model domain. Packages numerically implement various conceptual flow processes and their interactions with groundwater.

The boundary conditions present in the model domain provided guidelines for the model spatial and temporal scales. The time period of 1980 through 2013 was selected principally based on pumping and groundwater level elevation data availability. The numerical groundwater-flow model was constructed to simulate the conceptualized groundwater-flow system for steady-state 1980 conditions and transient conditions using annual stress periods from 1981 through 2013.

The spatial resolution of the model grid (model cell size) was based on the boundary conditions identified. As discussed in detail in Section 2.4, grid cell size varies by layer. Once the grid was developed, the hydrostratigraphic conceptual model (Montgomery and Associates, 2020) that was developed in Leapfrog® Geo (developed by Seequent) was imported into the model grid using Groundwater Vistas. Base-maps were also imported into Groundwater Vistas to identify county boundaries, rivers, and other features that generally orient the model.

Following model construction, preliminary model parameter estimates were generated (e.g. hydraulic conductivity parameterization) and boundary conditions (rivers, wells, recharge, evapotranspiration, and general head boundaries) were developed for steady-state 1980 conditions and transient 1981 through 2013 conditions. Calibration targets for water level elevations were developed for the steady-state and transient stress periods and imported into Groundwater Vistas (discussed in Section 3.0). The model was run in steady-state and transient modes to debug the datasets, establish convergence, and tune solver parameters for optimal simulation performance before moving on to the model calibration phase. Model calibration and sensitivity are discussed in Sections 3.0 and 4.0. Sections below provide details of model construction.

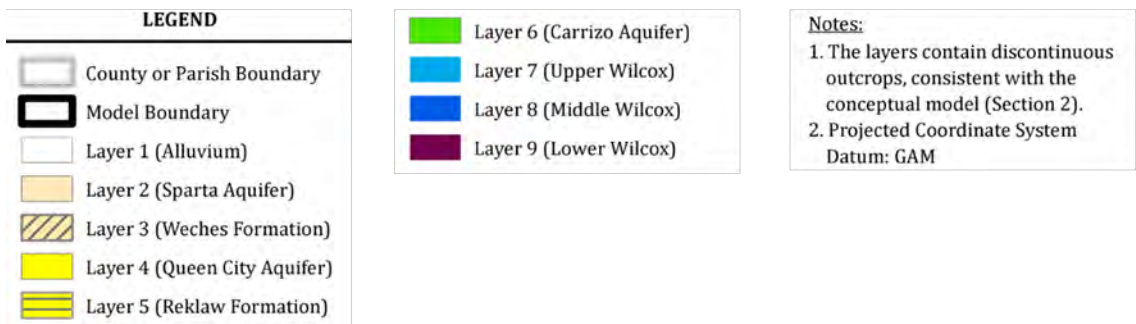
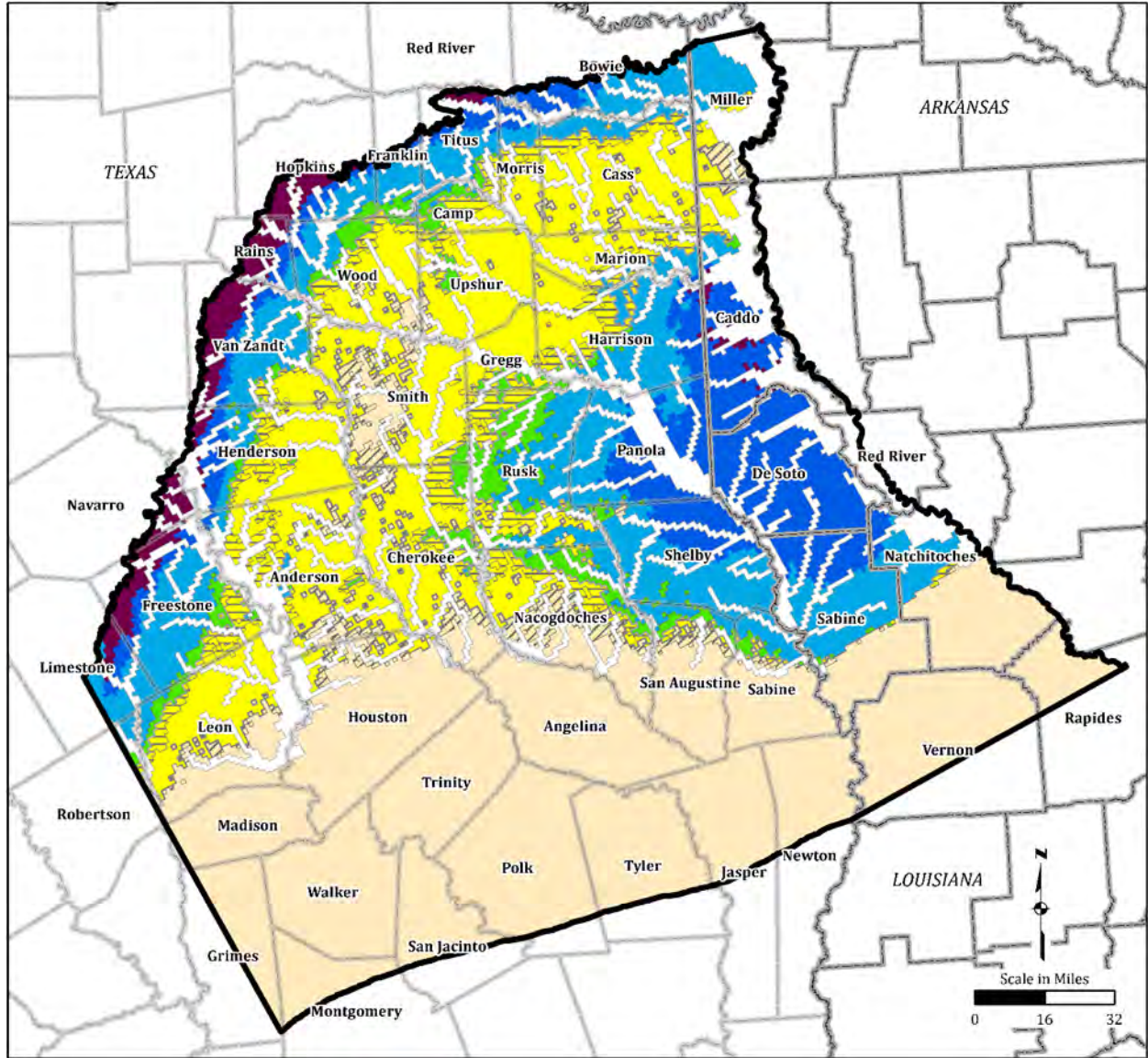
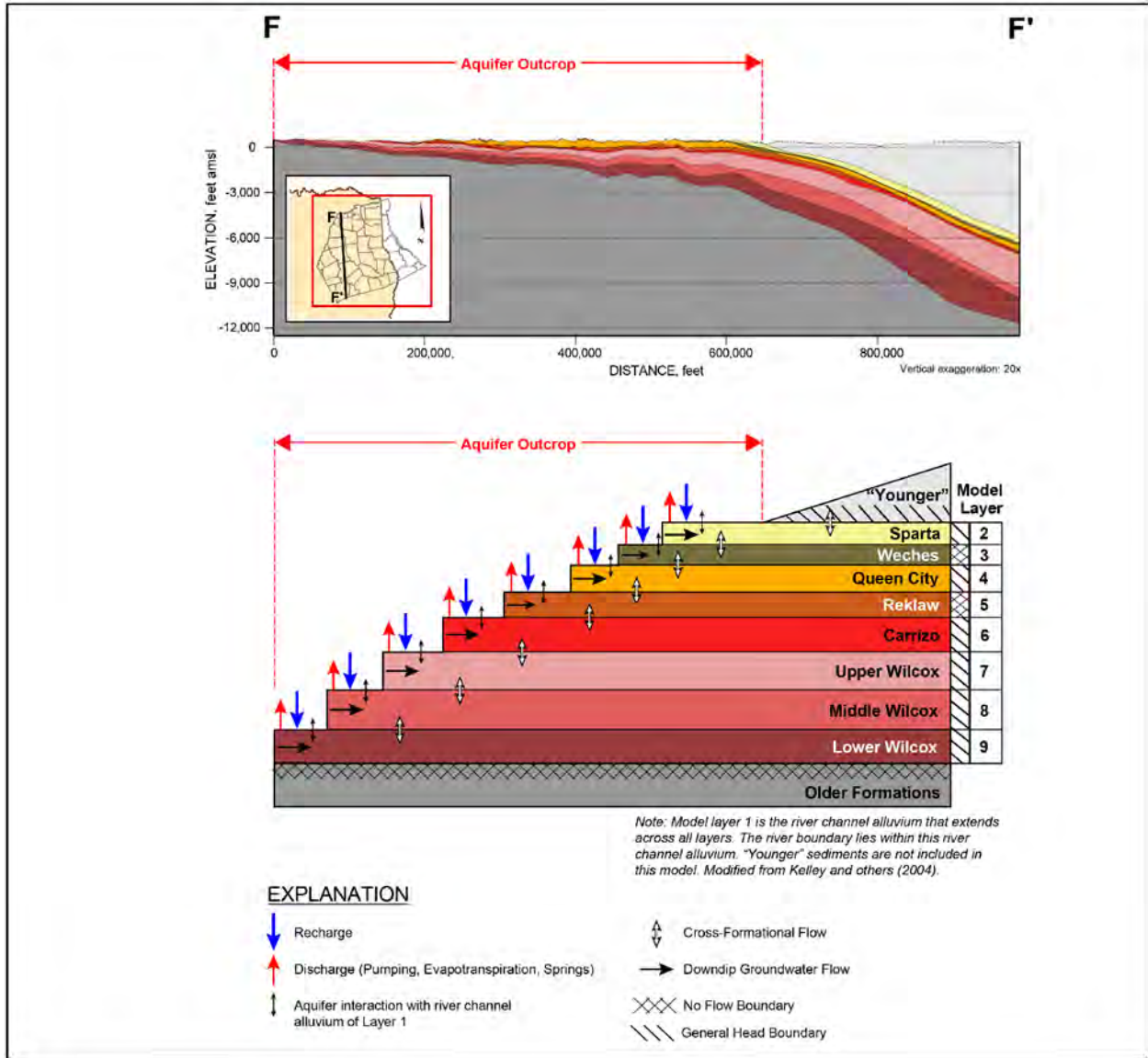


Figure 2.0-1. Aquifer Outcrops Simulated in the Groundwater Model



Notes:

1. amsl = above mean sea level
2. The block diagram was provided by Montgomery and Associates, November 2020.

Figure 2.0-2. Conceptual Block Diagram

2.1 MODFLOW 6 Overview

The MODFLOW 6 groundwater modeling software was used to construct the model within the Groundwater Vistas (version 7) interface. MODFLOW 6 is the newest version of the MODFLOW code, released in 2017 by the United States Geological Survey (Langevin and others, 2017). The code is appropriate for this work as it can meet the simulation requirements and challenges for this project. Elements of the code and packages pertinent to the groundwater availability model for the northern portion of the Queen City, Sparta, and Carrizo-Wilcox aquifers flow simulations are discussed here.

The MODFLOW 6 groundwater model (Langevin and others, 2017) contains most of the functionality of previous MODFLOW codes, including MODFLOW-2005 (Harbaugh, 2005), MODFLOW-NWT (Niswonger and others, 2011), MODFLOW-USG (Panday and others, 2013), and MODFLOW-LGR (Mehl and Hill, 2005).

Simulations were also evaluated with MODFLOW-2005 and MODFLOW-NWT. However, these software were not ultimately used for modeling in favor of MODFLOW 6. This was done for several reasons. First, MODFLOW-2005 uses an outdated scheme that has issues with drying and rewetting of cells which may then be overcome using heuristic methods, if at all. This approach makes the solution unreliable if it does converge. Simulations attempted with MODFLOW-2005 for the current project did not converge. Most of the simulation domain became inactive due to large fluctuations in water level elevations during the solution iterations. Rewetting schemes did not work. Carrying on with non-converged solutions provided meaningless results with large mass balance errors. Therefore, MODFLOW-2005 could not be applied successfully for the project.

Simulations were also conducted using MODFLOW-NWT. MODFLOW-NWT contains more robust schemes so it was used to run a coarse grid model of the study area. The model did converge and produced meaningful results. However, pinch-out features and geological displacements at faults could not be represented by the regular finite difference grid of MODFLOW-NWT. Also, it was impractical to create finer grids near surface-water features or wells to capture the required resolution due to the extremely large grid required. Therefore, the project was further conducted using MODFLOW 6 which has the flexibility to capture the geological features such as outcrops, pinch-outs, faults and displacements, and the fine grid resolution required to provide accuracy in regions of interest and around pumping wells and surface-water features. The MODFLOW-NWT test is discussed in Section 3.2.

MODFLOW 6 solves for three-dimensional flow of water in the subsurface using the control-volume finite-difference approach. The control-volume finite-difference numerical method “discretizes” the modeled domain into model cells that may have different sizes and shapes. Each model cell represents a part of the domain that is encompassed by that model cell and model inputs and outputs are generated for this discretized system. The control-volume finite-difference methodology allows for flexible gridding of the subsurface domain including: ability to refine the computational grid locally using nested grids to provide spatial resolution where required and accurately represent pinch-outs, faults, displacements and outcrops of geological layers.

As with the other MODFLOW codes, MODFLOW 6 consists of groups of “modules” or “packages” that perform various functions related to groundwater flow simulations. These packages compartmentalize the model into its various functional elements such as defining the model domain and its discretization, parameterizing the aquifer and flow processes, and implementing various pumping and boundary conditions to the modeled system. Table 2.1-1 shows the packages of MODFLOW 6 that were used for the groundwater availability model for the northern portion of the Queen City, Sparta, and Carrizo-Wilcox aquifers. Model input files were developed for each of the packages to represent the conceptual model of the system.

MODFLOW 6 is structured slightly differently from MODFLOW in that the solution is separated from the model. With the MODFLOW code, the entire domain is represented by one model, but in MODFLOW 6 it is possible to have multiple models (of different domains or different types) for the same solution. Therefore, in addition to the model related files shown on Table 2.1-1, MODFLOW 6 also includes files for the solution that contains the models (only one model in this case).

MODFLOW 6 simulation outputs are contained in several files. The main output is written in a run list file (LST) which also includes the mass balance information. Water level elevations output is provided in the heads file with the extension HDS. Modeled flows, storage flux, and boundary flux are output to the cell-by-cell flow file with extension CBB. Table 2.1-2 shows the relevant output files generated by MODFLOW 6.

Table 2.1-1. Summary of Model Input Packages

Package Type	Abbreviation	Description
Internal Packages		
Namefile	NAM	Controls all other model files and names
Initial Conditions	IC	Reads the starting heads
Discretization	DIS	Discretizes groundwater domain
Node Property Flow	NPF	Calculates flow between cells
Storage	STO	Calculates the change in water volume
Temporal discretization	TDIS	File containing model time discretization
Stress Packages		
Well	WEL	Implement sources/sinks
General Head Boundary	GHB	Implement head-dependent flux boundary
River	RIV	Implement river boundary
Recharge	RCH	Implement recharge
Evapotranspiration	EVT	Implement evapotranspiration

Table 2.1-2. Summary of Model Output Packages

Package Type	Abbreviation	Description
List file	LST	Lists model input, simulation summary, and mass balance
Groundwater Flow Head output	HDS	Contains head output for all GWF cells at all stress periods
Cell-by-cell flows	CBB	Contains CBB output for all cells at all stress periods
Output Control	OC	Control simulation output

2.2 NAME File

A MODFLOW 6 simulation includes two NAME files, one for the solution and another for the groundwater flow model.

The solution NAME file includes solution-related information such as solution options, time-stepping file name, NAME files for the various models (only one in this case), file names for the exchanges between models (none in this case), and file name for the solver. The CONTINUE option was used in the solution which allows for continuation of failed iterations; however, this option was not necessary as final model results converged to the prescribed tolerance limit.

The groundwater model NAME file contains the model options, the abbreviations of MODFLOW 6 packages used, and a file name for the input (or output) files that are used in the model. The Newton Raphson option was selected for linearizing the model flow equations.

2.3 Initial Conditions Package

The Initial Conditions (IC) package of MODFLOW 6 specifies initial water level elevations at all groundwater model cells in the domain. Since the first stress period of the model is a steady-state condition, the starting head values do not affect the result but are required to begin the iterative process. During calibration, the computational burden of deriving a numerical solution was reduced by using a previous calibration simulation output for starting heads. The binary output file of a simulation was renamed “start.hds” such that the first stress period values (the steady-state result of the previous calibration simulation) were used as the starting condition for the current simulation.

2.4 Discretization Packages

A MODFLOW 6 simulation includes two discretization packages, one for time discretization of the solution and the other for defining the discretization of the unstructured grid for the model.

The Stress Period Setup (TDIS) package of MODFLOW 6 defines the time discretization. The Discretization (DIS) package of MODFLOW 6 was used and defines the model discretization information for the 3-dimensional groundwater cells.

2.4.1 Stress Period Setup

The Stress Period Setup (TDIS) package of MODFLOW 6 defines the time discretization. The groundwater availability model for the northern portion of the Queen City, Sparta, and Carrizo-Wilcox aquifers was discretized into 34 stress periods. The first stress-period was simulated as steady-state representing 1980 conditions. The remaining stress periods were simulated as yearly and represented transient conditions from 1981 through 2013. The model was updated through 2013 in accordance with the project contract and based on pumping and groundwater level elevation data availability. The annual stress period discretization was considered sufficient for the regional planning objectives of the modeling effort. Table 2.4-1 shows the stress period details.

Table 2.4-1. Stress Period Setup

Stress Period	Time Steps	Representative Year	Length (days)	Type
1	1	1980	1	Steady State
2	5	1981	365	Transient
3	5	1982	365	Transient
4	5	1983	365	Transient
5	5	1984	366	Transient
6	5	1985	365	Transient
7	5	1986	365	Transient
8	5	1987	365	Transient
9	5	1988	366	Transient
10	5	1989	365	Transient
11	5	1990	365	Transient
12	5	1991	365	Transient
13	5	1992	366	Transient
14	5	1993	365	Transient
15	5	1994	365	Transient
16	5	1995	365	Transient
17	5	1996	366	Transient
18	5	1997	365	Transient
19	5	1998	365	Transient
20	5	1999	365	Transient
21	5	2000	366	Transient
22	5	2001	365	Transient
23	5	2002	365	Transient
24	5	2003	365	Transient
25	5	2004	366	Transient
26	5	2005	365	Transient
27	5	2006	365	Transient
28	5	2007	365	Transient
29	5	2008	366	Transient
30	5	2009	365	Transient
31	5	2010	365	Transient
32	5	2011	365	Transient
33	5	2012	366	Transient
34	5	2013	365	Transient

2.4.2 Model Domain Discretization

The Discretization (DIS) package of MODFLOW 6 defines the model discretization information for the 3-dimensional groundwater cells. The domain and stratigraphy for the groundwater availability model for the northern portion of the Queen City, Sparta, and Carrizo-Wilcox aquifers were established during conceptual model development and are shown on Figure 2.0-2. Nine geologic units in the model domain were discretized into 9 numerical layers, as shown on Figure 2.4-1 and summarized in Table 2.4-2.

The model domain's northern and north-western boundary represent the northern extent of the Carrizo-Wilcox Aquifer as shown on Figure 2.0-1 (Figure 4-3 of the Conceptual Model Report). The model domain includes the north-eastern portions of the Sparta and Queen City Aquifers (Figure 2.0-1) (Figure 4-3 of the Conceptual Model Report). The major and minor aquifers are described in detail in the Conceptual Model Report (Montgomery and Associates, 2020) (Figures 2-2 and 2-3 of the Conceptual Model Report).

The hydrostratigraphic unit Younger Units was excluded from the active model domain. The Younger Units have a limited extent along the southern portion of the model domain and flux between the Younger Units and the Sparta Aquifer was simulated as a general head boundary within Layer 2, as described in Section 2.8.

Figures 2.4-2 through 2.4-21 (Figures 4-5 through 4-22 of the Conceptual Model Report) show the stratigraphic elevations and thicknesses of the geologic units simulated by the model. The top of Layer 2 and the thickness of Layer 2 represent the Sparta Aquifer (Figure 2.4-5 and 2.4-7). Discontinuous sections of geologic units, as described in the Conceptual Model Report, are simulated in the model. These cells are not isolated but connected to cells vertically and may be connected to cells in layers above or below.

The structural features described in the Conceptual Model Report, which include the East Texas Embayment, Houston Embayment, Sabine Uplift, and Sabine Arch, are shown on Figure 2.4-22 (Figure 2-19 of the Conceptual Model Report). These structural features dictate the outcrop pattern of the geologic units. The Carrizo Aquifer and Wilcox hydrostratigraphic units outcrop along a belt along the northern extent of the model domain and also in the eastern portion of the model domain in the Sabine Uplift. The Sparta Aquifer and Queen City Aquifer hydrostratigraphic units outcrop in the central portion of the model domain along the East Texas Embayment. In the southern portion of the model domain, the surface geology and outcrop pattern are oriented southwest-northeast and the hydrostratigraphic units dip to the southeast.

The domain was discretized using a parent grid-block size of one square mile (5,280 feet length of each side) (Table 2.4-2) on a base grid containing 193 rows, 201 columns, and 9 layers. An oct-patch refinement procedure was implemented along the rivers to provide a finer spatial resolution along these features. The oct-patch feature refines the grid in the horizontal and vertical direction. Figures 2.4-23 through 2.4-31 show the discretization of the groundwater domain. Model Layer 1, representing the Quaternary Alluvium hydrostratigraphic unit, has the greatest refinement level of 4, giving square cells measuring 660 feet for each side along the river (Figure 2.4-23 and Table 2.4-2).

MODEL LAYER	HYDROSTRATIGRAPHIC UNITS
Layer 1	Quaternary Alluvium
Layer 2	Sparta Aquifer
Layer 3	Weches Formation
Layer 4	Queen City Aquifer
Layer 5	Reklaw Formation
Layer 6	Carrizo Aquifer
Layer 7	Upper Wilcox
Layer 8	Middle Wilcox
Layer 9	Lower Wilcox

Figure 2.4-1. Geologic Units and Model Layers

Table 2.4-2. Summary of Model Domain Discretization

Layer	Hydrostratigraphic Unit	Number of cells	Smallest grid cell size (feet)	Largest grid cell size (feet)
1	Quaternary Alluvium	307,787	660	5,280
2	Sparta Aquifer	63,072	1,320	5,280
3	Weches Formation	23,916	1,320	5,280
4	Queen City Aquifer	39,640	1,320	5,280
5	Reklaw Formation	33,467	1,320	5,280
6	Carrizo Aquifer	28,480	1,320	5,280
7	Upper Wilcox	50,692	1,320	5,280
8	Middle Wilcox	50,843	1,320	5,280
9	Lower Wilcox	39,639	1,320	5,280

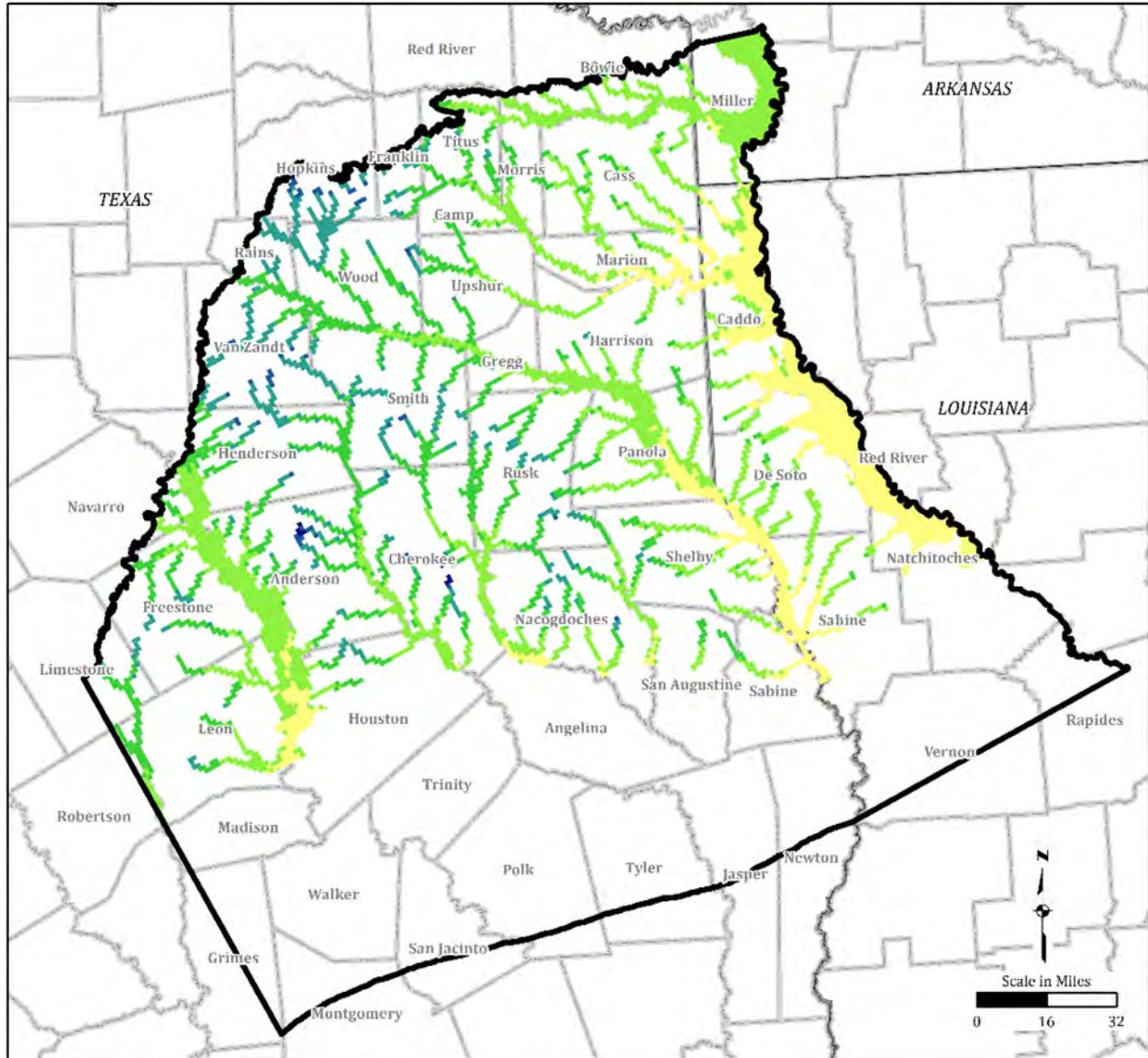


Figure 2.4-2. Modeled Top Elevation for Quaternary Alluvium (Model Layer 1)

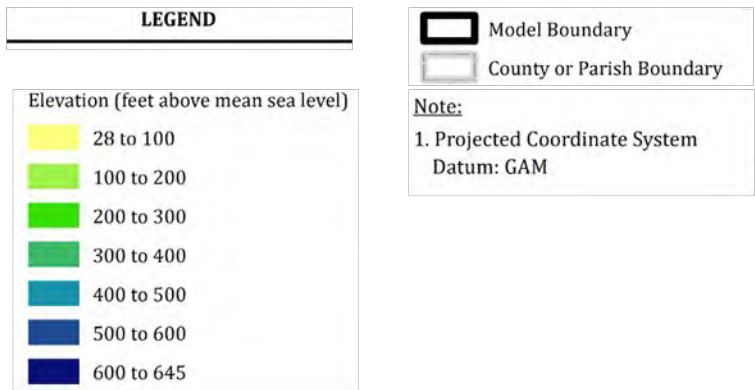
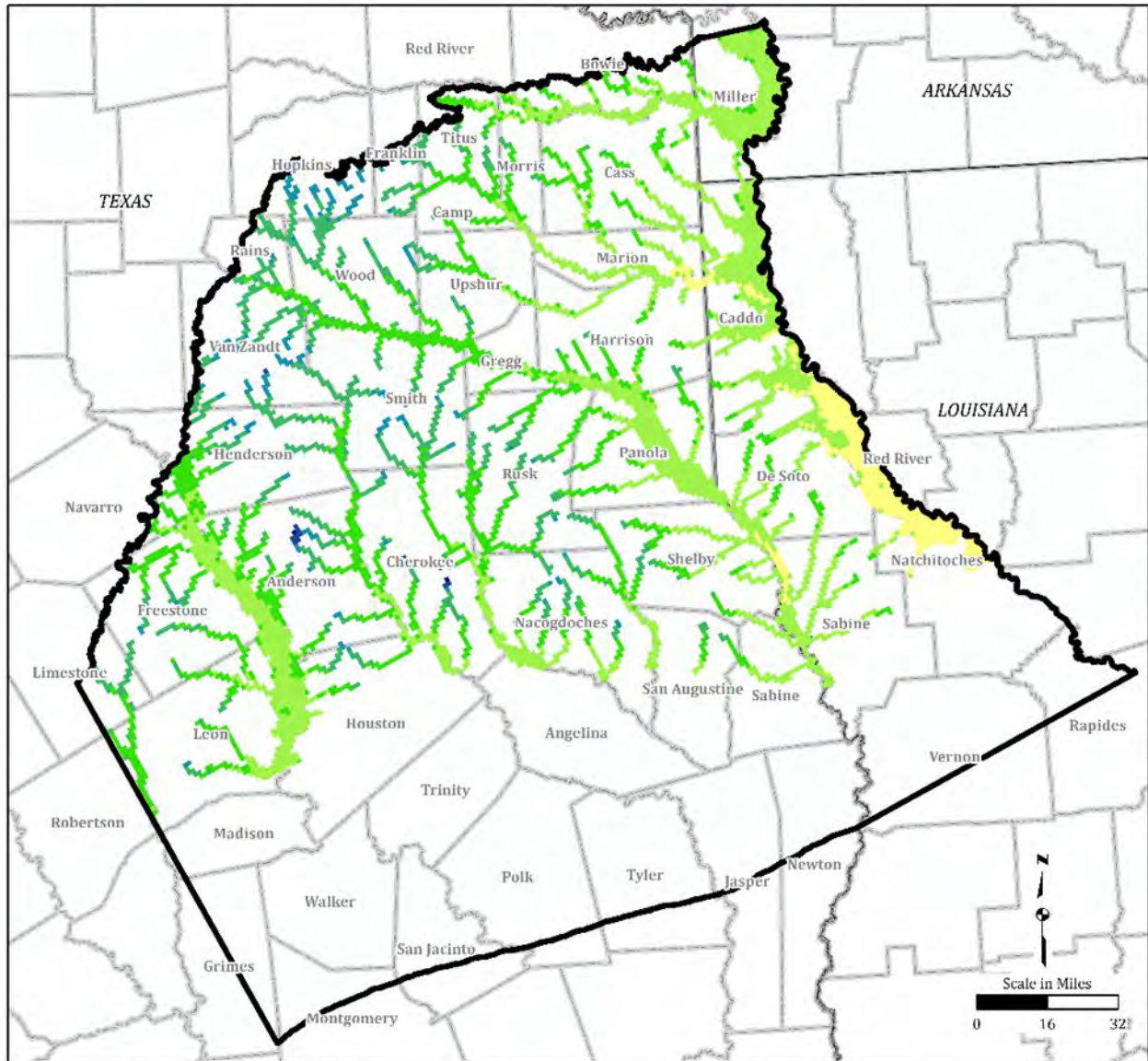


Figure 2.4-3. Modeled Bottom Elevation for Quaternary Alluvium (Model Layer 1)

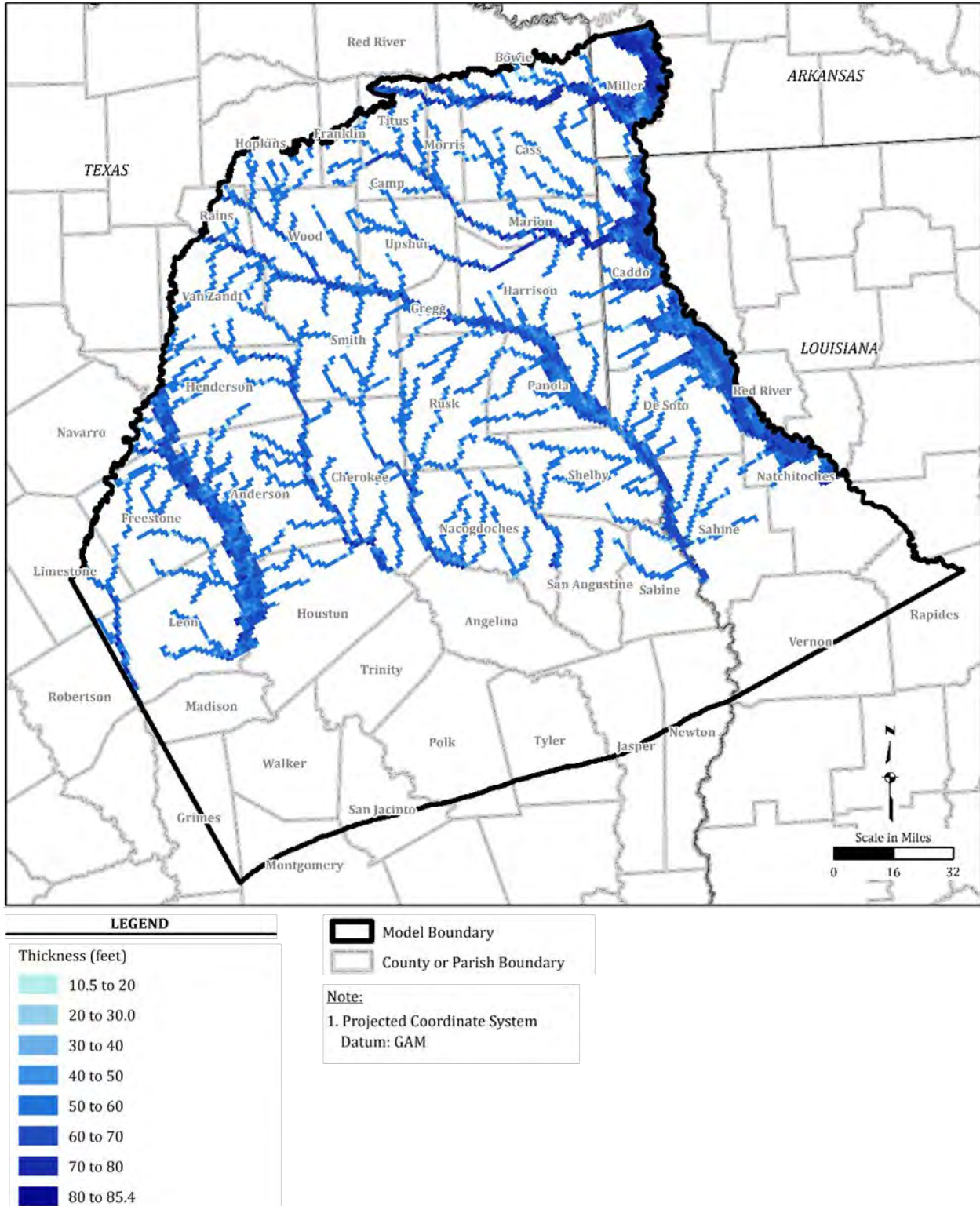
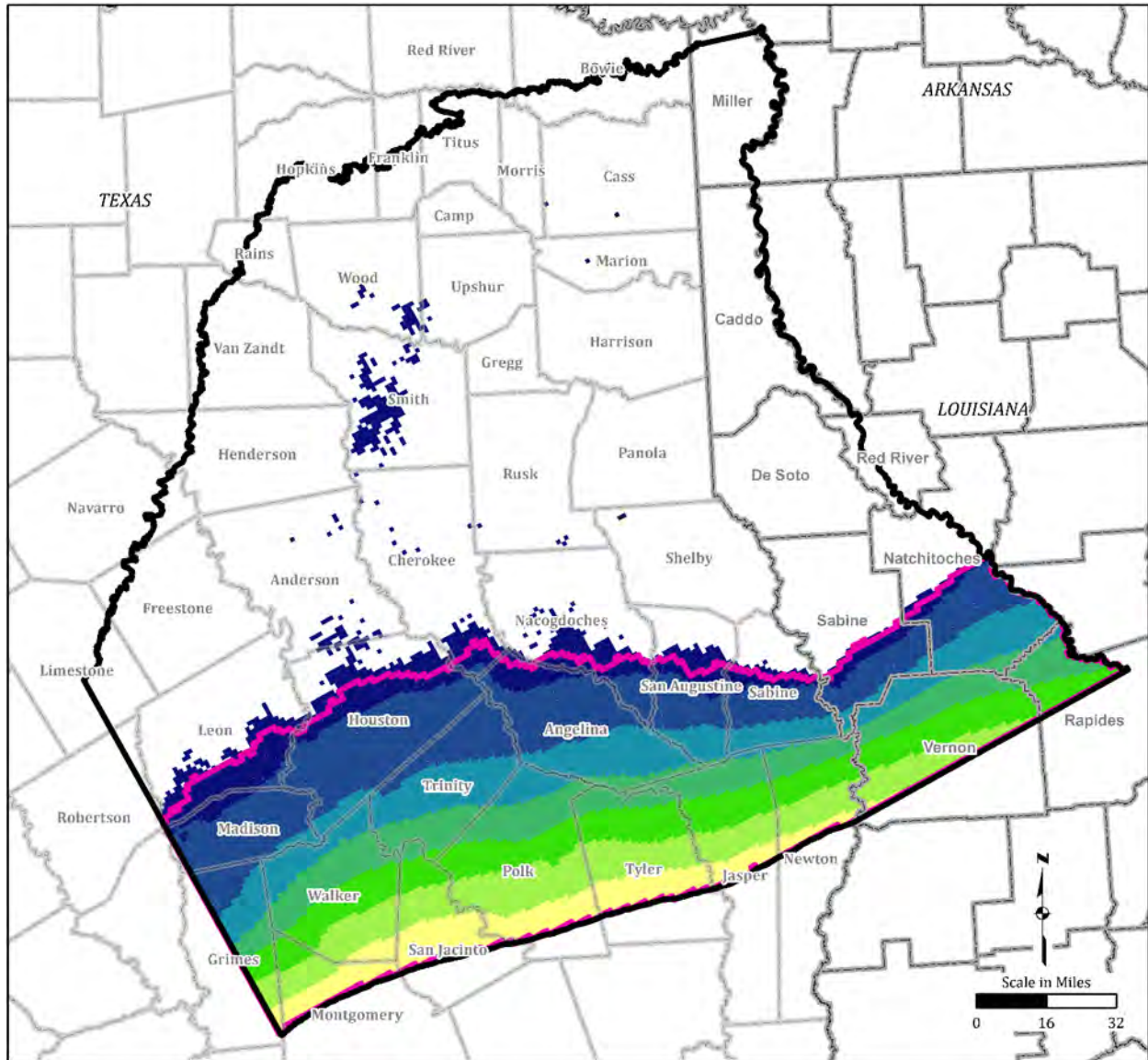


Figure 2.4-4. Modeled Thickness of Quaternary Alluvium (Model Layer 1)



LEGEND	
Elevation (feet above mean sea level)	
	-6229 to -5000
	-5000 to -4000
	-4000 to -3000
	-3000 to -2000
	-2000 to -1000
	-1000 to 0
	0 to 676

- Model
- Extent of General Head Boundary
- County or Parish Boundary

Notes:

1. The general head boundary in Layer 2 represents the Younger Units.
2. The layer contains discontinuous outcrops, consistent with the conceptual model (Section 2).
3. Projected Coordinate System Datum: GAM.

Figure 2.4-5. Modeled Top Elevation for Sparta Aquifer (Model Layer 2)

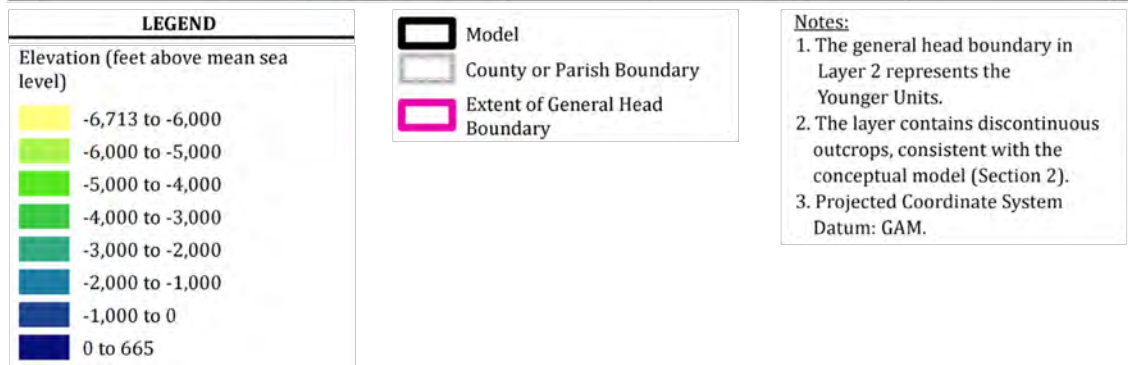
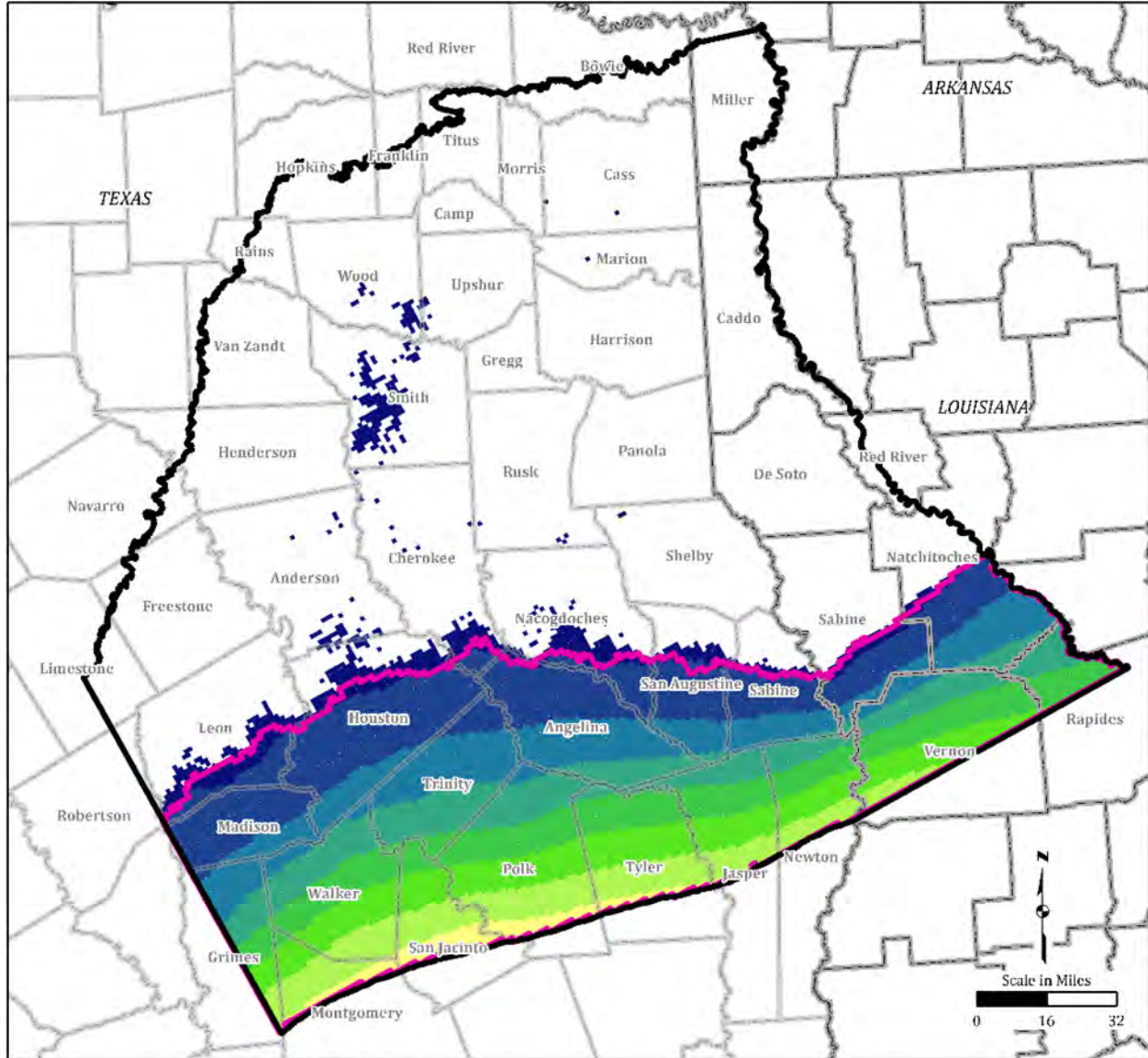
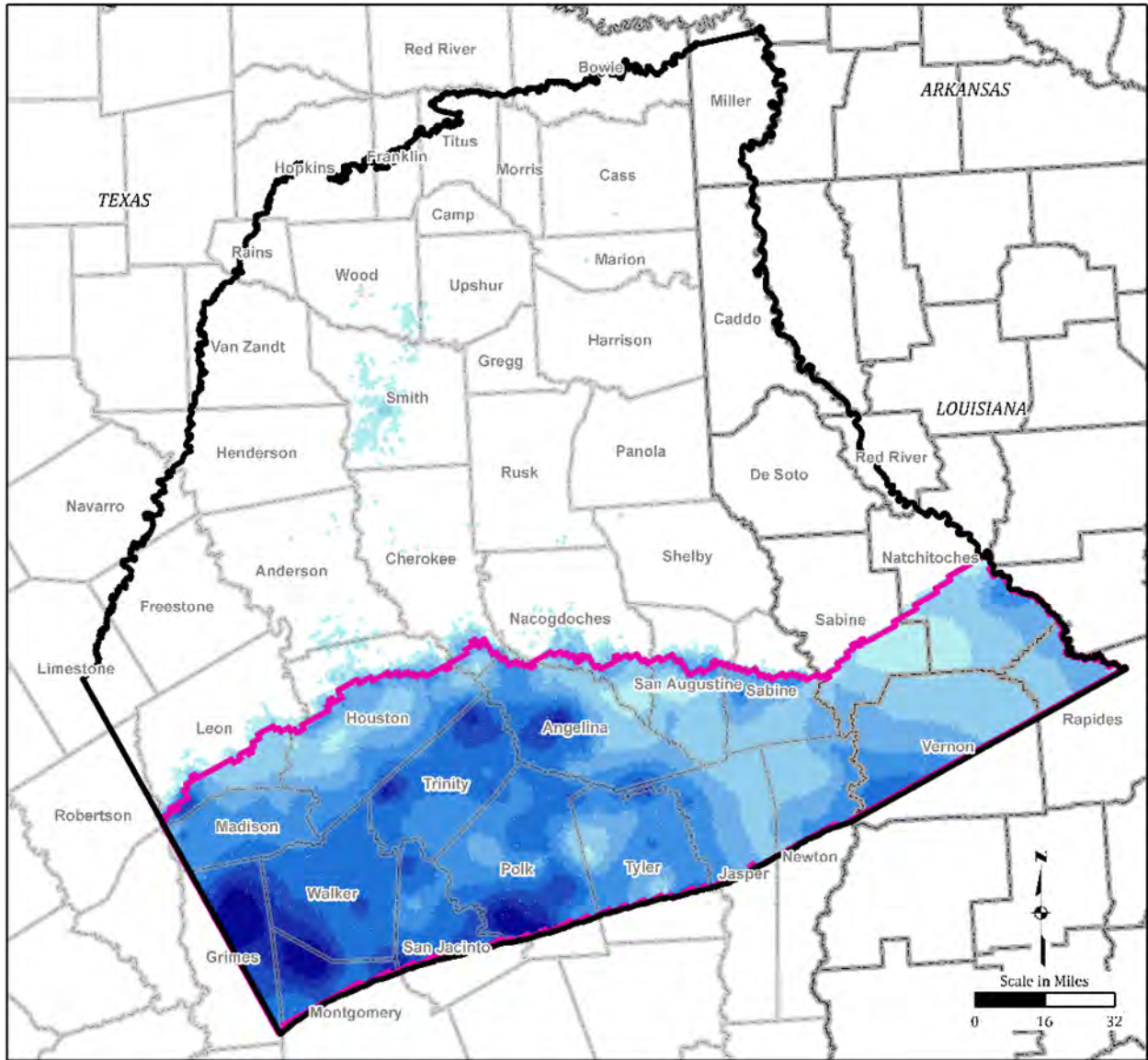


Figure 2.4-6. Modeled Bottom Elevation for Sparta Aquifer (Model Layer 2)



LEGEND	
Thickness (feet)	
	10 to 100
	100 to 200
	200 to 300
	300 to 400
	400 to 500
	500 to 600
	600 to 700
	700 to 915

	Model
	County or Parish Boundary
	Extent of General Head Boundary

- Notes:**
1. The general head boundary in Layer 2 represents the Younger Units.
 2. The layer contains discontinuous outcrops, consistent with the conceptual model (Section 2).
 3. Projected Coordinate System Datum: GAM.

Figure 2.4-7. Modeled Thickness for Sparta Aquifer (Model Layer 2)

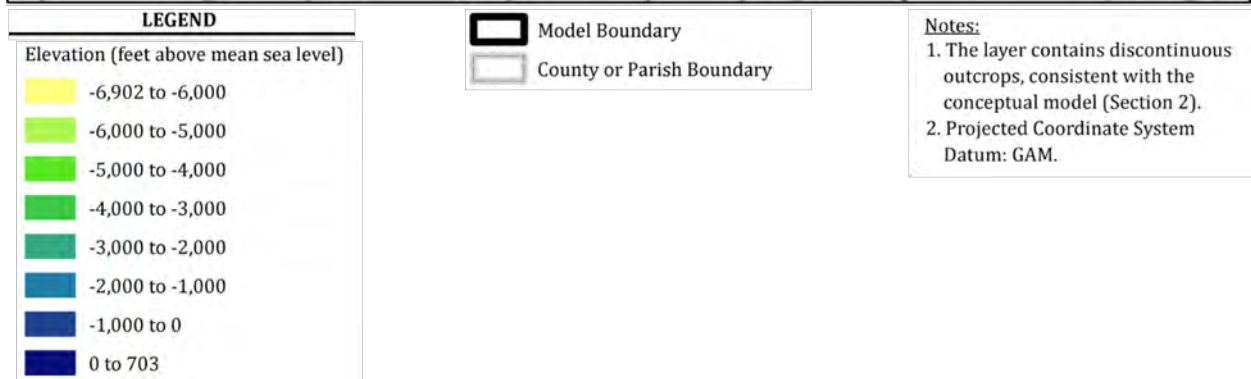
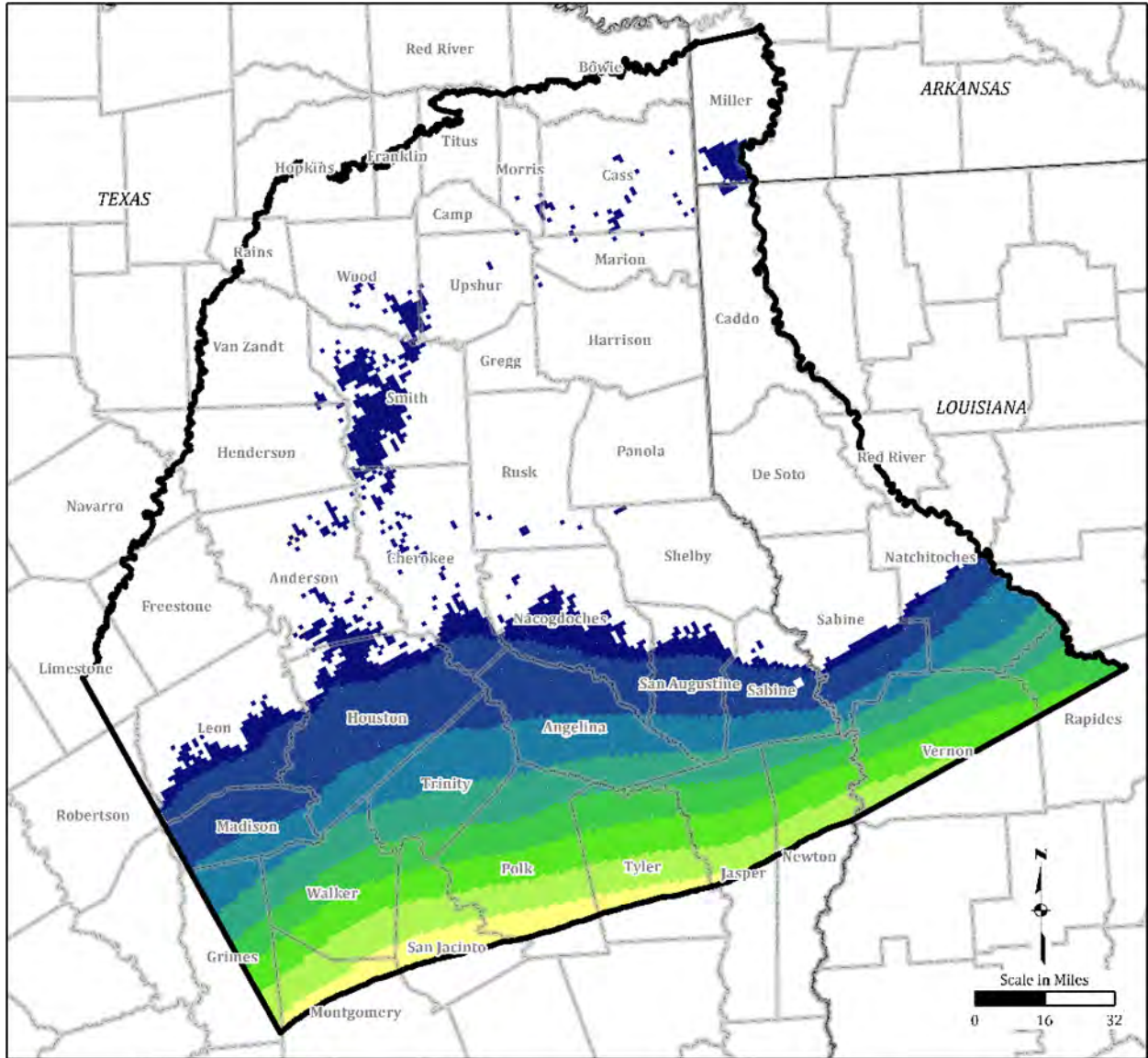
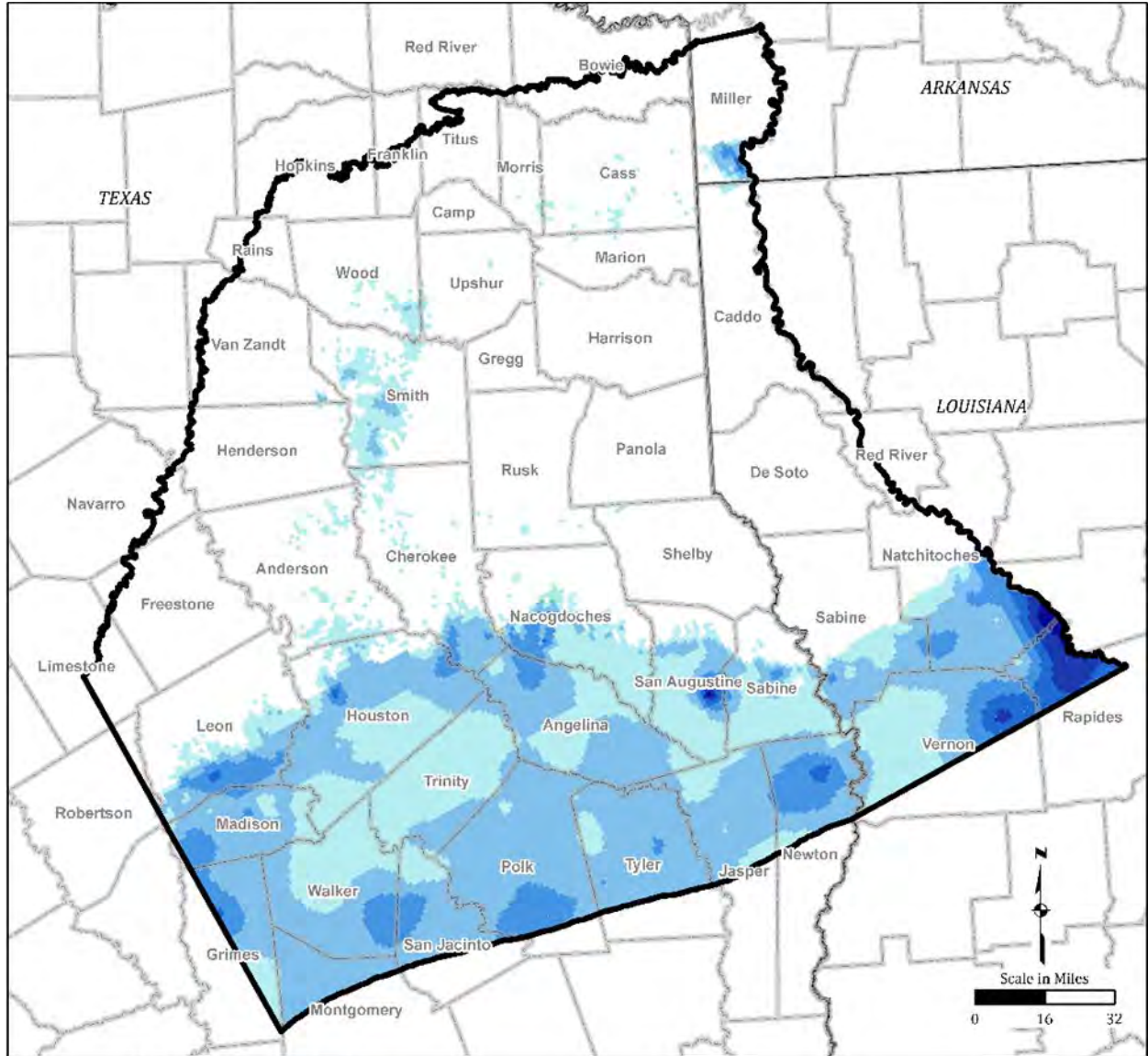


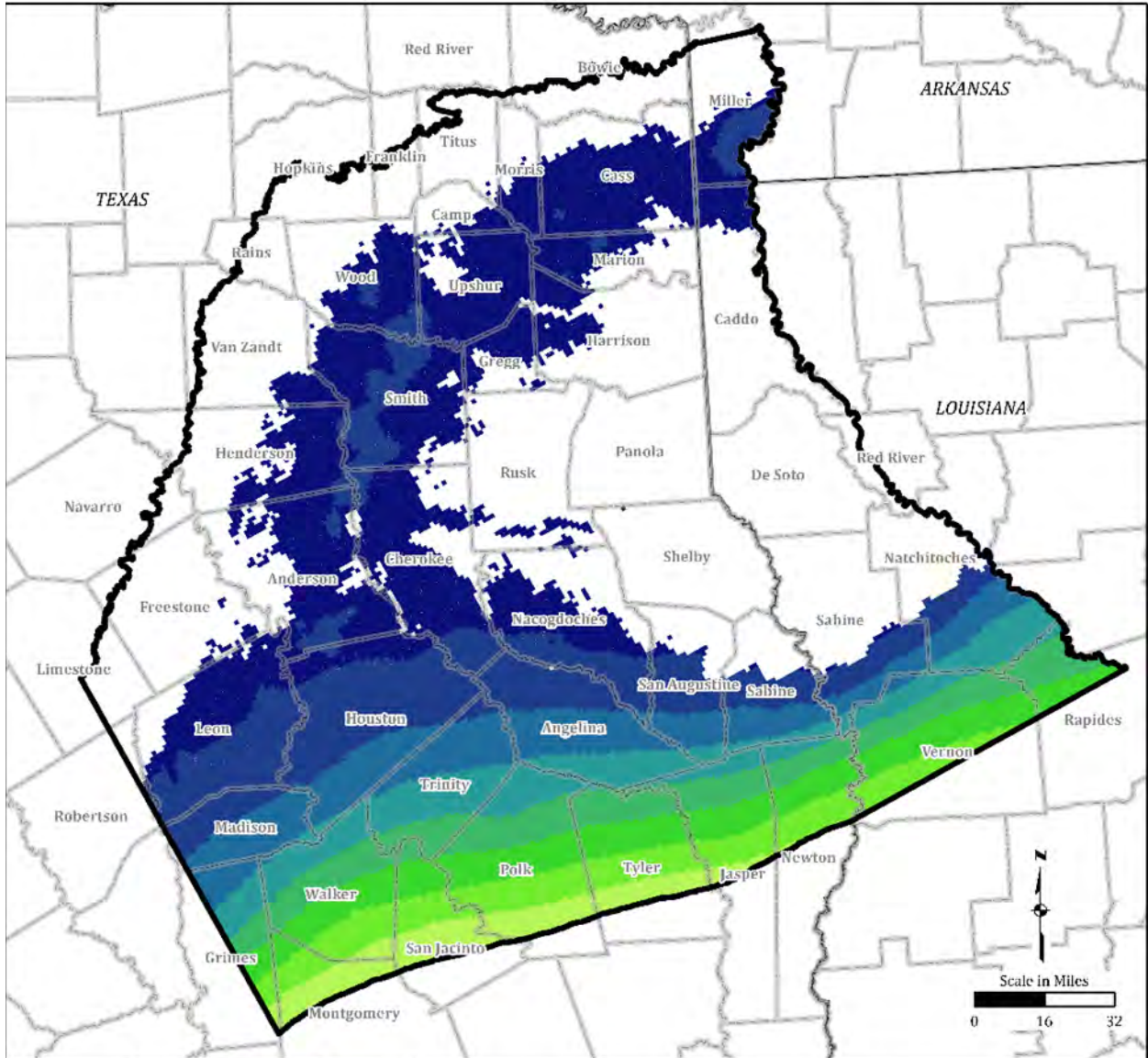
Figure 2.4-8. Modeled Bottom Elevation for Weches Formation (Model Layer 3)



LEGEND	
	Model Boundary
	County or Parish Boundary
Thickness (feet)	
	10 to 100
	100 to 200
	200 to 300
	300 to 400
	400 to 500
	500 to 559

Notes:
 1. The layer contains discontinuous outcrops, consistent with the conceptual model (Section 2).
 2. Projected Coordinate System Datum: GAM.

Figure 2.4-9. Modeled Thickness for Weches Formation (Model Layer 3)



LEGEND	
Elevation (feet above mean sea level)	
	-7,062 to -7,000
	-7,000 to -6,000
	-6,000 to -5,000
	-5,000 to -4,000
	-4,000 to -3,000
	-3,000 to -2,000
	-2,000 to -1,000
	-1,000 to 0
	0 to 517

	Model Boundary
	County or Parish Boundary

- Notes:**
1. The layer contains discontinuous outcrops, consistent with the conceptual model (Section 2).
 2. Projected Coordinate System Datum: GAM.

Figure 2.4-10. Modeled Bottom Elevation for Queen City Aquifer (Model Layer 4)

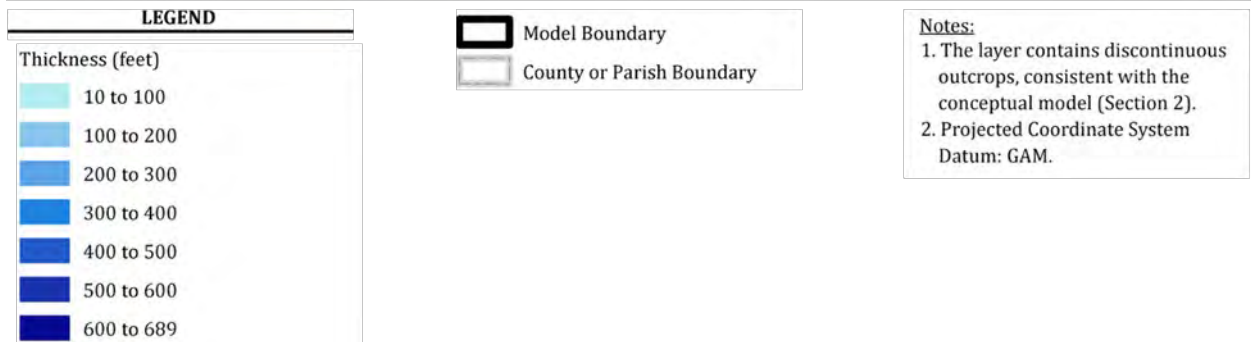
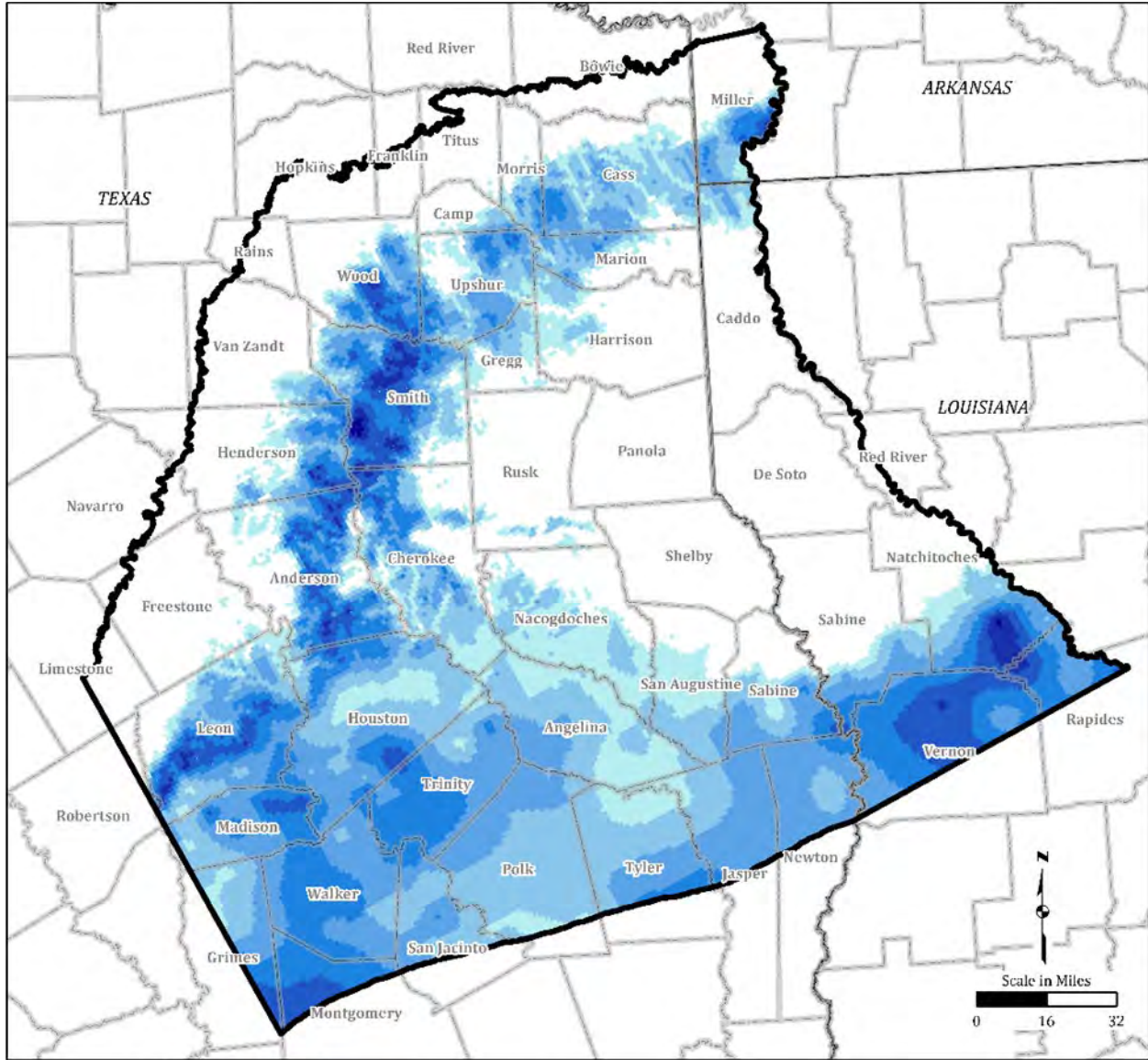


Figure 2.4-11. Modeled Thickness for Queen City Aquifer (Model Layer 4)

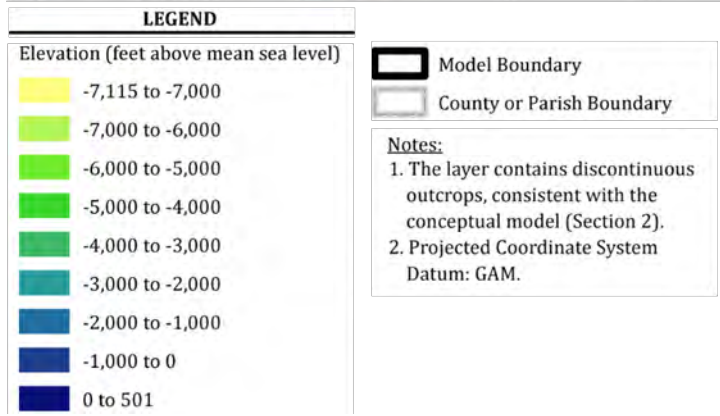
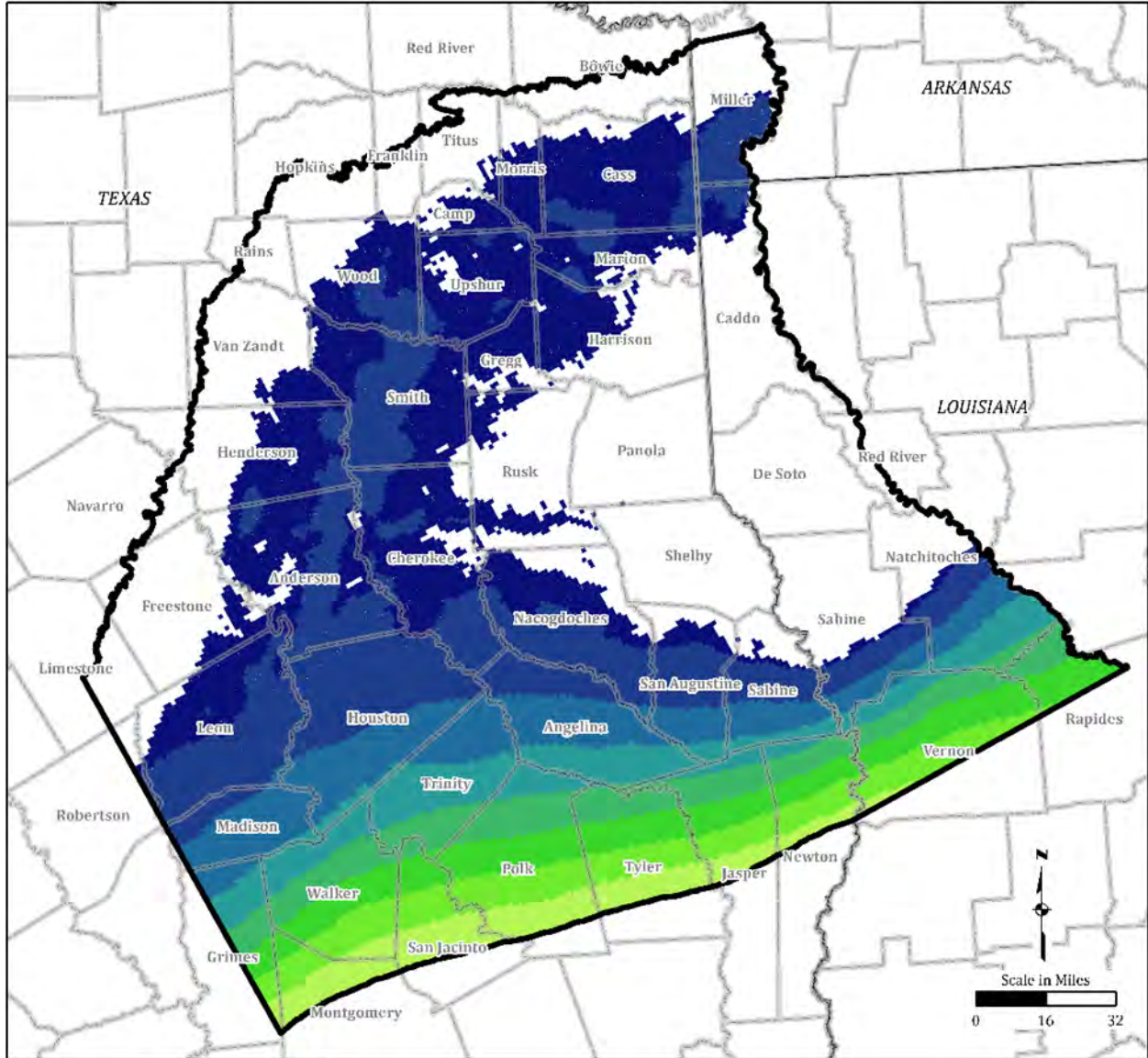


Figure 2.4-12. Modeled Bottom Elevation for Reklaw Formation (Model Layer 5)

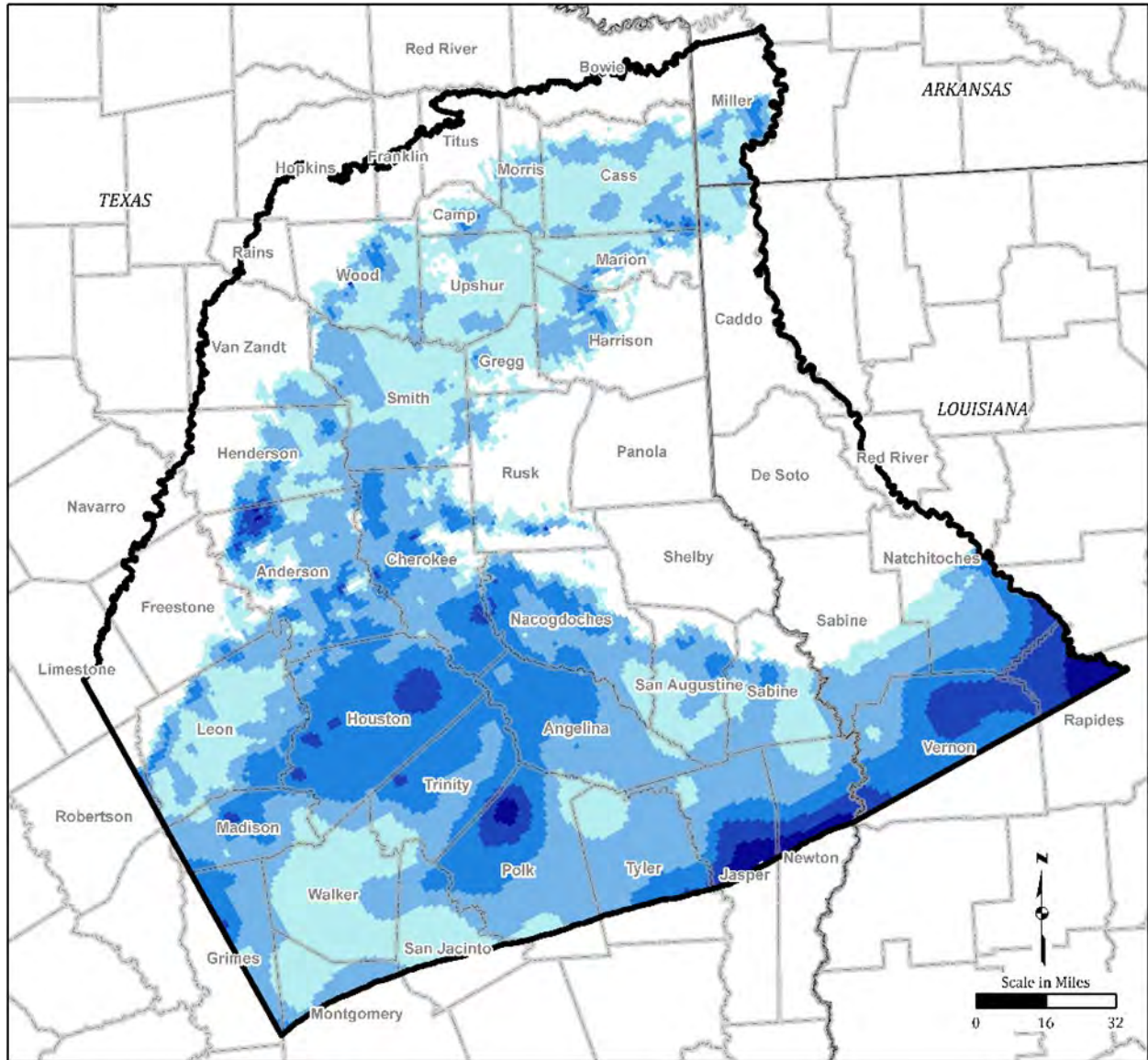
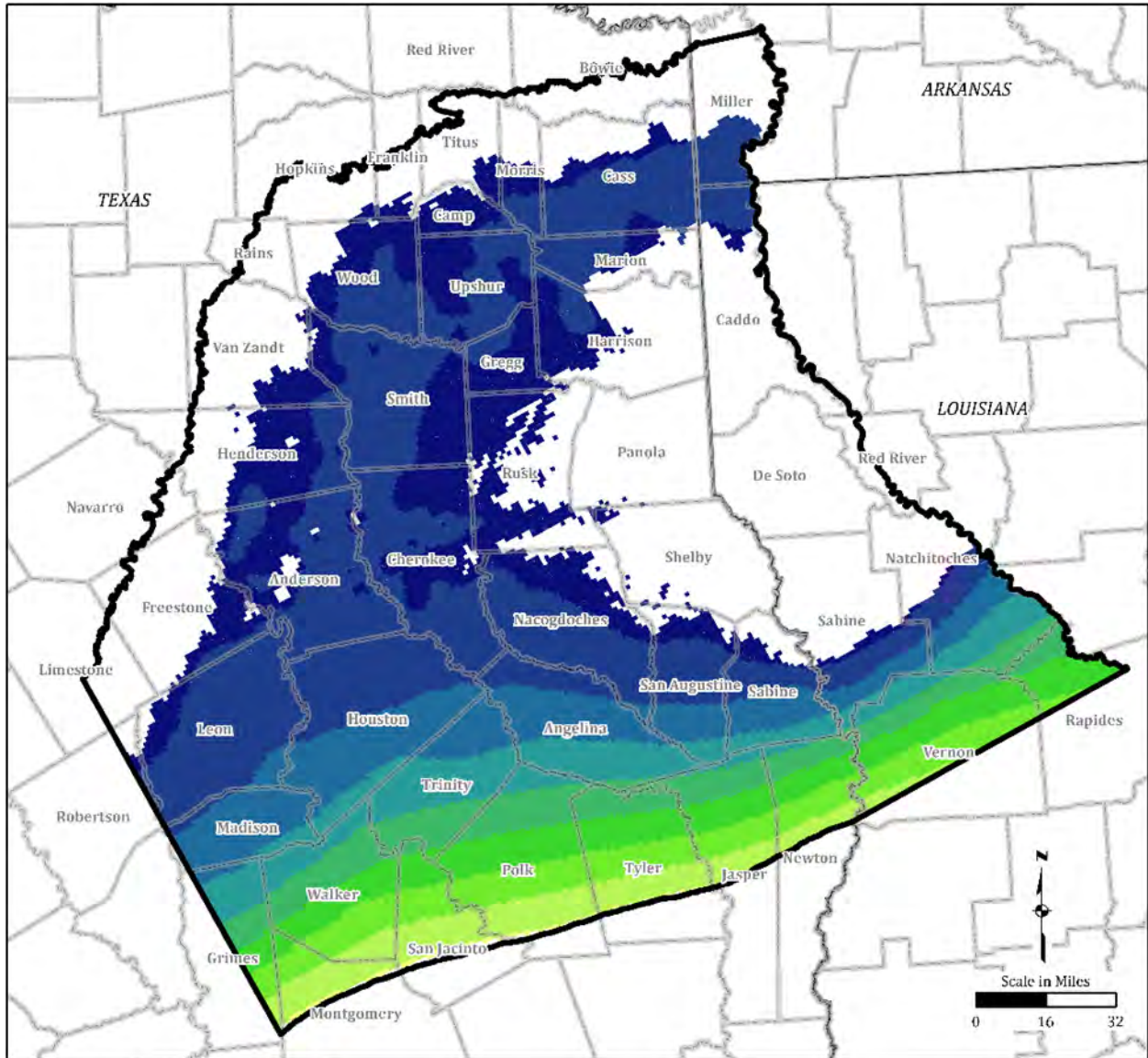


Figure 2.4-13. Modeled Thickness for Reklaw Formation (Model Layer 5)



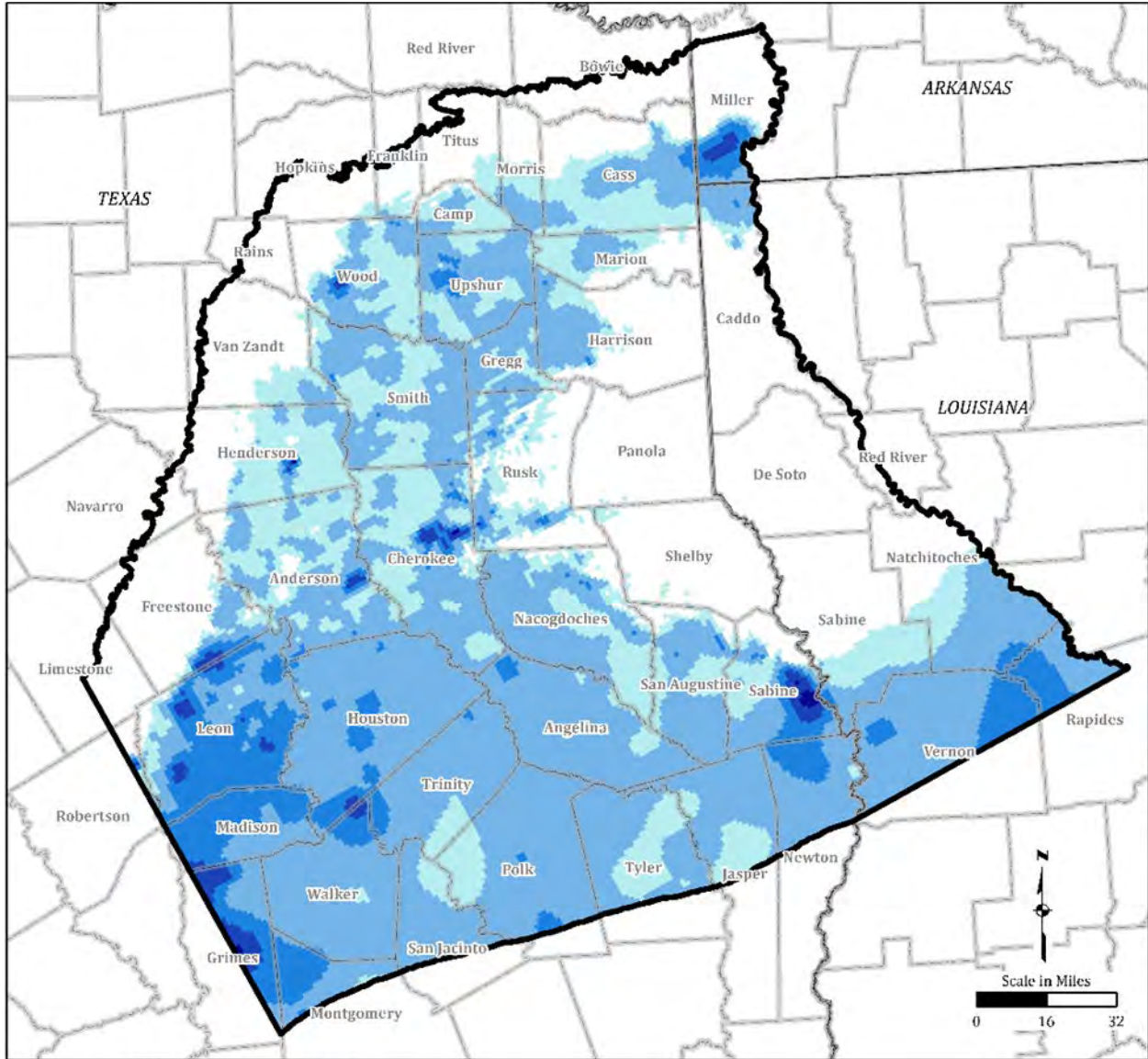
LEGEND

Elevation (feet above mean sea level)	
	-7,251 to -7,000
	-7,000 to -6,000
	-6,000 to -5,000
	-5,000 to -4,000
	-4,000 to -3,000
	-3,000 to -2,000
	-2,000 to -1,000
	-1,000 to 0
	0 to 571

	Model Boundary
	County or Parish Boundary

Notes:
 1. The layer contains discontinuous outcrops, consistent with the conceptual model (Section 2).
 2. Projected Coordinate System Datum: GAM.

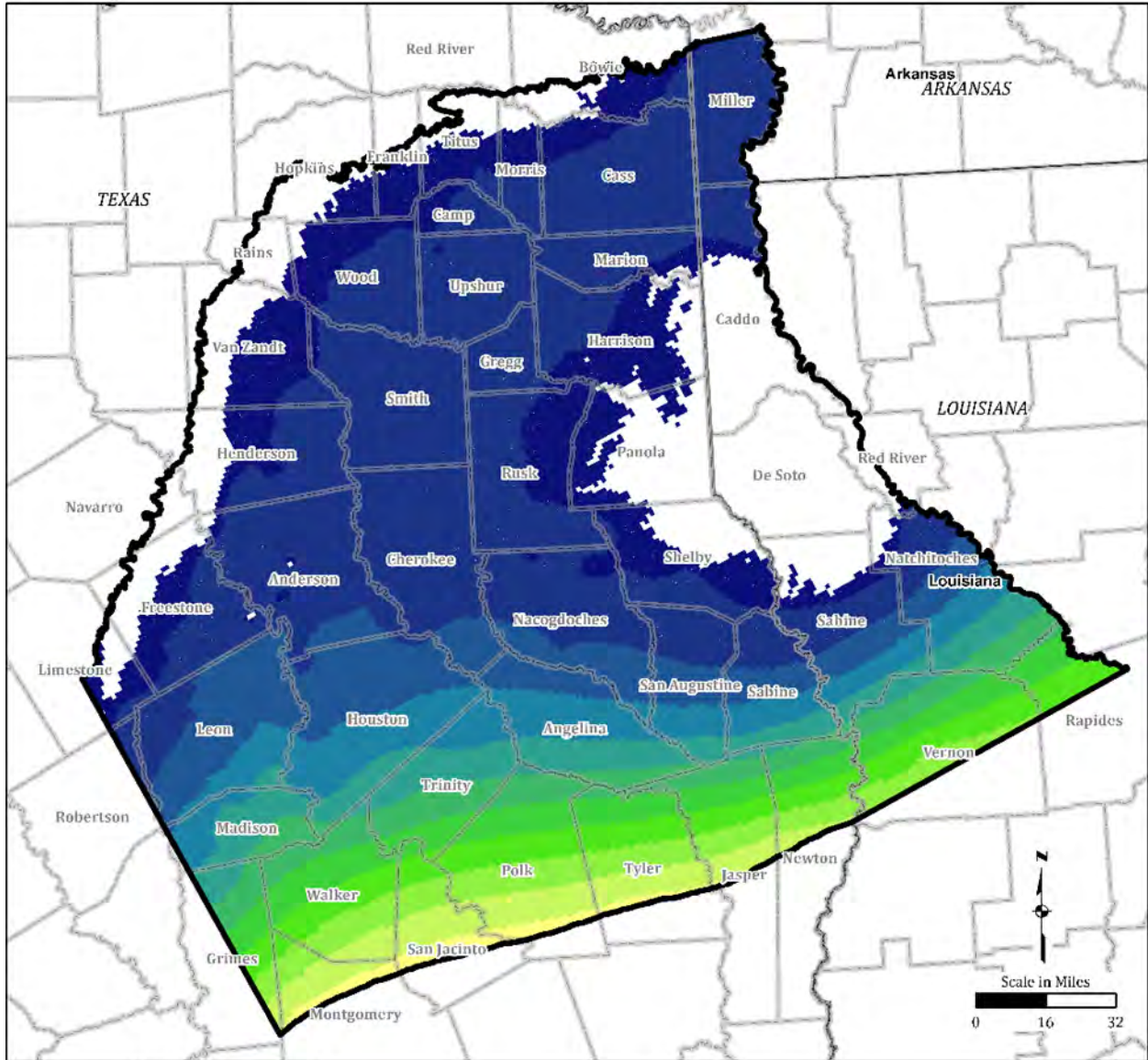
Figure 2.4-14. Modeled Bottom Elevation for Carrizo Aquifer (Model Layer 6)



LEGEND	
	Model Boundary
	County or Parish Boundary
Thickness (feet)	
	10 to 100
	100 to 200
	200 to 300
	300 to 400
	400 to 467

Notes:
 1. The layer contains discontinuous outcrops, consistent with the conceptual model (Section 2).
 2. Projected Coordinate System Datum: GAM.

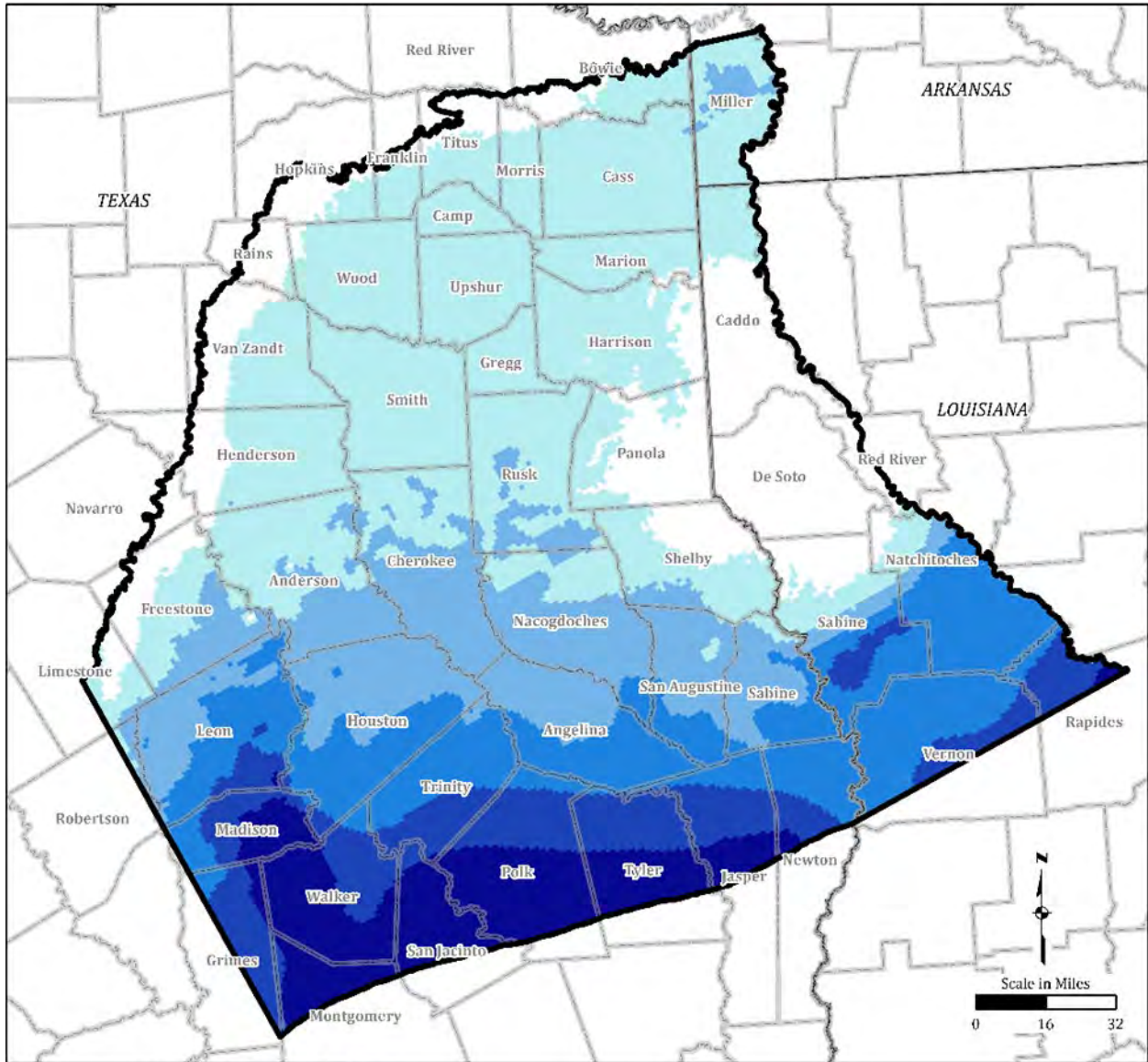
Figure 2.4-15. Modeled Thickness for Carrizo Aquifer (Model Layer 6)



LEGEND

Elevation (feet above mean sea level)		Notes:		
Yellow	-9,491 to -9,000	Light Blue	-3,000 to -2,000	1. The layer contains discontinuous outcrops, consistent with the conceptual model (Section 2). 2. Projected Coordinate System Datum: GAM.
Light Green	-9,000 to -8,000	Medium Blue	-2,000 to -1,000	
Green	-8,000 to -7,000	Dark Blue	-1,000 to 0	
Dark Green	-7,000 to -6,000	Very Dark Blue	0 to 546	
Lightest Green	-6,000 to -5,000	Thick Black Line	Model Boundary	
Medium Green	-5,000 to -4,000	Thin Grey Line	County or Parish Boundary	
Dark Green	-4,000 to -3,000			

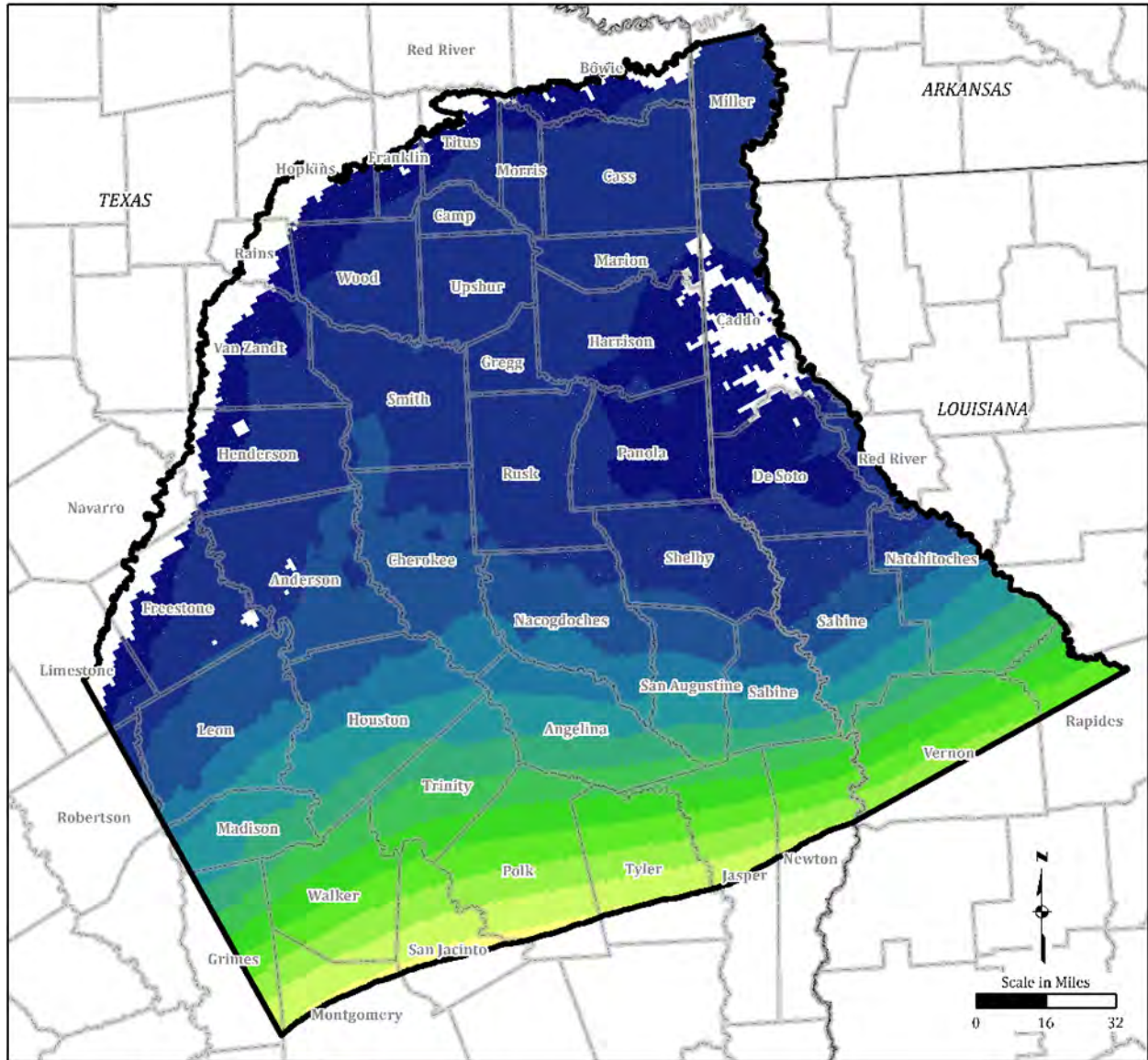
Figure 2.4-16. Modeled Bottom Elevation for Upper Wilcox (Model Layer 7)



LEGEND	
	Model Boundary
	County or Parish Boundary
Thickness (feet)	
	10 to 500
	500 to 1,000
	1,000 to 1,500
	1,500 to 2,000
	2,000 to 2,371

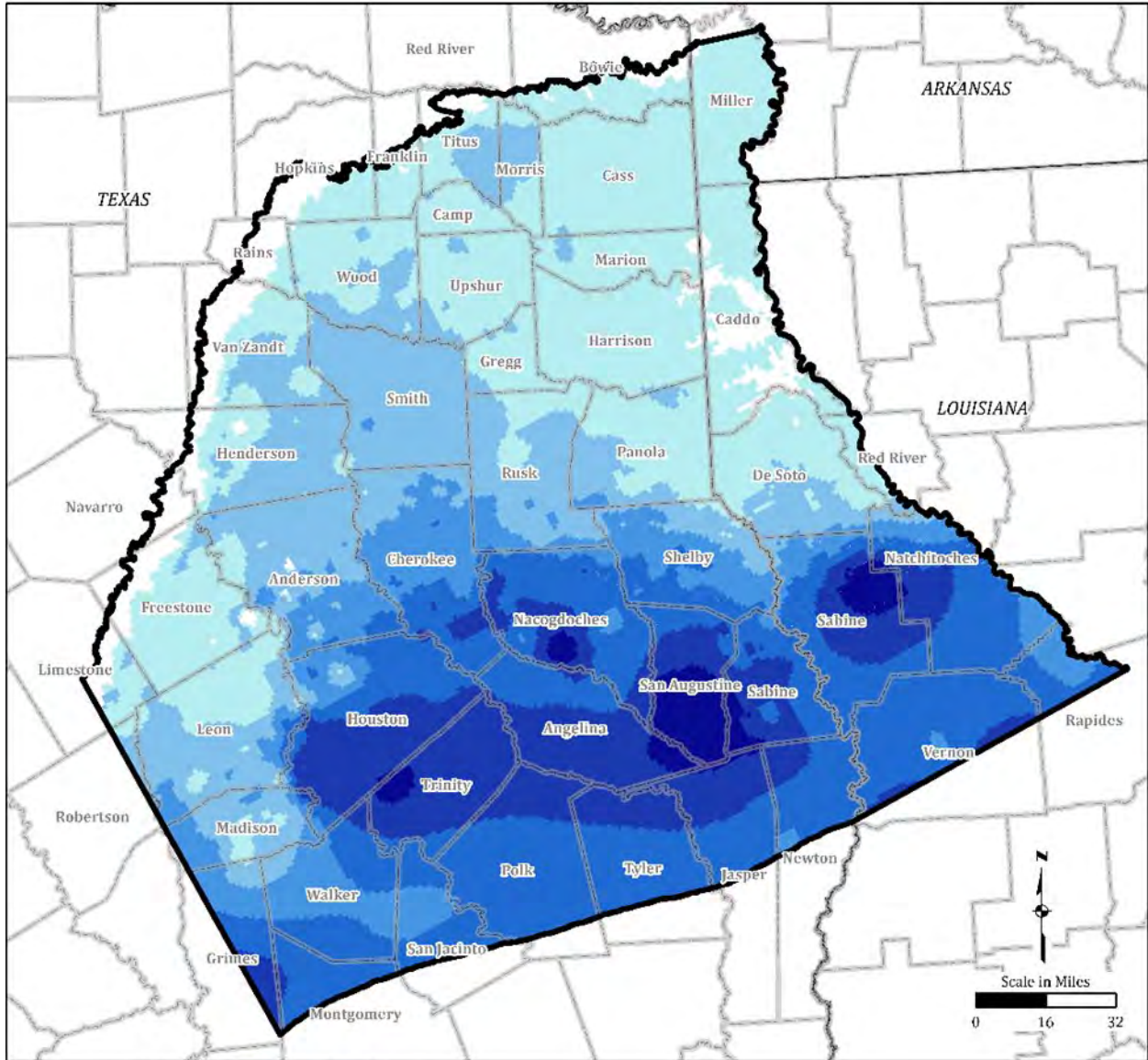
Notes:
 1. The layer contains discontinuous outcrops, consistent with the conceptual model (Section 2).
 2. Projected Coordinate System Datum: GAM.

Figure 2.4-17. Modeled Thickness for Upper Wilcox (Model Layer 7)



LEGEND		Notes:
	Model Boundary	
	County or Parish Boundary	
Elevation (feet above mean sea level)		1. The layer contains discontinuous outcrops, consistent with the conceptual model (Section 2). 2. Projected Coordinate System Datum: GAM.
	-10,406 to -10,000	
	-10,000 to -9,000	
	-9,000 to -8,000	
	-8,000 to -7,000	
	-7,000 to -6,000	
	-6,000 to -5,000	
	-5,000 to -4,000	
	-4,000 to -3,000	
	-3,000 to -2,000	
	-2,000 to -1,000	
	-1,000 to 0	
	0 to 512	

Figure 2.4-18. Modeled Bottom Elevation for Middle Wilcox (Model Layer 8)



LEGEND	
	Model Boundary
	County or Parish Boundary
Thickness (feet)	
	10 to 250
	250 to 500
	500 to 750
	750 to 1,000
	1,000 to 1,250
	1,250 to 1,558

Notes:
 1. The layer contains discontinuous outcrops, consistent with the conceptual model (Section 2).
 2. Projected Coordinate System Datum: GAM.

Figure 2.4-19. Modeled Thickness for Middle Wilcox (Model Layer 8)

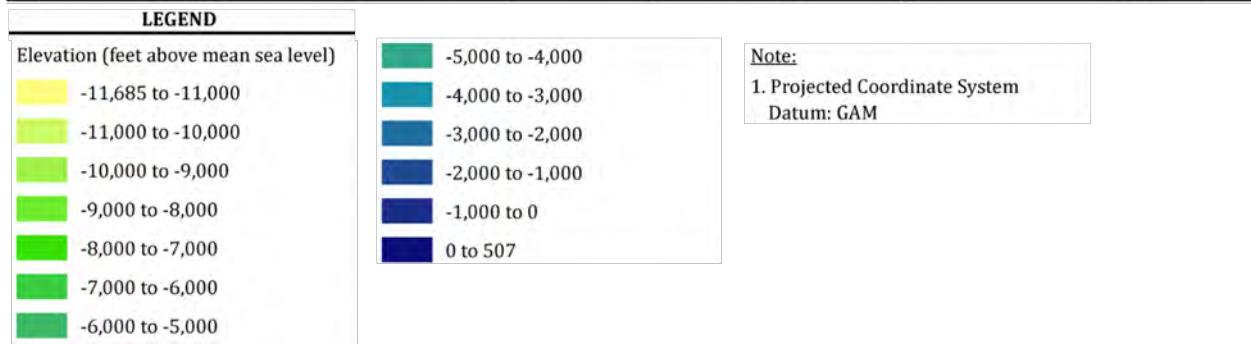
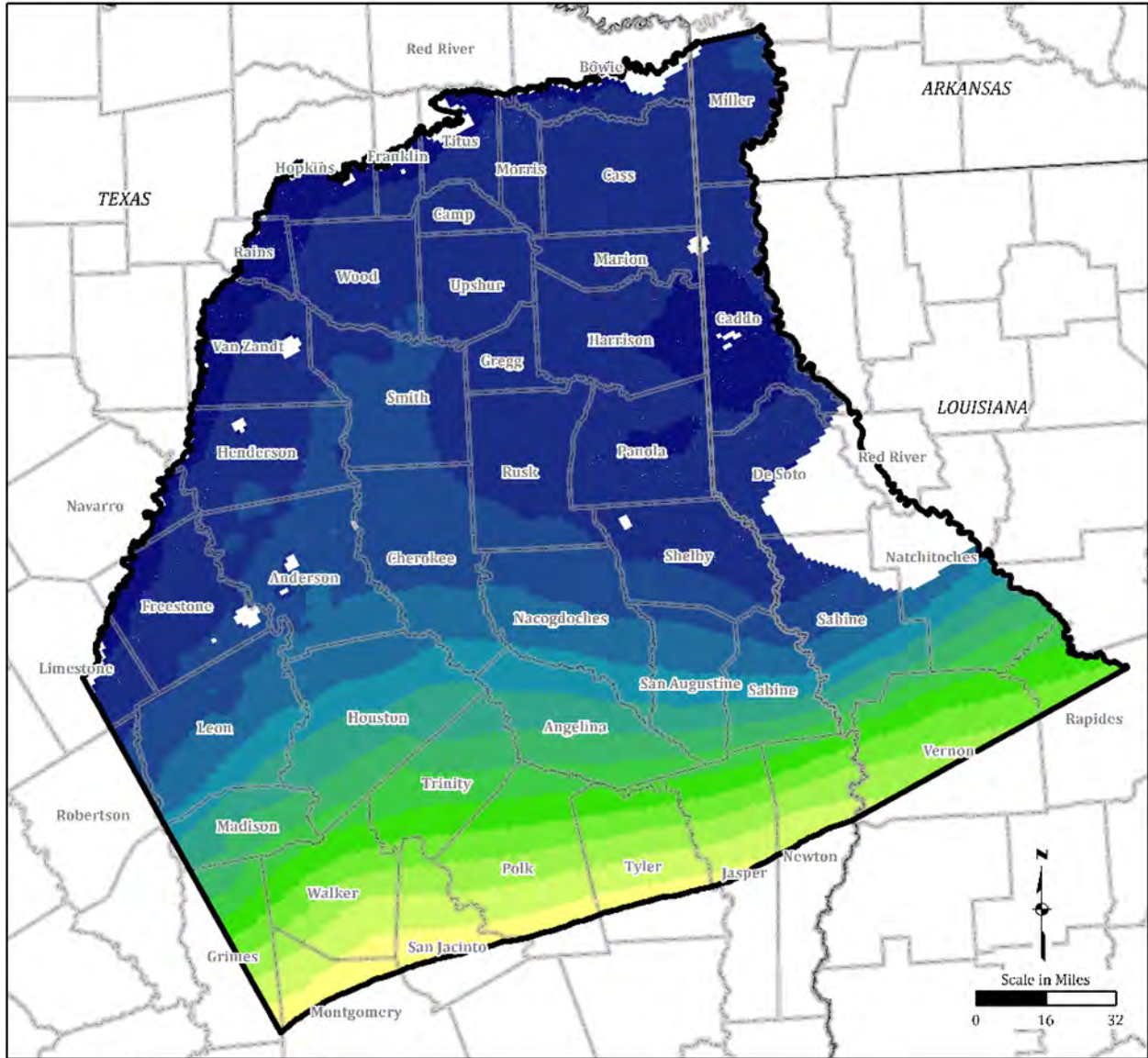
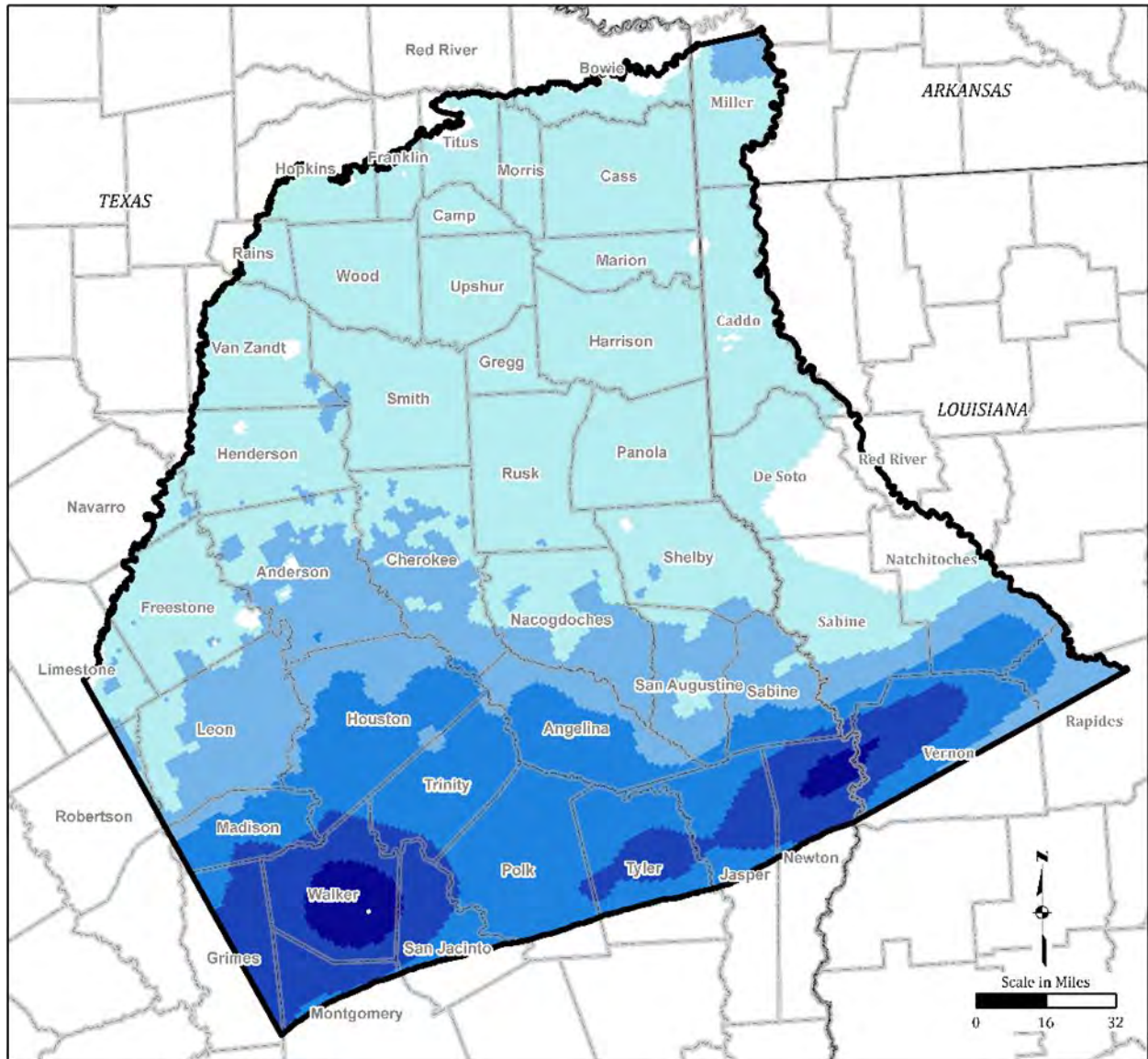


Figure 2.4-20. Modeled Bottom Elevation for Lower Wilcox (Model Layer 9)



LEGEND

- Model Boundary
- County or Parish Boundary

Thickness (feet)

- 10 to 500
- 500 to 1,000
- 1,000 to 1,500
- 1,500 to 2,000
- 2,000 to 2,501

Note:
 1. Projected Coordinate System
 Datum: GAM

Figure 2.4-21. Modeled Thickness for Lower Wilcox (Model Layer 9)

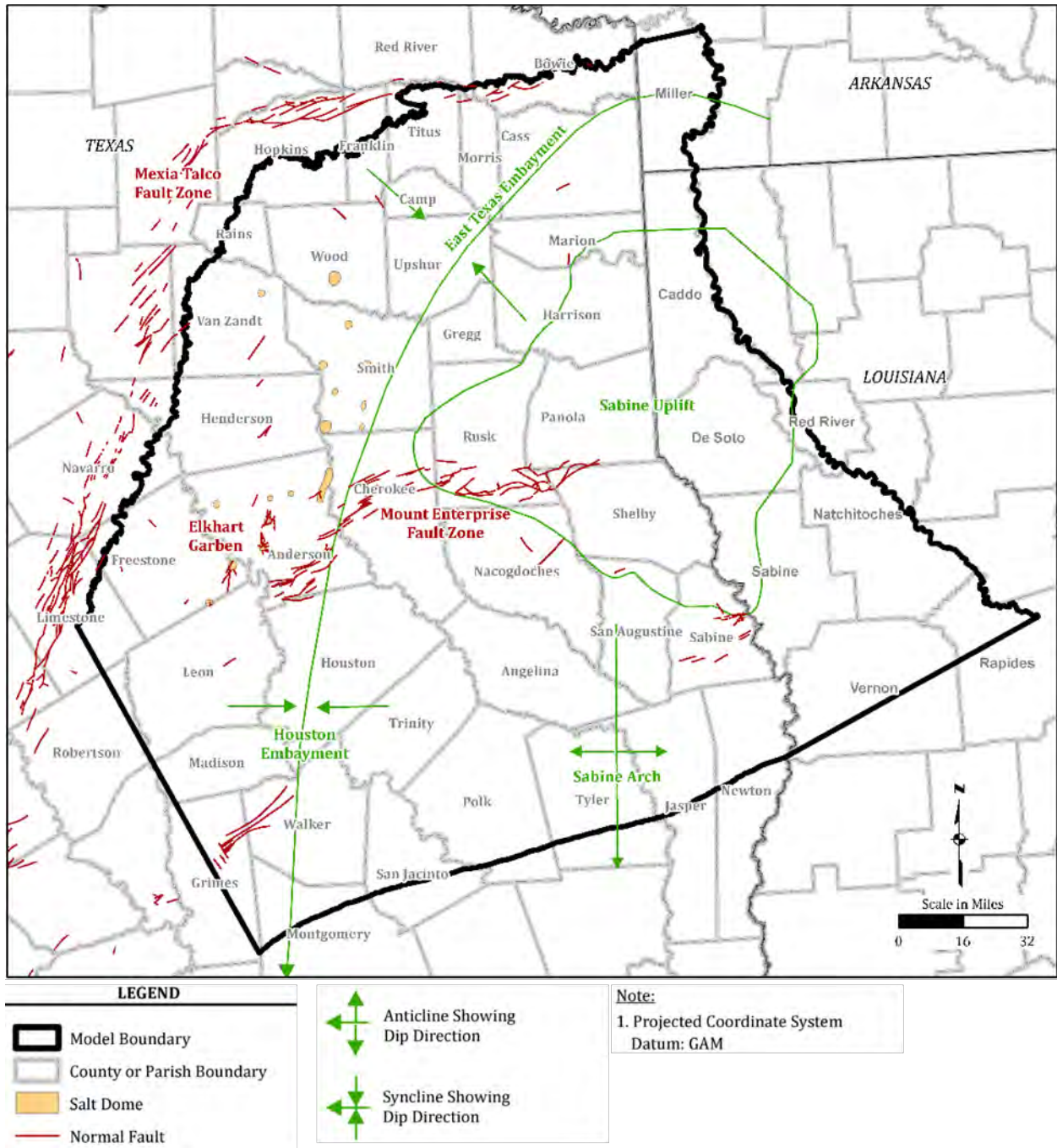
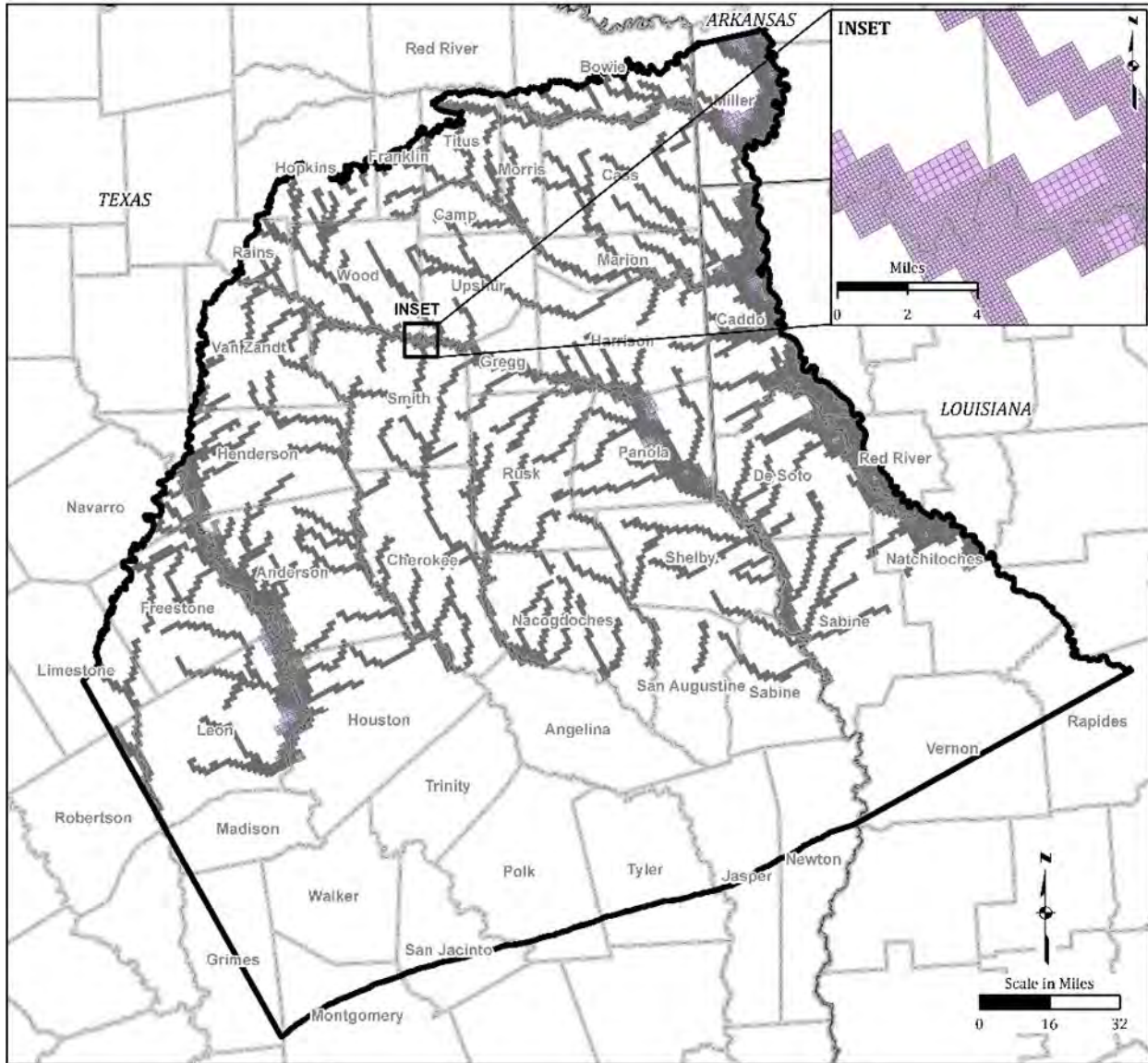





Figure 2.4-22. General Structural Setting



LEGEND

-  Model Boundary
-  County or Parish Boundary
-  Model Layer 1 Cells

Note:
 1. Projected Coordinate System
 Datum: GAM

Figure 2.4-23. Groundwater Model Domain Discretization for Quaternary Alluvium (Model Layer 1)

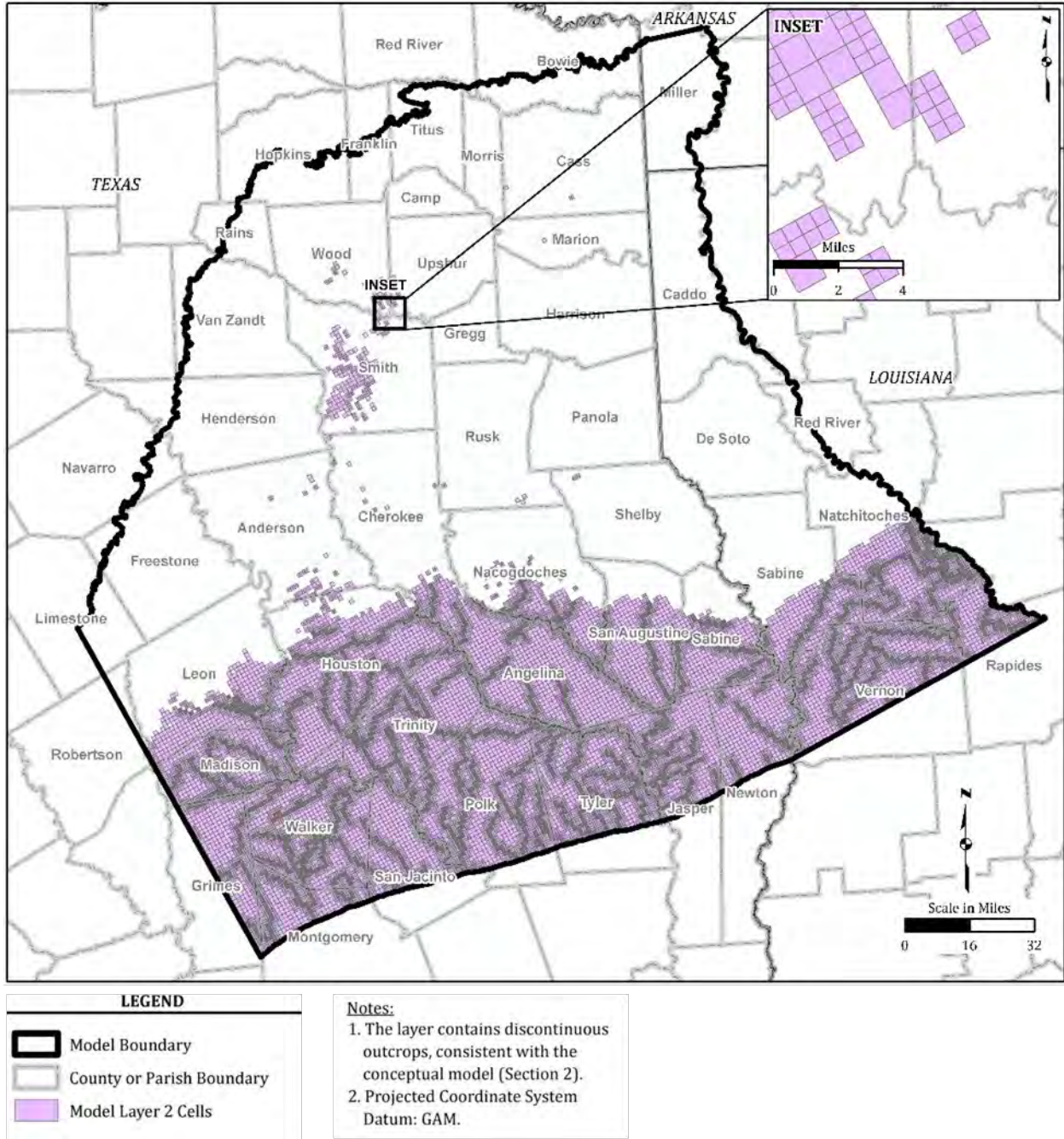


Figure 2.4-24. Groundwater Model Domain Discretization for Sparta Aquifer (Model Layer 2)

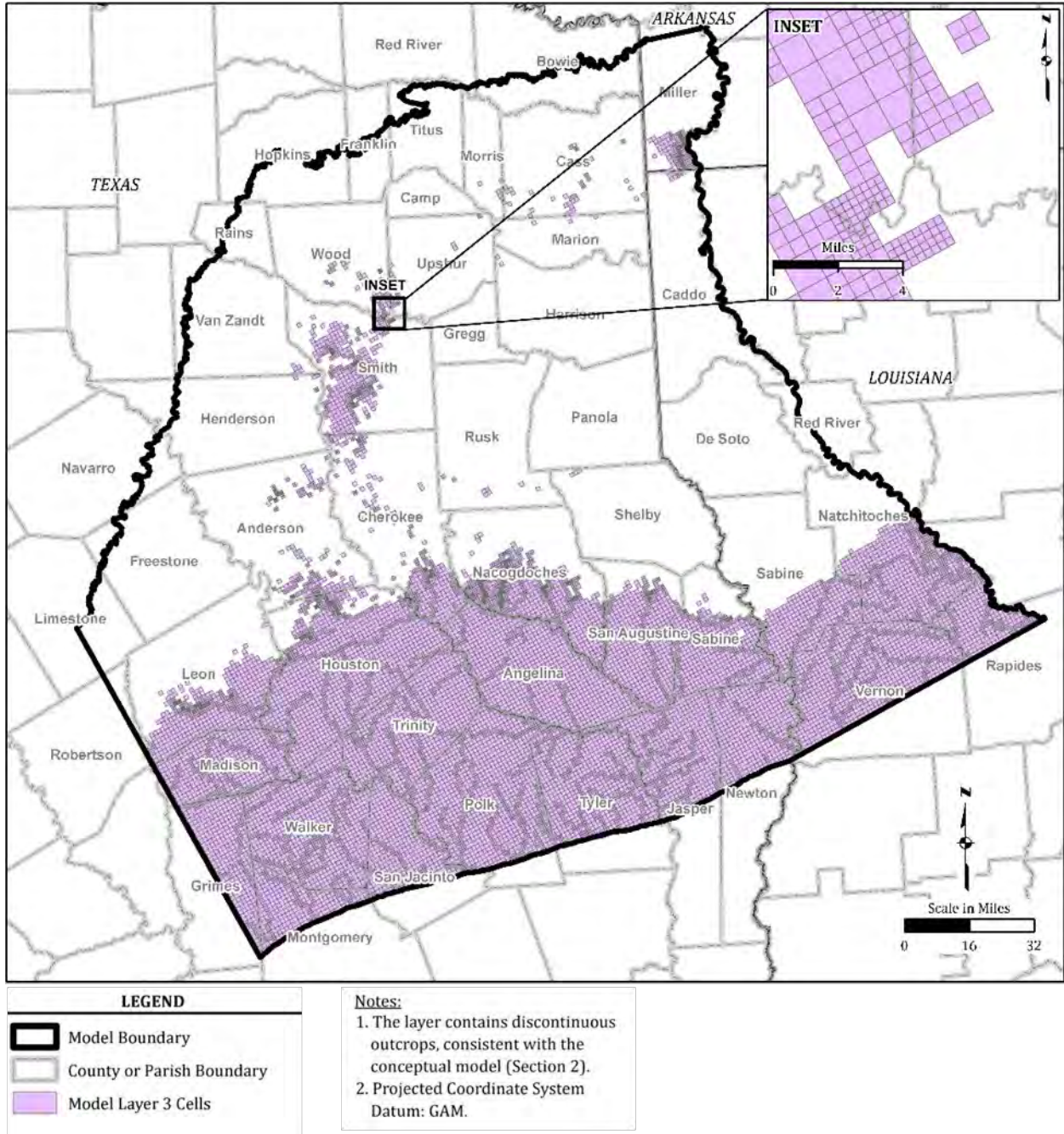


Figure 2.4-25. Groundwater Model Domain Discretization for Weches Formation (Model Layer 3)

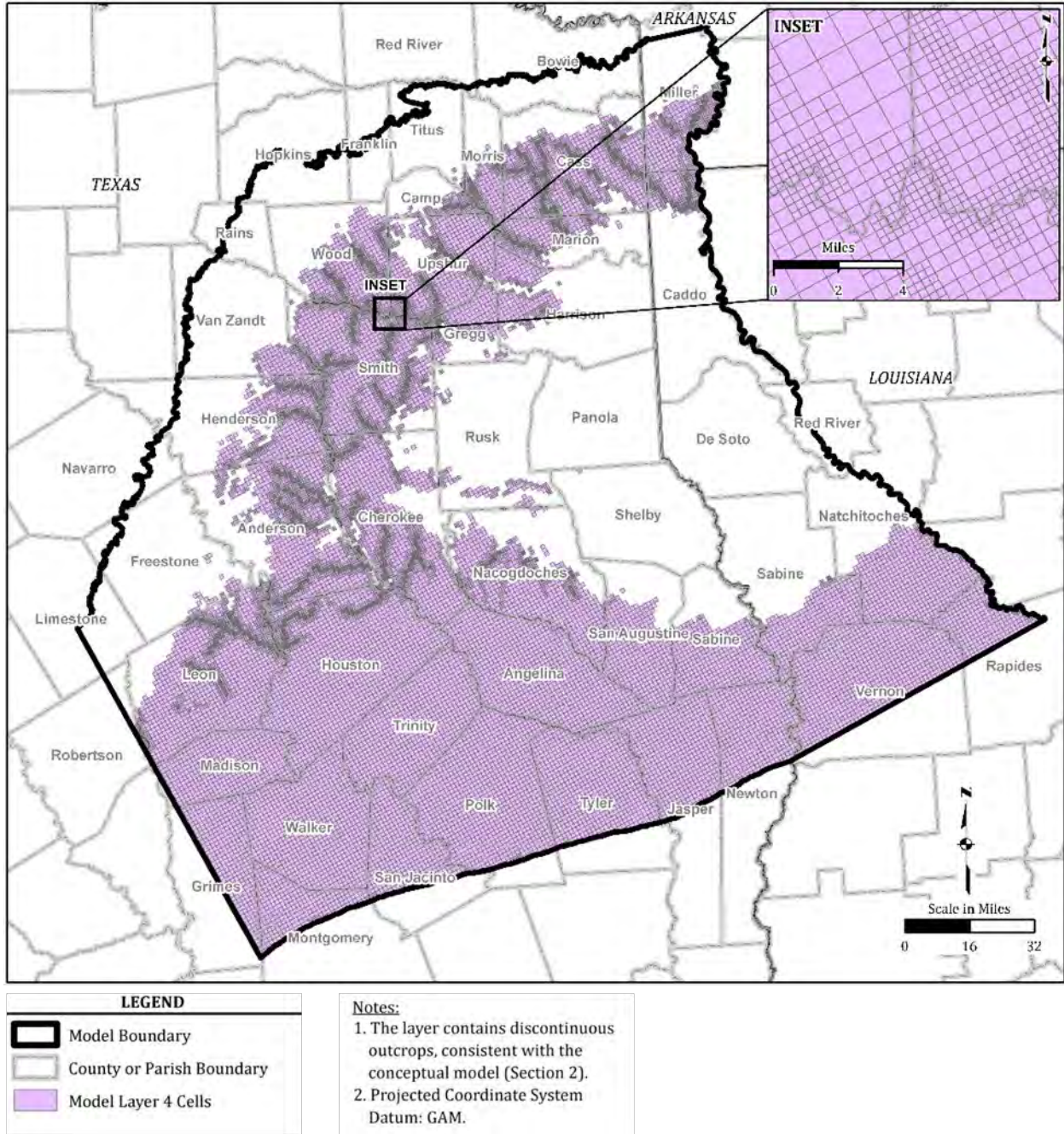


Figure 2.4-26. Groundwater Model Domain Discretization for Queen City Aquifer (Model Layer 4)

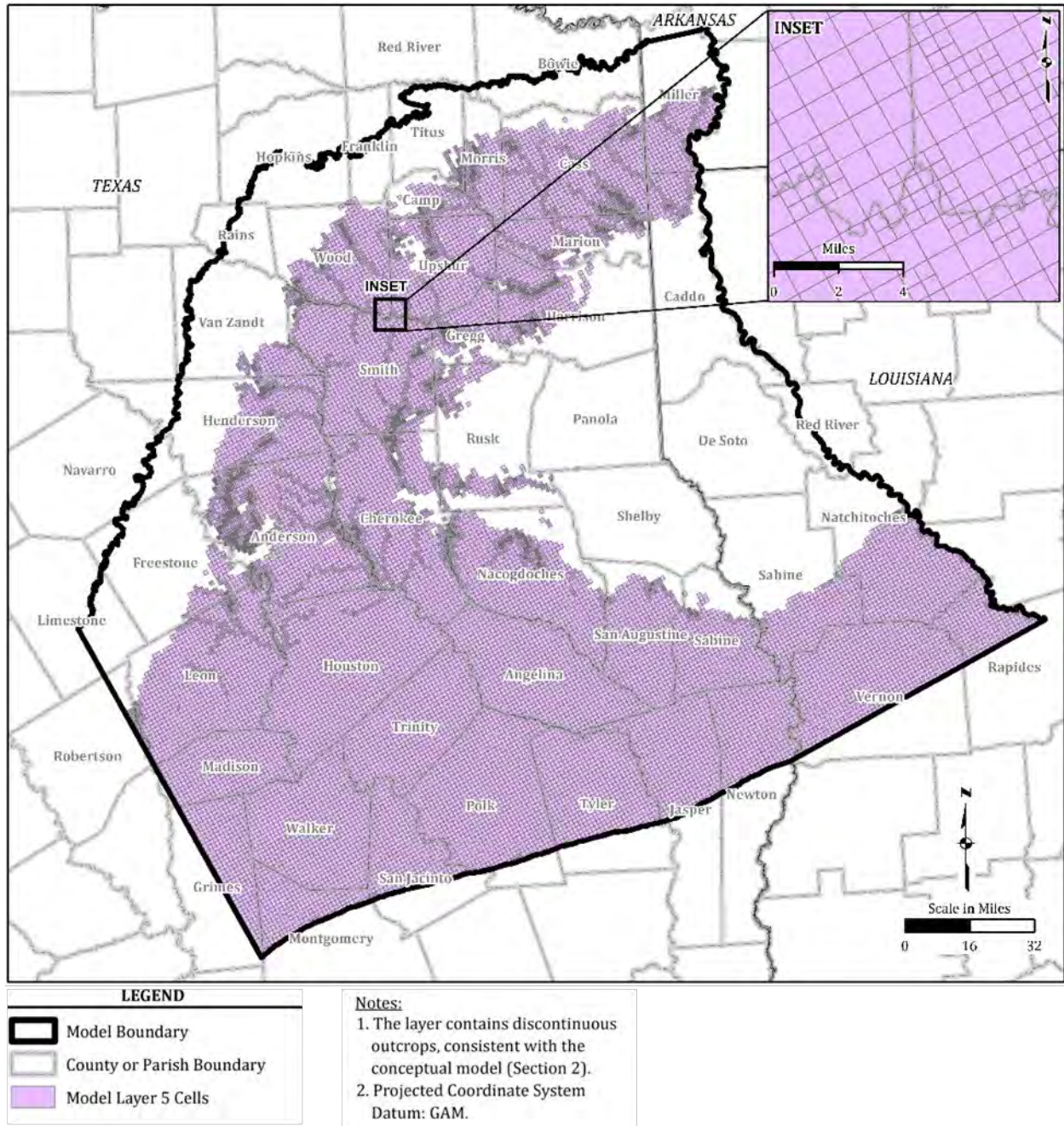


Figure 2.4-27. Groundwater Model Domain Discretization for Reklaw Formation (Model Layer 5)

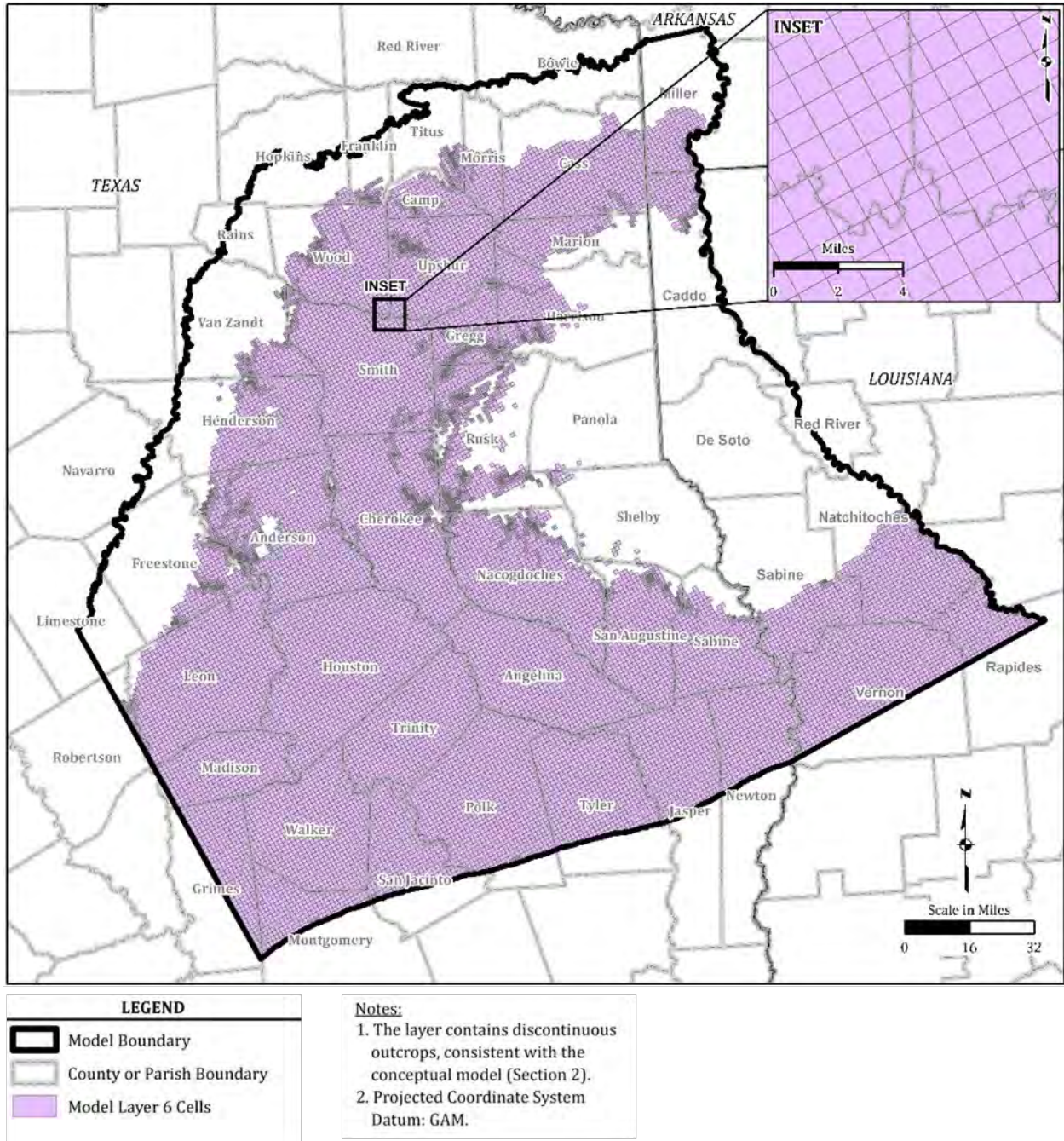


Figure 2.4-28. Groundwater Model Domain Discretization for Carrizo Aquifer (Model Layer 6)

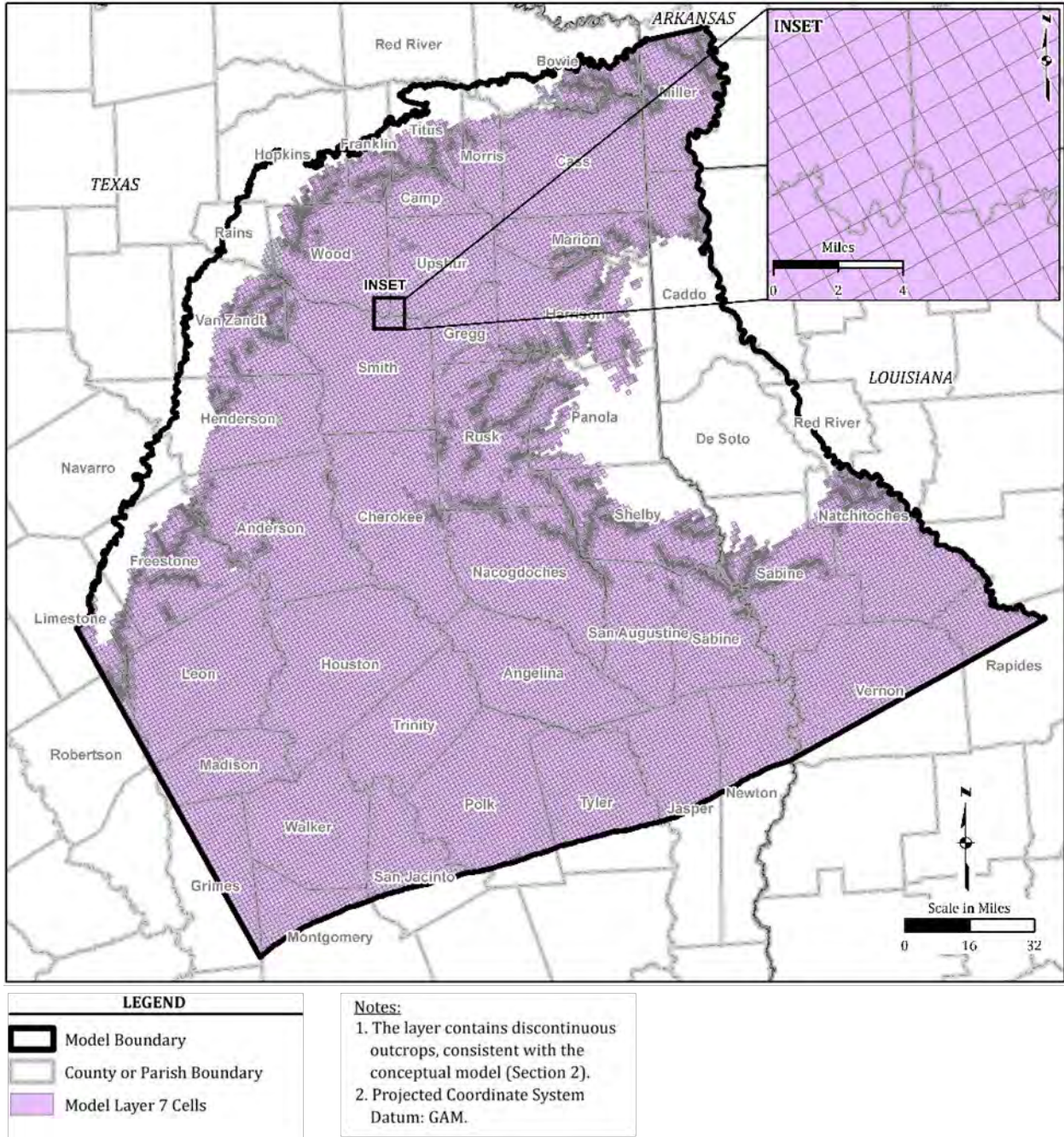


Figure 2.4-29. Groundwater Model Domain Discretization for Upper Wilcox (Model Layer 7)

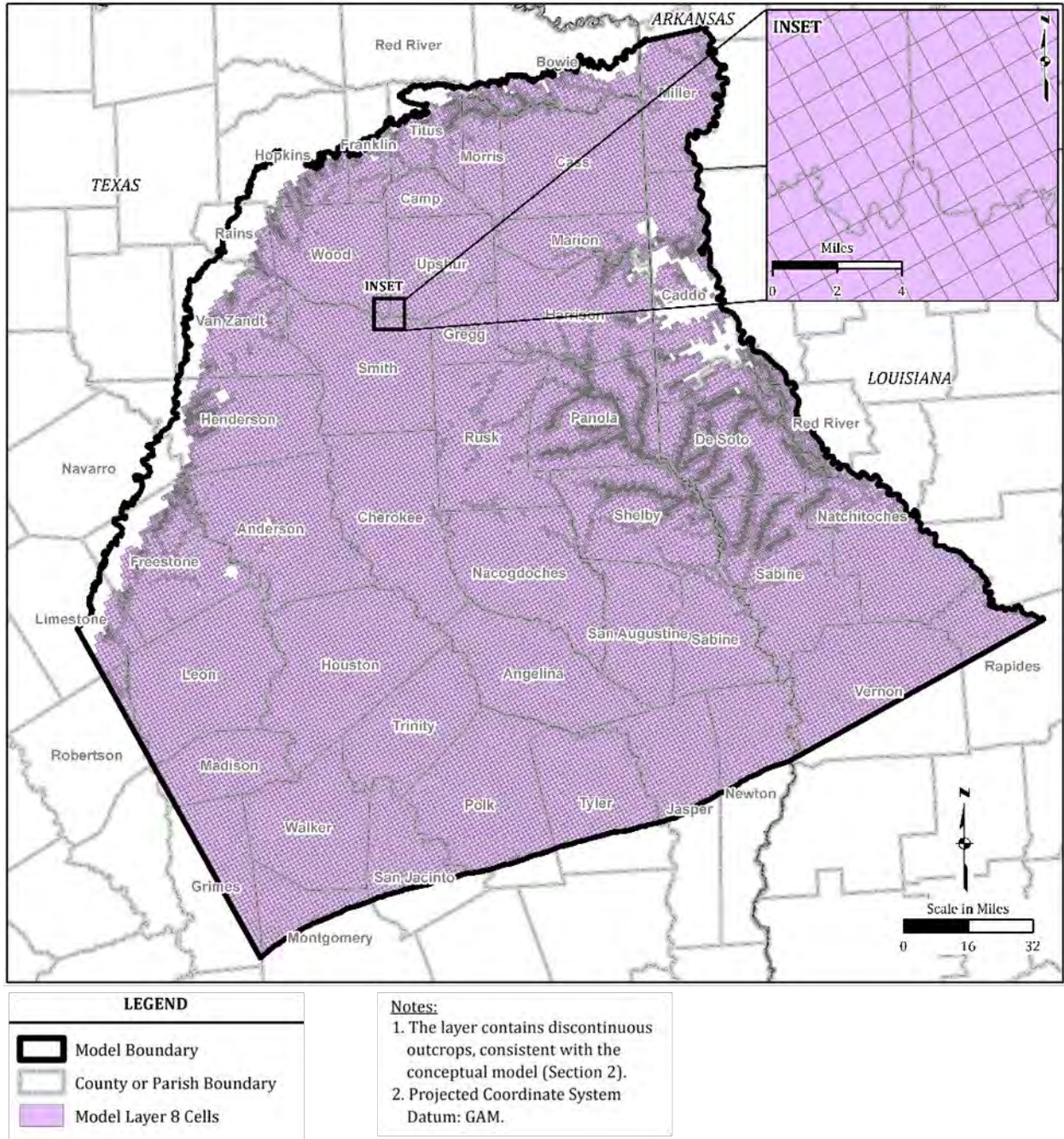
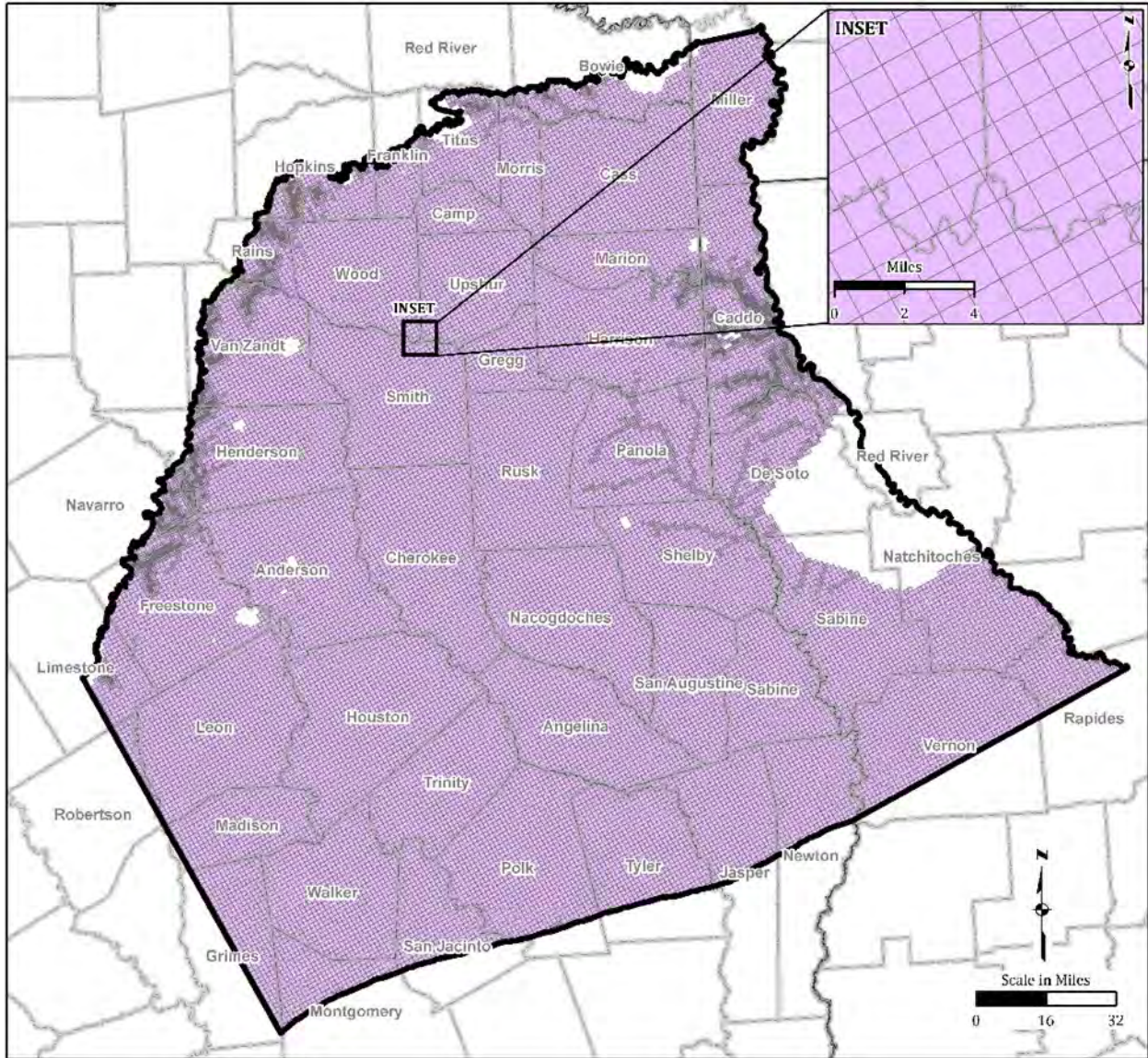





Figure 2.4-30. Groundwater Model Domain Discretization for Middle Wilcox (Model Layer 8)



LEGEND

-  Model Boundary
-  County or Parish Boundary
-  Model Layer 9 Cells

Note:

1. Projected Coordinate System
Datum: GAM

Figure 2.4-31. Groundwater Model Domain Discretization for Lower Wilcox (Model Layer 9)

The grid coarsens for deeper layers, with a coarsening of one level for every active layer found beneath the alluvium cells. Layer cells were eliminated where the geologic layer pinches out or where the geologic layer is absent and the underlying layer outcrops to the surface, as shown on Figures 2.4-23 through 2.4-31. The model grid consists of 637,536 cells. As discussed above, discontinuous sections of geologic units, as described in the Conceptual Model Report, are simulated in the model. These cells are not isolated but connected to cells vertically and may be connected to cells in layers above or below.

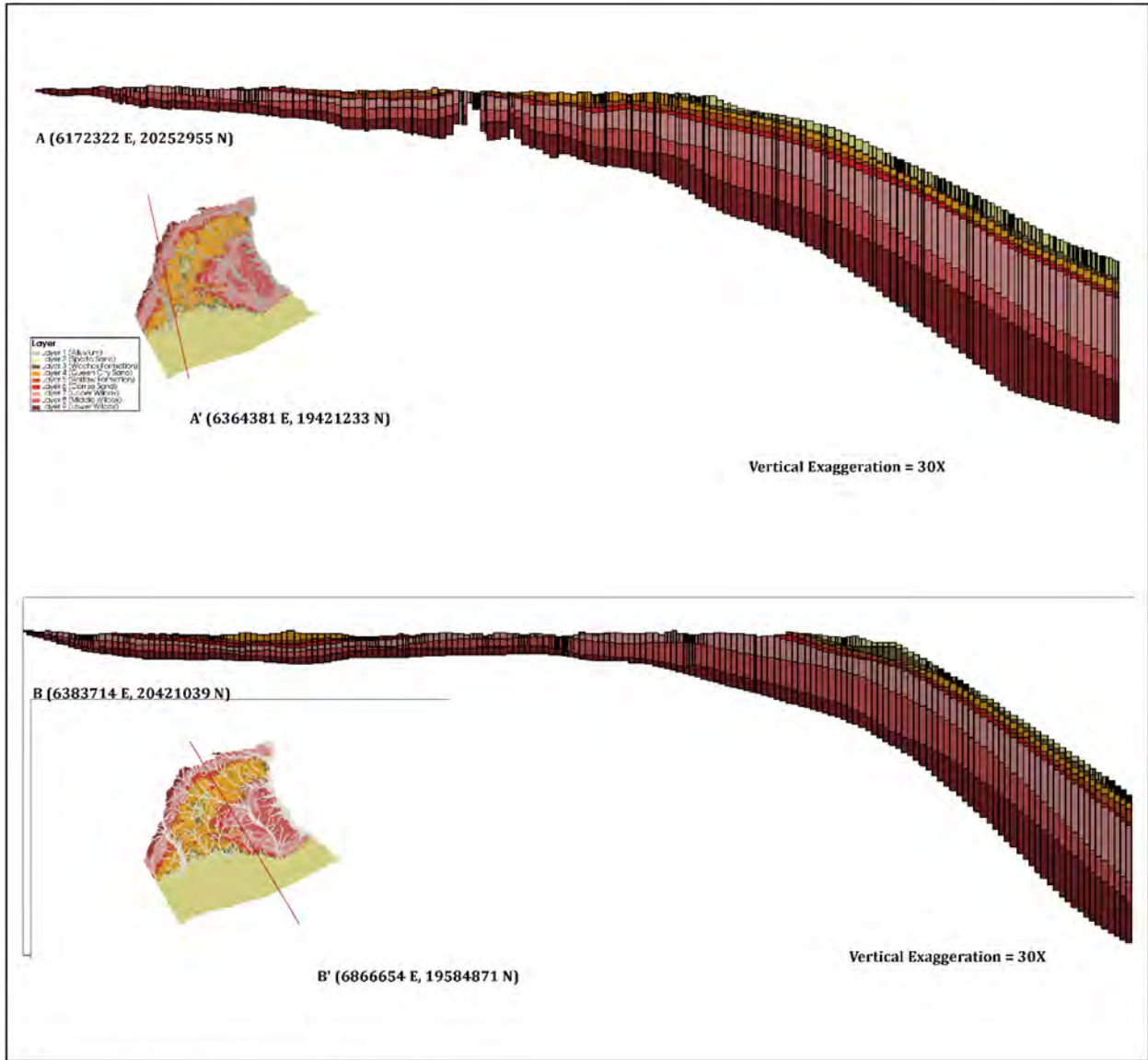
MODFLOW 6 accommodates pinch-outs and Groundwater Vistas eliminates pinched-out model cells automatically, resulting in much more efficient and robust simulations. MODFLOW 6 also accommodates displaced model layers along faults and Groundwater Vistas creates the cross-layer connections between the hydrogeologic units. Figure 2.4-32 shows cross-sections of the numerical model with a north-south cross-section A-A' and northwest to southeast cross-section B-B'. The cross-sections show the model layering honors the conceptual model including the salt dome feature shown in cross-section A-A', and pinch outs as shown in both cross sections (Figure 2.4-32).




2.5 Node Property Flow Package

The Node Property Flow (NPF) package and Storage (STO) package replace previous MODFLOW packages that characterize the aquifer properties including the Layer Property Flow (LPF), Block-Centered Flow (BCF), and Upstream Weighting (UPW) packages. The NPF Package was used to specify aquifer flow parameters (hydraulic properties) and define individual cells as confined or convertible for the groundwater domain. Aquifer flow parameters required by the NPF Package include horizontal and vertical hydraulic conductivities. The parameter values were established during calibration using the automated parameter estimation software, PEST; this process is discussed further in the Calibration Section (Section 3.0). The parameterization approach for hydraulic conductivity is discussed here.

Hydraulic conductivity values for the aquifers in the domain have previously been estimated at various locations as noted in the Conceptual Model Report; however, it is difficult to apply these values across a geologic unit. Therefore, hydraulic conductivity in each model layer was parameterized using the estimated distributions of sand fraction within each of the geologic units and across the model domain. Figures 2.5-1 through 2.5-5 show the sand fraction distributions for the Sparta Aquifer (model layer 2), Queen City Aquifer (model layer 4), Upper Wilcox (model layer 7), Middle Wilcox (model layer 8), and Lower Wilcox (model layer 9) units, respectively.

Sand fraction information was not available for two transmissive units, the Quaternary Alluvium (model layer 1) and the Carrizo Aquifer (model layer 6); or for the aquitards, the Weches Formation (model layer 3) and the Reklaw Formation (model layer 5). A uniform value was used to parameterize these units. The sand fraction value of 0.70 was used for the transmissive units; the sand fraction value of 0.10 was used for the aquitards. Sand fractions are summarized in Table 2.5-1.



LEGEND	
	Layer 1 (Alluvium)
	Layer 2 (Sparta Aquifer)
	Layer 3 (Weches Formation)
	Layer 4 (Queen City Aquifer)
	Layer 5 (Reklaw Formation)
	Layer 6 (Carrizo Aquifer)
	Layer 7 (Upper Wilcox)
	Layer 8 (Middle Wilcox)
	Layer 9 (Lower Wilcox)

Note:
1. Groundwater Desktop was used to visualize the groundwater flow model cross sections.

Figure 2.4-32. Cross Sections of Gridded Model Layers in the Groundwater Flow Model

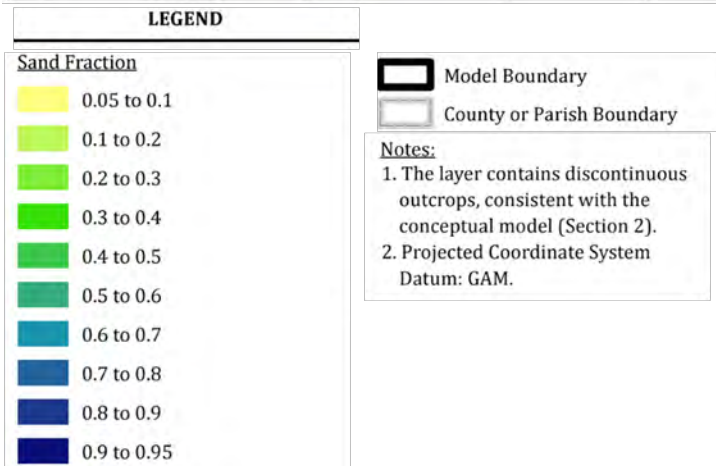
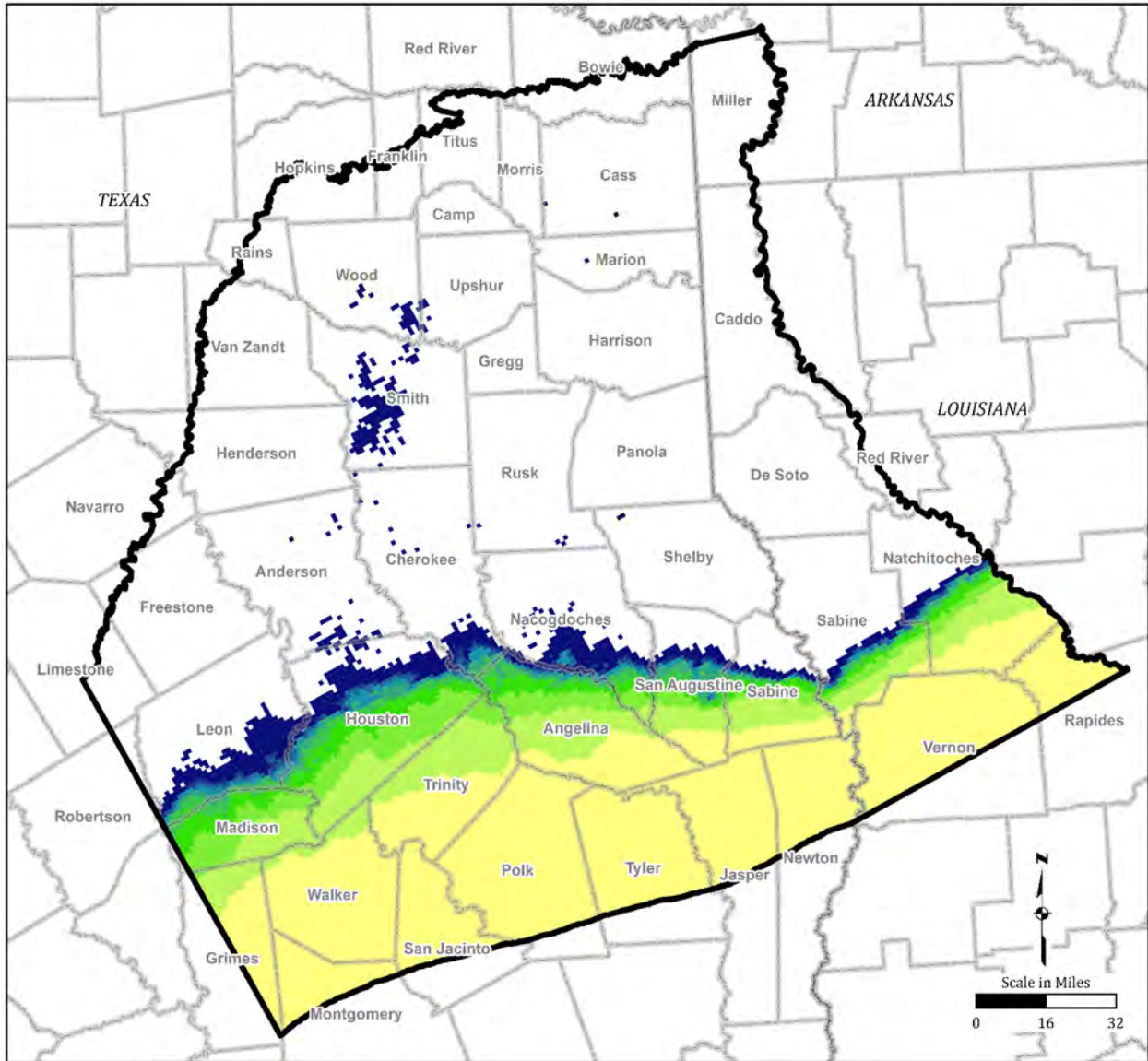


Figure 2.5-1. Estimated Sand Fraction Distribution for Sparta Aquifer (Model Layer 2)

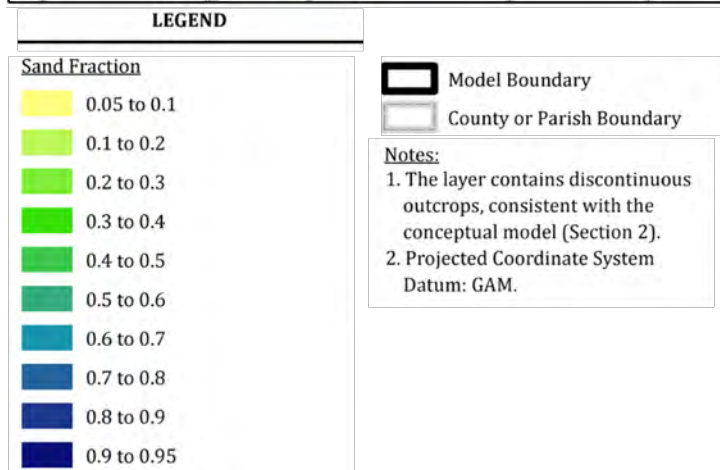
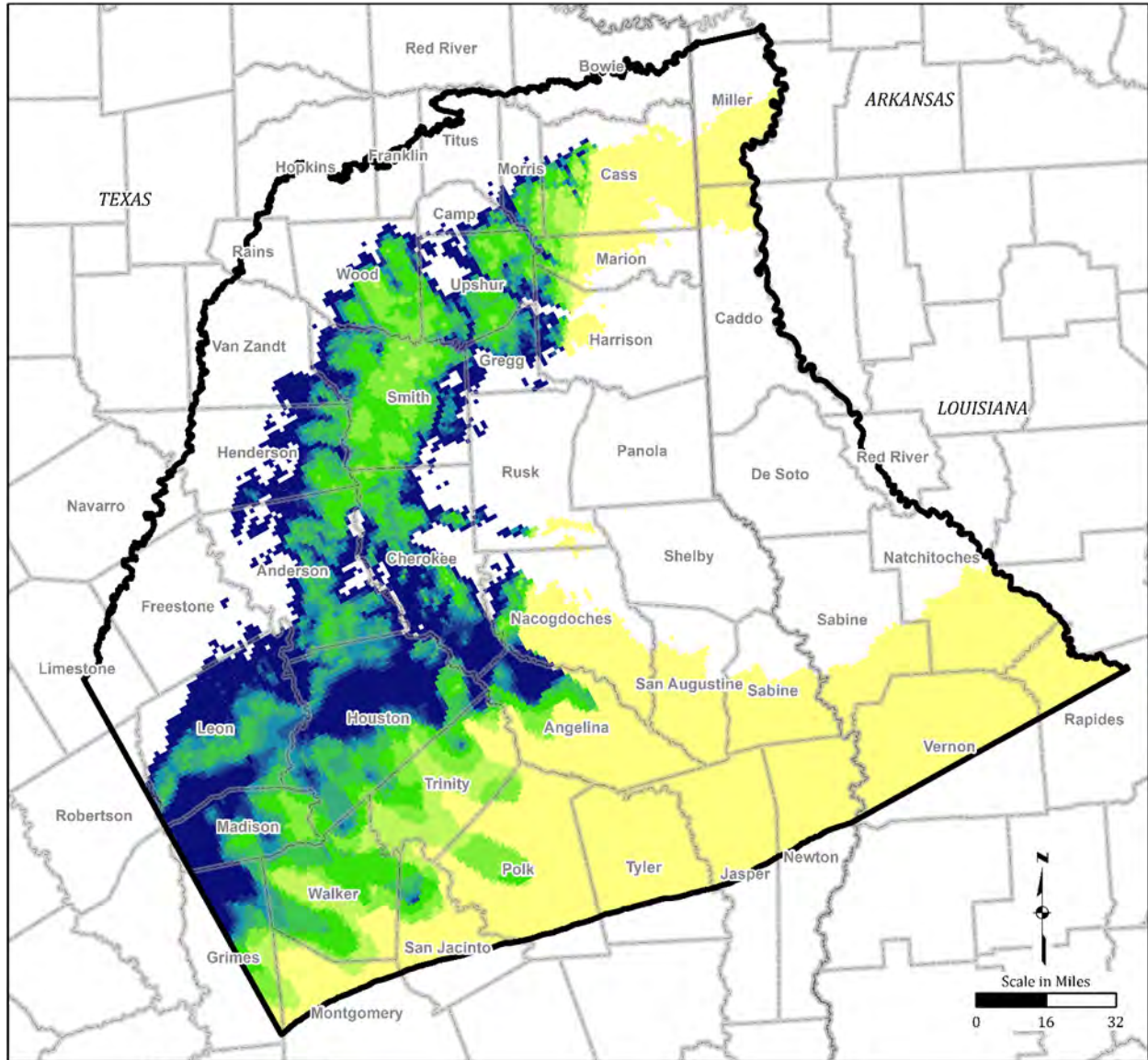


Figure 2.5-2. Estimated Sand Fraction Distribution for Queen City Aquifer (Model Layer 4)

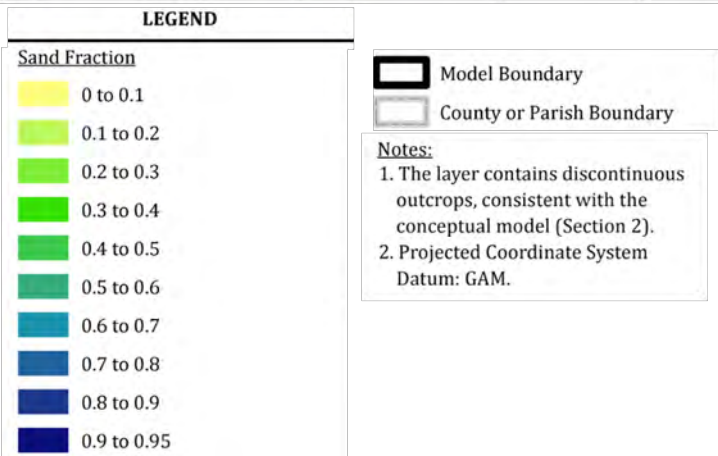
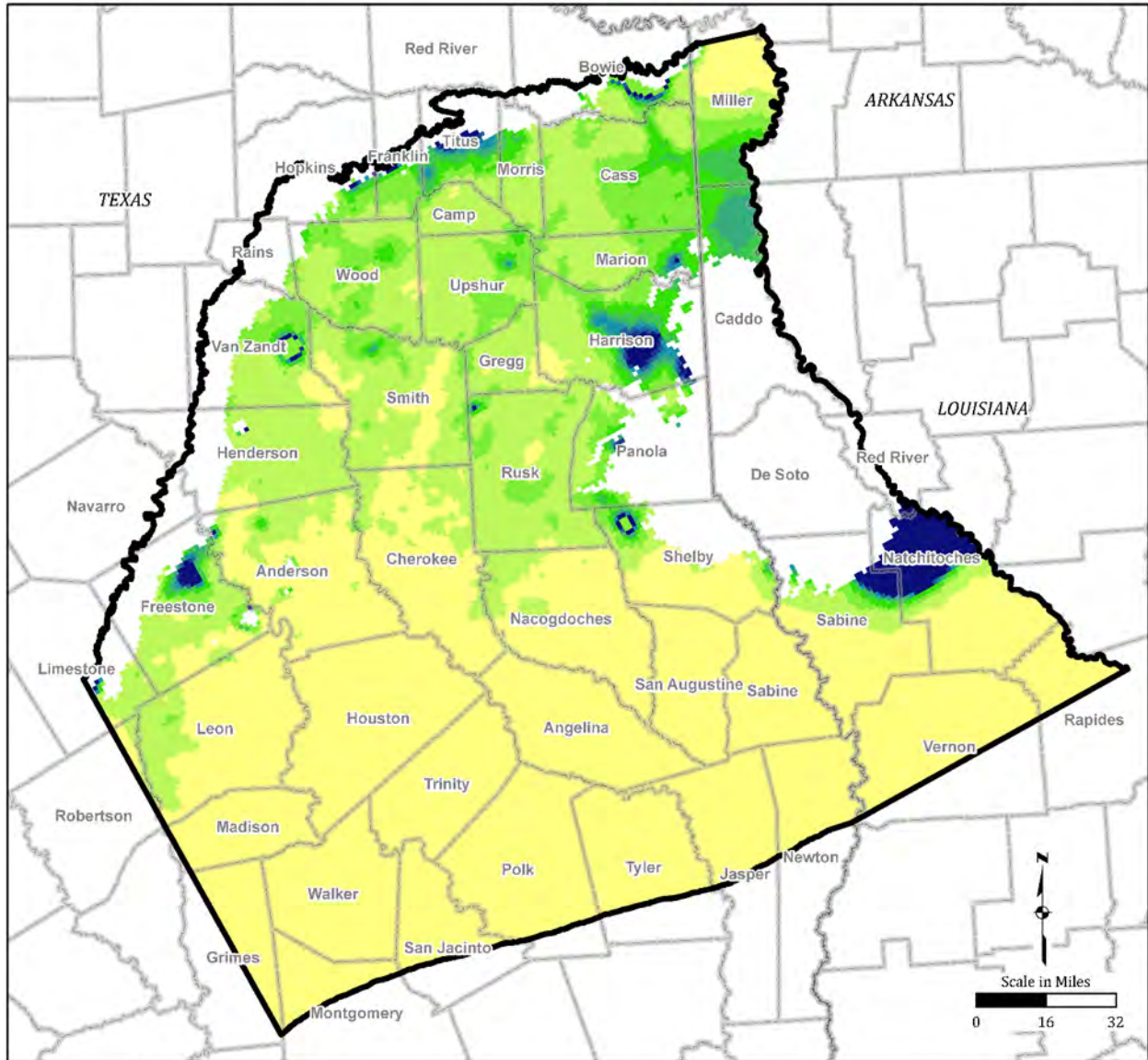


Figure 2.5-3. Estimated Sand Fraction Distribution for Upper Wilcox (Model Layer 7)

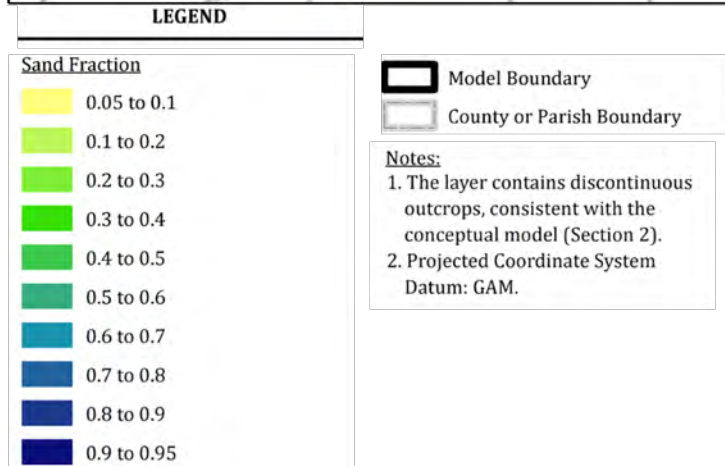
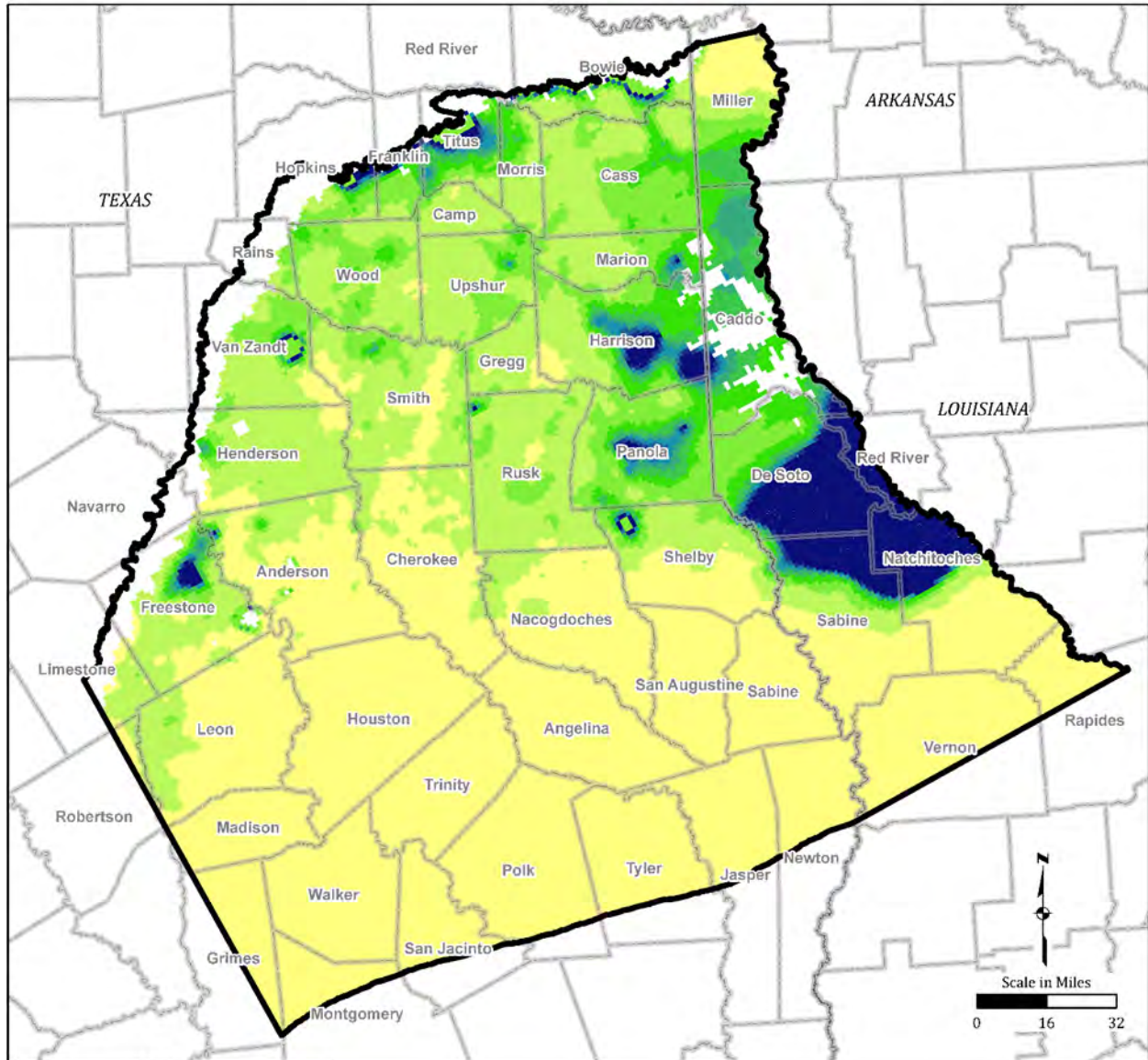


Figure 2.5-4. Estimated Sand Fraction Distribution for Middle Wilcox (Model Layer 8)

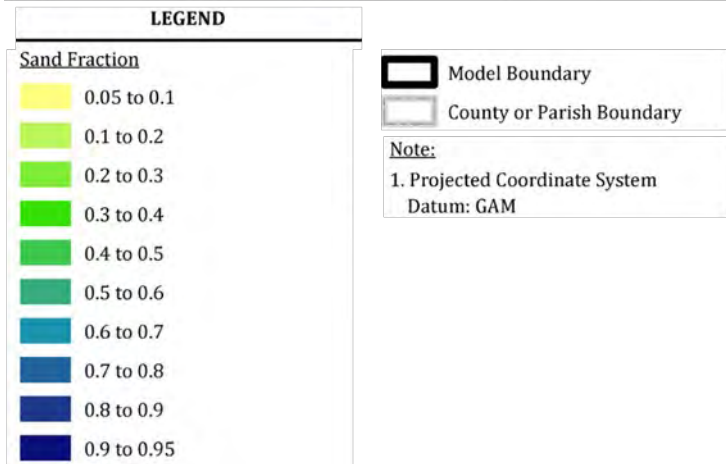
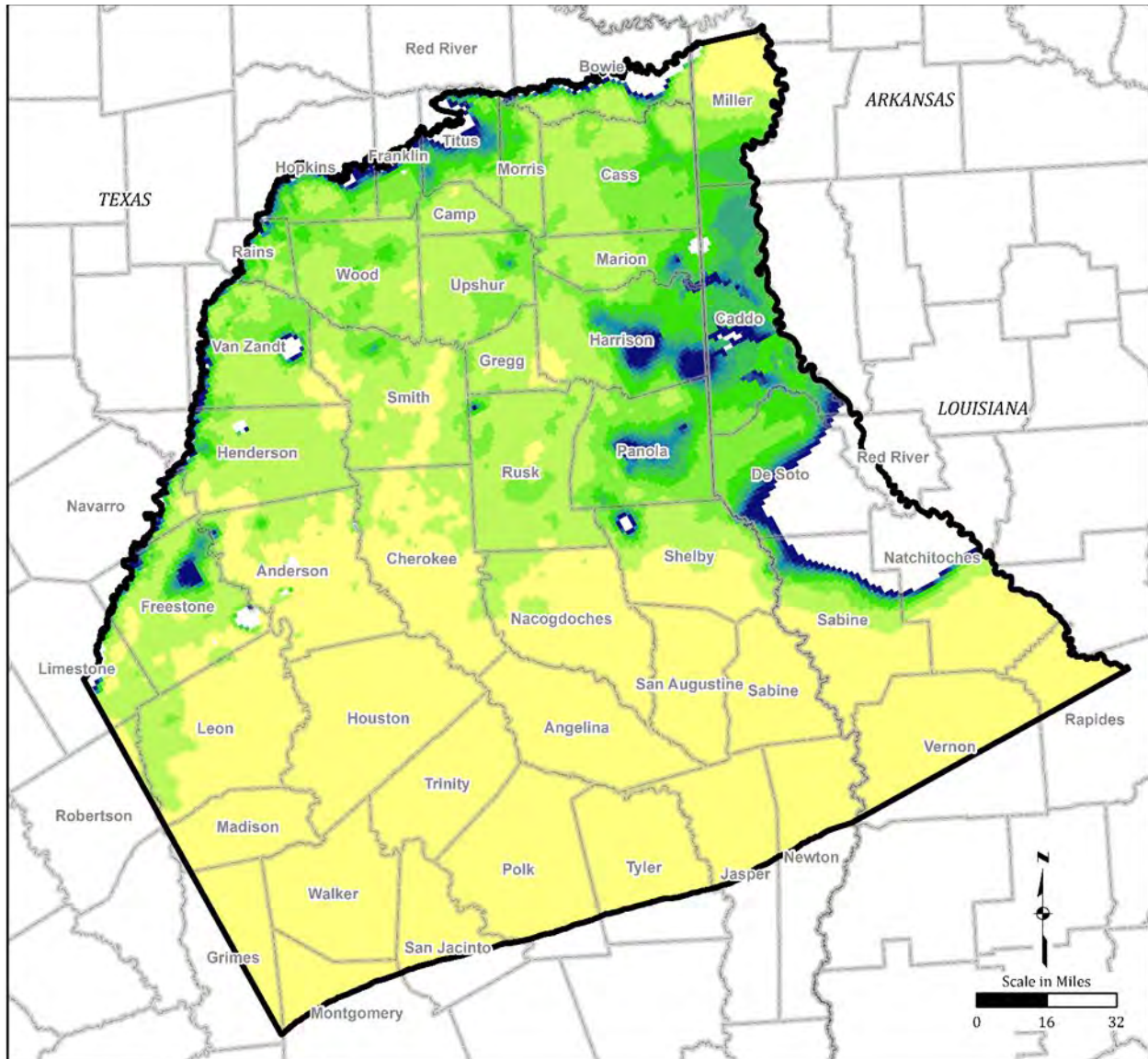


Figure 2.5-5. Estimated Sand Fraction Distribution for Lower Wilcox (Model Layer 9)

Table 2.5-1. Sand Fraction Range for Each Layer

Model Layer	Hydrostratigraphic Unit	Sand Fraction Range
1	Quaternary Alluvium	0.70
2	Sparta Aquifer	0.05 - 0.95
3	Weches Formation	0.10
4	Queen City Aquifer	0.05 - 0.95
5	Reklaw Formation	0.10
6	Carrizo Aquifer	0.70
7	Upper Wilcox	0 - 0.95
8	Middle Wilcox	0.05 - 0.95
9	Lower Wilcox	0.05 - 0.95

Hydraulic conductivity parameterization was conducted as follows. A higher parameterization hydraulic conductivity value was associated with a sand fraction of unity, and a lower value was associated with a sand fraction of zero for each geologic layer (the assumption being that each geologic unit has its own type of soil or rock and that, within each unit, less sand implies higher clay or rock content with an associated lower effective hydraulic conductivity). The horizontal hydraulic conductivity for any computational cell in the domain is calculated as an average, weighted by the sand fraction value of the cell; this provides a linear relationship between the highest and lowest value within each geologic unit.

The relationship between sand fraction, parameterized hydraulic conductivity values, and model hydraulic conductivity can be written as:

$$K_h = f_s K_s + (1 - f_s) K_c$$

Where K_h is the horizontal hydraulic conductivity of a cell; f_s is the sand fraction of a cell; K_s is the parameterization hydraulic conductivity value for sand for a geologic unit, and K_c is the parameterization hydraulic conductivity value for clay or rock for the geologic unit.

For vertical hydraulic conductivity, a weighted harmonic mean value was applied. Thus,

$$K_v = \frac{1}{[f_s / K_s + (1 - f_s) / K_c]}$$

Where K_v is the vertical hydraulic conductivity of a cell.

With this parameterization, sand hydraulic conductivity governs horizontal flow in the model since the arithmetic average tends towards the mid-point value for equal fractions of sand and clay. The clay hydraulic conductivity would generally govern vertical flow in the model since the harmonic average tends to be biased towards the lower (clay) conductivity value for equal fractions of sand and clay.

The sand fraction values are stored in the “Leakance” property within Groundwater Vistas. When the MODFLOW comment-line includes the phrase “Sand Fractions stored as Leakance”, Groundwater Vistas creates a text file with the extension ‘sand’ representing the sand fraction for each cell. Groundwater Vistas then performs the computations for horizontal hydraulic conductivity, K_h , and vertical hydraulic conductivity, K_v , for each cell using the formulas above to create the NPF datasets. The horizontal and vertical hydraulic conductivity values are saved in the text files with the extensions ‘kx’ and ‘kv’, respectively. Note that this computation is also done during PEST simulations for calibration.

The specific storage and specific yield parameters were estimated as uniform for the model domain. There is less data available for these parameters and adding complexity to these model parameters was deemed unwarranted. The influence of these parameters on the system and model solution was tested with a sensitivity analysis, discussed in Section 4.0.

Faults or flow barriers were not implemented in the calibrated model. However, the Mount Enterprise Fault Zone shown on Figure 2.4-22 (Figure 2-19 of the Conceptual Model Report) contains displacements along the faults causing inter-unit connections. MODFLOW 6 handles such connections allowing lateral flow from one geologic layer to multiple layers across a fault with displacement. These cross-layer connections at the Enterprise Fault location were generated in Groundwater Vistas as an “OPTION” under the “vertical geometry” tab depending on layer elevations across the fault.

2.6 Storage Package

The Storage (STO) package is only used for transient conditions to provide compressible storage contributions. The STO package was used in the model to specify the aquifer storage parameters which include specific storage and specific yield. Input for the STO package are the specific storage and specific yield of each model cell. Specific storage values are stored in the text file with the extension ‘ss’ and the specific yield values are stored in the text file with the extension ‘sy’, both of which are created by Groundwater Vistas and called by the STO package. If the STO package is not included in the model NAME file, then a steady-state simulation is conducted. The mass balance output for the STO package provides information on the confined and unconfined components of the total storage. Thus,

$$Q_{STO} = Q_{SS} + Q_{SY}$$

Where Q_{SS} is the volumetric flow rate from specific storage in units of length cubed over time (L^3/T) and Q_{SY} is the volumetric flow rate from specific yield in similar units (L^3/T).

2.7 Well Package

The Well (WEL) package was used in the model to simulate groundwater pumping wells. During initial model development, raw pumping data from the Conceptual Model Report was input into Groundwater Vistas as analytical element wells. Each well was screened within a single model layer based on available data from the Conceptual Model. After analyzing the raw pumping data, additional data clean up and the following changes to the raw pumping data were applied.

1. Wells placed in one of the two aquitards (model layers 3 and 5) were moved into the layer above;
2. Pumping records for the years 1981, 1982, and 1983 were not available, thus values for these years were established by linearly interpolating between 1980 and 1984;
3. Pumping outliers were removed for the dataset; and
4. An apparent shift in the pumping rate that occurred after 1999 was smoothed out for data in counties that displayed this pattern.

Simulations using the corrected data further identified issues with the pumping. Specifically, water level elevations were rising with increasing pumping and vice versa at several locations. Crucially, the pumping data did not show a general trend between 1980 and 2013 while water level elevations showed a general decline at many wells. The water level elevation datasets were considered to be the more reliable dataset because they are directly measured values; by contrast, the water use estimates in the TWDB database include values which are estimated from indirect methods. In addition, it appears that several counties changed the way they estimated pumping volumes after 1999; these individual practices introduced large inconsistencies and uncertainties within the pumping dataset. A calibration of the pumping variations via PEST on a county-by-county basis was conducted to address these uncertainties. However, upon implementation, it was noticed that the sensitivity of water level elevations changes to variations in pumping was very small and therefore the PEST optimization process failed.

The pumping data from the existing groundwater availability model (Kelley and others, 2004) model was evaluated and it was noted that increases in pumping within that dataset caused appropriate declines in observed water level elevations. Therefore, the TWDB pumping database was not used for the current model; instead, the current model pumping is based on pumping from the existing groundwater availability model.

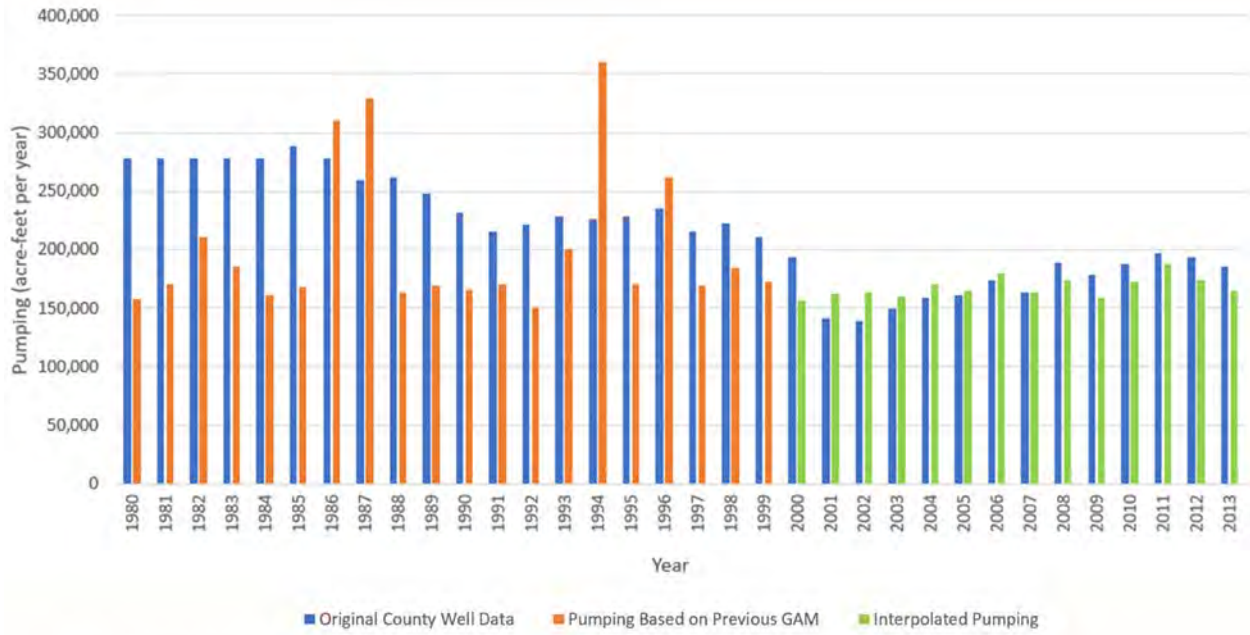
The pumping data presented in the existing groundwater availability model (Kelley and others, 2004) consisted of pumping wells in 54,729 model cells and in single model layers. The existing model data represented pumping from 1980 through 1999. Pumping from 2000 through 2013 was simulated as domain wide changes in pumping that approximate the trends over time from the TWDB database. Table 2.7-1 compares the total pumping per layer between the raw conceptual model data, the corrected conceptual model data, and the current model (based on previous groundwater availability model pumping). Figure 2.7-1 compares the original county well data and the pumping data used in the current model.

Table 2.7-1. Pumping Dataset Comparison

Hydrostratigraphic Unit	Model Layer	Conceptual Model Report Pumping (acre-ft)	Corrected Conceptual Model Report Pumping (acre-ft)	Current Model Total Pumping (acre-ft)
Quaternary Alluvium	1	79,896	155,763	0
Sparta Aquifer	2	274,874	537,688	140,745
Weches Formation	3	115,826	0	0
Queen City Aquifer	4	529,423	1,000,226	346,221
Reklaw Formation	5	301,848	0	0
Carrizo Aquifer	6	750,757	910,271	3,292,702
Upper Wilcox	7	2,299,622	2,660,318	1,219,102
Middle Wilcox	8	1,394,278	1,608,434	1,100,444
Lower Wilcox	9	1,110,469	1,324,976	287,559
Total Model Pumping		6,856,993	8,197,676	6,386,773

Notes:

1. Total pumping shown is for the model period 1980 to 2013.
2. Conceptual Model Report: Montgomery and Associates, 2020.
3. The current model pumping is based on pumping from the existing GAM groundwater model (Kelley and others, 2004).



Note: Previous GAM from Kelley and others, 2004.

Figure 2.7-1. Model Pumping Comparison

Since the existing model does not have a layer representing the alluvium, this model update contains no pumping in model layer 1 (Table 2.7-1). As there is little pumping in the alluvium layer in the conceptual model, the loss of pumping in layer 1 is minor. The majority of the pumping in the existing model is in the Carrizo Aquifer and the Upper, Middle, and Lower Wilcox. This compares well to the original conceptual model pumping (Table 2.7-1) at least in terms of bulk cumulative values between 1980 and 2013.

Each pumping well in the current model is screened within a single model layer. Figures 2.7-2 through 2.7-7 show the total pumping volume of each well during the model time period (1980 to 2013) for each layer. There are no wells screened within the Weches Formation (model layer 3) or the Reklaw Formation (model layer 5) which are aquitards. Groundwater is pumped from the Queen City Aquifer, Sparta Aquifer, and Carrizo-Wilcox aquifers for municipal, irrigation, industrial, domestic, and stock uses.

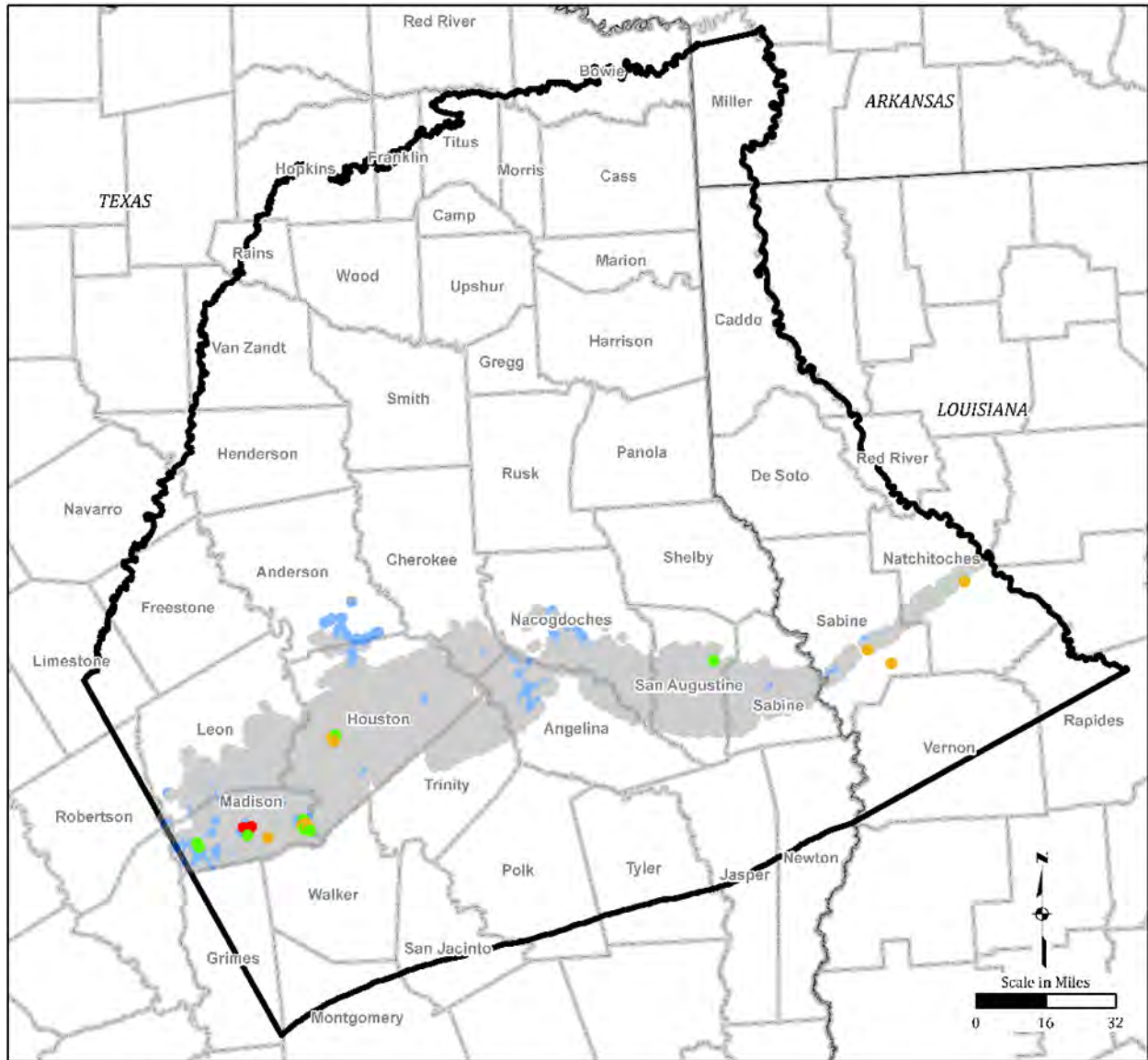
Appendix Table 1 provides total pumping for each county or parish within the model domain for each stress period (each year) and each layer of the model simulation. Figures 2.7-8a through 2.7-8e display these values graphically as individual county charts showing total pumping. Pumping sums for counties that straddle the model boundary do not reflect total pumping from that county but only the pumping portion that overlaps the model. In general, most pumping is from the Upper, Middle, and Lower Wilcox stratigraphic units.

The pumping data may contain outliers and unrealistic data. For example, there are three years of increased pumping rates for Morris County and four years of increased pumping rates for Hopkins County, as shown on Figure 2.7-8b. The pumping data and their associated water level elevation drawdowns should be further evaluated using data science techniques for a more reliable pumping data set. Improved pumping estimates will result in a better calibrated groundwater model.

The WEL package of MODFLOW 6 was used to apply a sink within the cell for each pumping well. The sink was applied on an annual stress period for 34 stress periods representing 1980 to 2013 conditions. The WEL Package includes an "AUTOFLOWREDUCE" option that ensures that pumping demand does not draw water level elevations below the bottom elevation of the cell. This option is turned on for the simulations and any associated simulated reduction in pumping is reported in a "well flow-reduction" file. All wells were pumping their desired volumes during model calibration.

2.8 General Head Boundary Package

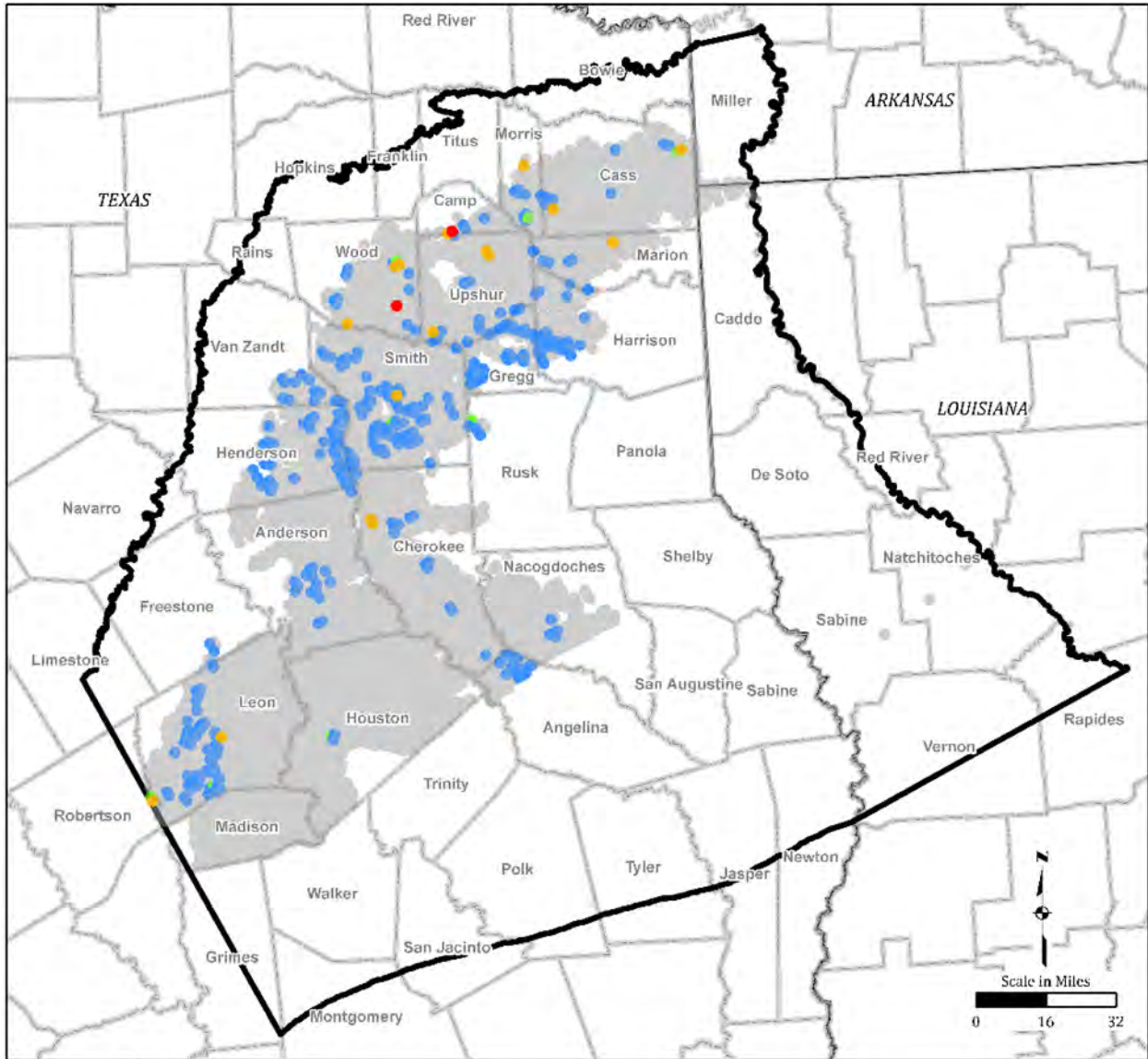
Flow into or out of the model domain from the southern model boundary was simulated using the General Head Boundary (GHB) package, in accordance with the conceptual model shown on Figure 2.0-2. Figure 2.8-1 shows the modeled GHB conditions in the current model. The GHB package was used to simulate the interaction of the model with the Younger Units which were not explicitly simulated. The model layer 2, Sparta Aquifer, GHB simulates exchange of water with the Younger Units. The GHB condition in model layers 4 and 6 through 9 (Queen City, Carrizo, and Wilcox Aquifers) along the southern model boundary allow flow of water into or out of the model domain and the respective aquifers. The GHB conditions account for the southern model boundary not being a natural aquifer boundary. The heads along the GHB boundaries approximate interpolated head contours



LEGEND	
1980 to 2013 Total Pumping (Acre-feet)	
■	0.01 to 100
■	100 to 500
■	500 to 1,000
■	1,000 to 10,000
■	10,000 to 17,373
	Model Boundary
	County or Parish Boundary

Notes:
 1. The layer contains discontinuous outcrops, consistent with the conceptual model (Section 2).
 2. Projected Coordinate System Datum: GAM.

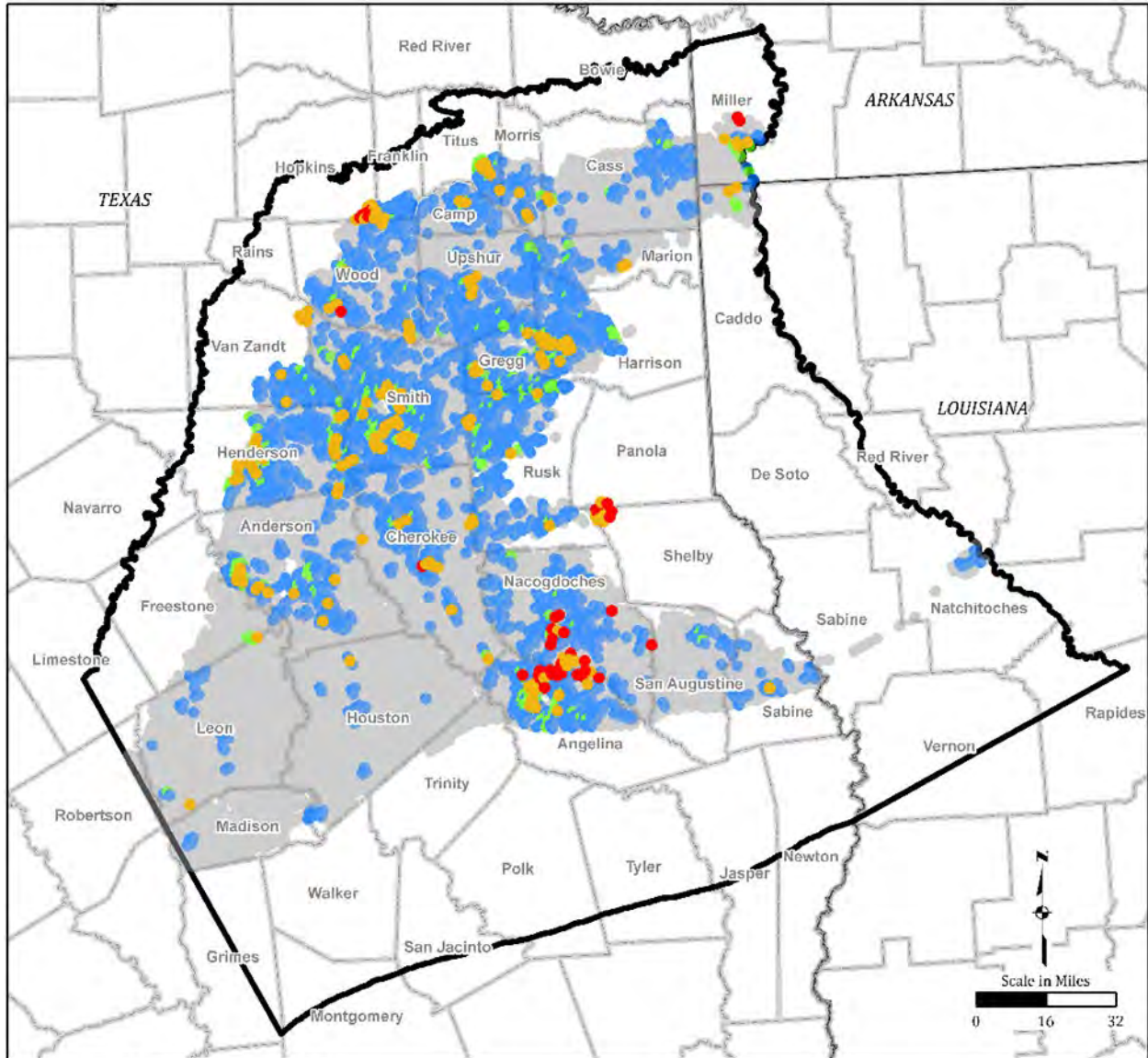
Figure 2.7-2. Pumping Well Total Pumping Volume in Sparta Aquifer (Layer 2)



LEGEND	
1980 to 2013 Total Pumping (Acre-feet)	
●	0.01 to 100
●	100 to 500
●	500 to 1,000
●	1,000 to 10,000
●	10,000 to 38,114
	Model Boundary
	County or Parish Boundary

Notes:
 1. The layer contains discontinuous outcrops, consistent with the conceptual model (Section 2).
 2. Projected Coordinate System Datum: GAM.

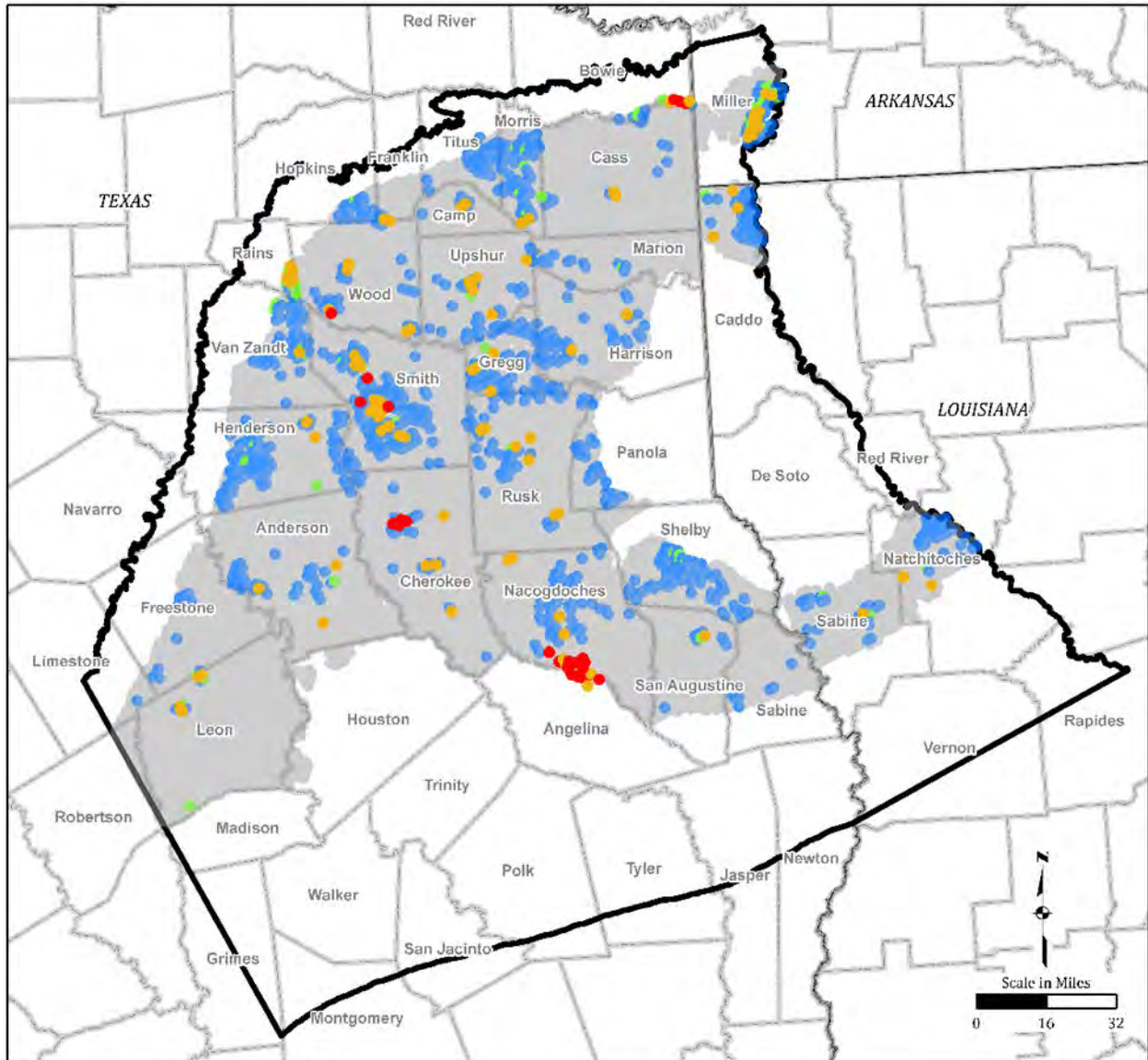
Figure 2.7-3. Pumping Well Total Pumping Volume in Queen City Aquifer (Layer 4)



LEGEND	
1980 to 2013 Total Pumping (Acre-feet)	
●	0.01 to 100
●	100 to 500
●	500 to 1,000
●	1,000 to 10,000
●	10,000 to >100,000
	Model Boundary
	County or Parish Boundary

Notes:
 1. The layer contains discontinuous outcrops, consistent with the conceptual model (Section 2).
 2. Projected Coordinate System Datum: GAM.

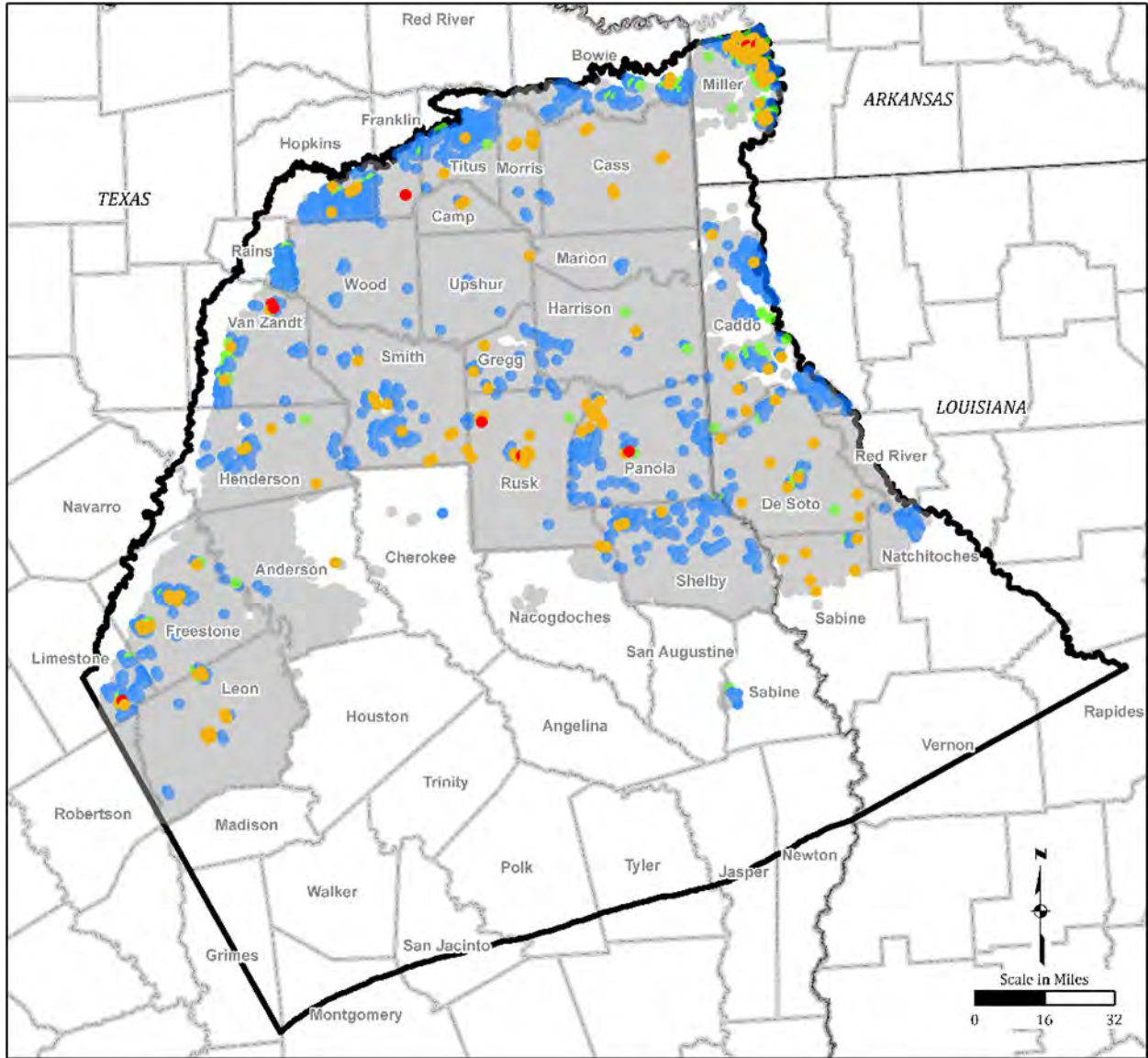
Figure 2.7-4. Pumping Well Total Pumping Volume in Carrizo Aquifer (Layer 6)



LEGEND	
1980 to 2013 Total Pumping (Acre-feet)	
●	0.01 to 100
●	100 to 500
●	500 to 1,000
●	1,000 to 10,000
●	10,000 to 35,770
▬	Model Boundary
▬	County or Parish Boundary

Notes:
 1. The layer contains discontinuous outcrops, consistent with the conceptual model (Section 2).
 2. Projected Coordinate System Datum: GAM.

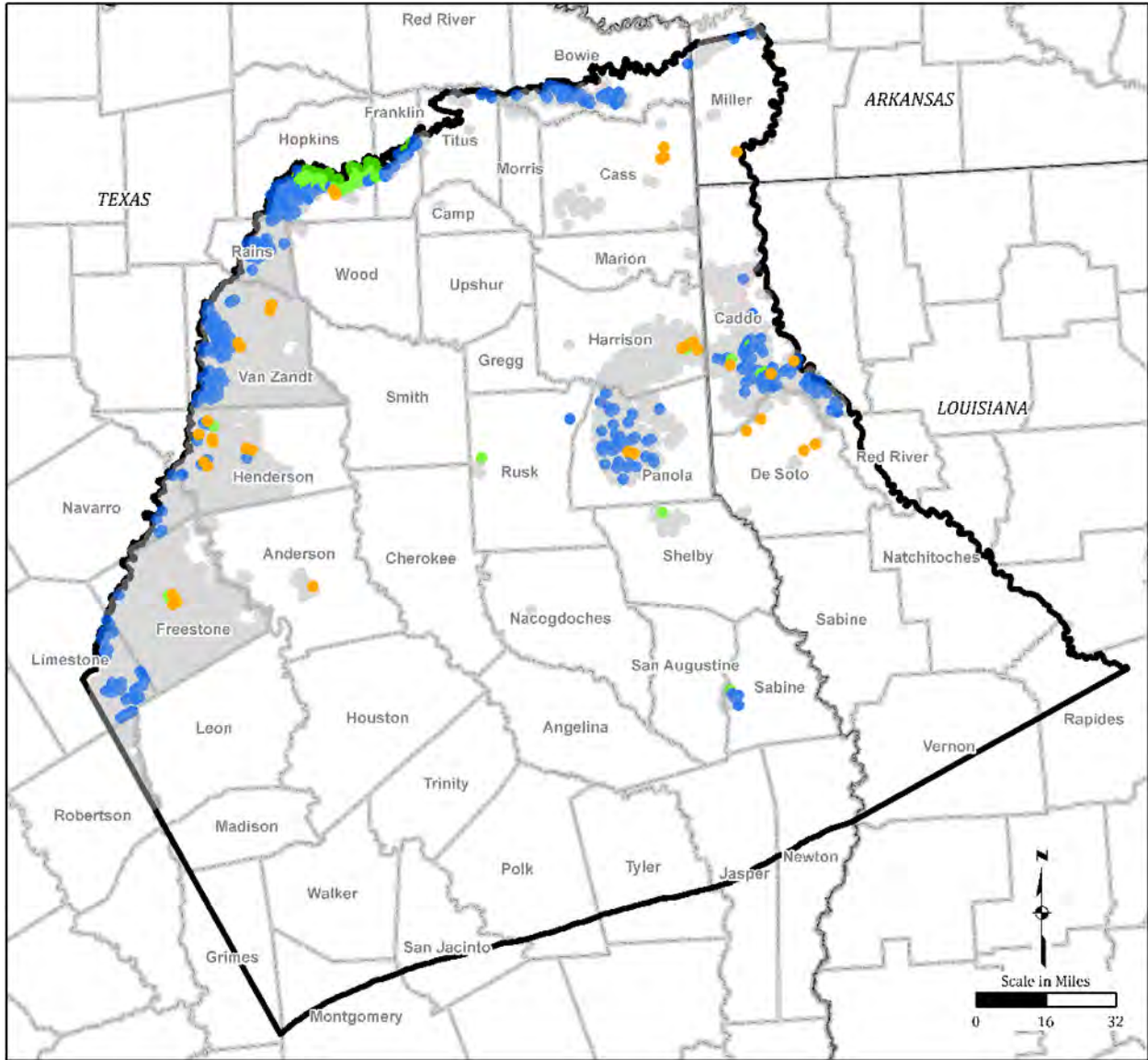
Figure 2.7-5. Pumping Well Total Pumping Volume in Upper Wilcox (Layer 7)



LEGEND	
1980 to 2013 Total Pumping (Acre-feet)	
●	0.01 to 100
●	100 to 500
●	500 to 1,000
●	1,000 to 10,000
●	10,000 to 24,770
▭	Model Boundary
▭	County or Parish Boundary

Notes:
 1. The layer contains discontinuous outcrops, consistent with the conceptual model (Section 2).
 2. Projected Coordinate System Datum: GAM.

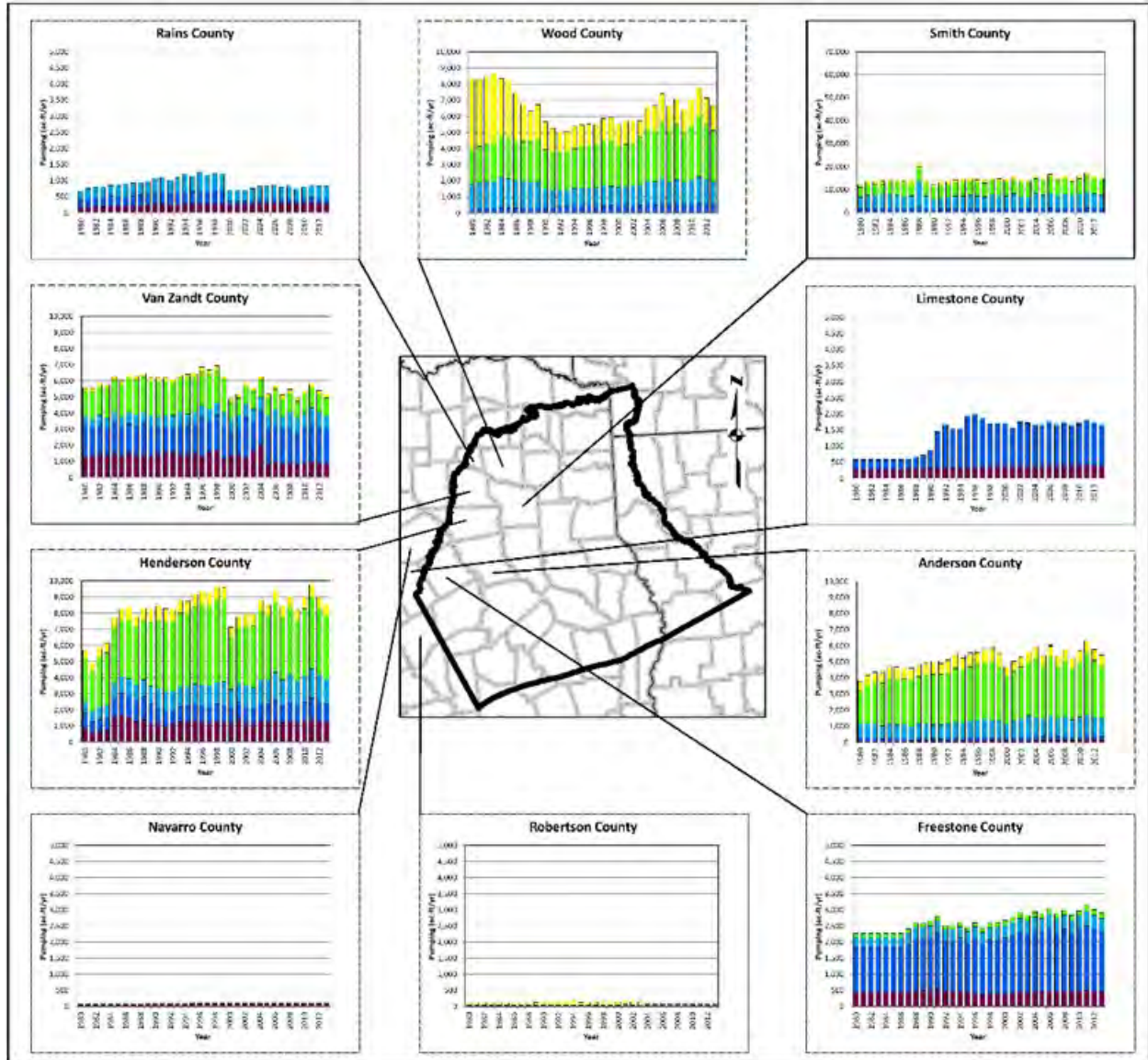
Figure 2.7-6. Pumping Well Total Pumping Volume in Middle Wilcox (Layer 8)



LEGEND	
1980 to 2013 Total Pumping (Acre-feet)	
●	0.01 to 100
●	100 to 500
●	500 to 1,000
●	1,000 to 9,750
▭	Model Boundary
▭	County or Parish Boundary

Note:
1. Projected Coordinate System
Datum: GAM

Figure 2.7-7. Pumping Well Total Pumping Volume in Lower Wilcox (Layer 9)

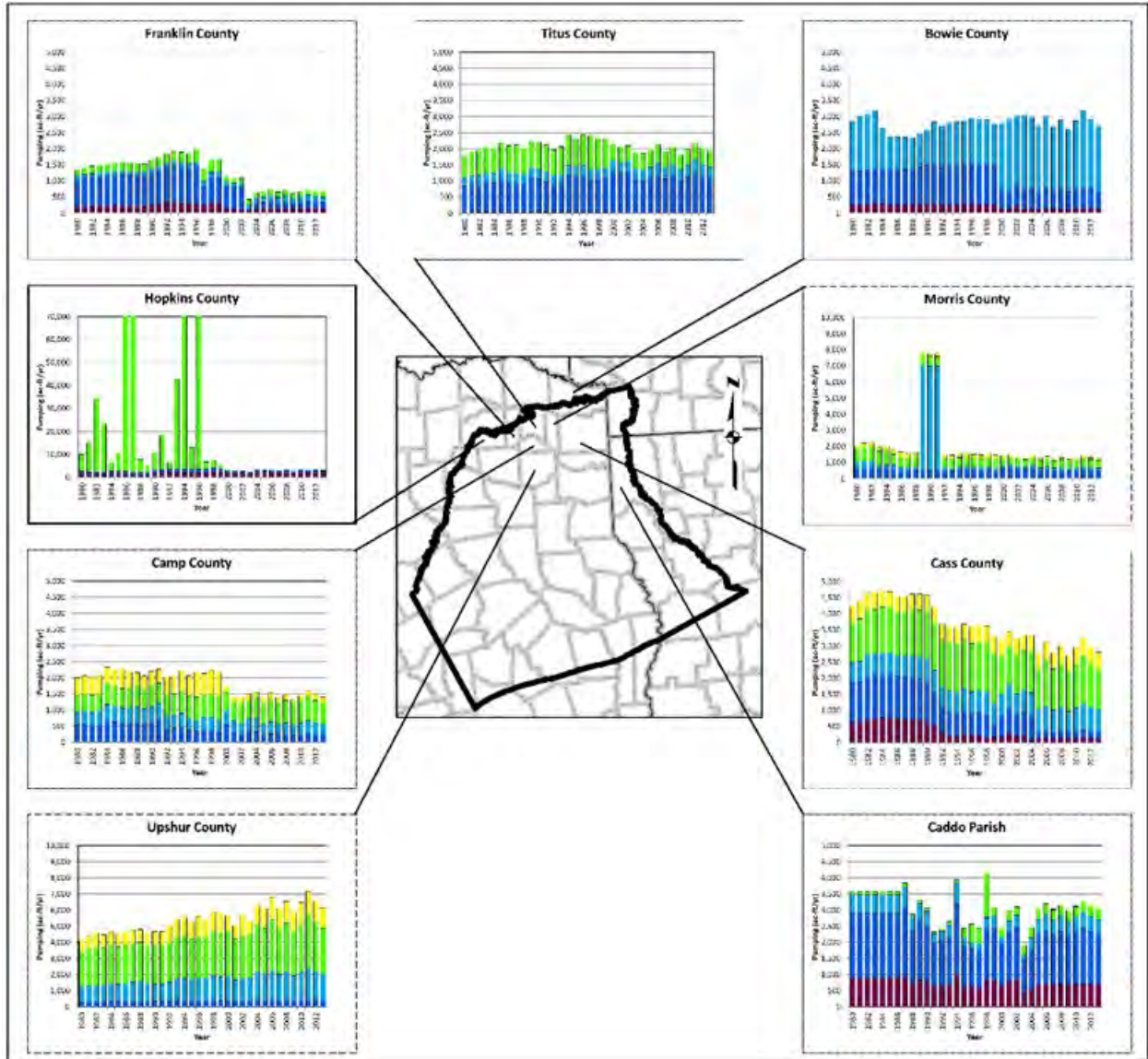


LEGEND

- Model Boundary
- County or Parish Boundary
- Layer Color**
- Quaternary Alluvium (Layer 1)
- Sparta Aquifer (Layer 2)
- Queen City Aquifer (Layer 4)
- Carrizo Aquifer (Layer 6)
- Upper Willcox (Layer 7)
- Middle Wilcox (Layer 8)
- Lower Willcox (Layer 9)

- Pumping Y-axis Range**
- 70,000 Acre Feet/Year
- 20,000 Acre Feet/Year
- 10,000 Acre Feet/Year
- 5,000 Acre Feet/Year

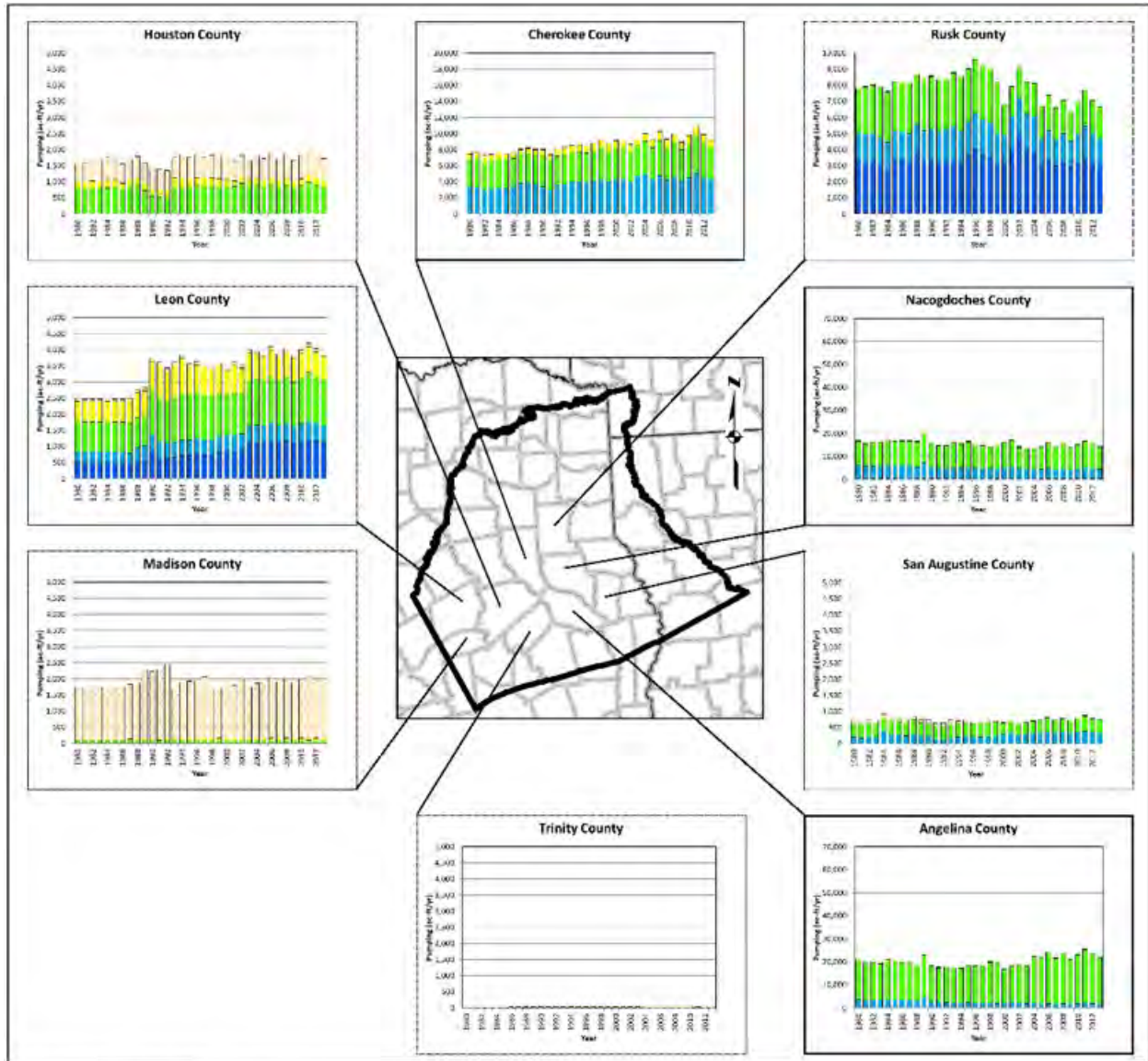
Figure 2.7-8a. Pumping per County



- LEGEND**
- Model Boundary
 - County or Parish Boundary
 - Layer Color**
 - Quaternary Alluvium (Layer 1)
 - Sparta Aquifer (Layer 2)
 - Queen City Aquifer (Layer 4)
 - Carrizo Aquifer (Layer 6)
 - Upper Willcox (Layer 7)
 - Middle Willcox (Layer 8)
 - Lower Willcox (Layer 9)

- Pumping Y-axis Range**
- 70,000 Acre Feet/Year
 - 20,000 Acre Feet/Year
 - 10,000 Acre Feet/Year
 - 5,000 Acre Feet/Year

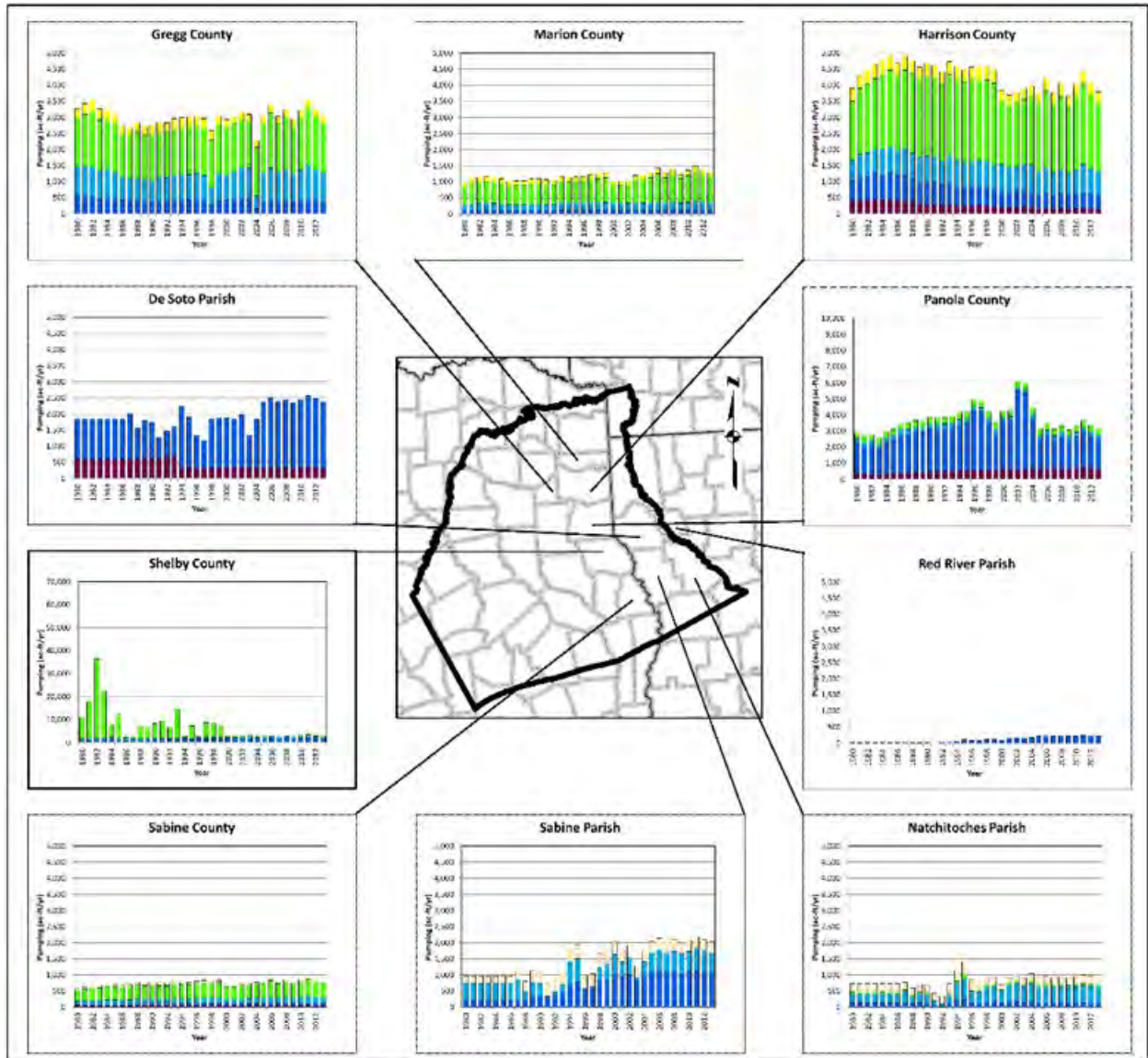
Figure 2.7-8b. Pumping per County



- LEGEND**
- Model Boundary
 - County or Parish Boundary
- Layer Color**
- Quaternary Alluvium (Layer 1)
 - Sparta Aquifer (Layer 2)
 - Queen City Aquifer (Layer 4)
 - Carrizo Aquifer (Layer 6)
 - Upper Willcox (Layer 7)
 - Middle Wilcox (Layer 8)
 - Lower Willcox (Layer 9)

- Pumping Y-axis Range**
- 70,000 Acre Feet/Year
 - 20,000 Acre Feet/Year
 - 10,000 Acre Feet/Year
 - 5,000 Acre Feet/Year

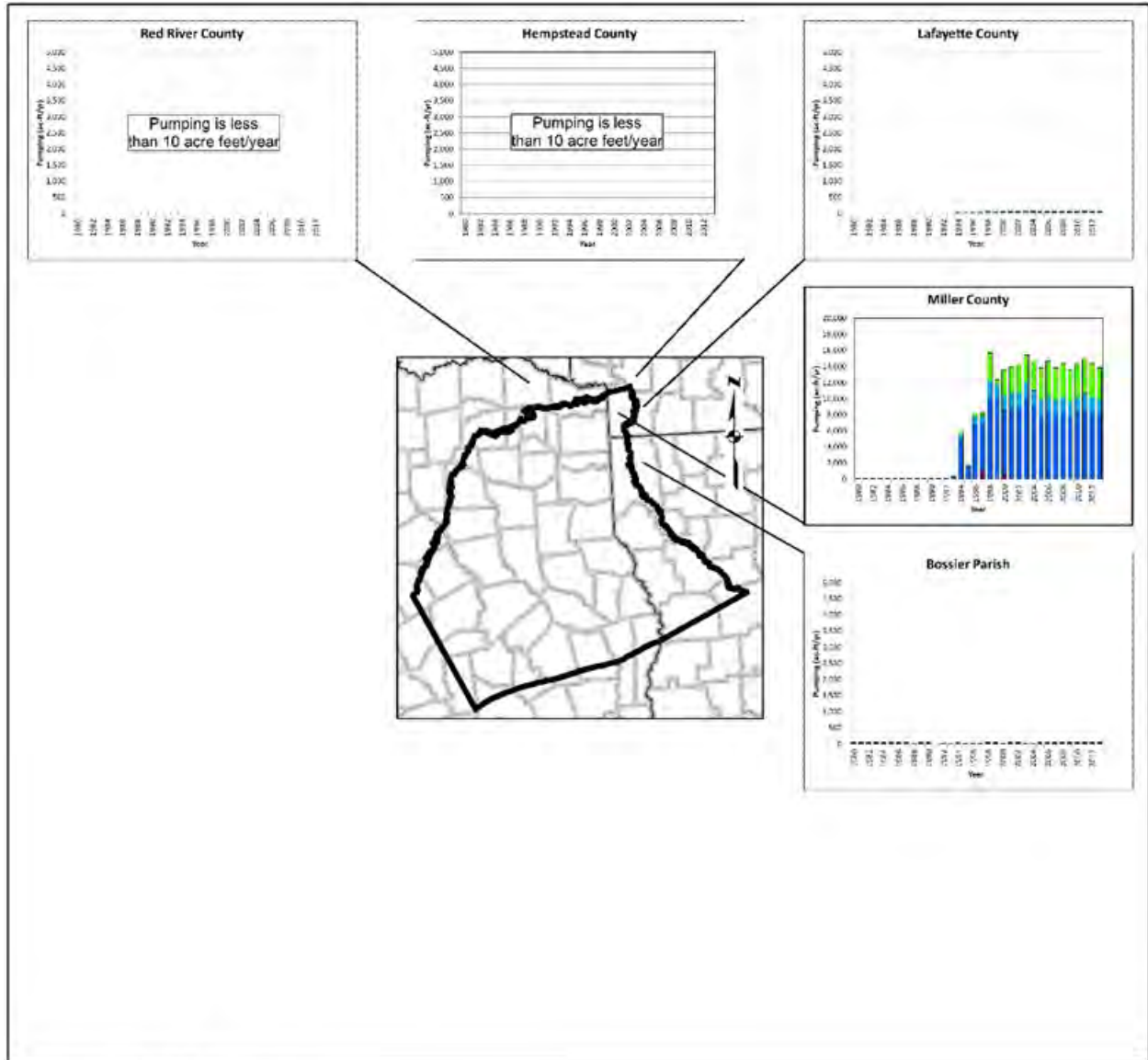
Figure 2.7-8c. Pumping per County



- LEGEND**
- Model Boundary
 - County or Parish Boundary
 - Layer Color**
 - Quaternary Alluvium (Layer 1)
 - Sparta Aquifer (Layer 2)
 - Queen City Aquifer (Layer 4)
 - Carrizo Aquifer (Layer 6)
 - Upper Willcox (Layer 7)
 - Middle Willcox (Layer 8)
 - Lower Willcox (Layer 9)

- Pumping Y-axis Range**
- 70,000 Acre Feet/Year
 - 20,000 Acre Feet/Year
 - 10,000 Acre Feet/Year
 - 5,000 Acre Feet/Year

Figure 2.7-8d. Pumping per County



- LEGEND**
- Model Boundary
 - County or Parish Boundary
- Layer Color**
- Quaternary Alluvium (Layer 1)
 - Sparta Aquifer (Layer 2)
 - Queen City Aquifer (Layer 4)
 - Carrizo Aquifer (Layer 6)
 - Upper Willcox (Layer 7)
 - Middle Willcox (Layer 8)
 - Lower Willcox (Layer 9)

- Pumping Y-axis Range**
- 70,000 Acre Feet/Year
 - 20,000 Acre Feet/Year
 - 10,000 Acre Feet/Year
 - 5,000 Acre Feet/Year

Figure 2.7-8e. Pumping per County

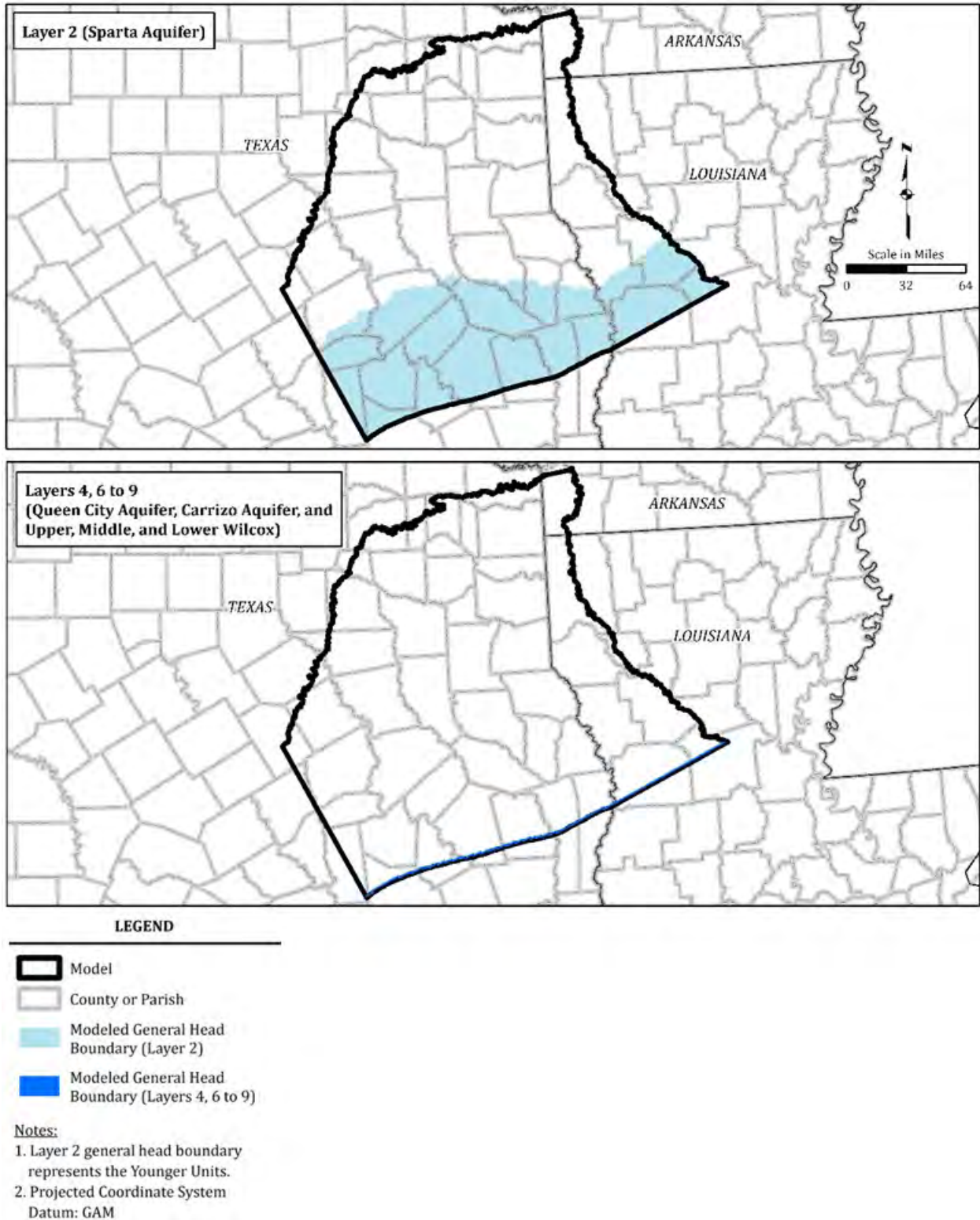


Figure 2.8-1. Modeled General Head Boundary Conditions

in the region; GHB heads are constant through the model simulation. Table 2.8-1 shows the GHB head range and conductance values for each layer.

2.9 River Package

The River (RIV) package of MODFLOW 6 was used to simulate the rivers in the model area. The RIV package simulates flow in or out of the aquifer to surface-water features such as canals, springs, reservoirs, rivers, and streams. Thus, flow within the surface-water features is not simulated, but the groundwater interaction is taken into account. In the model, the RIV package simulates area rivers and creeks.

Springs, or rejected recharge and subsequent runoff, occur in the model area in topographically low areas along river valleys. Springs that contribute to river flows are indirectly simulated using the RIV Package. Those that do not contribute and are isolated have low flows and negligible impact on groundwater. Springs are not directly simulated in this model.

Reservoirs within the model domain are located along rivers and are simulated using the RIV package. Small lakes not connected to the rivers have negligible contribution to groundwater. Lakes are not directly simulated in this model.

Figures 2.9-1 through 2.9-5 show the annual stream flows at stream gages located on the major rivers in the model domain, the Trinity River, Neches River, Sabine River, Big Cypress Creek, and Sulphur River. Rivers generally flow from north to south. The flow difference between stream gages was calculated at select river segments with unmanaged flows. A positive difference in seasonal flow means the river is gaining along the reach, and a negative difference in seasonal flow means the river is losing along the reach. The rivers simulated in the model are primarily gaining streams.

Figure 2.9-6 shows the simulated river boundary condition within the model domain. River width, bed thickness and bed conductance were taken as 1 foot, 1 foot, and 25 feet per day (feet/day), respectively, and the river segment length intersecting each groundwater cell was calculated by Groundwater Vistas for computation of the conductance coefficient. The river stage was estimated from the topography and the riverbed elevation was taken as a foot below the stage.

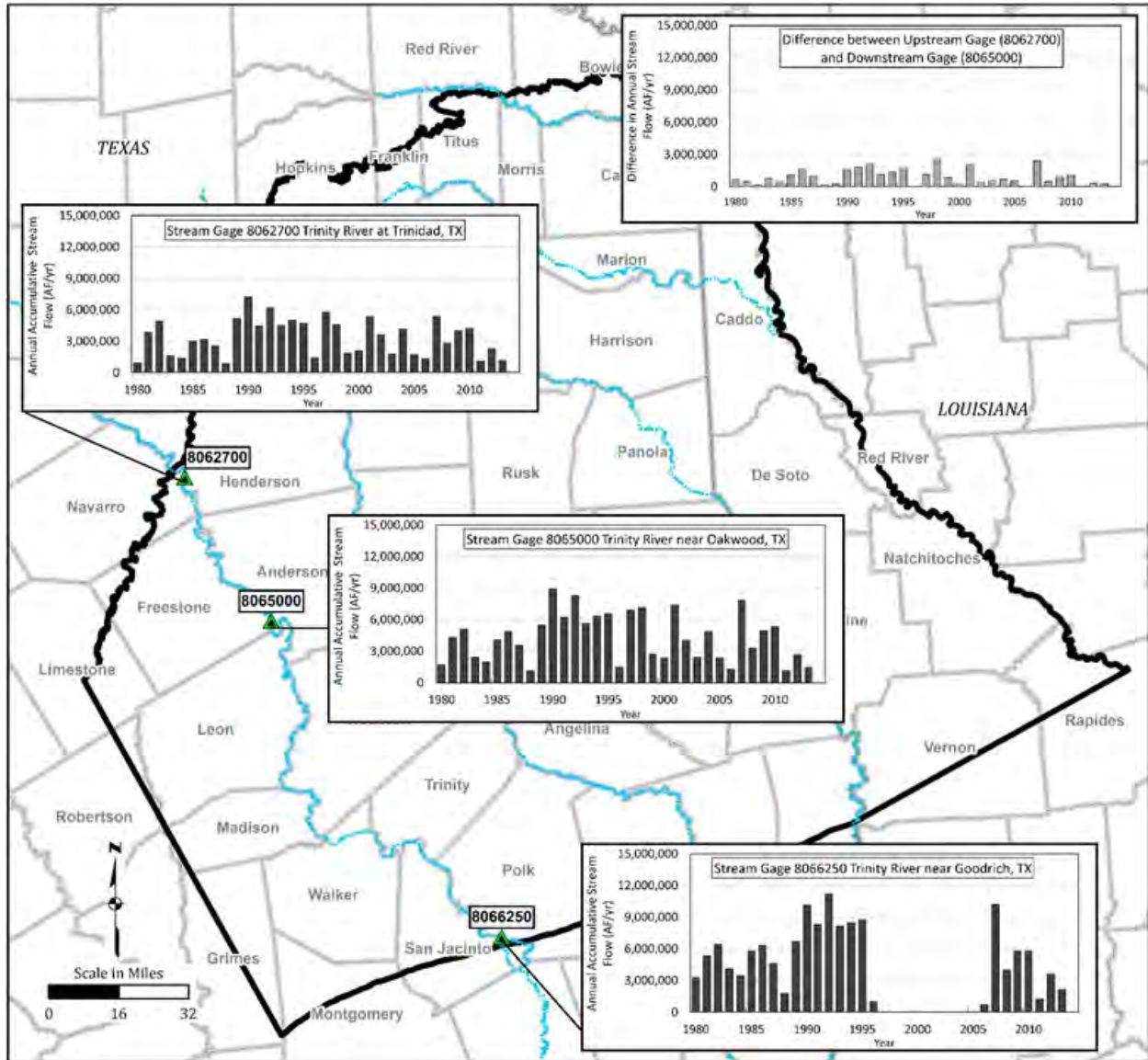
Preliminary model simulations used the Stream (STR) package of MODFLOW 6. However, the simulations encountered long runtimes and occasional convergence difficulties. Because the river flow is managed with controlled releases from the area reservoirs, estimating reliable baseflow values for the gaged reaches is difficult. The RIV package is able to satisfy the objectives of the project with these data limitations.

2.10 Recharge Package

The Recharge (RCH) package was used to simulate recharge. Estimation of recharge from percolation of precipitation was evaluated during conceptual model development. Annual average recharge rates were estimated to be up to 2.5 inches per year over the model area with recharge being proportional to the hydraulic conductivity of the outcrop material, as described in the Conceptual Model Report (Montgomery and Associates, 2020).

Table 2.8-1. General Head Boundary Conditions

Layer	Hydrostratigraphic Unit	Number of GHB Cells	GHB Head (feet)	GHB Conductance (feet/day)	Hydraulic Feature
Layer 2	Sparta Aquifer	59,512	min = 52.864	min = 0.378125	Interaction with the Younger Units
			max = 482.014	max = 83.83	
Layer 4	Queen City Aquifer	244	min = 150	90.961681	Lateral boundary
			max = 179.61772		
Layer 6	Carrizo Aquifer	241	min = 150.225917	993.24725	Lateral boundary
			max = 224.730862		
Layer 7	Upper Wilcox	240	min = 75.047346	10.839841	Lateral boundary
			max = 174.242096		
Layer 8	Middle Wilcox	234	min = 0	11.325211	Lateral boundary
			max = 118.782266		
Layer 9	Lower Wilcox	236	min = 50	58.1002	Lateral boundary
			max = 118.377152		



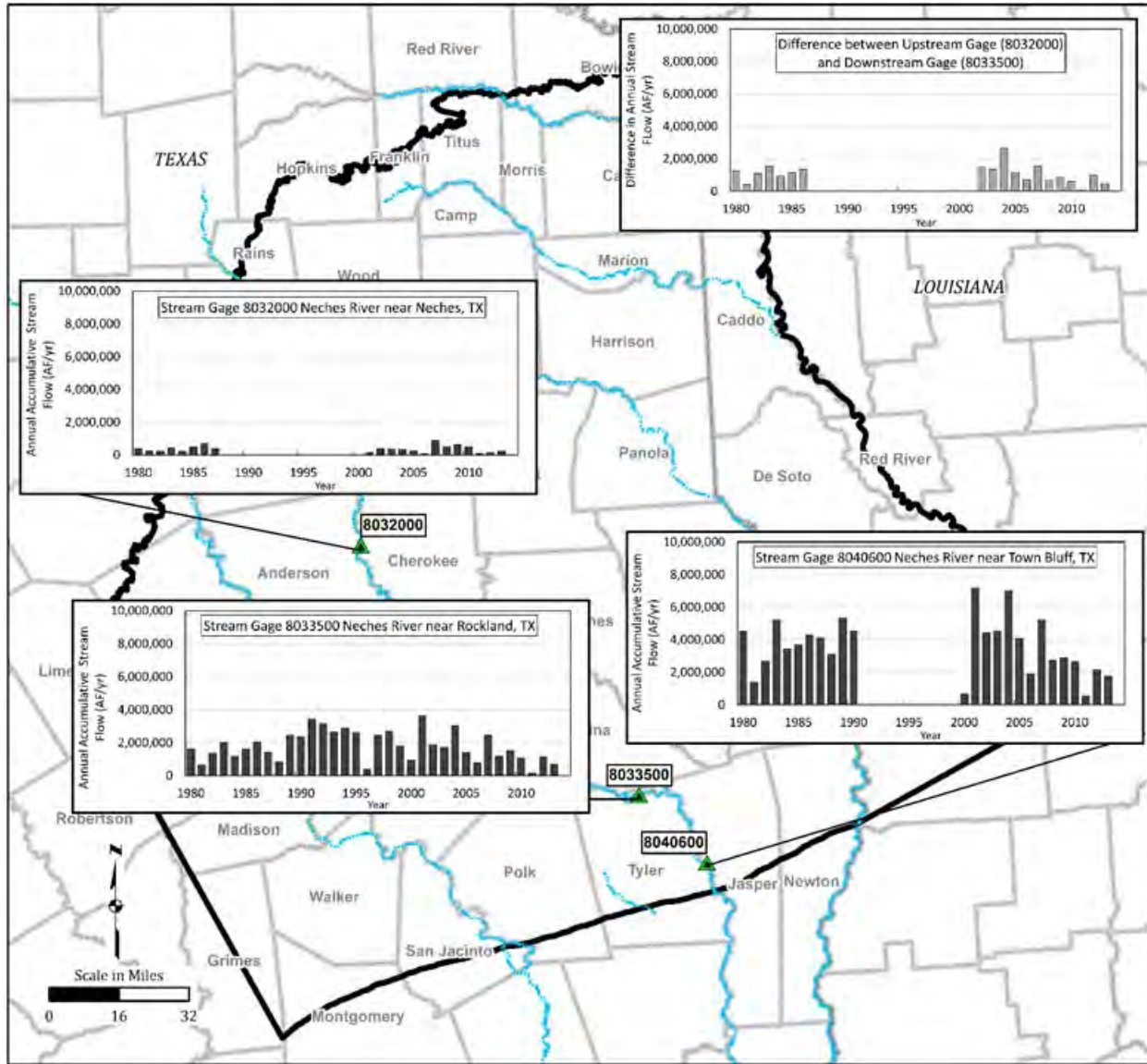
LEGEND

- USGS Stream Gage
- River
- Model Boundary
- County or Parish Boundary

Notes:

1. USGS = United States Geological Survey
2. AF/yr = acre-feet per year
3. Projected Coordinate System
Datum: GAM

Figure 2.9-1. Estimated Annual Streamflows for Trinity River



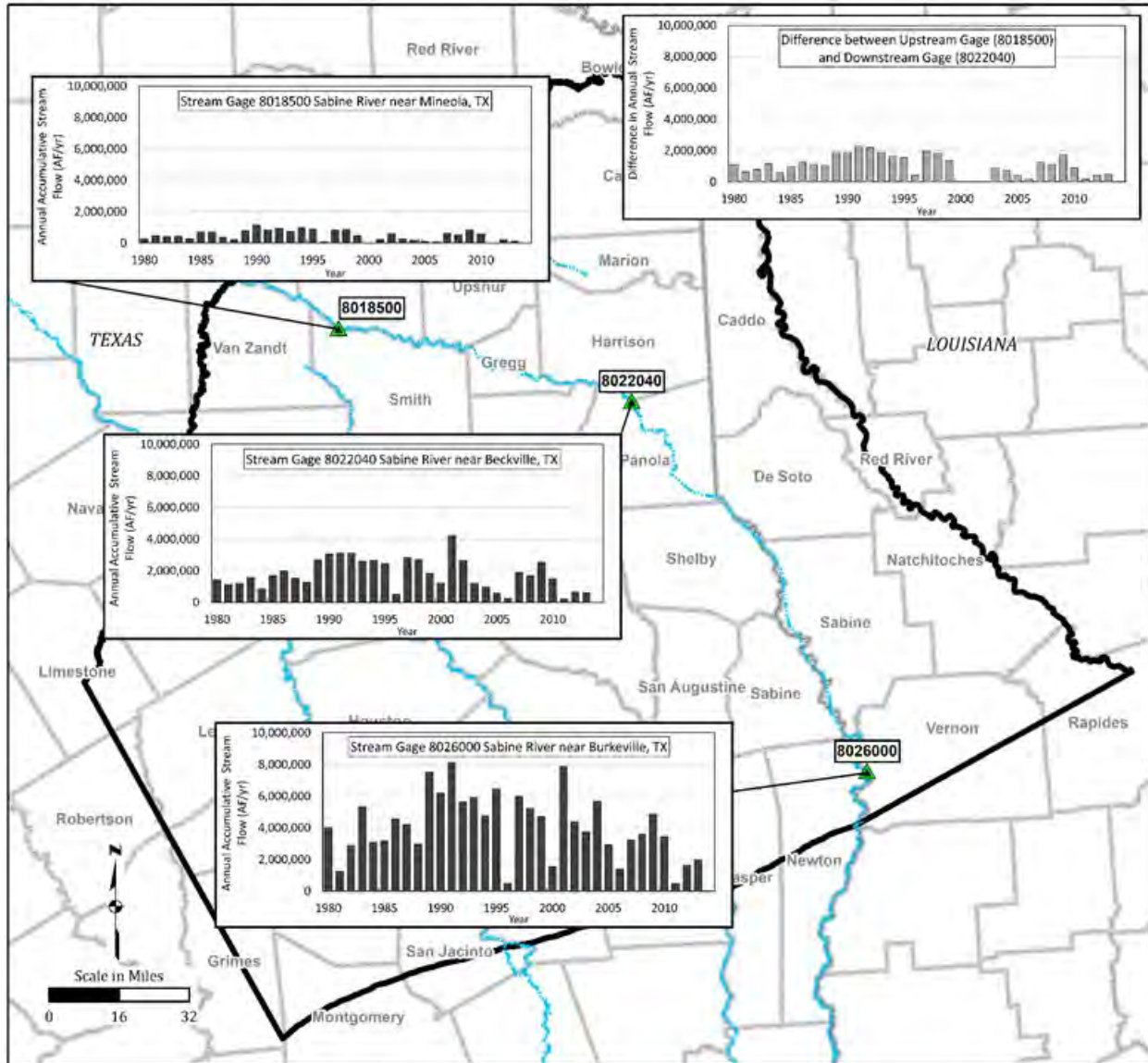
LEGEND

- USGS Stream Gage
- River
- Model Boundary
- County or Parish Boundary





Notes:

1. USGS = United States Geological Survey
2. AF/yr = acre-feet per year
3. Projected Coordinate System
Datum: GAM

Figure 2.9-2. Estimated Annual Streamflows for Neches River



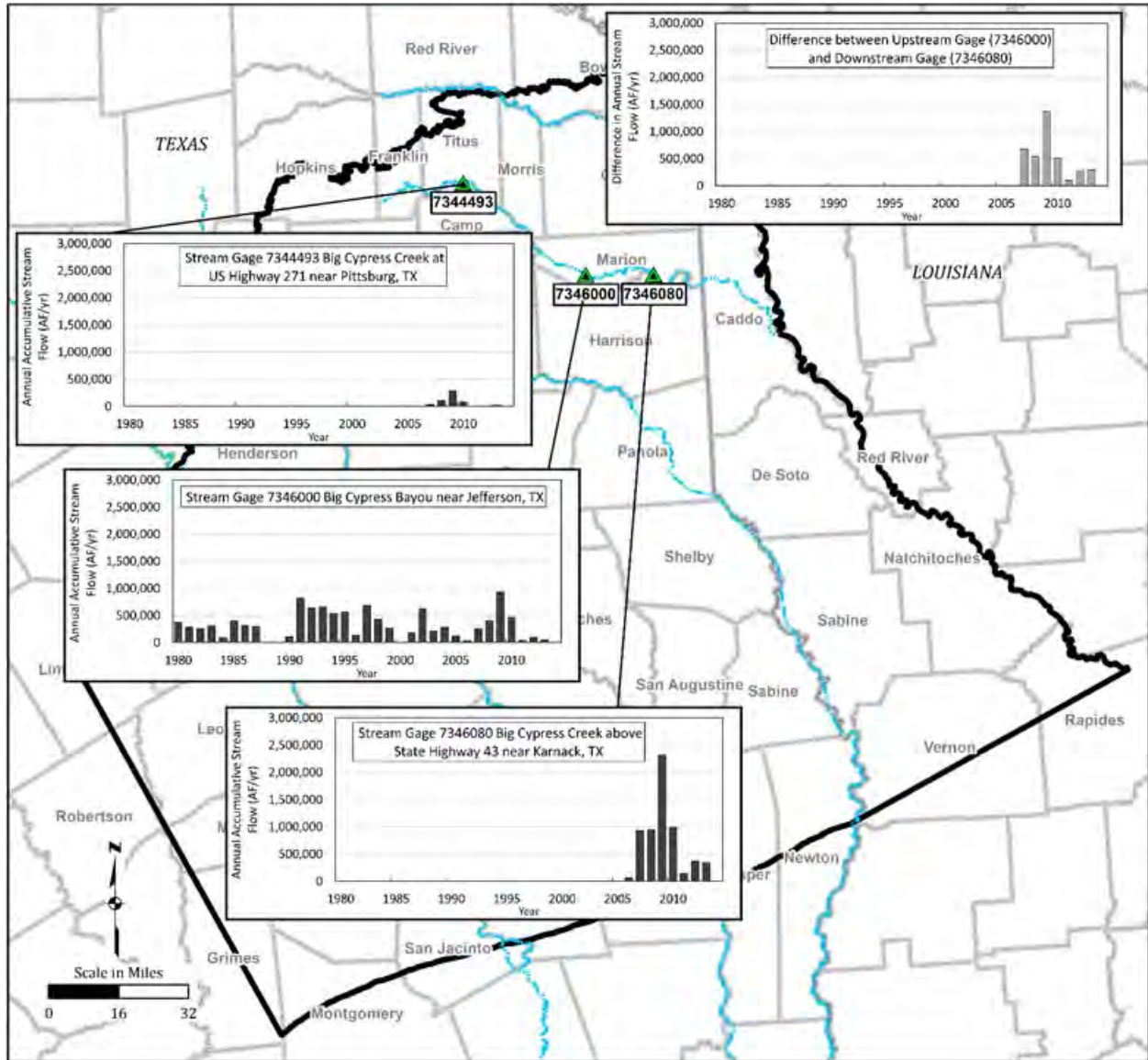
LEGEND

-  USGS Stream Gauge
-  River
-  Model Boundary
-  County or Parish Boundary

Notes:

1. USGS = United States Geological Survey
2. AF/yr = acre-feet per year
3. Projected Coordinate System
Datum: GAM

Figure 2.9-3. Estimated Annual Streamflows for Sabine River



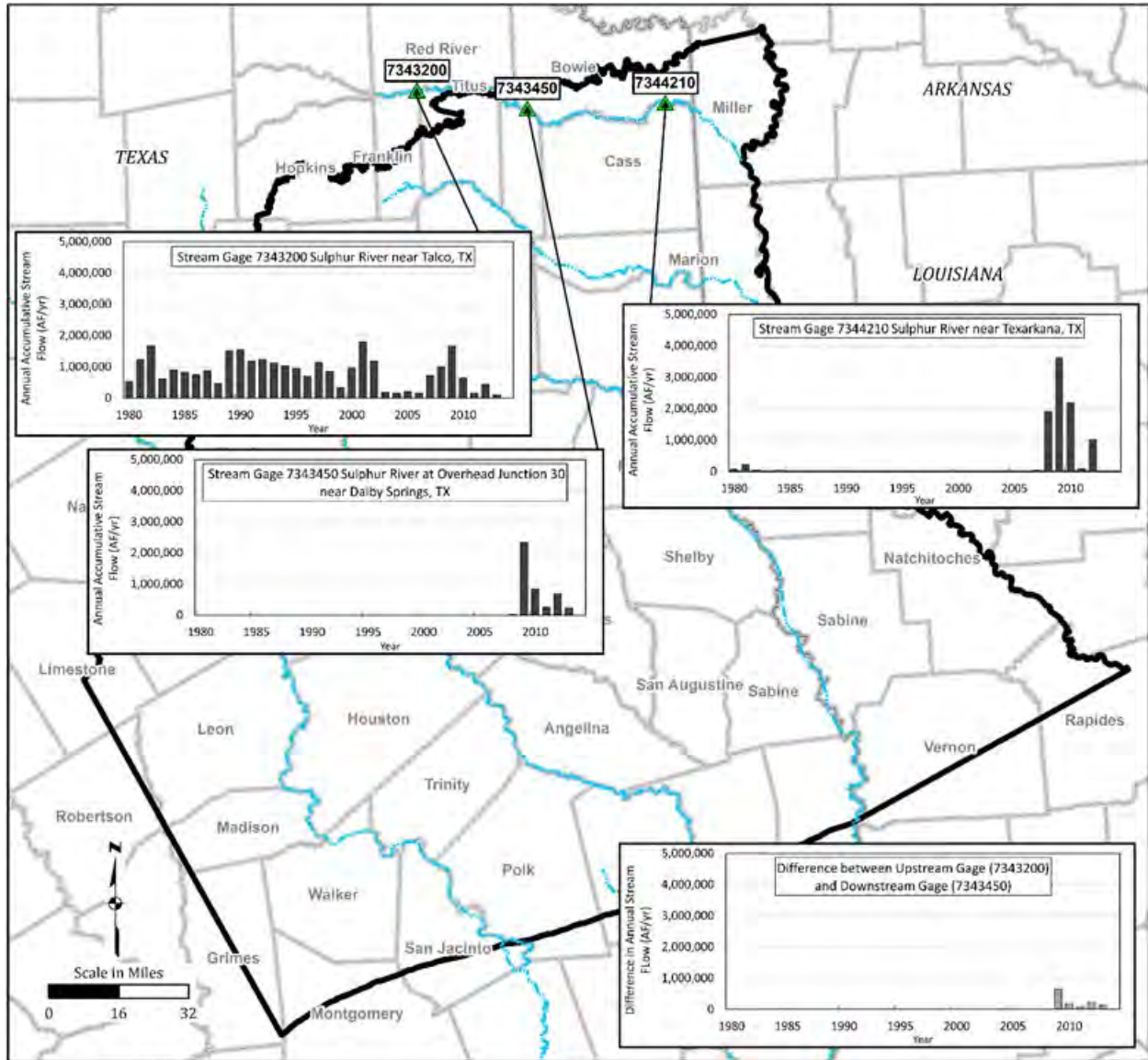
LEGEND

- USGS Stream Gage
- River
- Model Boundary
- County or Parish Boundary

Notes:

1. USGS = United States Geological Survey
2. AF/yr = acre-feet per year
3. Projected Coordinate System Datum: GAM

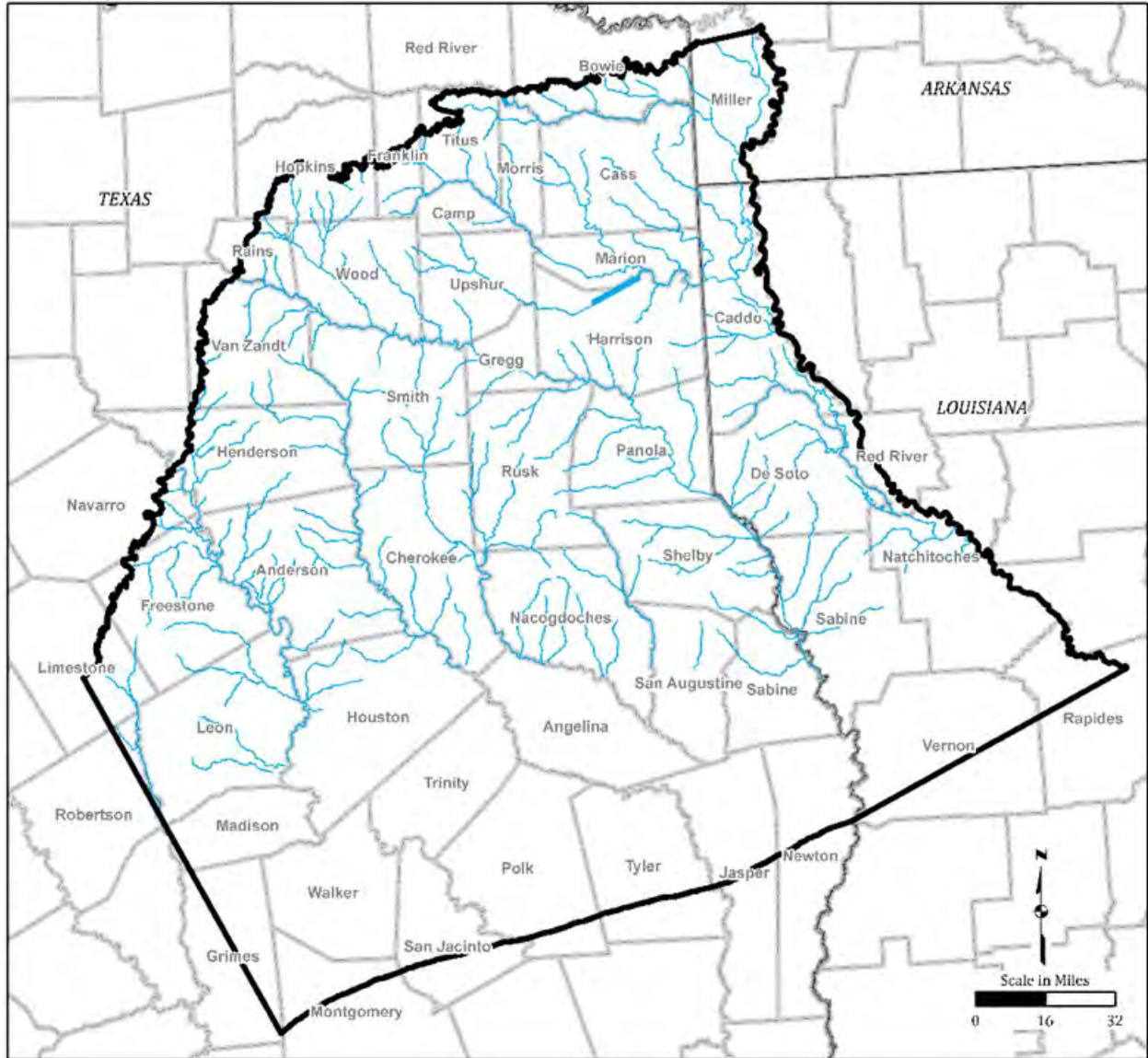
Figure 2.9-4. Estimated Annual Streamflows for Big Cypress Creek






- LEGEND**
- USGS Stream Gage
 - River
 - Model Boundary
 - County or Parish Boundary

- Notes:**
1. USGS = United States Geological Survey
 2. AF/yr = acre-feet per year
 3. Projected Coordinate System
Datum: GAM

Figure 2.9-5. Estimated Annual Streamflows for Sulphur River



LEGEND

-  Model Boundary
-  County or Parish Boundary
-  River Boundary Conditions

Note:

1. Projected Coordinate System
Datum: GAM

Figure 2.9-6. Simulated River Boundary Conditions

Figure 2.10-1 shows the model 1980 recharge rates which represent annual average estimates of recharge within the domain and across the various aquifers that crop out at the surface. Since recharge is related to hydraulic conductivity of the material, the recharge spatial distribution was noted to be generally similar between years, with locations of higher recharge having higher recharge throughout the simulation period. Therefore, the 1980 recharge distribution shown on Figure 2.10-1 was used as the basis for model recharge and was scaled for subsequent years to represent greater or lower precipitation.

The recharge scaling factors developed for 1981 through 2013 were used as initial recharge conditions in the model (Table 2.10-1). Initial recharge scaling factors are also charted on Figure 2.10-2. Groundwater Vistas allows import of these as “multiplication factors” applied to the 1980 recharge conditions and this produces the initial recharge values for years 1981 through 2013 in the model. The recharge values were implemented in MODFLOW 6 via the RCH package, with recharge applied to the topmost active cell as computed by Groundwater Vistas.

2.11 Evapotranspiration Package

The Evapotranspiration (EVT) package of MODFLOW 6 was used to apply evapotranspiration to the model. The EVT package applies a Potential Evapotranspiration (PET) flux (in units of length per time) to each associated model cell in the domain. The actual evapotranspiration flux depends on a user-defined PET that is applied to each cell when the water table is at or above the “evapotranspiration surface” of that cell (taken equal to the land surface elevation). The PET declines linearly to zero as the water table depth drops down to an “extinction depth”.

Estimation of PET and the extinction depth are discussed in the conceptual model. The distribution of maximum evapotranspiration rates in the model is shown on Figure 2.11-1. Evapotranspiration was applied to the topmost active cell as computed by Groundwater Vistas.

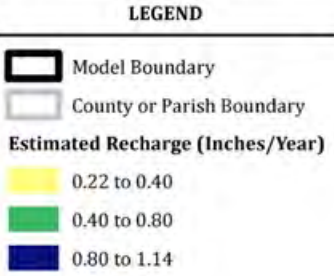
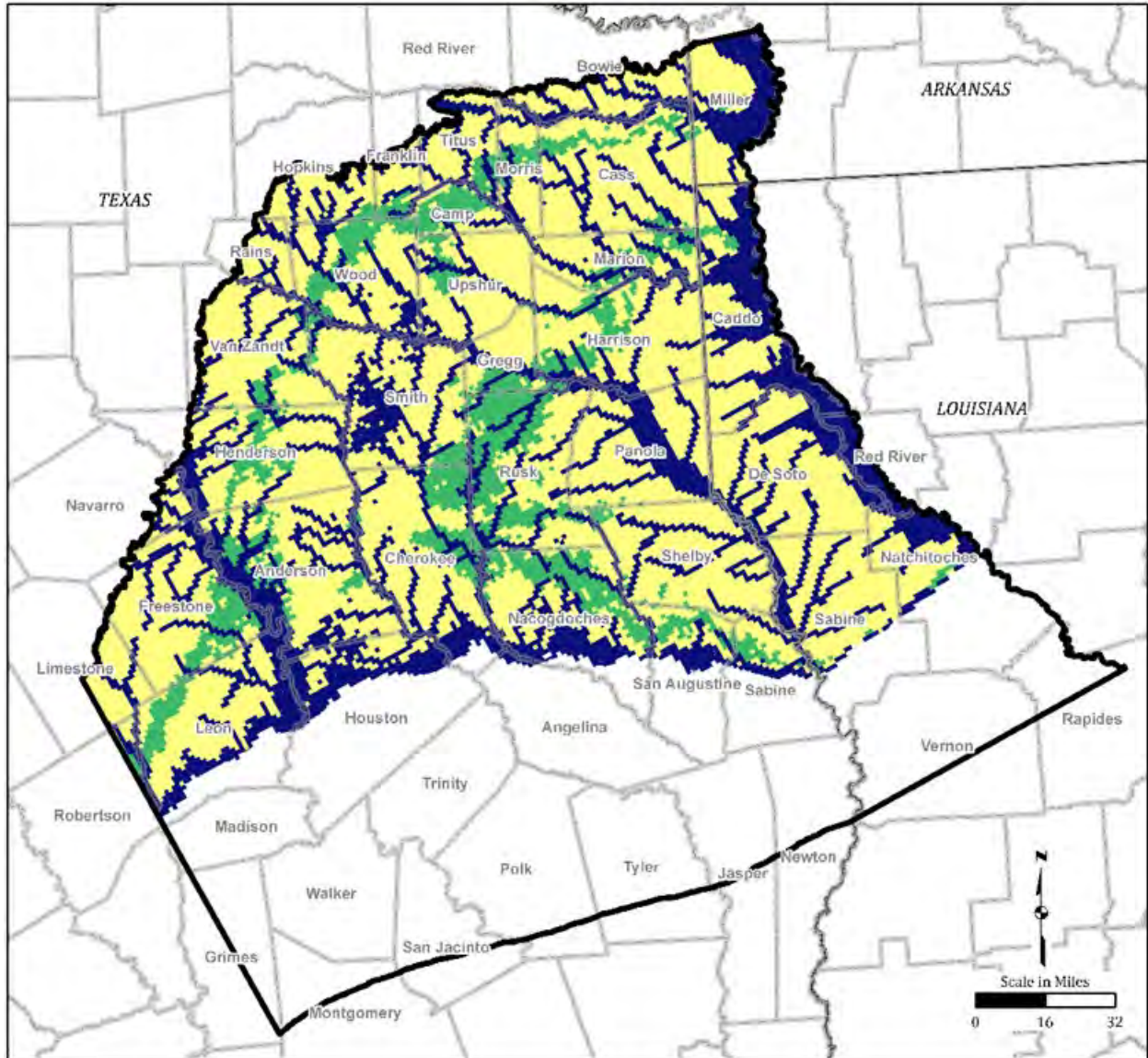
2.12 Output Control Package

The Output Control (OC) package of MODFLOW 6 controls how water levels, fluxes, and water budget information are saved during a simulation. The Output Control file was set up to save these results at the end of each stress period. Thus, output was provided for the steady-state 1980 stress-period and at the end of each year of the 1980 to 2013 transient simulation period.

2.13 Iterative Matrix Solver Package

The Iterative Matrix Solver (IMS) package of MODFLOW 6 sets up the solution methodologies and linear solver selection for a simulation.

Nonlinear iterations using the Newton-Raphson linearization scheme were controlled using residual reduction and under-relaxation. The under-relaxation parameters that are a default for MODFLOW 6 (the default parameters in Groundwater Vistas interface reflect these parameter values) are not very sensitive and were not changed for the simulations. The residual reduction parameters are generally tightened when nonlinear convergence



Note:
 1. Projected Coordinate System
 Datum: GAM

Figure 2.10-1. Distribution of Average Estimated Annual Recharge Rates for 1980

Table 2.10-1. Recharge Multiplication Factors

Stress Period	Representative Year	Recharge Multiplier
1	1980	1
2	1981	1
3	1982	0.9235
4	1983	0.9627
5	1984	0.9988
6	1985	0.9669
7	1986	0.7067
8	1987	1.0482
9	1988	1.1294
10	1989	1.2864
11	1990	1.0412
12	1991	0.9706
13	1992	1.147
14	1993	0.9042
15	1994	0.8246
16	1995	1.152
17	1996	1.0659
18	1997	0.8142
19	1998	1.0351
20	1999	1.2623
21	2000	1.0902
22	2001	0.8916
23	2002	1.256
24	2003	0.6938
25	2004	0.99031
26	2005	1.0678
27	2006	0.967
28	2007	1.1605
29	2008	0.6912
30	2009	0.6571
31	2010	0.9698
32	2011	0.9923
33	2012	0.8996
34	2013	1.4333

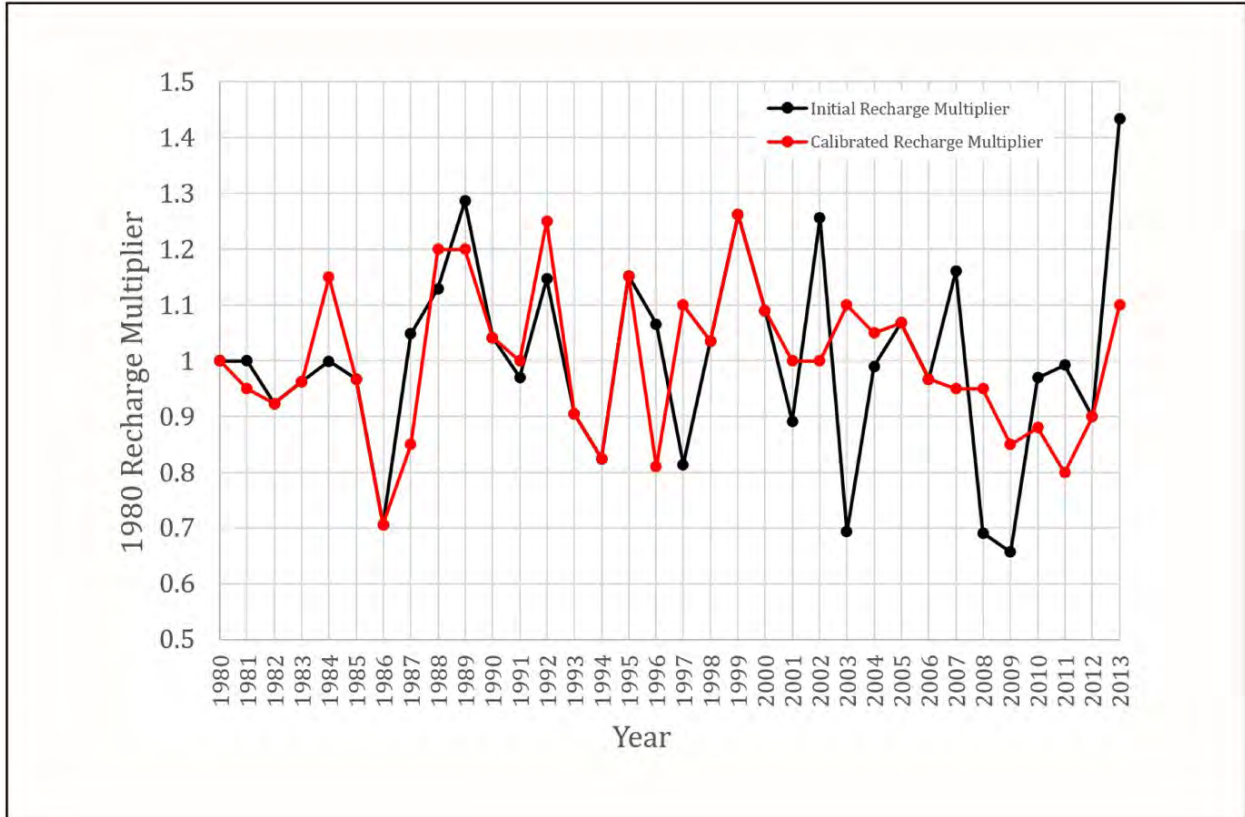
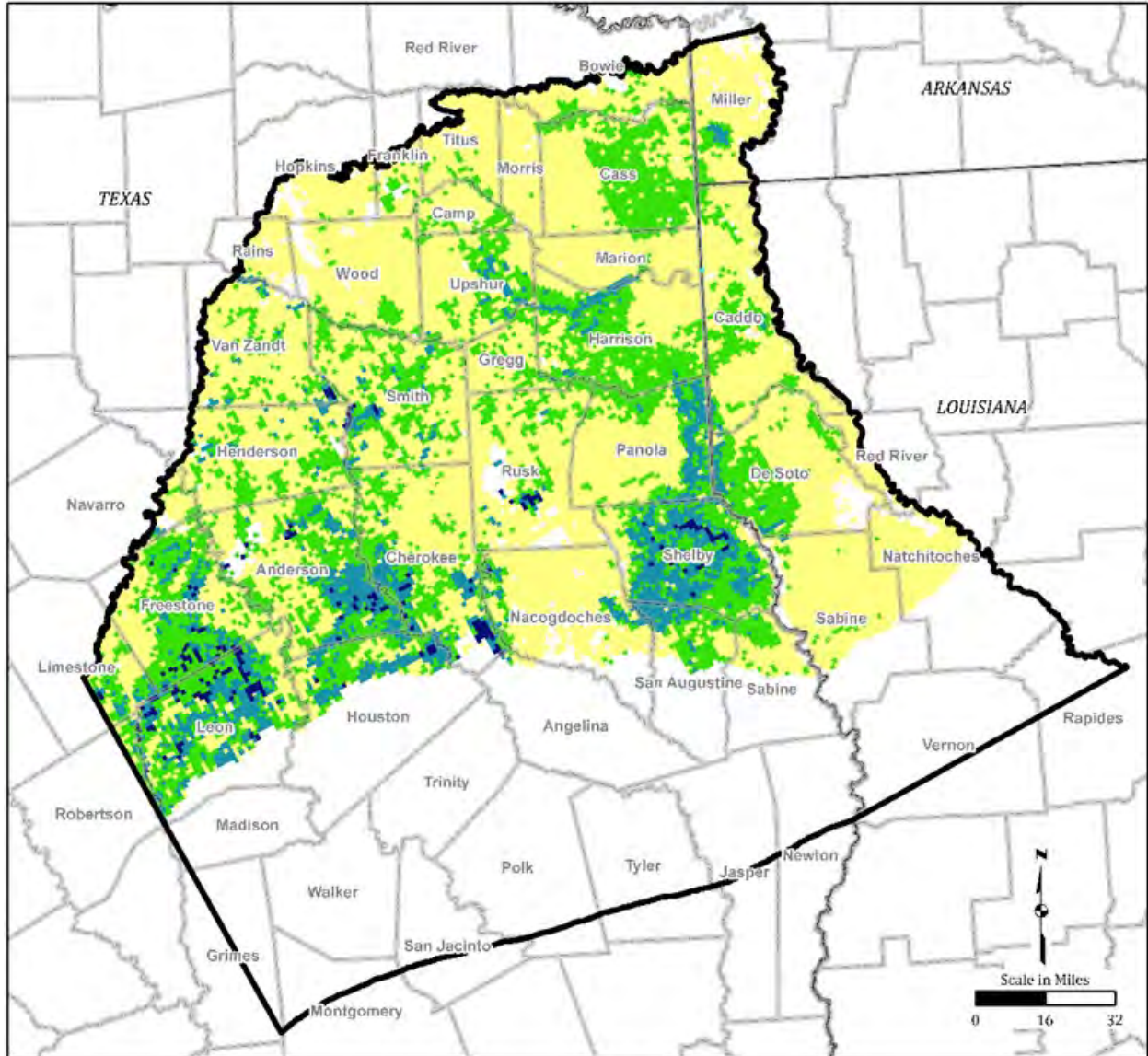

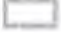






Figure 2.10-2. Model Precipitation Multipliers 1980 to 2013



LEGEND

-  Model Boundary
-  County or Parish Boundary
- Maximum Modeled Evapotranspiration Rate (Feet/Day)
 -  0 to 0.001
 -  0.001 to 0.002
 -  0.002 to 0.003
 -  0.003 to 0.0038

Note:

1. Projected Coordinate System
Datum: GAM

Figure 2.11-1. Distribution of Modeled Maximum Evapotranspiration Rates

difficulties are encountered but are relaxed when convergence eases. Specifically, the residual change tolerance term (BACKTRACKING_TOLERANCE) was varied between 10,000 and 1.1 at various stages of simulation. The final optimal value selected was 1.1.

The BiCGSTAB scheme was selected to solve the asymmetric system of linear equations. Linear solver parameters that were significant to the simulation included the matrix ordering scheme (REORDERING_METHOD), the level of fill (PRECONDITIONER_LEVELS), and number of orthogonal directions (NUMBER_ORTHOGONALIZATIONS). These parameters were varied depending on convergence behavior during calibration. Final calibrated simulation values were: PRECONDITIONER_LEVELS = 3; the RCM Ordering scheme; and NUMBER_ORTHOGONALIZATIONS = 14. The “drop tolerance” scheme was used with a drop-tolerance factor (PRECONDITIONER_DROP_TOLERANCE) equal to 1.0×10^{-3} .

Solver parameter tuning was done throughout model development and calibration. This was done to make sure that the simulations progressed as quickly as possible at every stage of the project.

3.0 Model Calibration and Results

The model was constructed as discussed above in Section 2. Upon model construction and prior to calibration, the model contained initial estimates for hydraulic conductivity, recharge rates, specific storage and specific yield, and general head boundary conditions. Preliminary simulations confirmed the model was appropriately assembled and showed the model could be executed successfully. Model behavior and sensitivity were also evaluated. Solver parameters were adjusted for robustness and efficiency and were tuned throughout the calibration process.

During model calibration, the recharge rates were adjusted within reasonable ranges to provide appropriate fluctuations in water levels; the hydraulic conductivity values for sand and clay were adjusted within reasonable parameter value bounds to provide appropriate flow behavior in the model domain; the specific storage and specific yield values of the units were adjusted within reasonable parameter value bounds to provide appropriate magnitude of fluctuations of water levels; and the conductance values for the general head boundary conditions in layers 2, 4, and 6 through 9 were adjusted within reasonable parameter values to provide appropriate fluxes into and out of the model domain.

The model was calibrated using an interactive expert approach (manual calibration evaluations) in conjunction with automatic model calibration using the parameter estimation code PEST (Doherty, 2010). Consistency with the conceptual model was also evaluated and adjustments were made to model aquifer parameters or conceptual elements until the model was considered calibrated. The model was further calibrated in response to comments received from TWDB dated November 4, 2020. Specifically, the hydraulic conductivity of the Carrizo Aquifer was increased from 0.12 feet per day (ft/day) to 7.04 ft/day to better match the observed range; and the calibration statistics were improved for the Queen City Aquifer (model layer 4) by moving eight target wells into the layers above (model layer 2) and below (model layer 6). Also, model layer 2 was updated

in the south to only reflect the thickness of the Sparta Aquifer (omitting the thickness of the Younger Units).

The model calibration procedure and results are described in sections below and in calibration figures and tables included in this report. Report appendices provide detailed modeling results. Appendix A contains the water budget for Texas Groundwater Conservation Districts or Texas counties in the model domain. Appendix B contains the final simulated groundwater elevation at individual wells and hydrographs of wells with thirty or more observed water level elevation measurements. Hydrographs compare the final calibrated model and the draft calibrated model. Appendix C presents the draft calibration model (prior to TWDB comments) and supporting documentation. Appendices D, E, and F present the model predictive simulations. Appendix G presents an evaluation of model pumping input and output. Appendix H shows comments received from TWDB and how each were addressed.

3.1 Calibration Procedures

This section discusses the methods used to calibrate the model and the calibration parameters: recharge, aquifer parameters, and GHBs. Measured groundwater level elevations were used to constrain the simulation results and calibration parameter adjustments.

Estimates of groundwater to surface-water flux in five Texas rivers were not used to constrain model calibration but were used to evaluate the final calibration. Baseflow in streams (movement of water between the stream and groundwater) is largely unknown and differences between river gages can reflect volume changes other than baseflow. Baseflow estimates can be obtained by evaluating recession hydrographs at stream gages after storms at different times of the year and for different years but this information was not available for the numerical model.

To aid calibration of hydraulic conductivity and GHB properties, a two-period steady-state model representing 1980 and 2013 conditions was used. This two-period model's short run times allowed calibration of selected properties using the automatic calibration method PEST.

The transient model, spanning 1980 through 2013, was calibrated to match water level fluctuations due to recharge and pumping, and to match the amplitude of water level elevations changes which are controlled by storage parameters of the aquifer materials. Calibration efforts showed there were significant issues with the pumping data resulting in replacing the TWDB database pumping with the previous groundwater availability model pumping (Kelley and others, 2004), as discussed in Section 2.7.

3.1.1 Calibration of Recharge

Recharge rates for each stress period were based on 1980 recharge rates and spatial distribution, as discussed in Section 2.10; individual stress period recharge multiplication factors were adjusted during calibration to best fit observed groundwater level elevations. As discussed in the Conceptual Model Report, annual average recharge rates were estimated to be up to 2.5 inches per year over the model area.

Adjustments during calibration were driven by observation wells in outcrop areas of aquifers (unconfined wells) as these are sensitive to recharge values. The calibrated recharge multiplication factors are summarized on Table 3.1-1 and charted on Figure 2.10-2. These values averaged to unity over the simulation period as did the pre-calibration estimated recharge factors in Table 2.10-1.

The predictive drawdown simulation presented in Appendix F does not use the 2013 recharge values from the calibrated model but uses the 1980 steady-state recharge based on a sensitivity analysis of the calibrated recharge (Appendix D). Thus, ending the model in 2013 does not have a significant impact on the predictive simulations.

3.1.2 Calibration of Aquifer Parameters

As discussed in Section 2.5, the horizontal and vertical hydraulic conductivities were parameterized using two datasets: the sand fraction within each simulated geologic layer, with the remaining fraction assumed to be clay; and hydraulic conductivity estimates for sand and clay in each of layer. Within Groundwater Vistas, each model layer horizontal hydraulic conductivity was calculated using the sand fraction and sand estimated hydraulic conductivity; each layer vertical hydraulic conductivity was calculated using the clay fraction and clay estimated hydraulic conductivity. Equations are provided in Section 2.5.

The hydraulic conductivity values for sand and clay were calibrated using PEST and adjusted manually to best fit observed groundwater level elevations. The two-period steady-state model was used for the PEST simulations. Though the 1980 and 2013 periods do not represent steady-state conditions, water level elevations were relatively stable during these two years, making them useful for estimating hydraulic conductivity. The resulting hydraulic conductivity values were considered reliable as the two-period model represented different stress conditions.

The PEST results were transferred to the transient model where further manual calibration was performed including evaluation of aquifer storage parameters. The model-wide specific storage and specific yield were adjusted manually resulting in calibrated values of 3.898×10^{-8} and 0.0007, respectively. The specific storage value reflects compressibility of water but not the matrix and therefore represents a low end of values. Water level fluctuations were best represented by lower values of the storage terms during the calibration process. The low specific yield value indicates there may be partial confinement of the aquifer system even in the outcrop (unconfined) regions. However, the sensitivity analyses later determined that simulated water level elevations were not overly sensitive to storage parameters and that the storage terms effect on the nature and magnitude of fluctuations was small. and that higher values provide similar results.

As discussed in Section 3.0, an initial draft model calibration was reviewed by TWDB and revised for further hydraulic conductivity and layering adjustment after comments. This draft model is provided in Appendix C as a technical report and supporting files.

Table 3.1-2 shows the calibrated model horizontal and vertical hydraulic conductivities. These are based on the final parameterized hydraulic conductivity values for sand and clay of the various layers and the layer sand fractions, also shown on the table. The calibrated

horizontal and vertical hydraulic conductivity distributions for model geologic units are shown in Figures 3.1-1 through 3.1-10.

The calibrated sand fraction within the Quaternary Alluvium (model layer 1) and the Carrizo Aquifer (model layer 6) was assumed to be uniform at 0.7, resulting in calibrated horizontal hydraulic conductivity values of 21.97 feet/day and 7.04 feet/day, respectively,

Table 3.1-1. Calibration of Recharge Multiplication Factors

Stress Period	Representative Year	Recharge Multiplier
1	1980	1
2	1981	0.95
3	1982	0.9235
4	1983	0.9627
5	1984	1.15
6	1985	0.9669
7	1986	0.7067
8	1987	0.85
9	1988	1.2
10	1989	1.2
11	1990	1.0412
12	1991	1
13	1992	1.25
14	1993	0.9042
15	1994	0.8246
16	1995	1.152
17	1996	0.81
18	1997	1.1
19	1998	1.0351
20	1999	1.2623
21	2000	1.0902
22	2001	1
23	2002	1
24	2003	1.1
25	2004	1.05
26	2005	1.0678
27	2006	0.967
28	2007	0.95
29	2008	0.95
30	2009	0.85
31	2010	0.88
32	2011	0.8
33	2012	0.9
34	2013	1.1

Note:

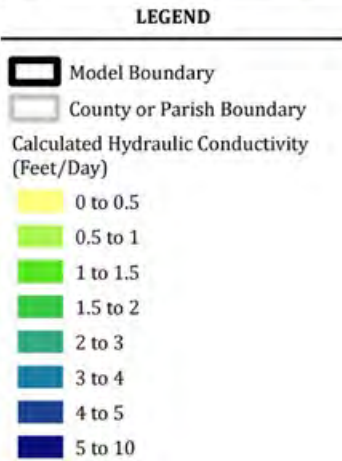
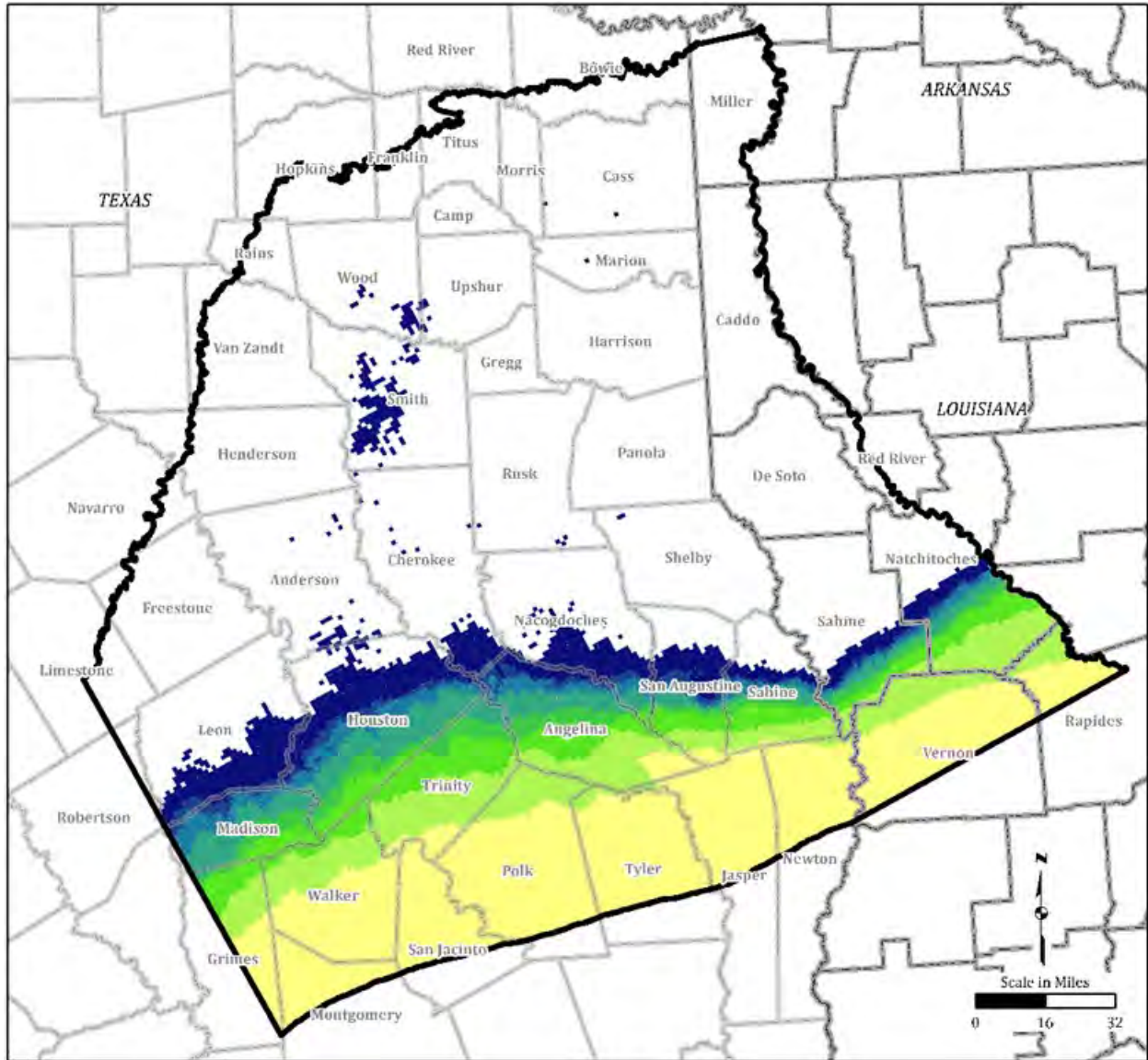
Multiplication factors modified during calibration are indicated in bold font.

Table 3.1-2. Calibrated Hydraulic Conductivity for Modeled Geologic Units

Model Layer	Hydrostratigraphic Unit	Model Sand Fraction	Parameterized Hydraulic Conductivity Values (feet per day)		Calibrated Model Hydraulic Conductivity (feet per day)		Conceptual Model Estimated Hydraulic Conductivity (feet per day)	
			Sand	Clay	Horizontal	Vertical	Range	Geometric Mean
1	Quaternary Alluvium	0.70	30	3.24	21.97	8.62	1 - 1000	165
2	Sparta Aquifer	0.05 to 0.95	10	4.50E-05	0.50 to 9.50	4.74E-05 to 9.00E-04	1 - 808	14
3	Weches Formation	0.10	1	6.70E-05	0.10	7.44E-05	0.2 - 65	5
4	Queen City Aquifer	0.05 to 0.95	7	8.46E-02	0.43 to 6.65	0.09 to 1.38	0.1 - 451	5
5	Reklaw Formation	0.10	2.55E-01	1.00E-05	0.03	1.11E-05	0.05 - 385	5
6	Carrizo Aquifer	0.70	10	1.31E-01	7.04	4.23E-01	0.3 - 198	6
7	Upper Wilcox	0 to 0.95	4.06	3.94	3.94 to 4.06	3.94 to 4.06	0.06 - 278	4
8	Middle Wilcox	0.05 to 0.95	8.77	3.70E-05	0.44 to 8.34	3.89E-05 to 7.40E-04	0.04 - 671	4
9	Lower Wilcox	0.05 to 0.95	2.31	1.67E-03	0.12 to 2.19	1.76E-03 to 3.30E-02	0.01 - 97	3

Notes:

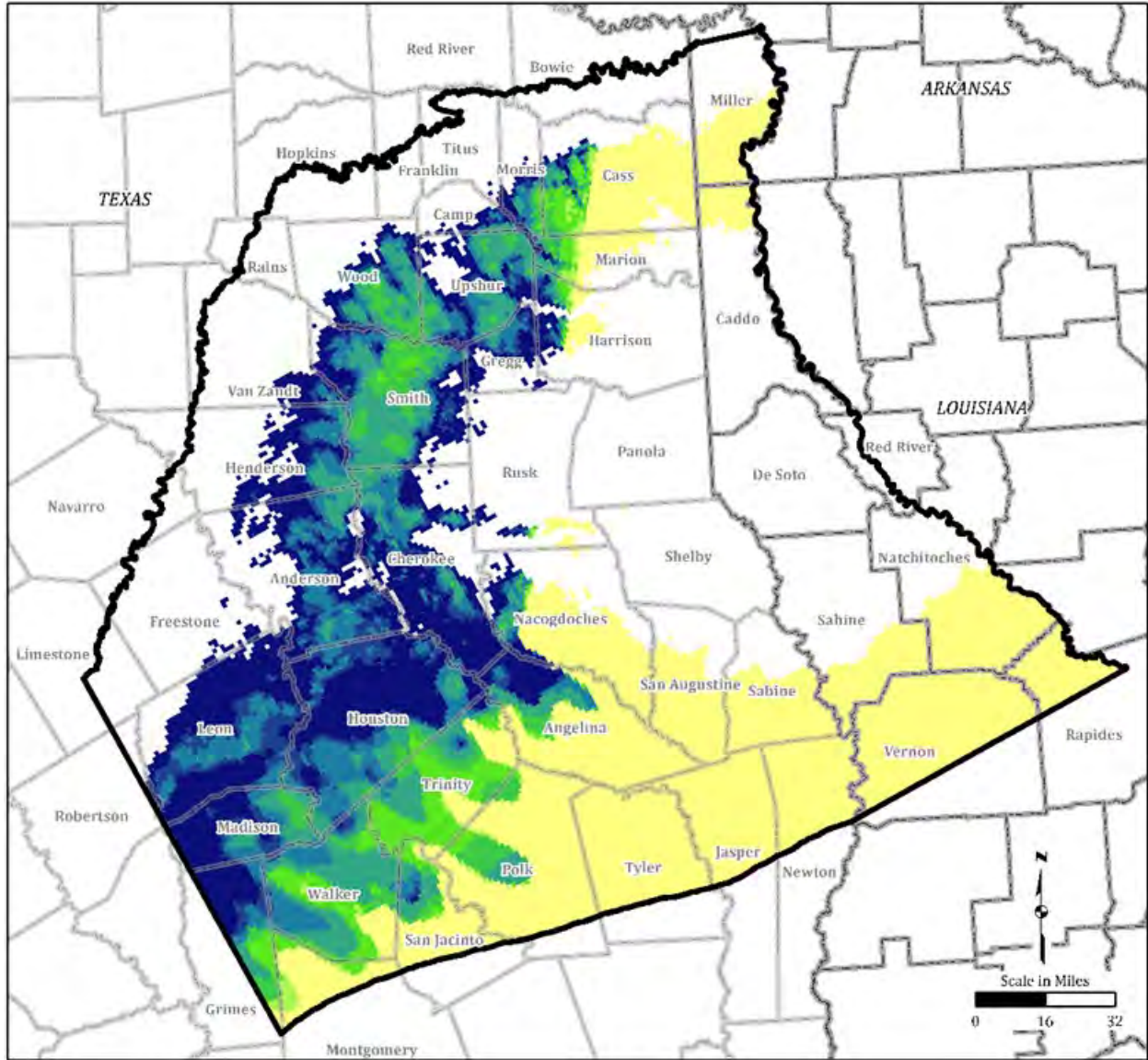
1. Calibrated horizontal and vertical hydraulic conductivities are based on sand fraction and parameterized hydraulic conductivity values. Equations for calculating horizontal and vertical hydraulic conductivity are discussed in Section 3.1.
2. Estimated hydraulic conductivities are from the 2020 Conceptual Model Report (Montgomery and Associates, 2020).



Notes:

1. The layer contains discontinuous outcrops, consistent with the conceptual model (Section 2).
2. Projected Coordinate System Datum: GAM.

Figure 3.1-1. Calculated Horizontal Hydraulic Conductivity for Sparta Aquifer (Model Layer 2)

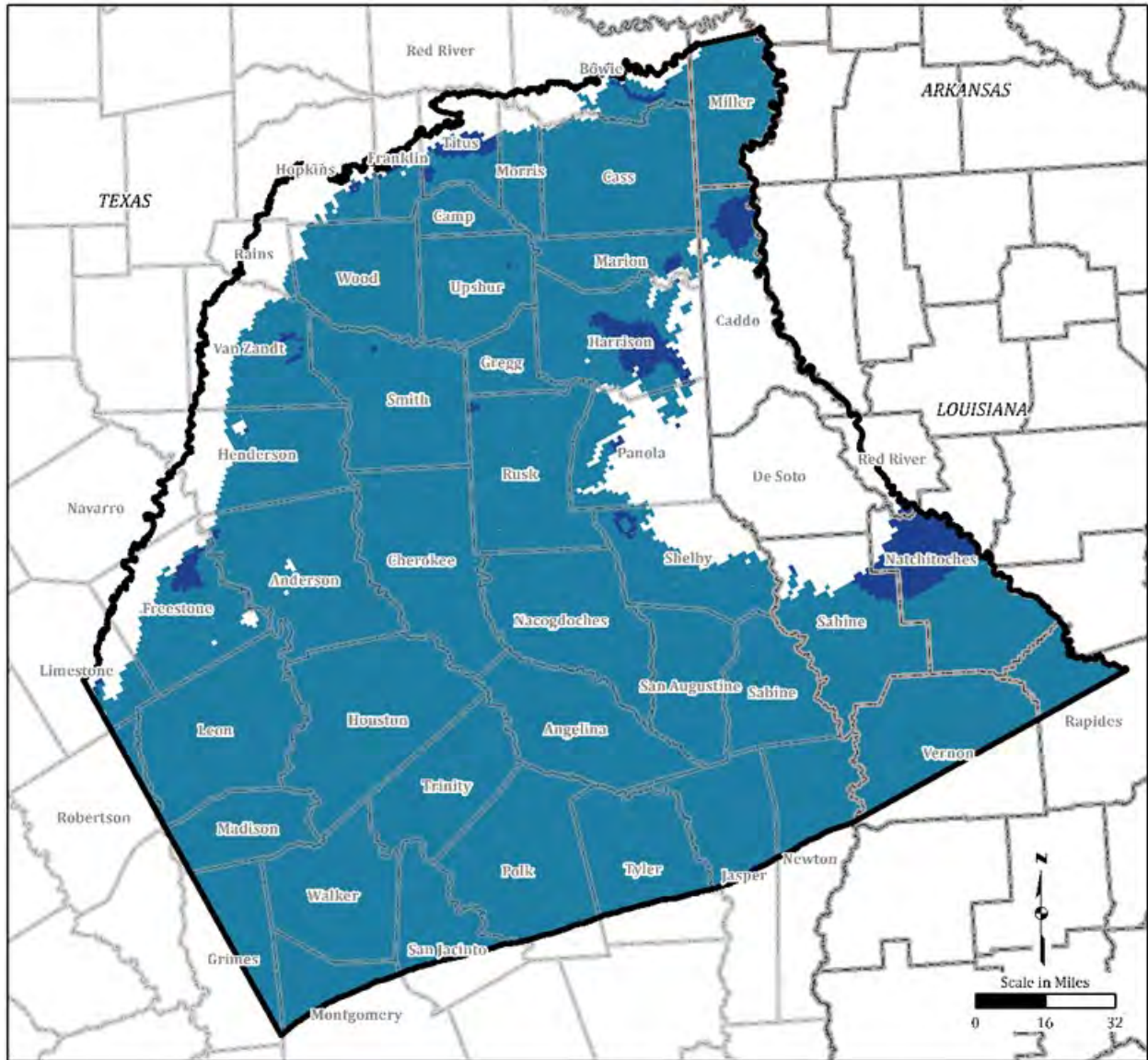


LEGEND

- Model Boundary
- County or Parish Boundary
- Calculated Hydraulic Conductivity (Feet/Day)
- 0 to 0.5
- 0.5 to 1
- 1 to 1.5
- 1.5 to 2
- 2 to 3
- 3 to 4
- 4 to 5
- 5 to 10

- Notes:**
1. The layer contains discontinuous outcrops, consistent with the conceptual model (Section 2).
 2. Projected Coordinate System Datum: GAM.

Figure 3.1-2. Calculated Horizontal Hydraulic Conductivity for Queen City Aquifer (Model Layer 4)

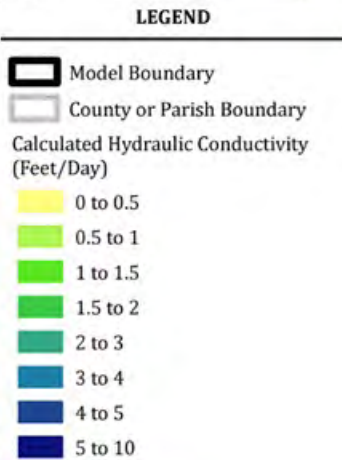
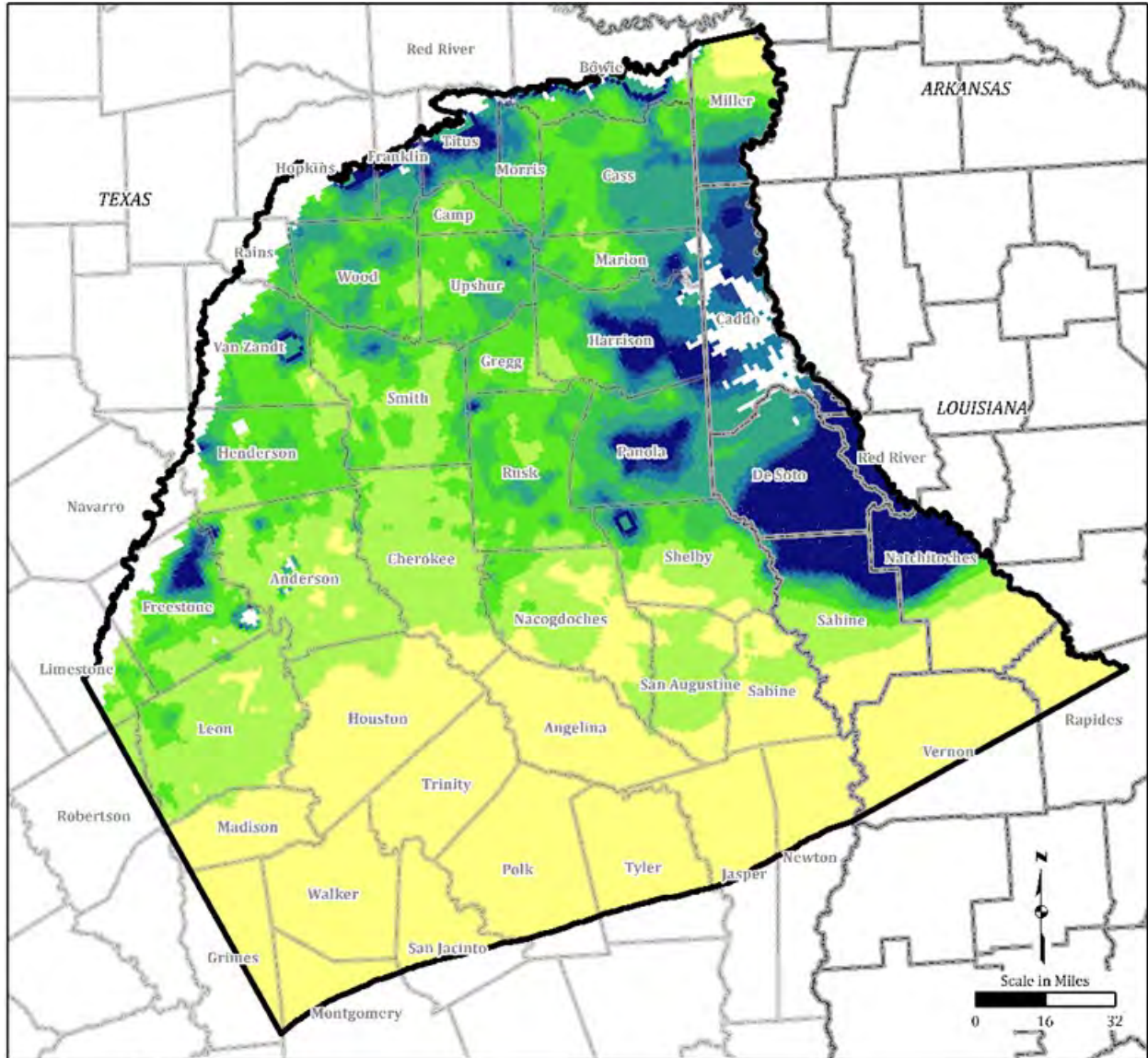


LEGEND

- Model Boundary
- County or Parish Boundary
- Calculated Hydraulic Conductivity (Feet/Day)
- 0 to 0.5
- 0.5 to 1
- 1 to 1.5
- 1.5 to 2
- 2 to 3
- 3 to 4
- 4 to 5
- 5 to 10

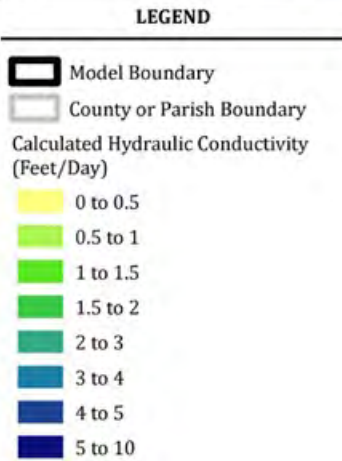
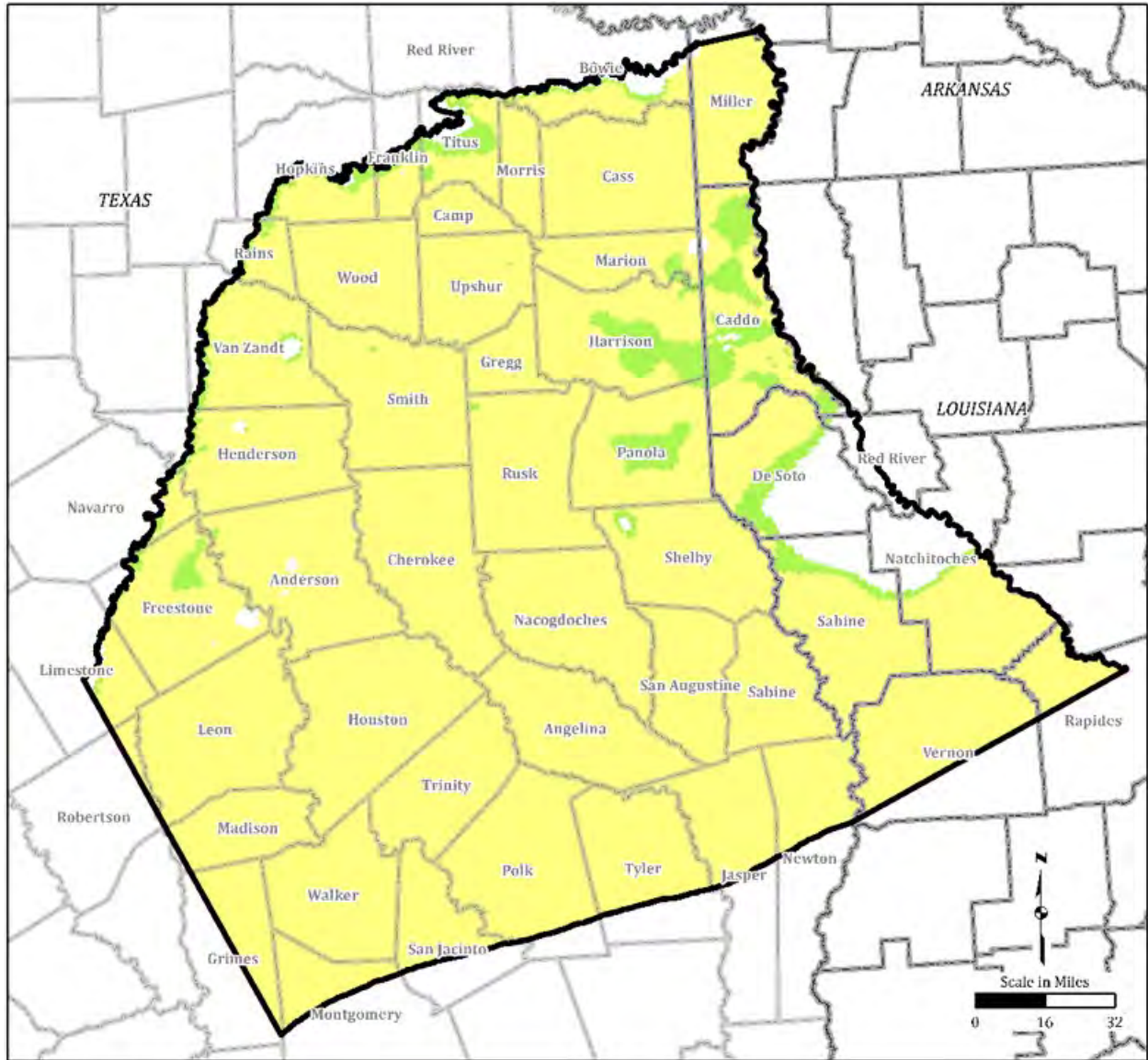
- Notes:**
1. The layer contains discontinuous outcrops, consistent with the conceptual model (Section 2).
 2. Projected Coordinate System Datum: GAM.

Figure 3.1-3. Calculated Horizontal Hydraulic Conductivity for Upper Wilcox (Model Layer 7)



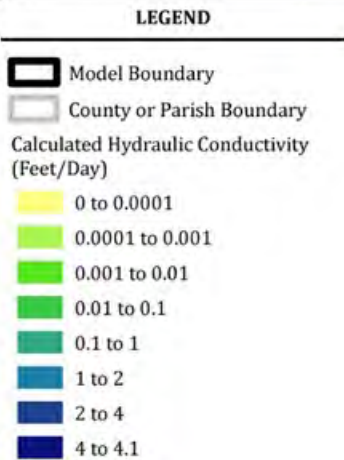
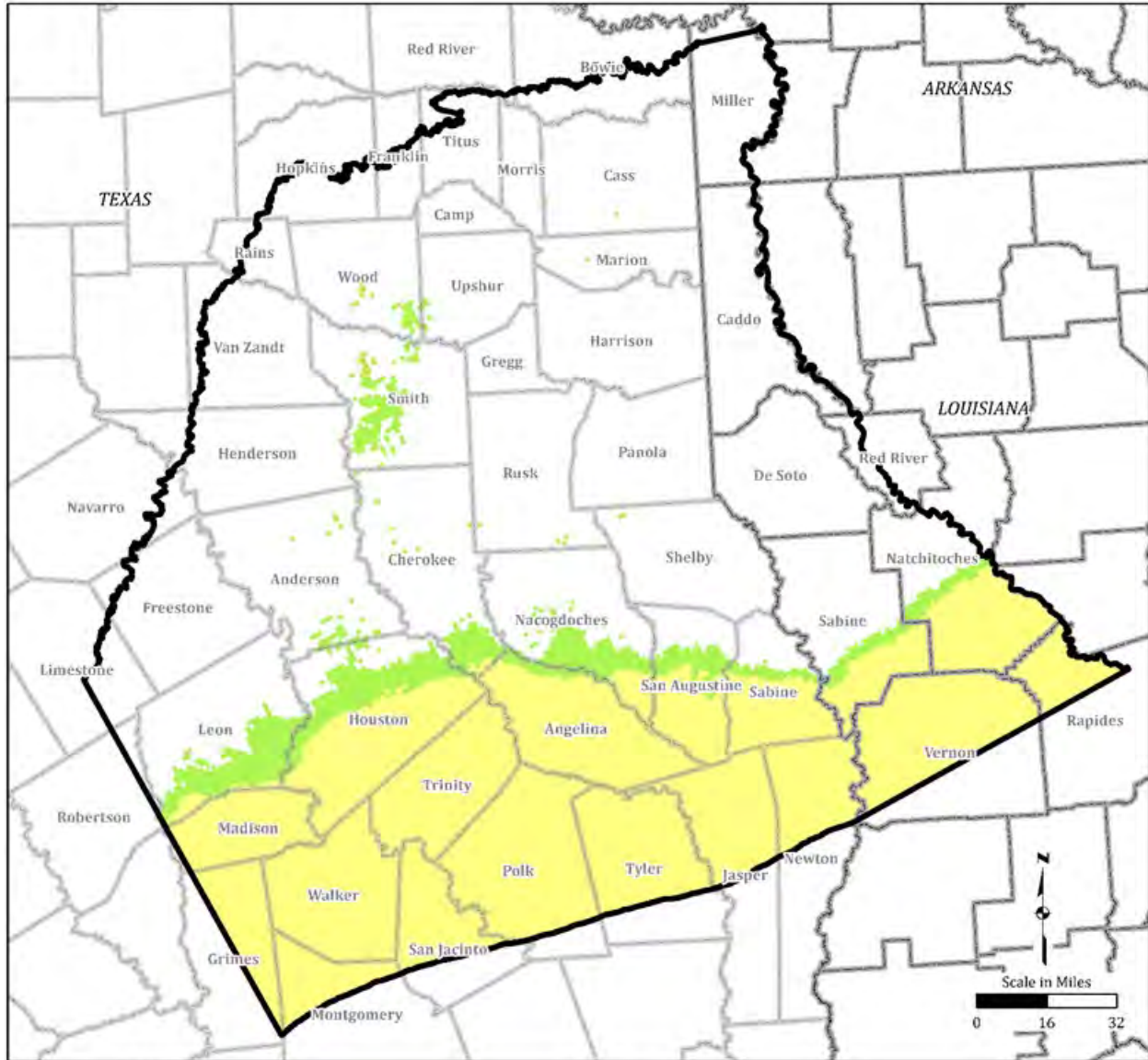
Note:
 1. Projected Coordinate System
 Datum: GAM

Figure 3.1-4. Calculated Horizontal Hydraulic Conductivity for Middle Wilcox (Model Layer 8)



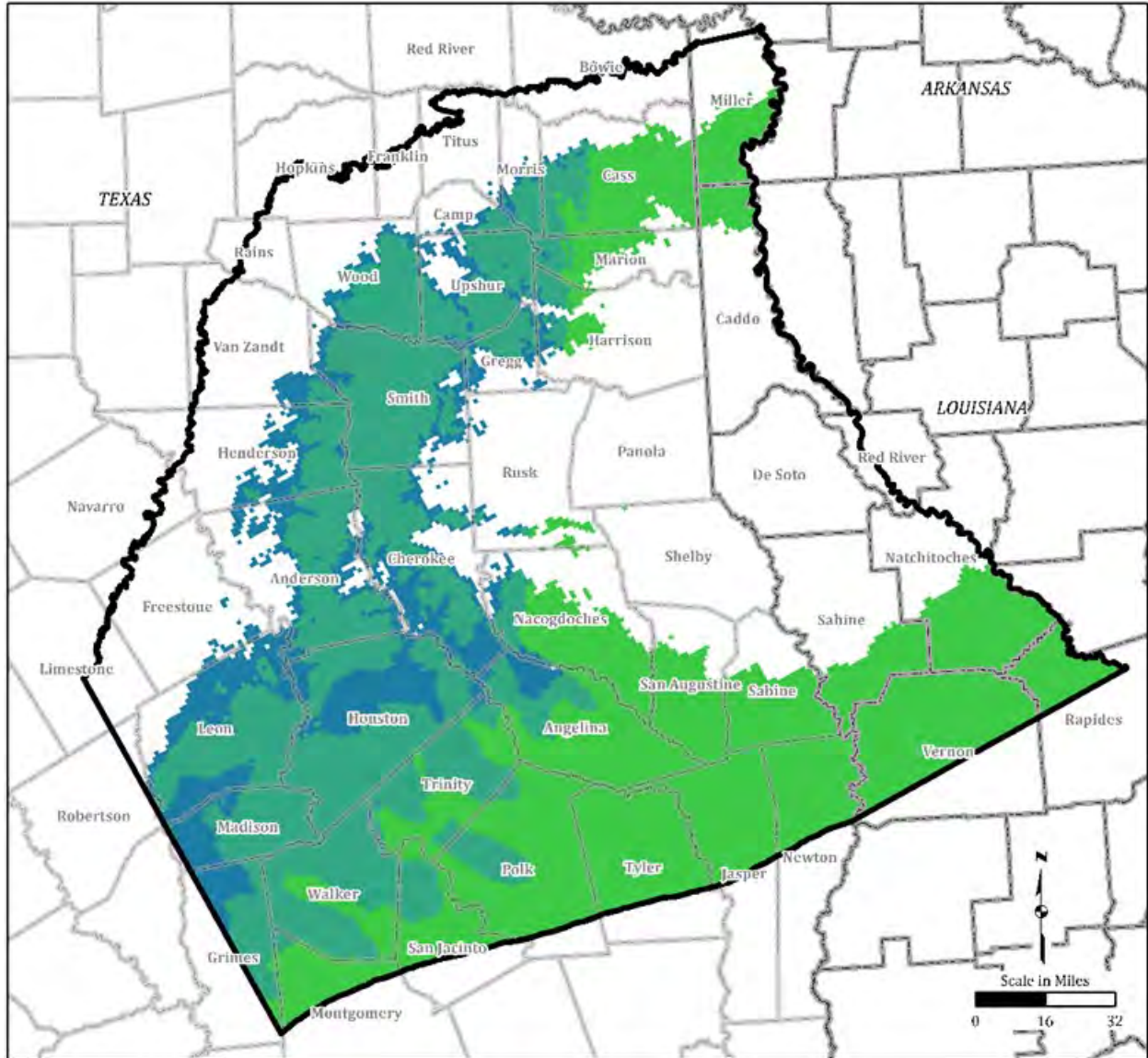
Note:
 1. Projected Coordinate System
 Datum: GAM

Figure 3.1-5. Calculated Horizontal Hydraulic Conductivity for Lower Wilcox (Model Layer 9)



Notes:
 1. The layer contains discontinuous outcrops, consistent with the conceptual model (Section 2).
 2. Projected Coordinate System Datum: GAM.

Figure 3.1-6. Calculated Vertical Hydraulic Conductivity for Sparta Aquifer (Model Layer 2)



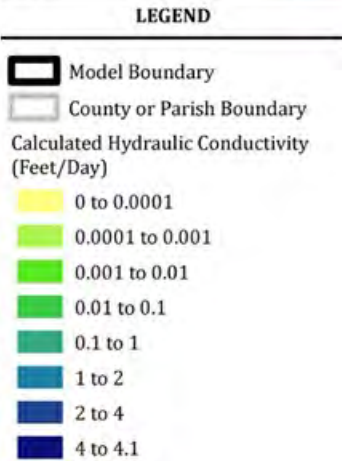
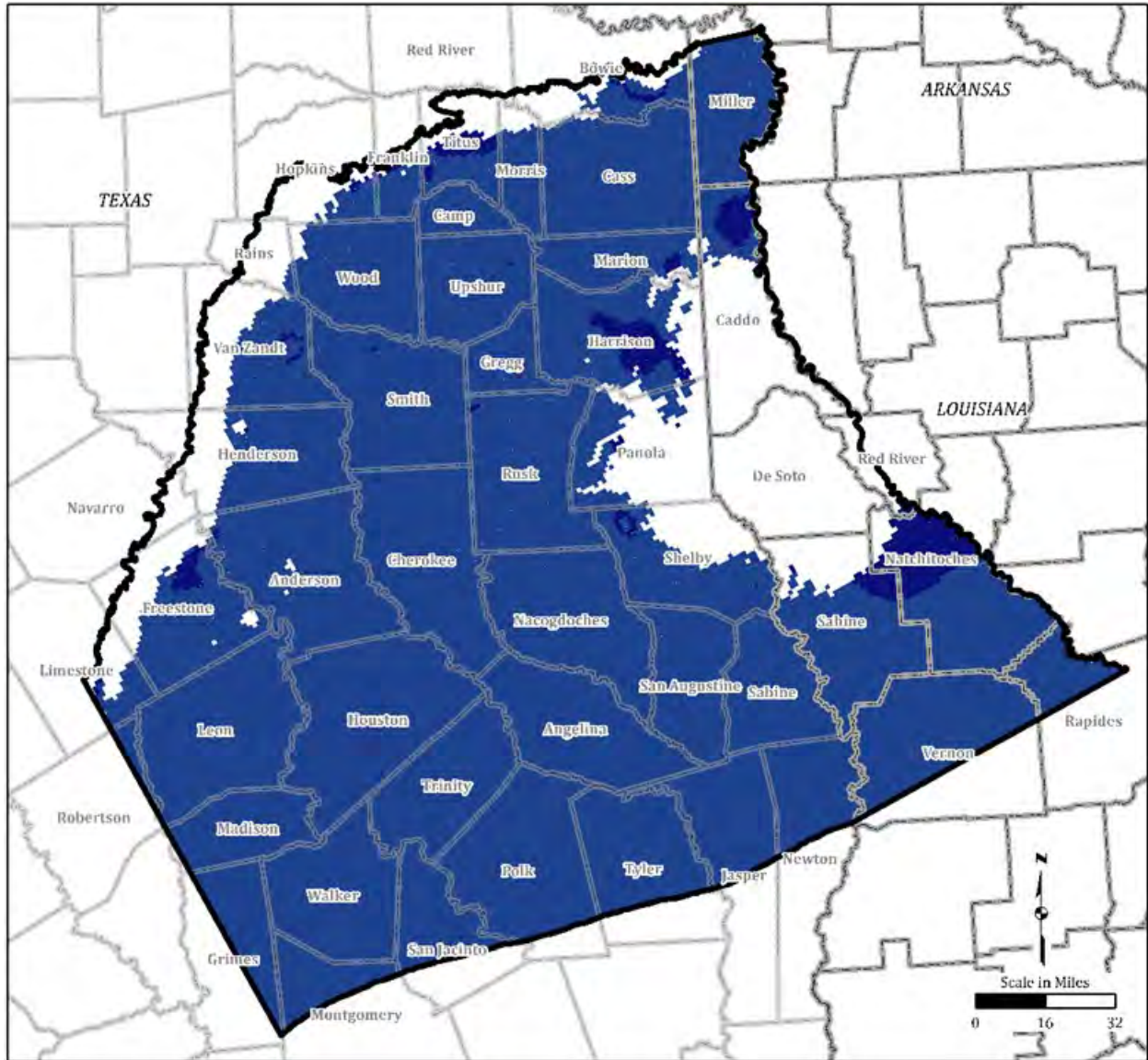
LEGEND

- Model Boundary
- County or Parish Boundary
- Calculated Hydraulic Conductivity (Feet/Day)
- 0 to 0.0001
- 0.0001 to 0.001
- 0.001 to 0.01
- 0.01 to 0.1
- 0.1 to 1
- 1 to 2
- 2 to 4
- 4 to 4.1

Notes:

1. The layer contains discontinuous outcrops, consistent with the conceptual model (Section 2).
2. Projected Coordinate System Datum: GAM.

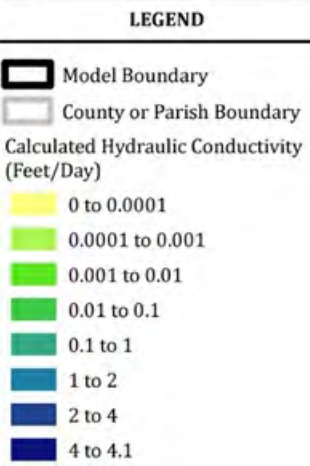
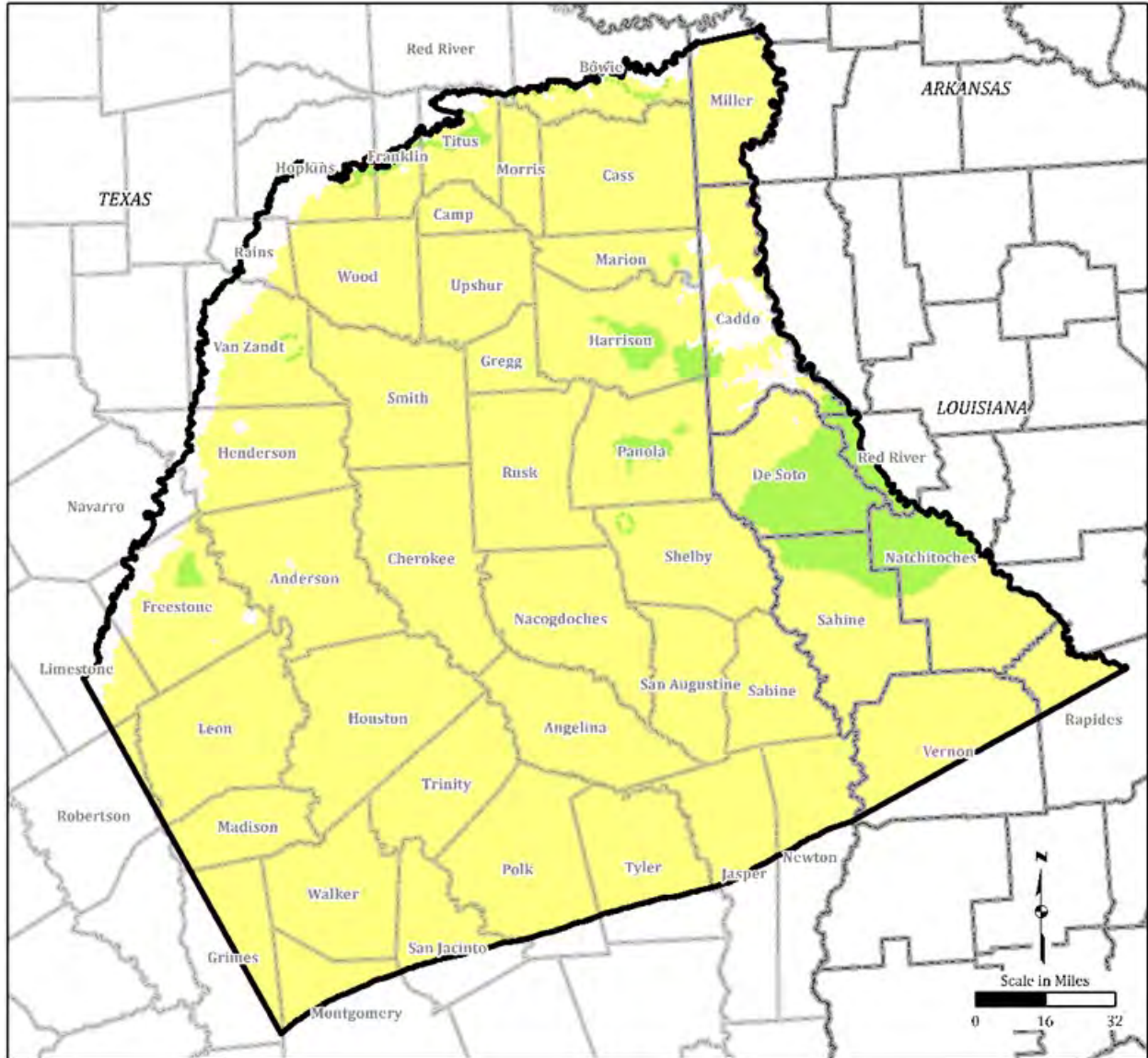
Figure 3.1-7. Calculated Vertical Hydraulic Conductivity for Queen City Aquifer (Model Layer 4)



Notes:

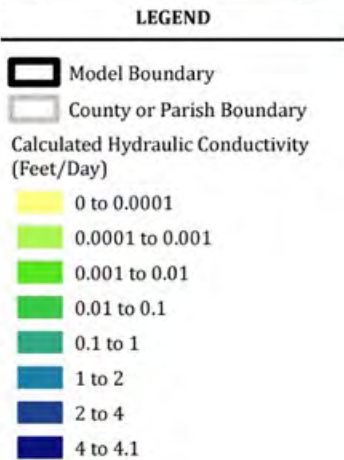
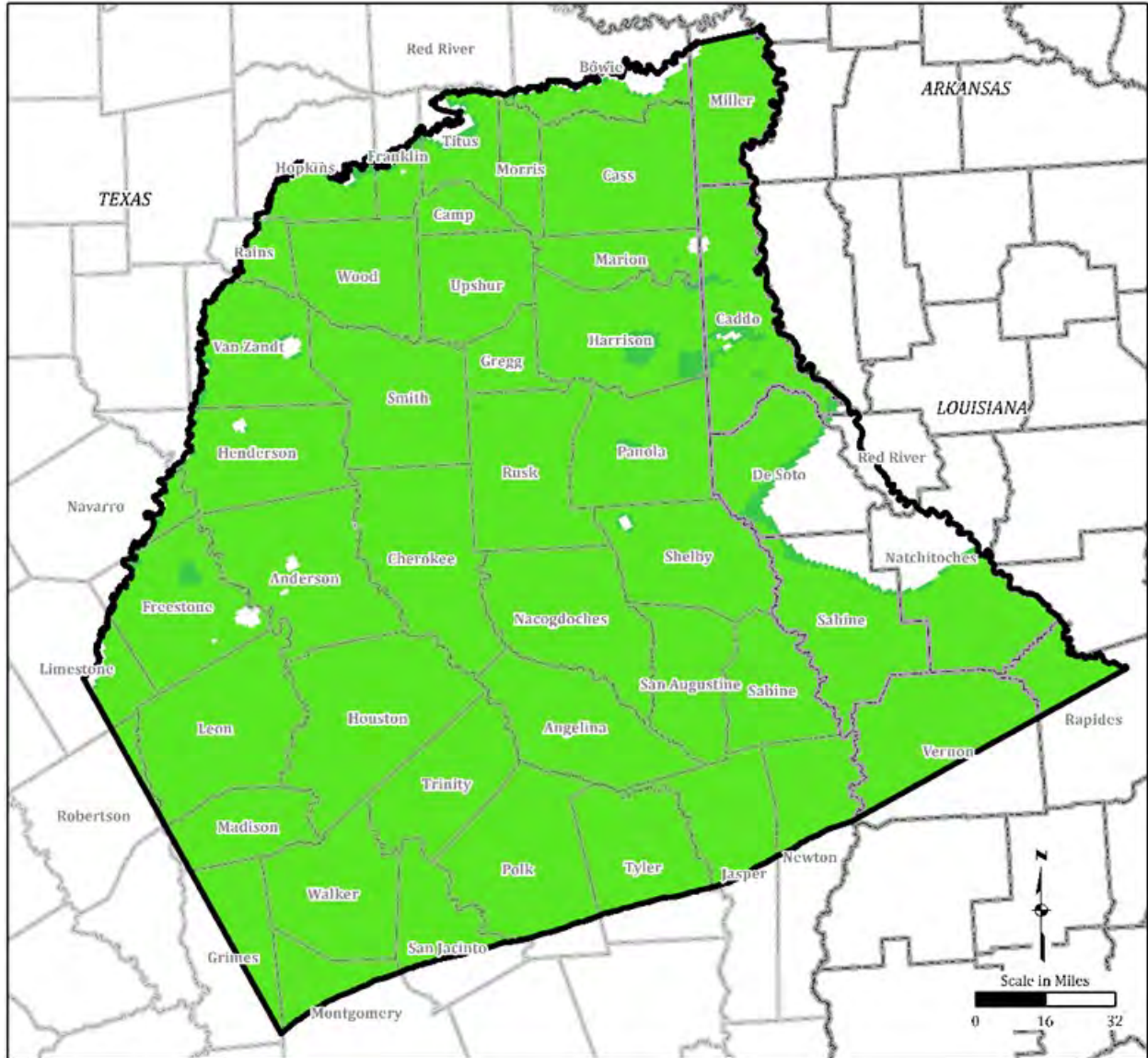
1. The layer contains discontinuous outcrops, consistent with the conceptual model (Section 2).
2. Projected Coordinate System Datum: GAM.

Figure 3.1-8. Calculated Vertical Hydraulic Conductivity for Upper Wilcox (Model Layer 7)



Note:
 1. Projected Coordinate System
 Datum: GAM

Figure 3.1-9. Calculated Vertical Hydraulic Conductivity for Middle Wilcox (Model Layer 8)



Note:
 1. Projected Coordinate System
 Datum: GAM

Figure 3.1-10. Calculated Vertical Hydraulic Conductivity for Lower Wilcox (Model Layer 9)

and calibrated vertical hydraulic conductivity values of 8.62 feet/day and 0.42 feet/day, respectively. For the Weches Formation (model layer 3) and the Reklaw Formation (model layer 5), the sand fraction was assumed to be uniform at 0.1, resulting in calibrated horizontal hydraulic conductivity values of 0.10 feet/day and 0.03 feet/day, respectively, and calibrated vertical hydraulic conductivity values of 7.44×10^{-5} feet/day and 1.11×10^{-5} feet/day, respectively.

The calibrated horizontal hydraulic conductivity values for the Sparta Aquifer (model layer 2) ranged from 0.50 to 9.50 feet/day and that of the Queen City Aquifer (model layer 4) ranged from 0.43 to 6.65 feet/day. The calibrated vertical hydraulic conductivity values for the Sparta Aquifer (model layer 2) ranged from 4.74×10^{-5} to 9.00×10^{-4} feet/day and that of the Queen City Aquifer (model layer 4) ranged from 0.09 to 1.38 feet/day. The calibrated horizontal hydraulic conductivity units of the Wilcox Aquifer (Upper, Middle, and Lower Wilcox) (model layers 7, 8, and 9) ranged from 0.12 to 8.34 feet/day. The calibrated vertical hydraulic conductivity units of the Wilcox Aquifer (Upper, Middle, and Lower Wilcox) (model layers 7, 8, and 9) ranged from 3.89×10^{-5} to 4.06 feet/day.

The calibrated hydraulic conductivity values were compared to the estimated hydraulic conductivity values and geometric means presented in the Conceptual Model Report in Section 4.5 (Montgomery and Associates, 2020) (Table 3.1-2). The calibrated horizontal hydraulic conductivity values are within the range of the estimated values, except for the Weches Formation (model layer 3) and Reklaw Formation (model layer 5), which are slightly below the estimated range. Use of a uniform sand/clay fraction for these aquitard units could also have caused the calibration to exceed the expected range. Calibrated horizontal hydraulic conductivity values in the Queen City Aquifer (model layer 4) (Figure 3.1-2), Carrizo Aquifer (model layer 6), and the Upper Wilcox Aquifer (model layer 9) (Figure 3.1-3) match the conceptual model geometric mean (Table 3.1-2).

Additional work may further correlate hydraulic conductivity zones with sand fraction distributions to improve understanding of groundwater flow, as noted in Section 7, Future Improvements.

3.1.3 Calibration of GHB

The GHB conductance was adjusted during calibration to provide a best fit between observed and simulated groundwater level elevations. As described in Section 2.8, the GHB controls flow in or out of the model domain along the southern model boundary in model layers 2, 4, and 6 through 9. The heads along the GHB boundaries were set according to interpolated head contours in the region. Within layer 2, Sparta Aquifer, the GHB was also used to represent interaction of the Sparta Aquifer with the overlying Younger Units.

GHB heads and conductance values were adjusted using PEST and the two-period steady-state model. Table 2.8-1 shows the GHB calibrated range in heads and conductance for each layer. The GHB conductance values did not change through the calibration. Since the GHB water level elevations did not change with time, wells within the Sparta Aquifer beneath the Younger Units showed only minor groundwater level elevation fluctuations.

3.2 Model Simulated Versus Measured Heads

Groundwater level elevations were used to constrain the model to observed conditions during the simulation period. This section discusses the development of the water level elevation target data set and the various qualitative as well as quantitative measures that were used to evaluate the simulated water level elevations.

3.2.1 Water Level Elevation Targets

A total of 19,473 water level elevation records from 1,811 wells are within the model domain in the simulated model layers (Younger Units, Midway Group, and Older Units are not simulated) and during the simulated model timeframe (1980 through 2013). 867 water level elevation records from 392 wells were removed due to following questionable data flags.

- pumping-level measurement;
- presence of oil and grease in well;
- possible incorrect well identification;
- flooding/runoff into the well casing;
- air leak in the sampling line;
- re-completion in different zone;
- well bridged or caved;
- previously flagged as questionable; and
- well water level elevations previously marked for exclusion.

Using well construction and geologic information, target wells were assigned to corresponding model layers and this layering was checked against respective water level elevations. Discrepancies consisted of wells with water level elevations below the bottom of the assigned layer and wells where water level elevations were below the top of an assigned layer in areas where the aquifer was confined. These discrepancies were resolved by moving problematic wells into a lower aquifer layer.

The observed water level dataset (target dataset) used for the model consisted of 18,606 water level elevation records from 1,797 wells. The wells were placed in all model layers except the two layers representing aquitards (Weches and Reklaw Formations, model layers 3 and 5). Distribution of wells in each layer is shown on Figures 3.2-1 through 3.2-7. The number of observed water level measurements at each well location is also shown.

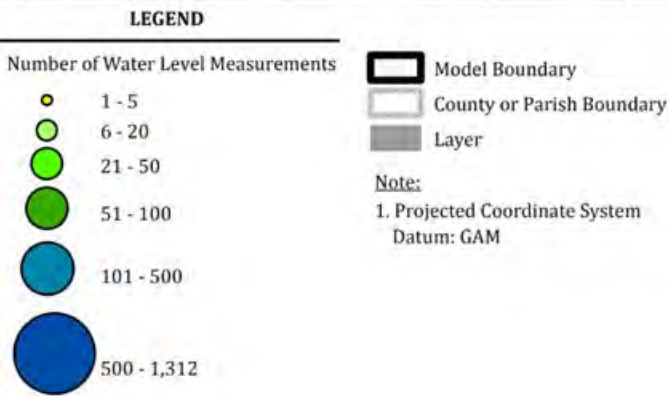
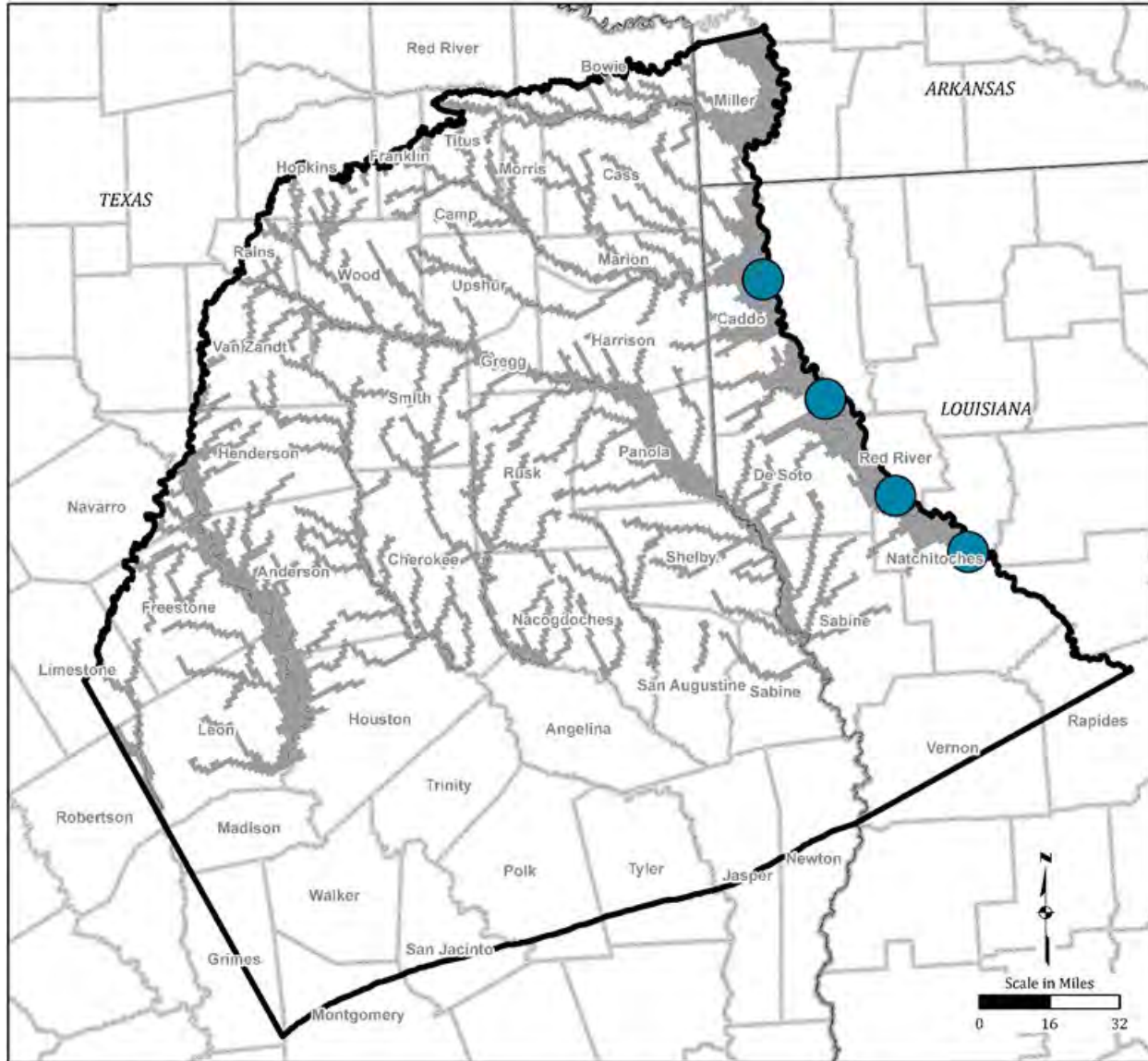


Figure 3.2-1. Location of Groundwater Observation Wells and Available Water Level Elevation Data - Quaternary Alluvium (Layer 1)

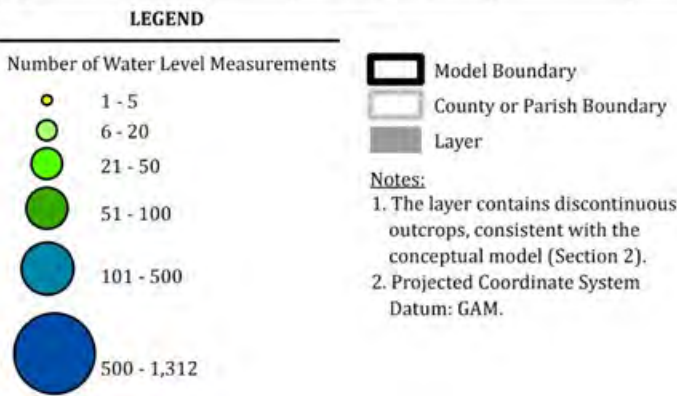
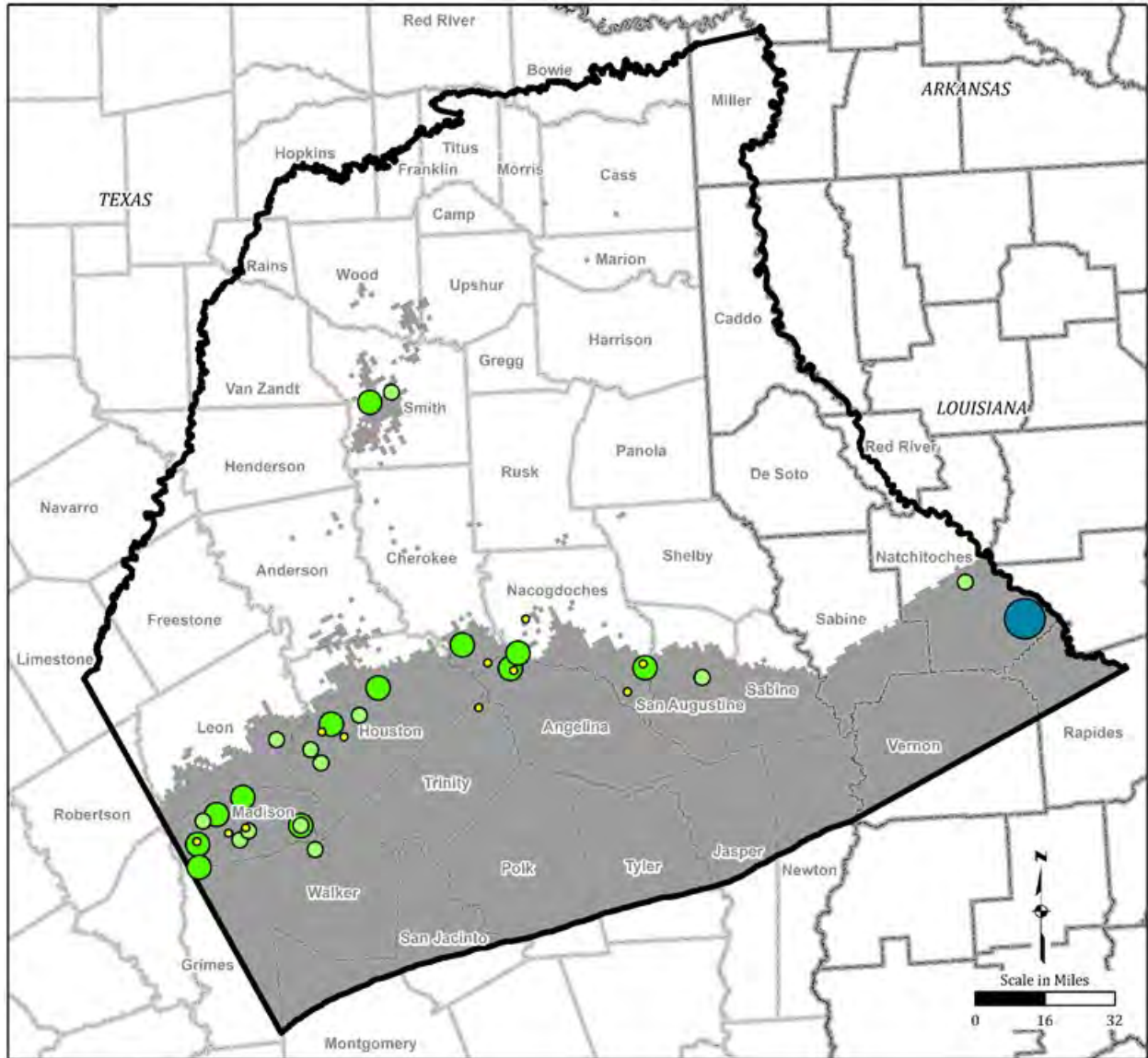


Figure 3.2-2. Location of Groundwater Observation Wells and Available Water Level Elevation Data - Sparta Aquifer (Layer 2)

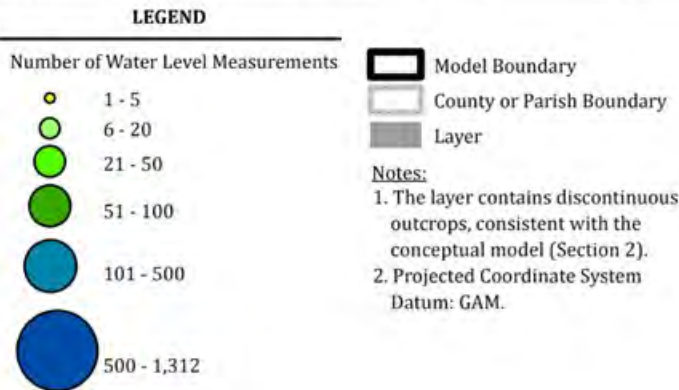
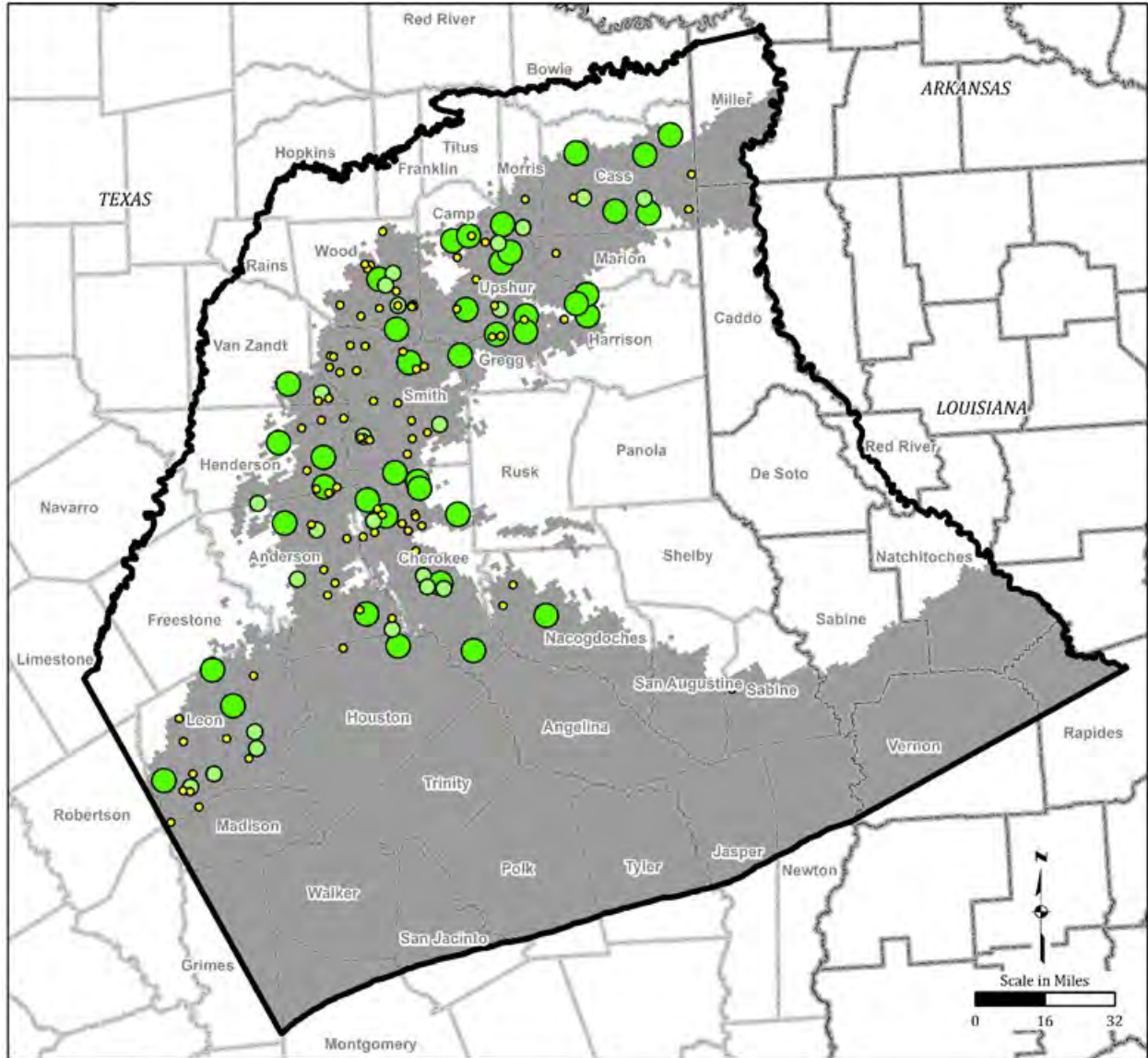


Figure 3.2-3. Location of Groundwater Observation Wells and Available Water Level Elevation Data - Queen City Aquifer (Layer 4)

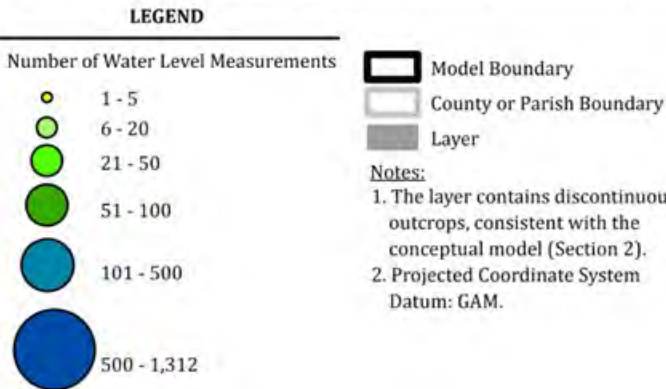
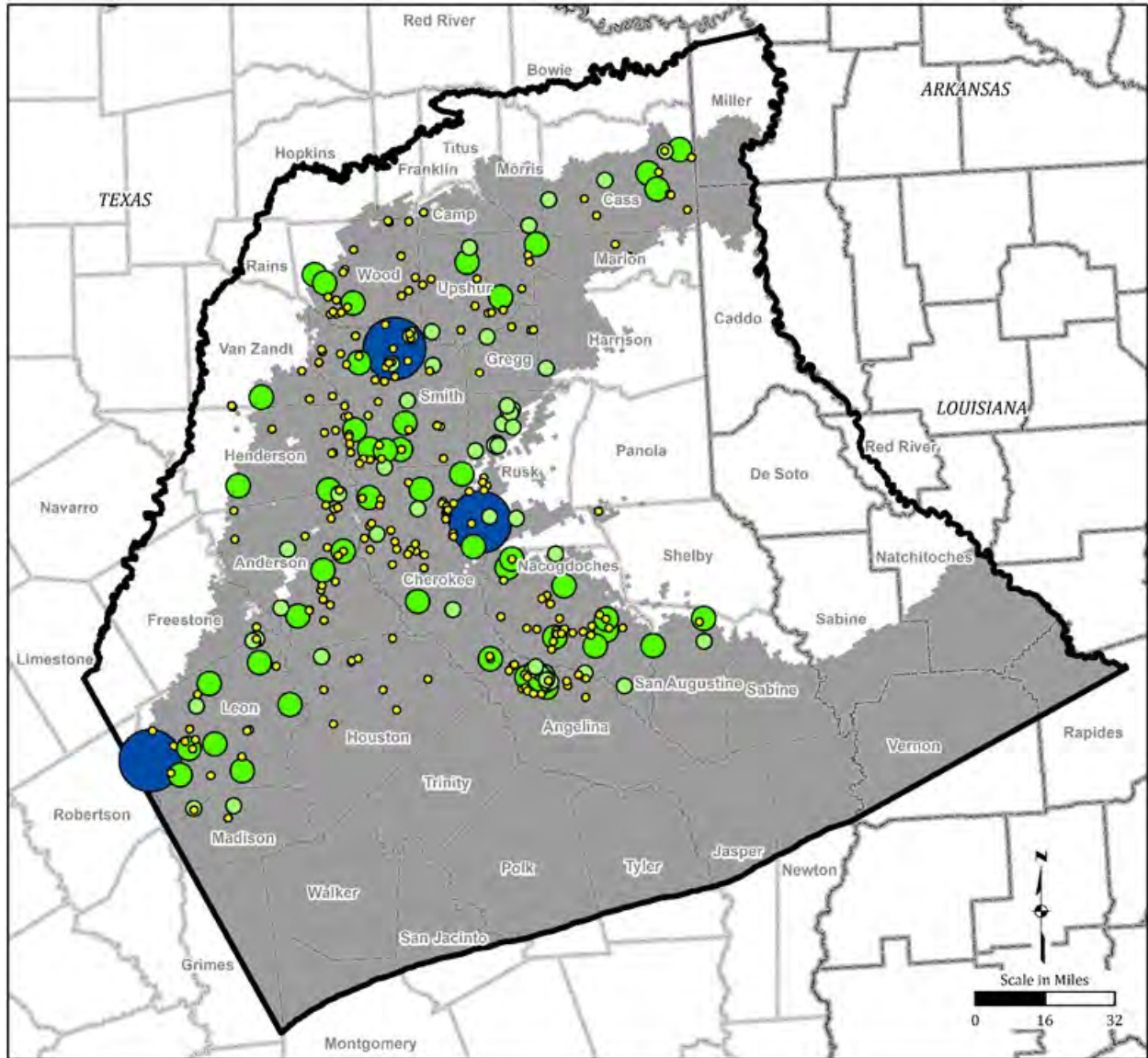


Figure 3.2-4. Location of Groundwater Observation Wells and Available Water Level Elevation Data - Carrizo Aquifer (Layer 6)

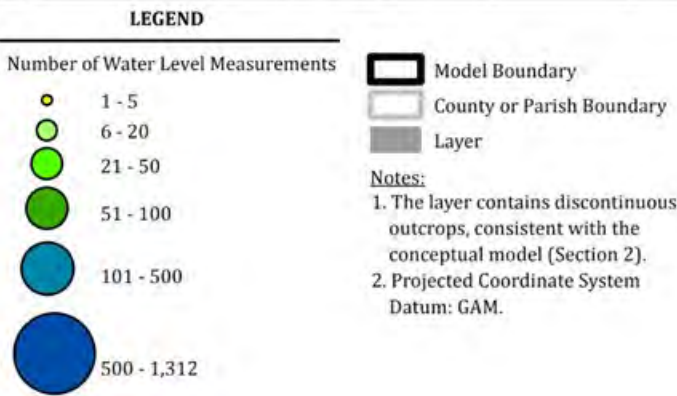
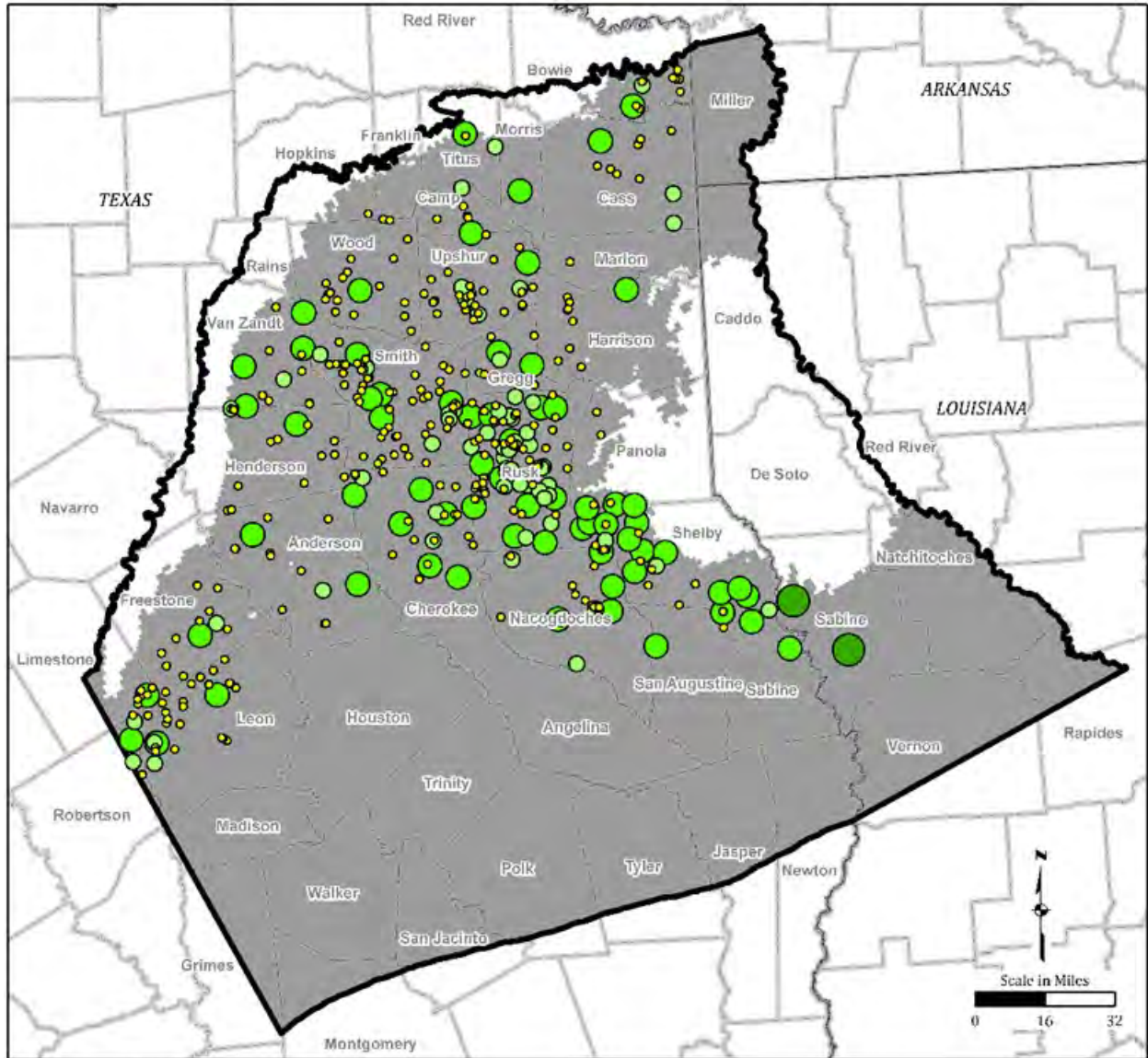


Figure 3.2-5. Location of Groundwater Observation Wells and Available Water Level Elevation Data - Upper Wilcox (Layer 7)

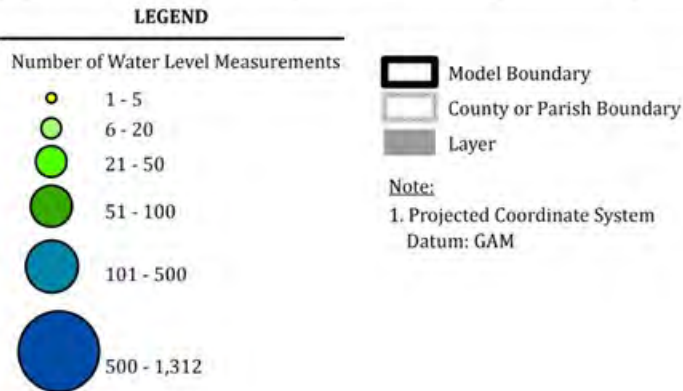
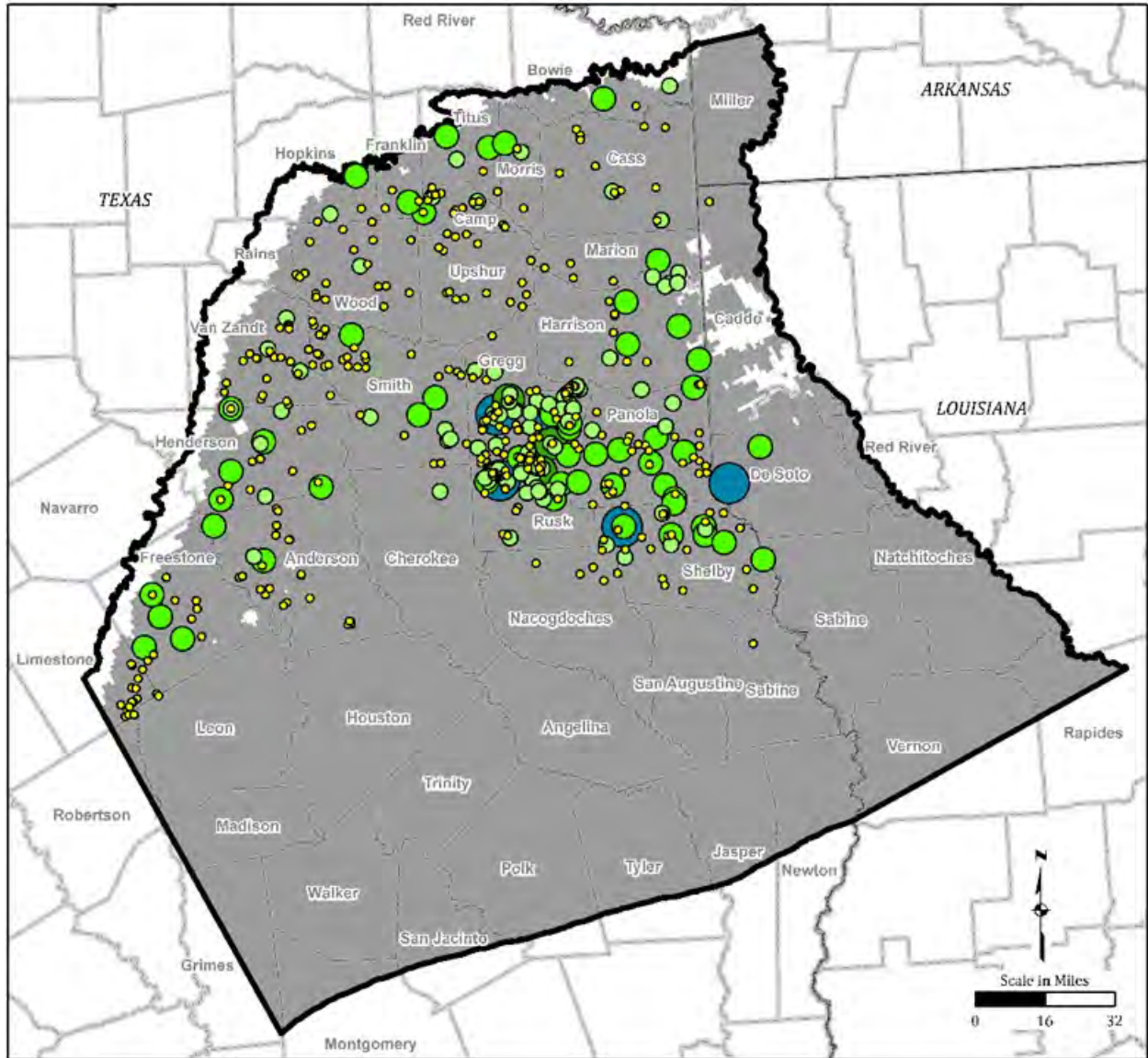
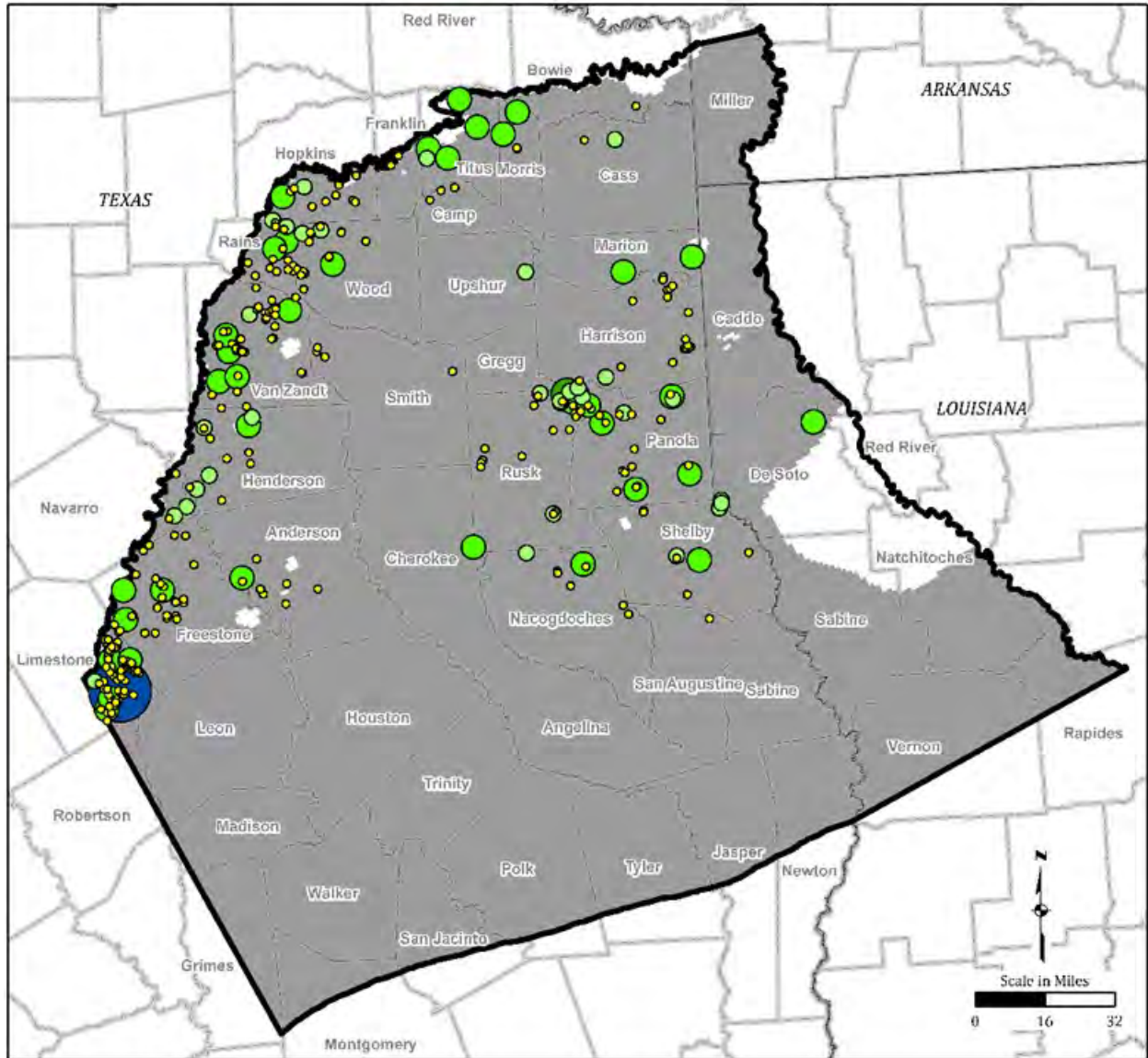
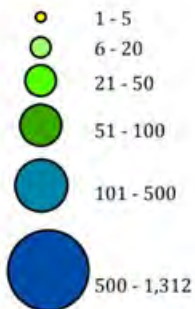


Figure 3.2-6. Location of Groundwater Observation Wells and Available Water Level Elevation Data - Middle Wilcox (Layer 8)



LEGEND

Number of Water Level Measurements



- Model Boundary
- County or Parish Boundary
- Layer

Note:

- 1. Projected Coordinate System
Datum: GAM

Figure 3.2-7. Location of Groundwater Observation Wells and Available Water Level Elevation Data - Lower Wilcox (Layer 9)

The target dataset was evaluated for additional quality control issues that may warrant applying a weight to individual water level elevation records. A weight factor applied to a water level measurement represents a measure of uncertainty in the data. Weight factors were applied for the following conditions.

- Reported recent pumping;
- nearby pumping;
- possible recharge activities nearby;
- measurements from ground surface prior to wellhead completion;
- wet or leaking casing;
- tape does not fall freely in well;
- well screened across multiple model layers; and
- wells with a single water level measurement.

A weight factor of 0.7 was applied to water level elevation records with a single quality control issue. In the case that more than one condition existed for a water level elevation record, a cumulative weighting factor was assigned as 0.5. Data without quality issues and single-layer screens were given a weight of 1. It is possible for a given well to have water level elevation records with varying weights. However, most records have a weight of 1. Within the target dataset, 1,739 records from 717 wells have a weight of 0.7; 585 records from 569 wells have a weight of 0.5; and 16,282 records from 707 wells have a weight of 1.

Although the target dataset set consists of 18,606 water level elevation records, the model targets consist of 18,421 water level elevation records. Water level elevation records were averaged for the 1980 steady-state stress period for each well, resulting in 185 less records for calibration. The water level elevation records with target weights and aquifer type designation are provided in Appendix B Table 1.

3.2.2 Simulated Versus Observed Heads

Table 3.2-1 shows the summary for weighted head calibration statistics for the two-period steady-state model representing 1980 and 2013 conditions. For the 1980 steady-state period, the residual mean of 6.62 is relatively close to zero, indicating a good calibration and no overall bias in the calibration. For the 1980 steady-state period, the absolute residual mean was 33.21 feet and the root mean squared (RMS) error was 47.86 feet. For the 2013 steady-state period, the residual mean was -9.00, the absolute residual mean was 46.29 feet, and the RMS error was 63.11 feet.

Table 3.2-2 shows the summary for weighted head calibration statistics for the transient simulation period 1980 through 2013. The weighted head calibration statistics are presented for all targets, and the confined and unconfined targets. The residual mean for all targets of -3.13 feet is slightly negative, indicating simulated water level elevations are slightly higher than observed overall. However, given the range of water level elevation measurements is 901.4 feet, the residual mean is relatively close to zero, indicating a good calibration. The absolute residual mean for all targets was 41.06 feet and the RMS error

Table 3.2-1. Weighted Calibration Statistics for the Steady-State 1980 and 2013 Simulation

Statistic	1980 Values	2013 Values
Number of targets	695	386
Number of observations	695	386
Range in observed values	805.78	852.78
Minimum residual	-166.50	-240.40
Maximum residual	223.87	218.79
Sum of squared residuals	1.59E+06	1.54E+06
Root mean square (RMS) error	47.86	63.11
Residual mean	6.62	-9.00
Absolute residual mean	33.21	46.29
Standard deviation	47.43	62.55
Scaled residual mean	0.008	-0.011
Scaled absolute residual mean	0.041	0.054
Scaled standard deviation	0.059	0.073
Scaled RMS error	0.059	0.074

Table 3.2-2. Weighted Calibration Statistics for the Transient 1980 to 2013 Simulation

Statistic	All Targets	Confined Targets	Unconfined Targets
Number of targets	1,797	1,328	469
Number of observations	18,421	12,395	6,026
Range in observed values	901.40	901.40	551.10
Minimum residual	-316.32	-316.32	-166.15
Maximum residual	250.62	250.62	168.12
Sum of squared residuals	5.85E+07	4.64E+07	1.21E+07
Root mean square (RMS) error	56.37	61.18	44.85
Residual mean	-3.13	-6.73	4.26
Absolute residual mean	41.06	44.80	33.37
Standard deviation	56.28	60.81	44.65
Scaled residual mean	-0.003	-0.007	0.008
Scaled absolute residual mean	0.046	0.050	0.061
Scaled standard deviation	0.062	0.067	0.081
Scaled RMS error	0.063	0.068	0.081

was 56.37 feet. The standard deviation for all targets of 56.28 feet is less than 10 percent of the range of observed values, indicating a good calibration. The residual mean for the confined targets was -6.73 and for the unconfined targets was 4.26, indicating simulated water level elevations are slightly higher for the confined areas and slightly lower for the unconfined, or outcrop areas. In general, the weighted head calibration statistics show the model is well calibrated in both the confined and unconfined areas.

Table 3.2-3 shows the summary for the weighted head calibration statistics for the transient simulation period for 1980 through 2013 conditions for each model layer. All model layer statistics meet the calibration criteria set forth by TWDB that requires the mean absolute error or RMS error to be less than 10 percent of the measured hydraulic-head drop across the model area for each model layer (Table 3.2-3). The scaled absolute residual mean is less than 10 percent for all model layers; the scaled RMS error is less than 10 percent for all layers except Layer 4 with an RMS of 12 percent (Table 3.2-3). The Queen City Aquifer is between two aquitard layers and target well screens generally extend into at least one of the aquitard layers. Calibration statistics for the Queen City Aquifer were improved by examining the target wells within this model layer and assigning eight target wells to the aquifer above (Sparta Aquifer) or below (Carrizo Aquifer) the Queen City Aquifer. This change resulted in a scaled RMS error equal to 0.122 for the Queen City Aquifer. More reliable water level elevation data and better well construction data will improve calibration, as discussed below in Section 7.0.

The steady-state and transient error statistics are less than 10 percent of the range of observations which is generally considered a reasonably good calibration. This number could not be improved further considering all the uncertainties in pumping and water level measurement locations discussed in Sections 2.7 and 3.2.1, respectively. All residuals are computed as observed minus simulated metrics. Thus, positive residuals indicate that simulated water level elevations are lower than observed, while negative residuals indicate that simulated water level elevations are higher than observed.

A transient 1980 through 2013 simulation, based on the draft model, using MODFLOW-NWT was performed for the model domain to evaluate the impact of a grid coarser than that used for the transient model simulation. The MODFLOW-NWT simulation used the 1-mile by 1-mile parent grid only and used the same parameterization of the draft model (minimum calibrated model cell size was 660 feet). The MODFLOW-NWT simulation residual mean was -7.9 feet, the absolute residual mean was 48.1 feet, and the RMS error was 70.8 feet. These values are similar to the draft transient model statistics summarized in Appendix C. This similarity indicates that the finer discretization of the transient simulation did not affect calibration, likely due to the coarseness of pumping estimates despite fine resolution along modeled streams.

Figure 3.2-8 shows the observed versus simulated water level elevations for the steady-state 1980 and 2013 conditions while Figure 3.2-9 and Figure 3.2-10 show these values based on whether the aquifer is confined or unconfined. The left panel shows the 1980 regression plot while the right panel shows the 2013 regression plot. The steady-state simulation results tightly surround the best-fit line with no noticeable bias across the range of observations. The regression coefficient (R^2) for the three plots are greater than 0.9,

Table 3.2-3. Weighted Calibration Statistics by Layer for the Transient 1980 to 2013 Simulation

Statistic	Layer 1 (Quaternary Alluvium)	Layer 2 (Sparta Aquifer)	Layer 4 (Queen City Aquifer)	Layer 6 (Carrizo Aquifer)	Layer 7 (Upper Wilcox)	Layer 8 (Middle Wilcox)	Layer 9 (Lower Wilcox)
Number of observations	707	681	1,629	4,969	3,458	4,147	2,830
Range in observed values	77.62	449.07	485.60	897.10	738.15	752.00	616.16
Minimum residual	-18.69	-101.13	-166.15	-243.53	-257.59	-291.13	-316.32
Maximum residual	12.48	57.42	230.69	250.62	233.30	215.75	100.29
Sum of squared residuals	3.61E+04	8.96E+05	5.70E+06	2.51E+07	1.38E+07	9.45E+06	3.54E+06
Root mean square (RMS) error	7.14	36.27	59.18	71.13	63.07	47.73	35.38
Residual mean	-3.45	-23.44	27.10	-8.95	-0.69	-6.80	-2.97
Absolute residual mean	5.75	31.59	41.60	58.74	48.31	32.26	24.84
Standard deviation	6.25	27.68	52.61	70.57	63.06	47.24	35.26
Scaled residual mean	-0.045	-0.052	0.056	-0.010	-0.001	-0.009	-0.005
Scaled absolute residual mean ¹	0.074	0.070	0.086	0.065	0.065	0.043	0.040
Scaled standard deviation	0.081	0.062	0.108	0.079	0.085	0.063	0.057
Scaled RMS error ²	0.092	0.081	0.122	0.079	0.085	0.063	0.057

Notes:

1. The scaled absolute residual mean for each layer is below 10 percent.
2. The scaled root mean square (RMS) error for each layer is less than 10 percent except in Layer 4.
3. Layers 3 and 5 (Weches and Reklaw Formations) do not contain water level elevations targets.

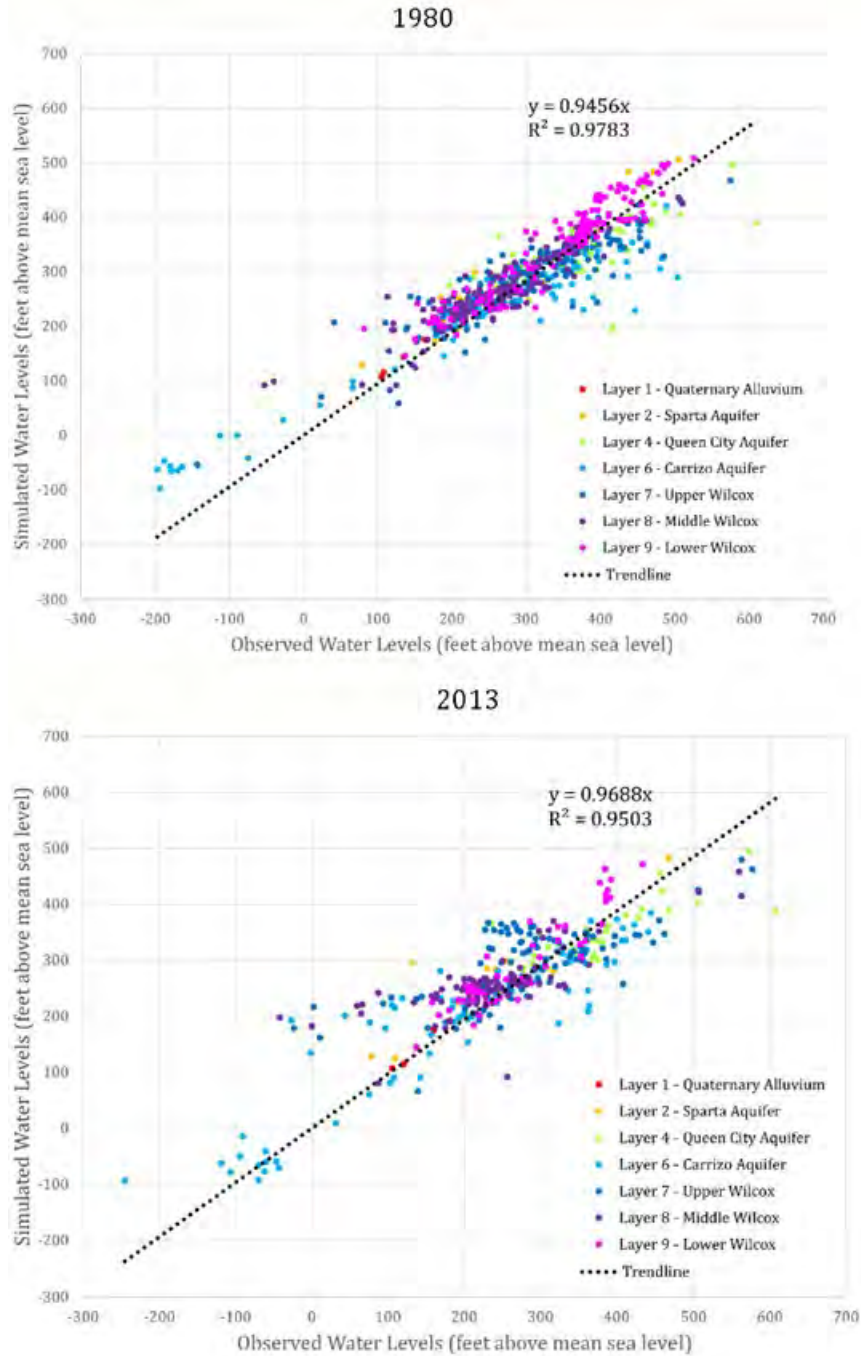


Figure 3.2-8. Observed vs. Simulated Water Level Elevations for Calibrated 1980 and 2013 Conditions

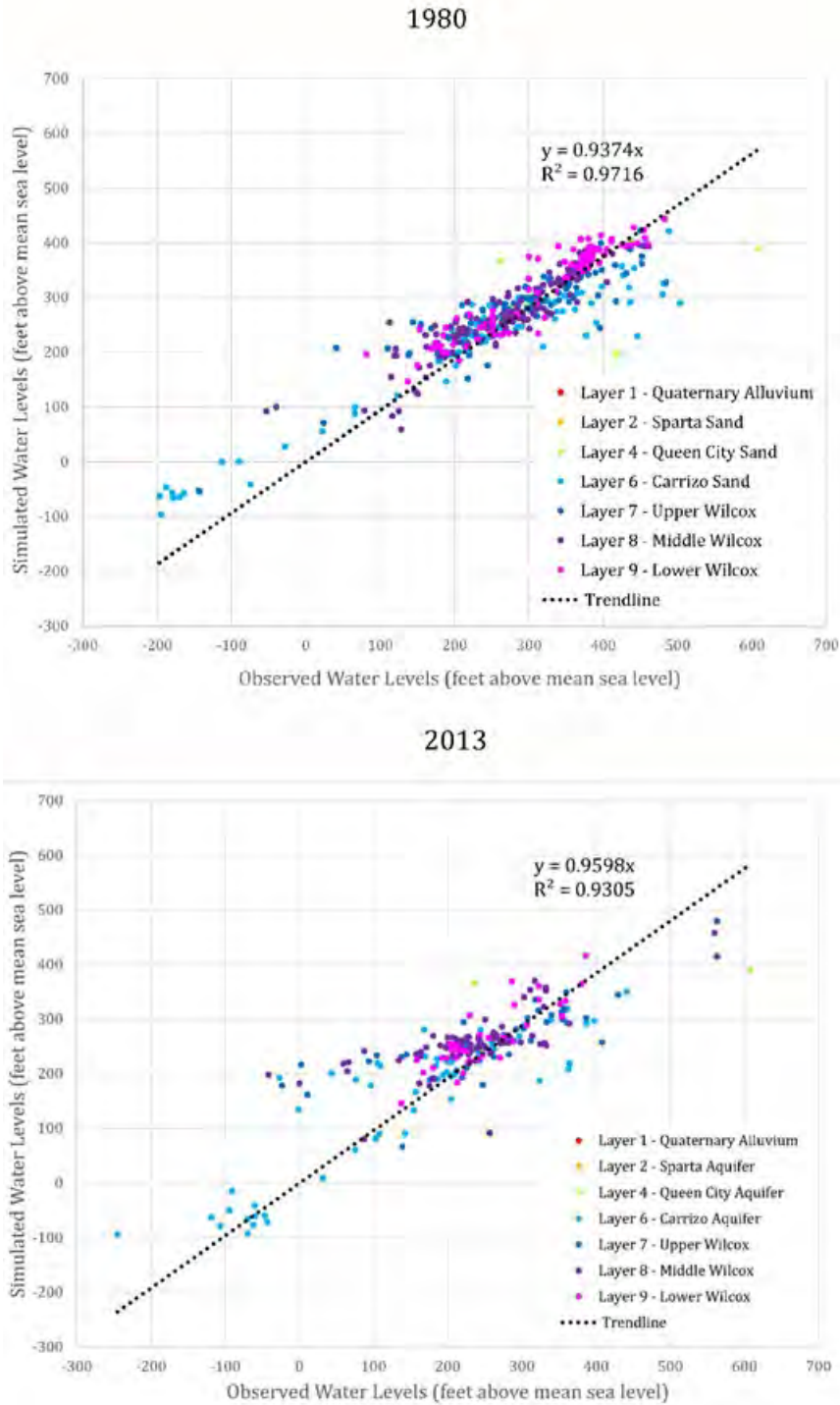


Figure 3.2-9. Observed vs. Simulated Confined Water Level Elevations for Calibrated 1980 and 2013 Conditions

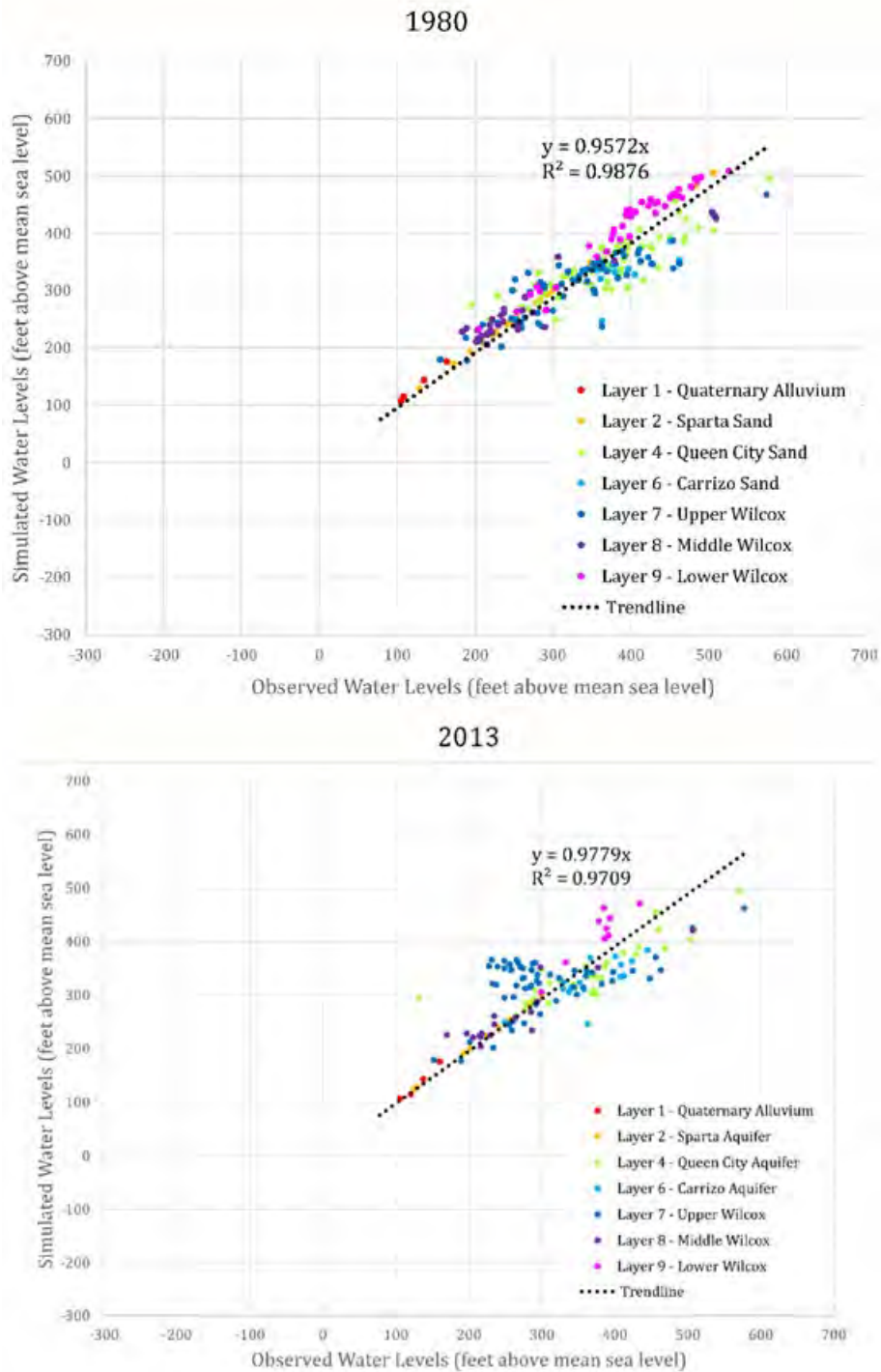


Figure 3.2-10. Observed vs. Simulated Unconfined Water Level Elevations for Calibrated 1980 and 2013 Conditions

indicating a good match between observed and simulated water level elevations for both confined and unconfined conditions.

Figure 3.2-11 shows the regression plot of observed versus simulated water level elevations for the transient 1980 through 2013 simulation period. Figure 3.2-12 shows the confined water level elevation regression plot and Figure 3.2-13 shows the unconfined water level elevation regression plot for the 1980 through 2013 simulation period. The transient simulation results tightly surround the best-fit line with no noticeable bias across the range of observations. The regression coefficient (R^2) for the three plots are greater than 0.9, indicating a good match between observed and simulated water level elevations of the transient simulation for both confined and unconfined conditions. Figure 3.2-14 shows the unconfined water level elevation regression plot for the 1980 through 2013 simulation period and plots the subset of unconfined wells which are overlain by the Quaternary Alluvium (model layer 1). There is no bias noted for unconfined targets overlain by Quaternary Alluvium.

Figures 3.2-15a through 15c show the observed versus simulated water level elevations for the 1980 through 2013 simulation period for each aquifer layer. The regression coefficient (R^2) for the plots range from about 0.92 to 0.99, indicating a good match between observed and simulated values in all layers. The Carrizo Aquifer (Layer 6) showed the poorest match with a regression coefficient of 0.92 while other aquifer layers had regression coefficients above 0.95.

Appendix B compares the final simulated water level elevation to each observed data point for all targets and includes the calculated residual value along with additional target data.

3.2.3 Spatial Distribution and Frequency of Residuals

The spatial distribution of head residuals for the 1980 through 2013 simulation period is shown for target wells without quality control issues on Figure 3.2-16. This figure plots 541 of the 1,797 total targets used for model calibration which had an average weight of 1.

The residual values plotted at each well are an average of all residuals (from 1980 to 2013) at that well. Residuals at these 541 wells range from -420 to 319 feet. Large clusters of residuals occur in Rusk, Smith, Upshur, and Van Zandt counties. Finer resolution on sand and clay heterogeneity or more accurate pumping locations might improve the calibration in these counties, especially as these counties have high pumping rates as shown on Figures 2.7-2 through 2.7-7. In general, negative and positive residuals are evenly distributed across the model domain with no noticeable bias.

Figures 3.2-17a and 3.2-17b show the frequency of residual values by model aquifer layer (layers 1, 2, 4, 6, 7, 8, and 9). Residuals cluster around a value of zero. The Carrizo Aquifer and Wilcox Aquifer (model layers 6, and 7 through 9) have more water level elevation data and also showed more spread in residual values but no noticeable bias towards high or low residuals. Appendix B compares the final simulated water level elevation to each observed data point for all targets and includes the calculated residual value along with additional target data.

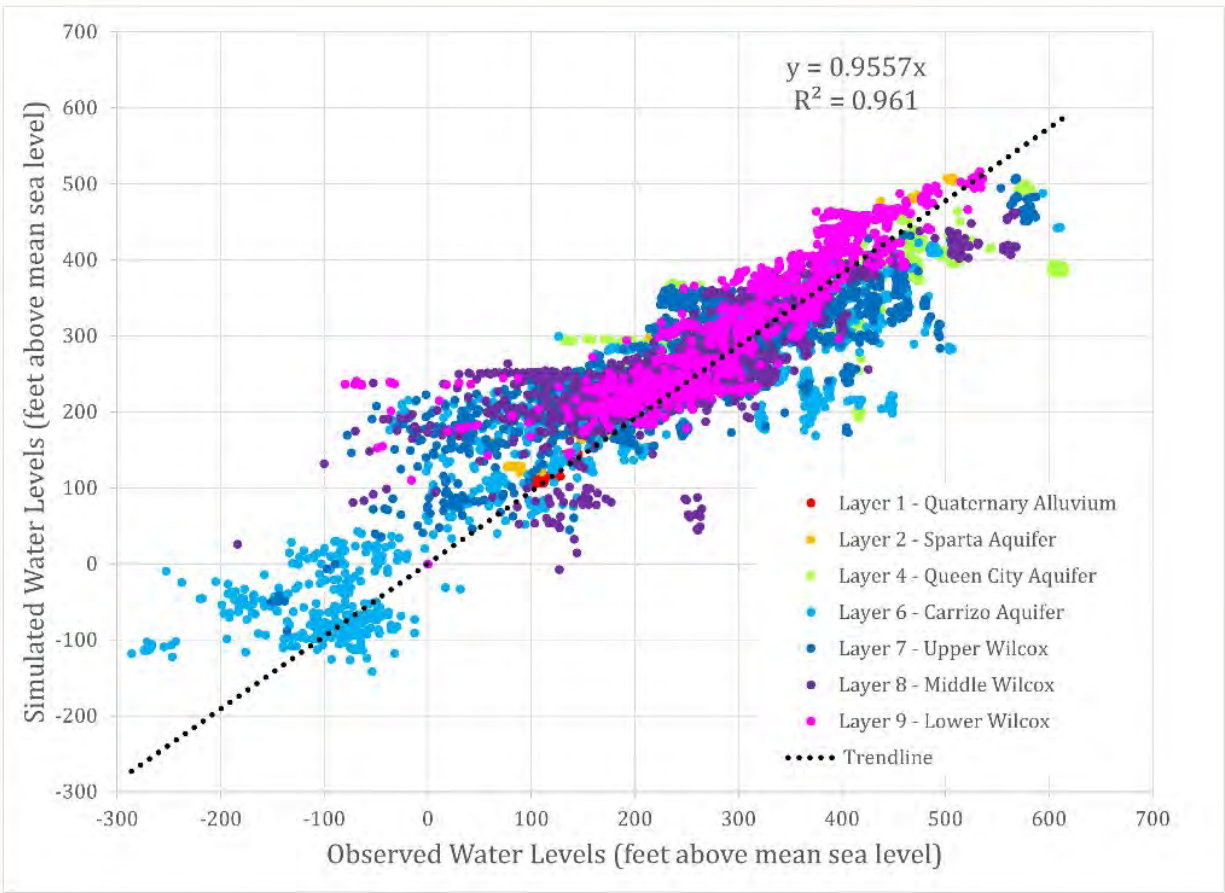


Figure 3.2-11. Observed vs. Simulated Water Level Elevations for Calibrated 1980 to 2013 Simulation

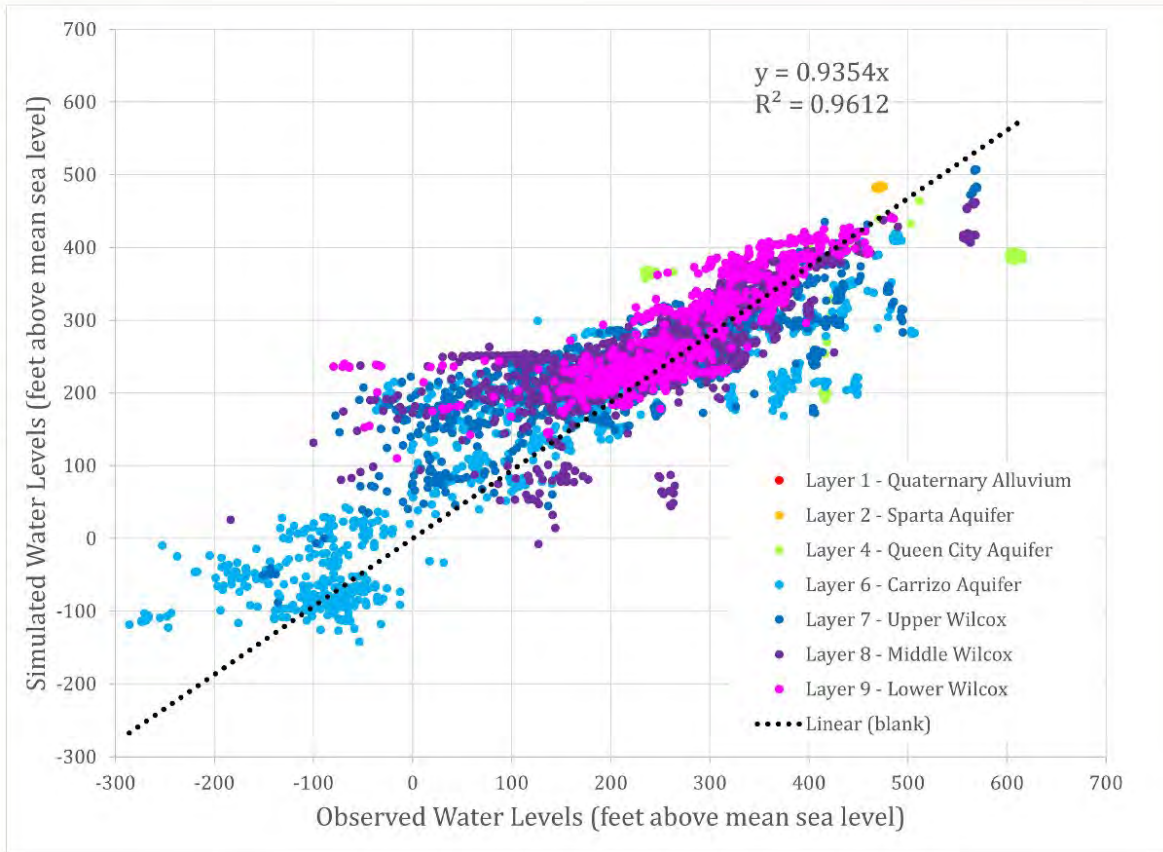


Figure 3.2-12. Observed vs. Simulated Confined Water Level Elevations for Calibrated 1980 to 2013 Simulation

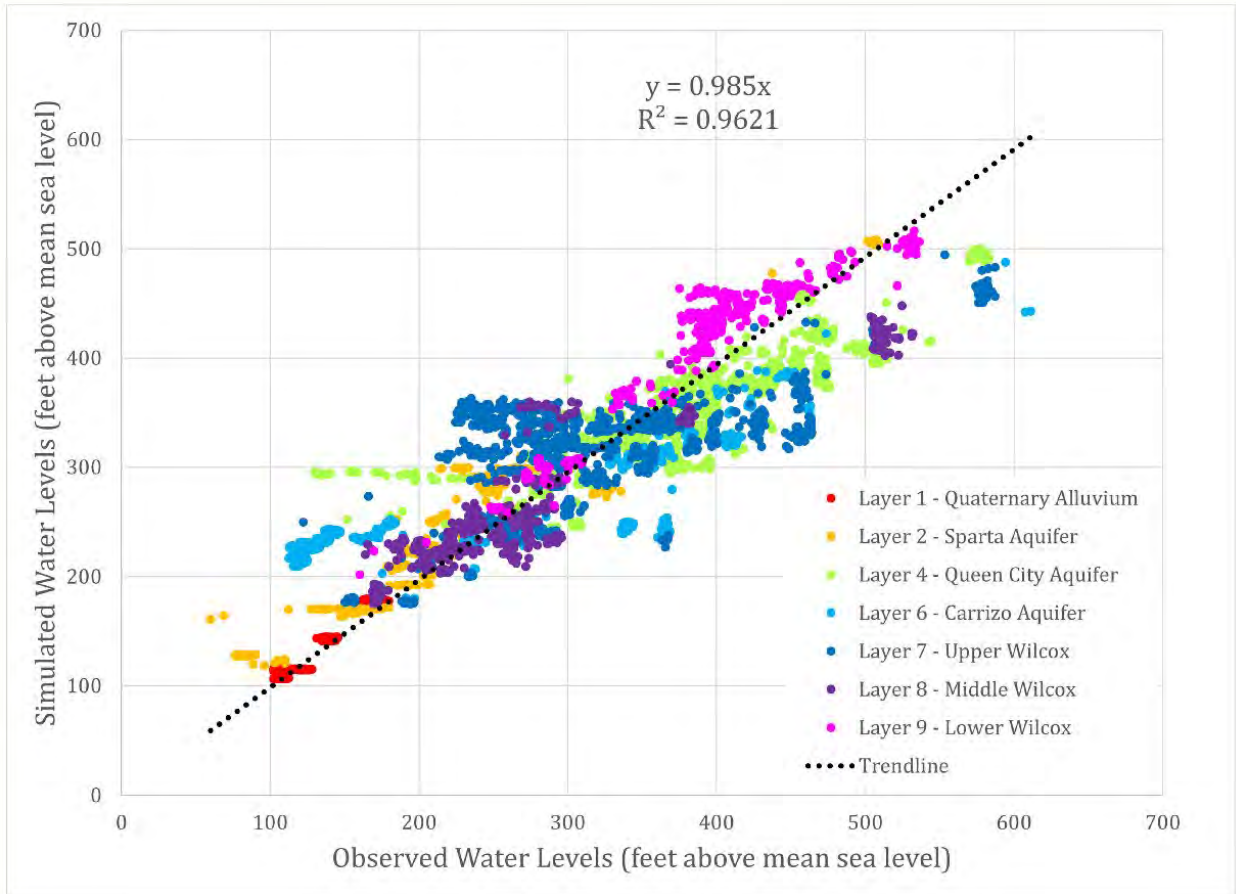


Figure 3.2-13. Observed vs. Simulated Unconfined Water Level Elevations for Calibrated 1980 to 2013 Simulation

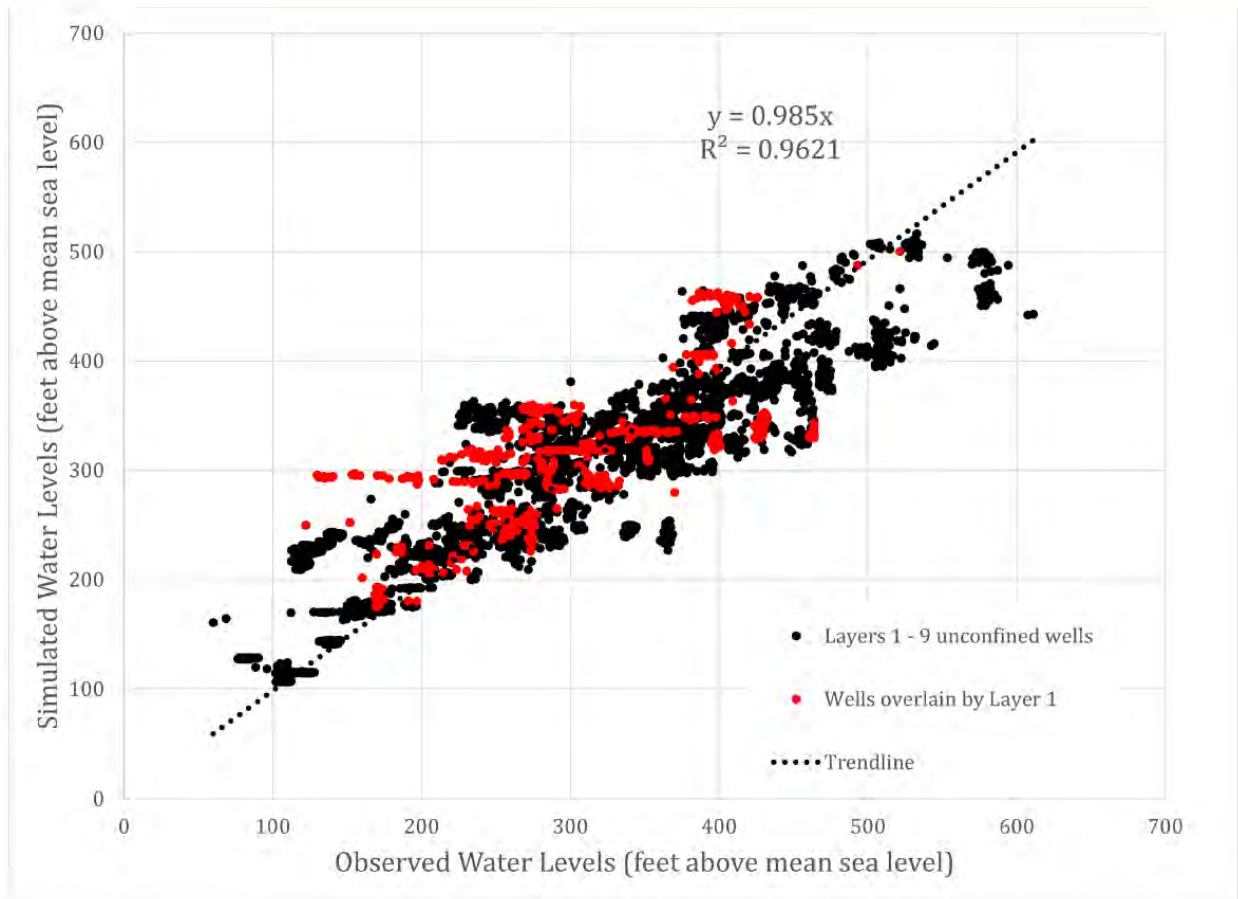


Figure 3.2-14. Observed vs. Simulated Unconfined Water Level Elevations for Calibrated 1980 to 2013 Simulation showing Wells Overlain by Layer 1

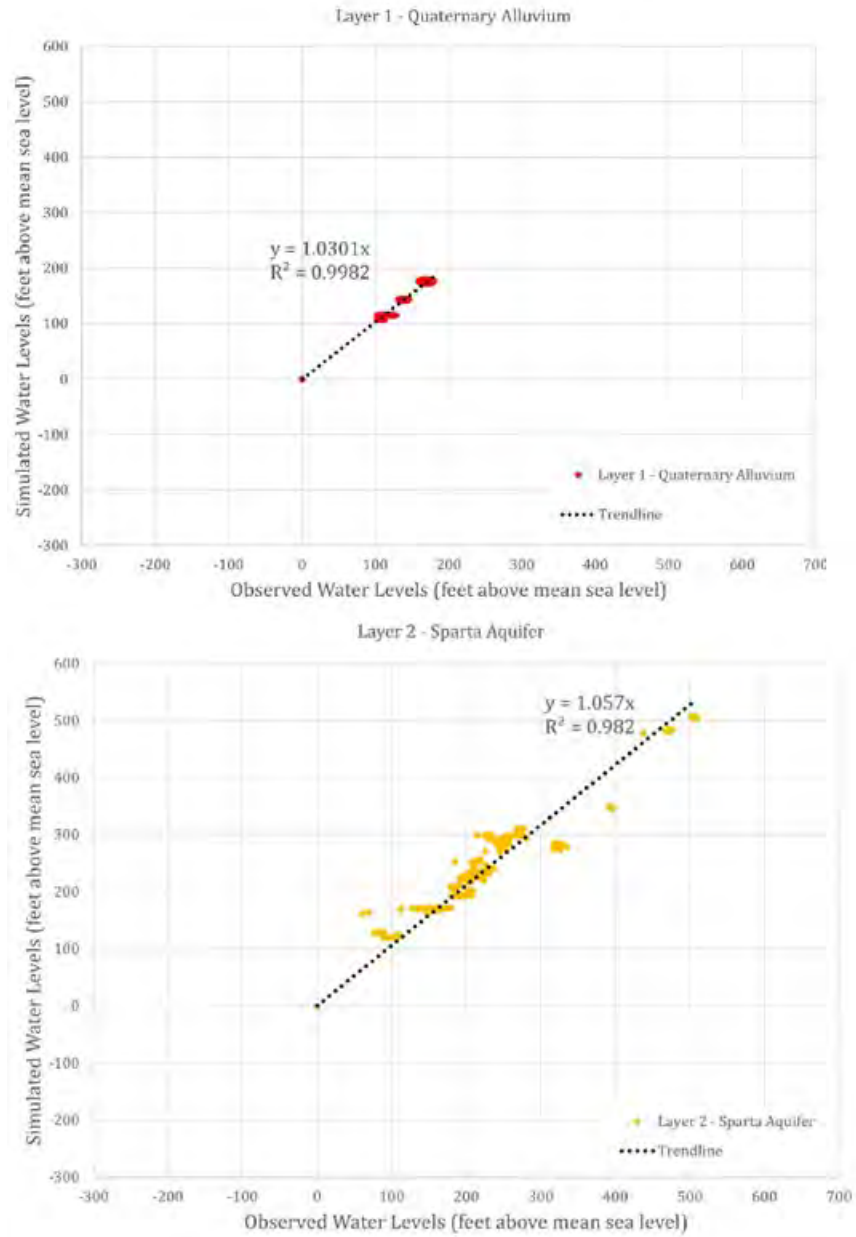


Figure 3.2-15a. Observed vs. Simulated Water Level Elevations for Calibrated 1980 to 2013 Simulation by Layer

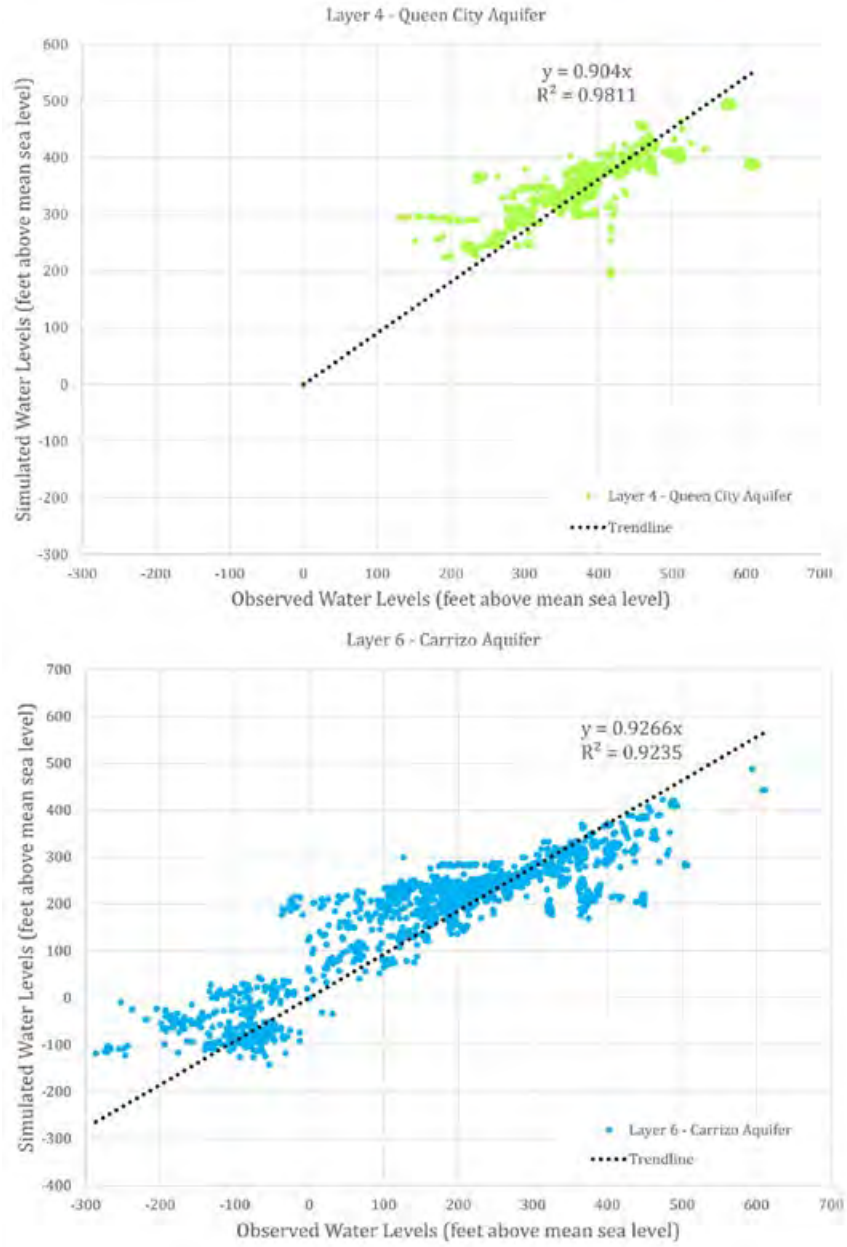


Figure 3.2-15b. Observed vs. Simulated Water Level Elevations for Calibrated 1980 to 2013 Simulation by Layer



Figure 3.2-15c. Observed vs. Simulated Water Level Elevations for Calibrated 1980 to 2013 Simulation by Layer

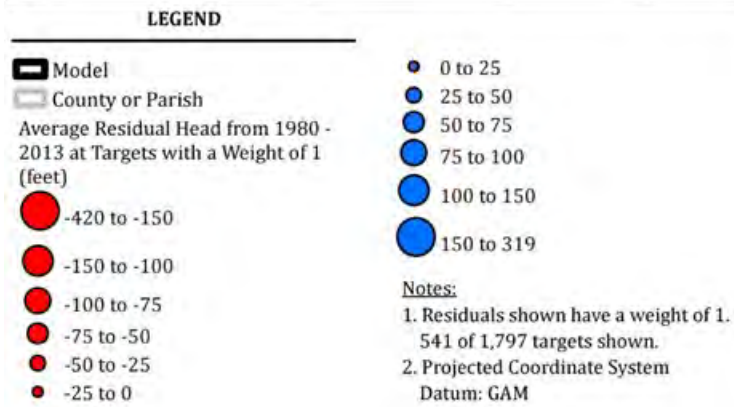
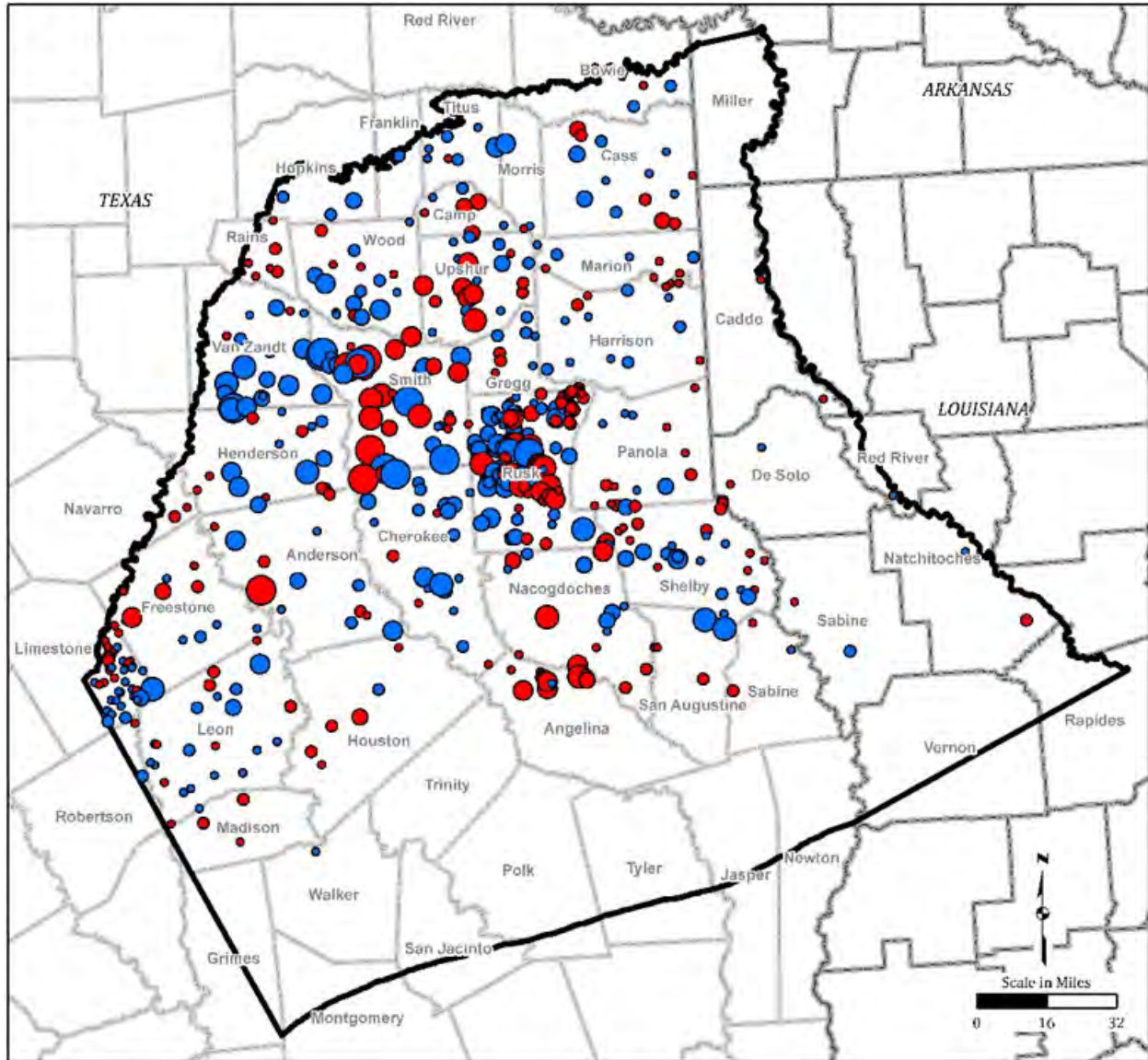


Figure 3.2-16. Distribution of Water Level Elevation Errors for Calibrated 1980 to 2013 Simulation at Weight = 1

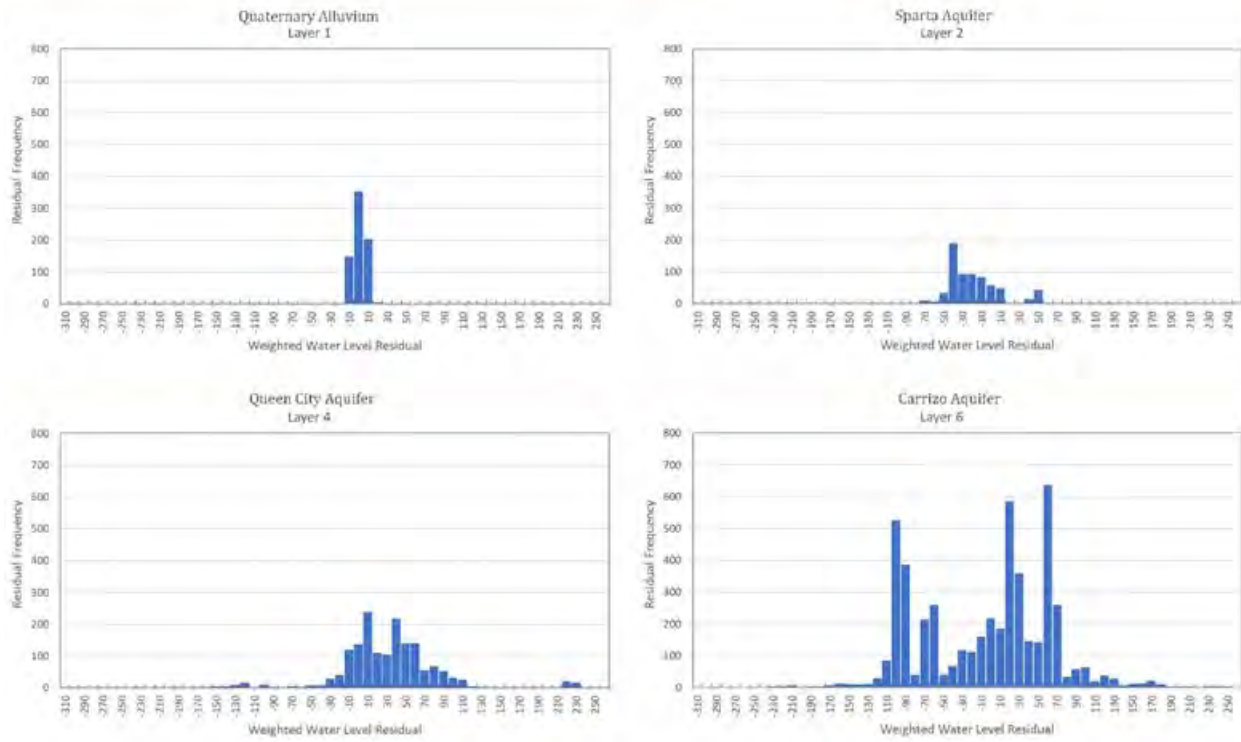


Figure 3.2-17a. Histograms of Water Level Elevation Residuals by Layer

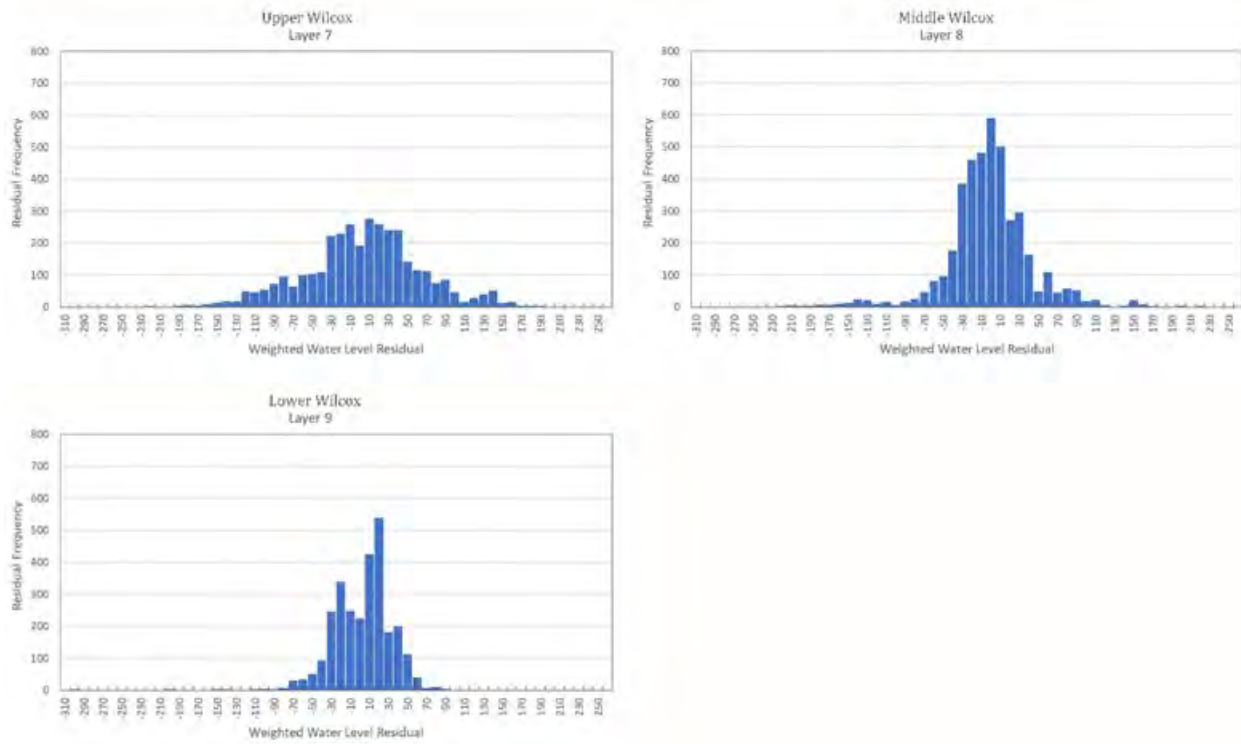


Figure 3.2-17b. Histograms of Water Level Elevation Residuals by Layer

3.2.4 Water Level Hydrographs

Figures 3.2-18 through 3.2-24 show the observed and simulated hydrographs for select wells with observations spanning the simulation period from 1980 through 2013 within the various aquifer units. Observed water level fluctuations are generally similar in frequency and amplitude. Simulated water level elevations match well to observed in the Quaternary Alluvium (model layer 1) except in the northern-most well in Caddo County where simulated water level elevations are generally higher than observed (as shown on Figure 3.2-18).

Simulated water level elevations in the Sparta Aquifer (model layer 2) are higher and lower compared to observed, depending on the location (Figure 3.2-19). However, fluctuations are of similar magnitude. Simulated water level elevations in the Queen City Aquifer (model layer 4) are generally lower than observed to the north and higher to the south, but general water level trends and fluctuations match observed trends and amplitudes, as shown on Figure 3.2-20. Simulated water level elevations in the Carrizo Aquifer (model layer 6) are generally lower than observed water level elevations, except for Cass County where simulated and observed water levels match well and Leon County where simulated water level elevations are greater than observed, as shown on Figure 3.2-21.

Simulated water level elevations in the Upper Wilcox (model layer 7) are generally lower than observed water level elevations, except for Sabine and Rusk counties where simulated and observed water levels match well, as shown on Figure 3.2-22. Frequency and amplitude of fluctuations are similar at most wells except the well in Leon County where simulated water level elevation declines are smaller than measured. Simulated water level elevations in the Middle Wilcox (model layer 8) generally match well to observed water level elevations, except for Camp County where the simulated water level elevations do not follow the observed water level trend and Harrison County where simulated groundwater is much lower than observed water level elevations, as shown on Figure 3.2-23. A better definition of increase in pumping through time in that area would better match the observed decline in water levels during the simulation period. Simulated water level elevations in model layer 9 are higher than observed at some wells and lower in others, as shown on Figure 3.2-24. The simulated water level elevations in Panola County show a dip in 2003 that is not shown in the observed data.

Appendix B provides water level hydrographs for target wells containing 30 or more observed water level elevations at the well. The hydrographs compare the draft and final simulated water level elevations and observed water level elevations for 143 wells with 30 or more measurements. The final simulated water level measurements closely match the draft measurements for most of the target wells shown. Though the final simulated water level measurements are higher or lower than the draft measurements at some locations, the general shape of response is consistent.

3.2.5 Simulated Water Levels

Figures 3.2-25 through 3.2-33 show the simulated water level elevations in the 9 modeled layers, respectively, at the end of the simulation period in 2013. Water level elevations show water flows generally to the southern boundary in all layers. Model layer 1, representing the Quaternary Alluvium, reflects flow in the river channels, as shown on

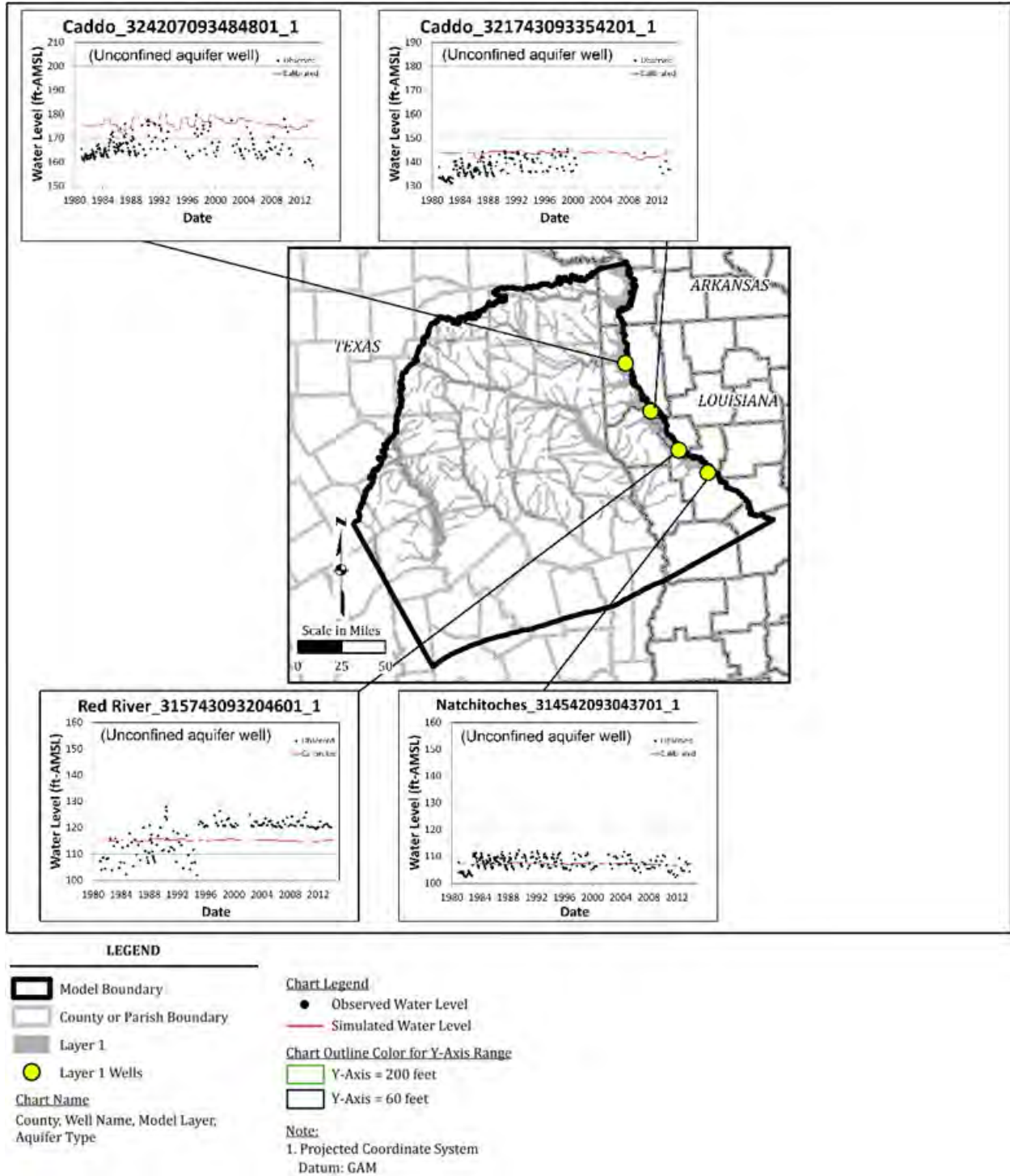
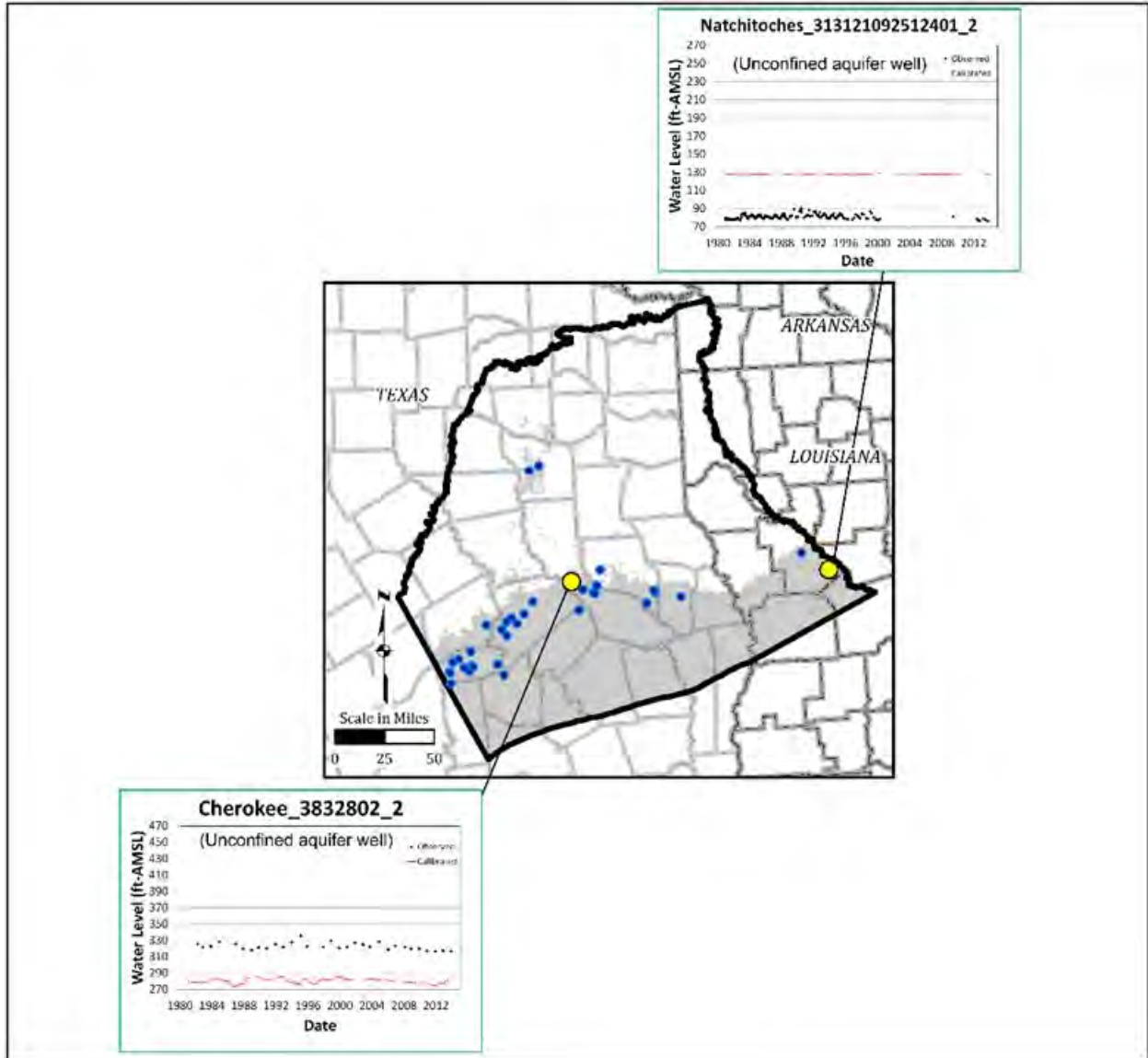


Figure 3.2-18. Measured and Simulated Water Level Elevation Hydrographs for Select Wells - Quaternary Alluvium (Layer 1)



LEGEND

- Model Boundary
- County or Parish Boundary
- Layer
- Select Layer 2 Wells
- Layer 2 Wells

Chart Name
County, Well Name, Model Layer, Aquifer Type

Chart Legend

- Observed Water Level
- Simulated Water Level

Chart Outline Color for Y-Axis Range

- Y-Axis = 200 feet
- Y-Axis = 60 feet

Notes:

1. The layer contains discontinuous outcrops, consistent with the conceptual model (Section 2).
2. Projected Coordinate System Datum: GAM.

Figure 3.2-19. Measured and Simulated Water Level Elevation Hydrographs for Select Wells - Sparta Aquifer (Layer 2)

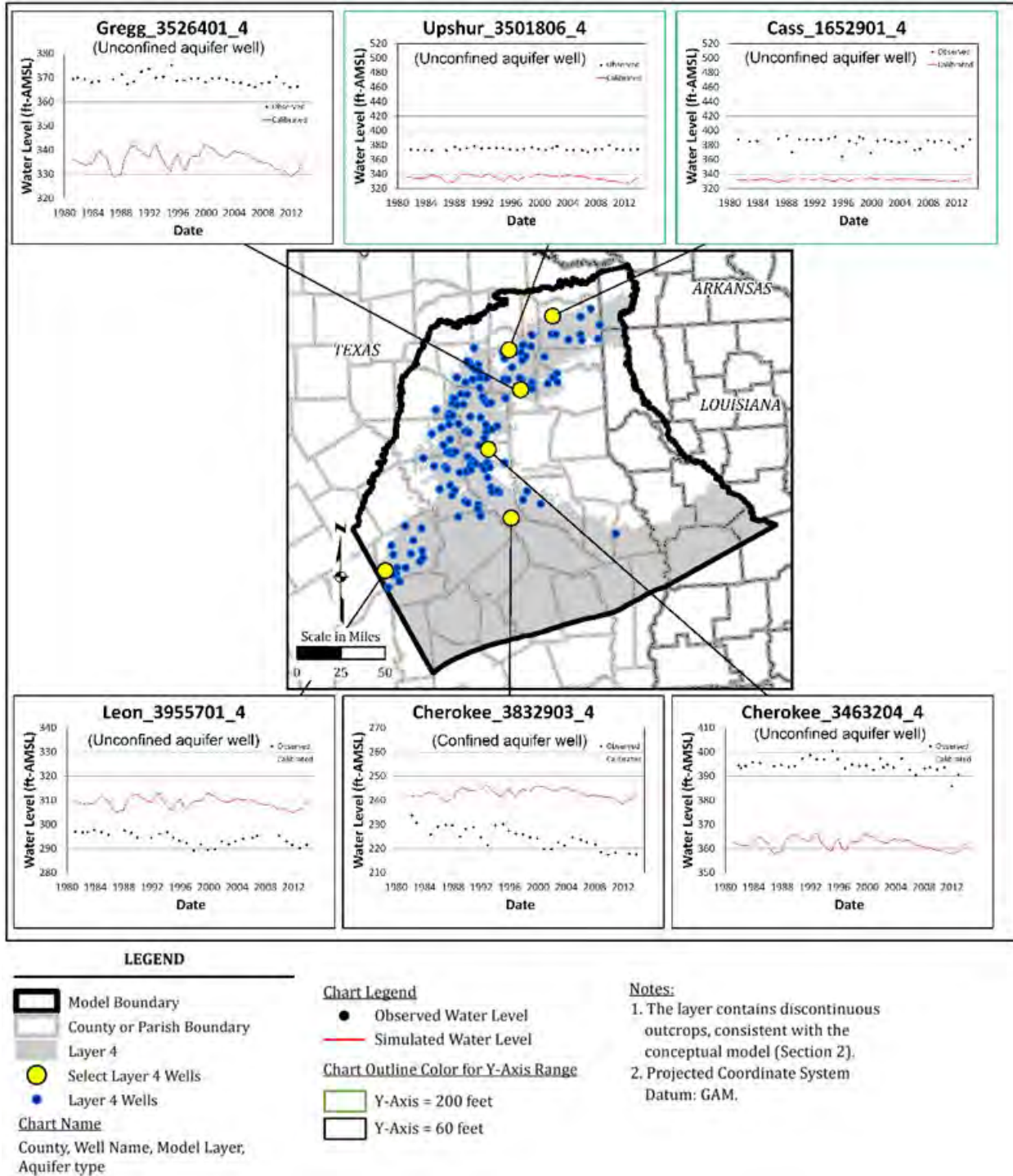


Figure 3.2-20. Measured and Simulated Water Level Elevation Hydrographs for Select Wells - Queen City Aquifer (Layer 4)

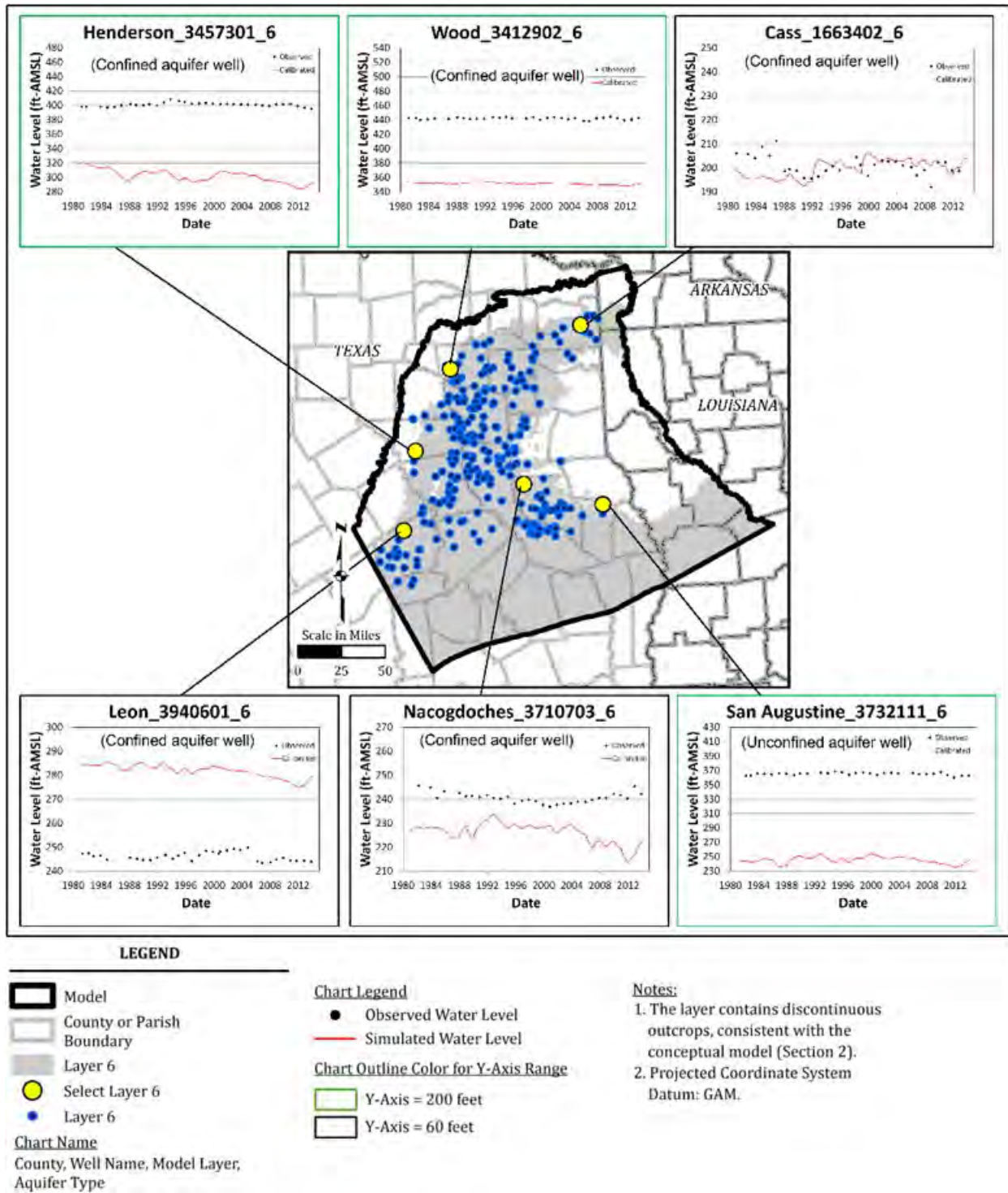


Figure 3.2-21. Measured and Simulated Water Level Elevation Hydrographs for Select Wells - Carrizo Aquifer (Layer 6)

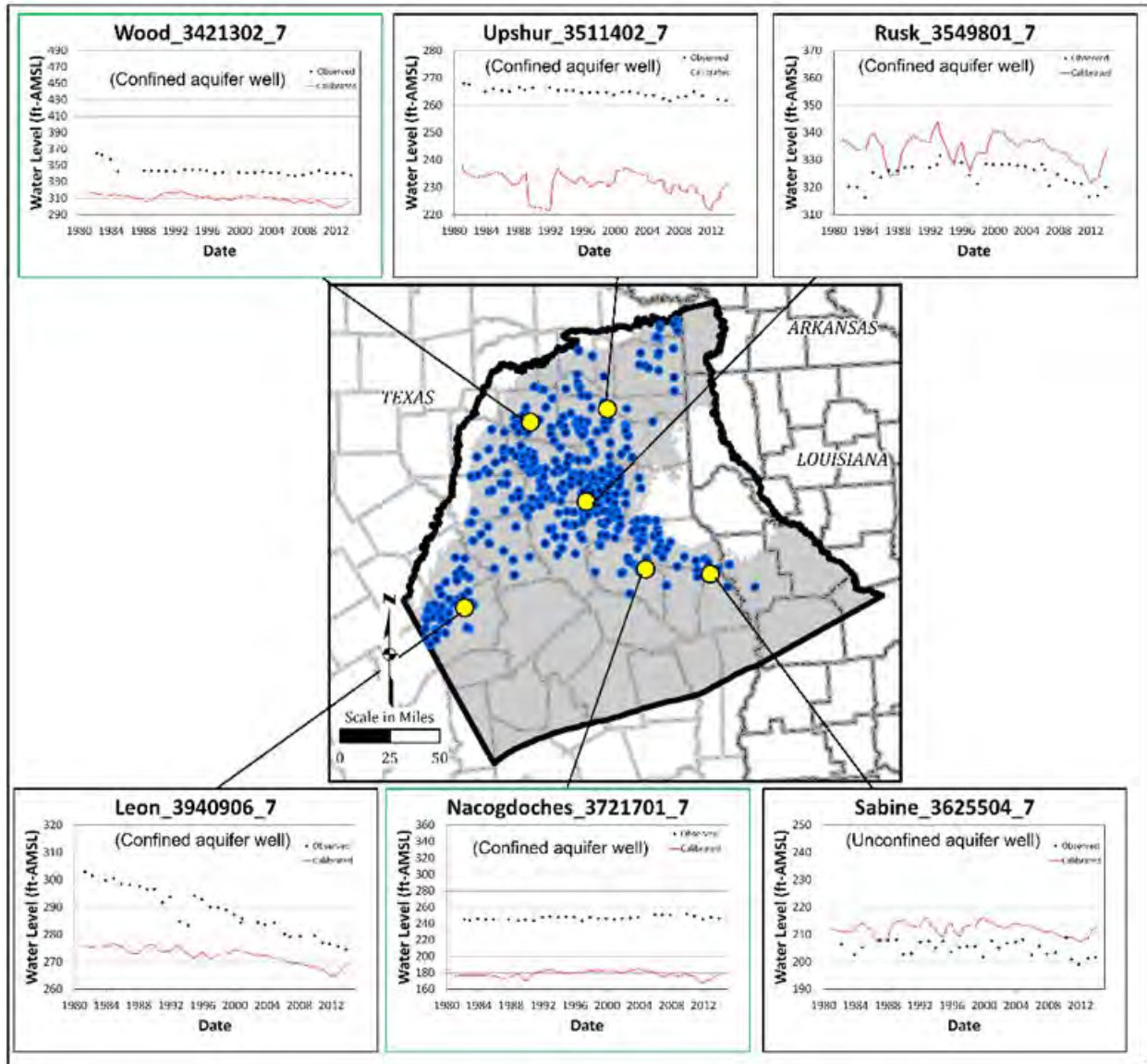


Figure 3.2-22. Measured and Simulated Water Level Elevation Hydrographs for Select Wells - Upper Wilcox (Layer 7)

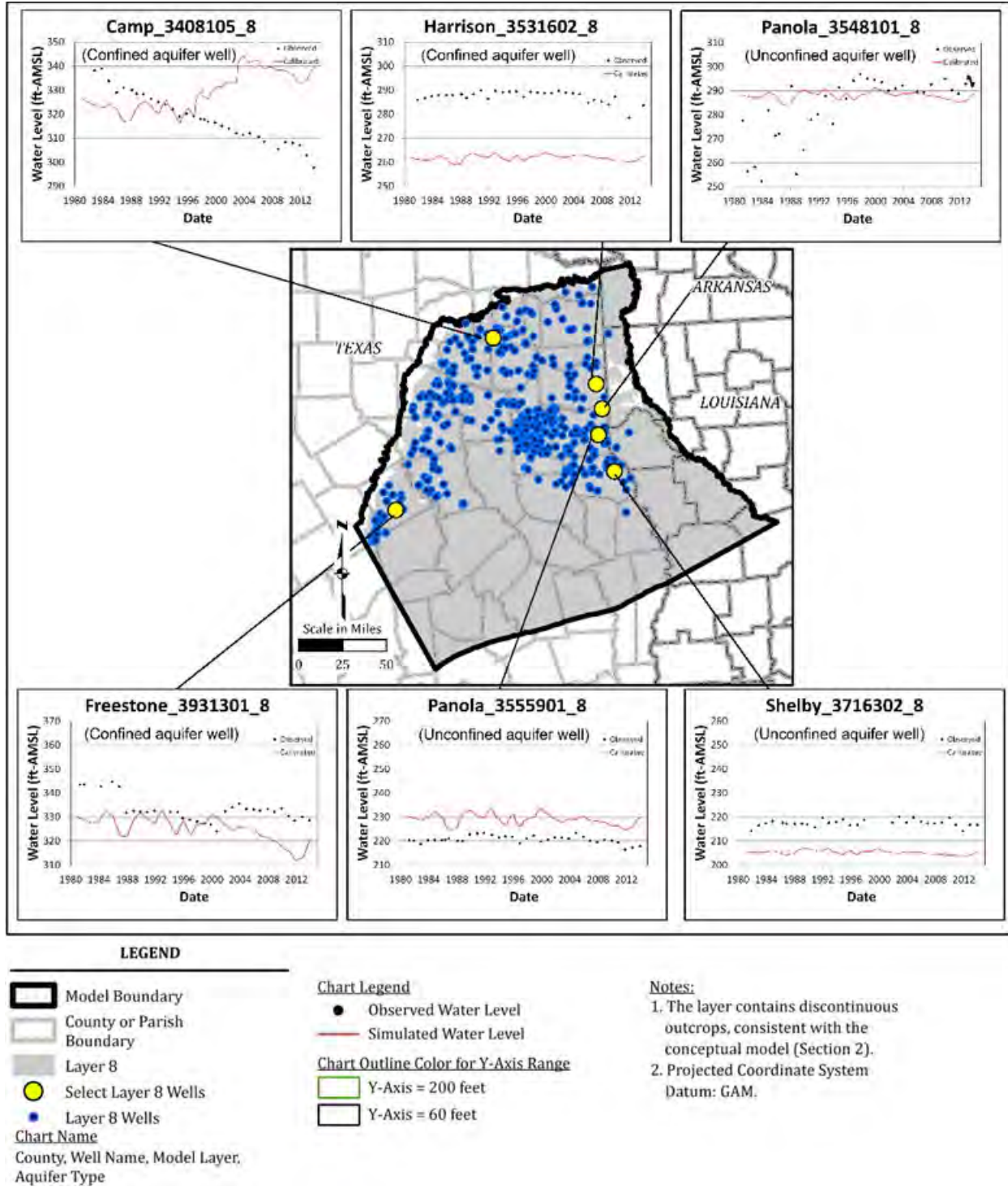


Figure 3.2-23. Measured and Simulated Water Level Elevation Hydrographs for Select Wells - Middle Wilcox (Layer 8)

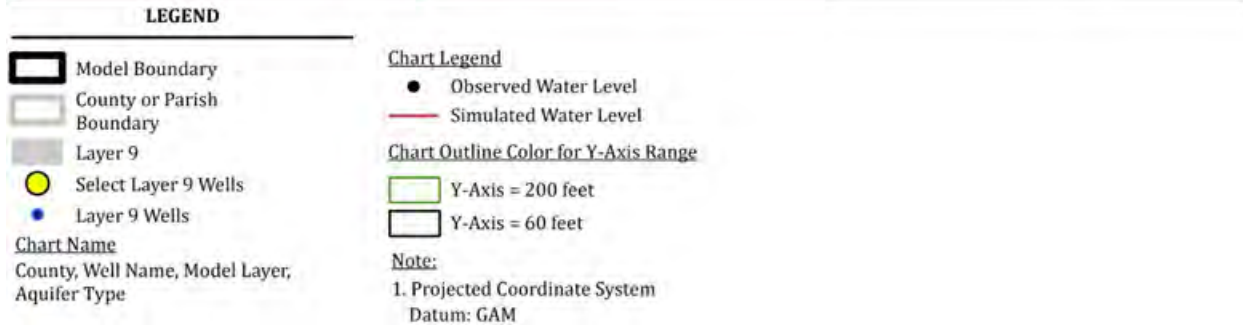
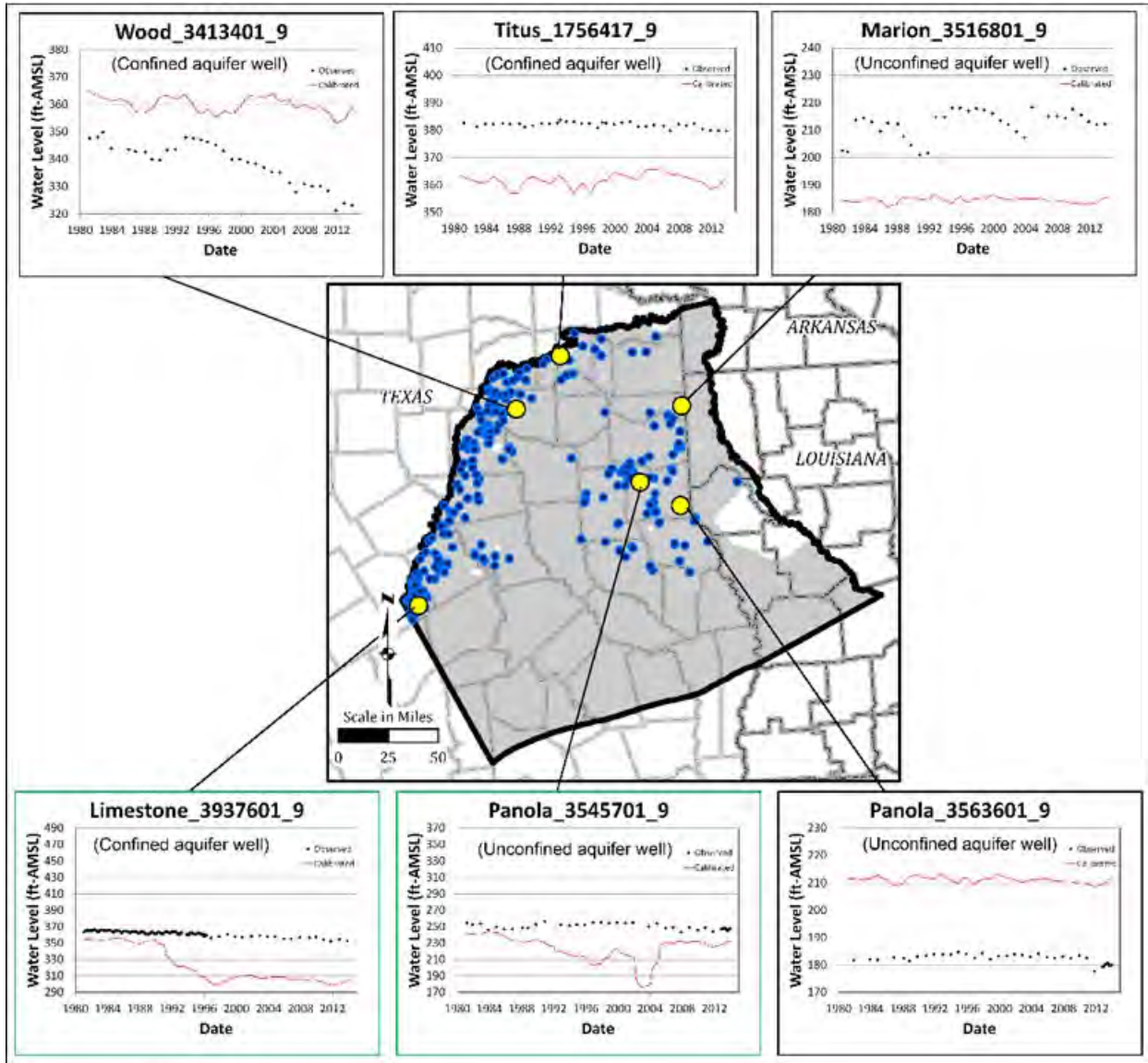
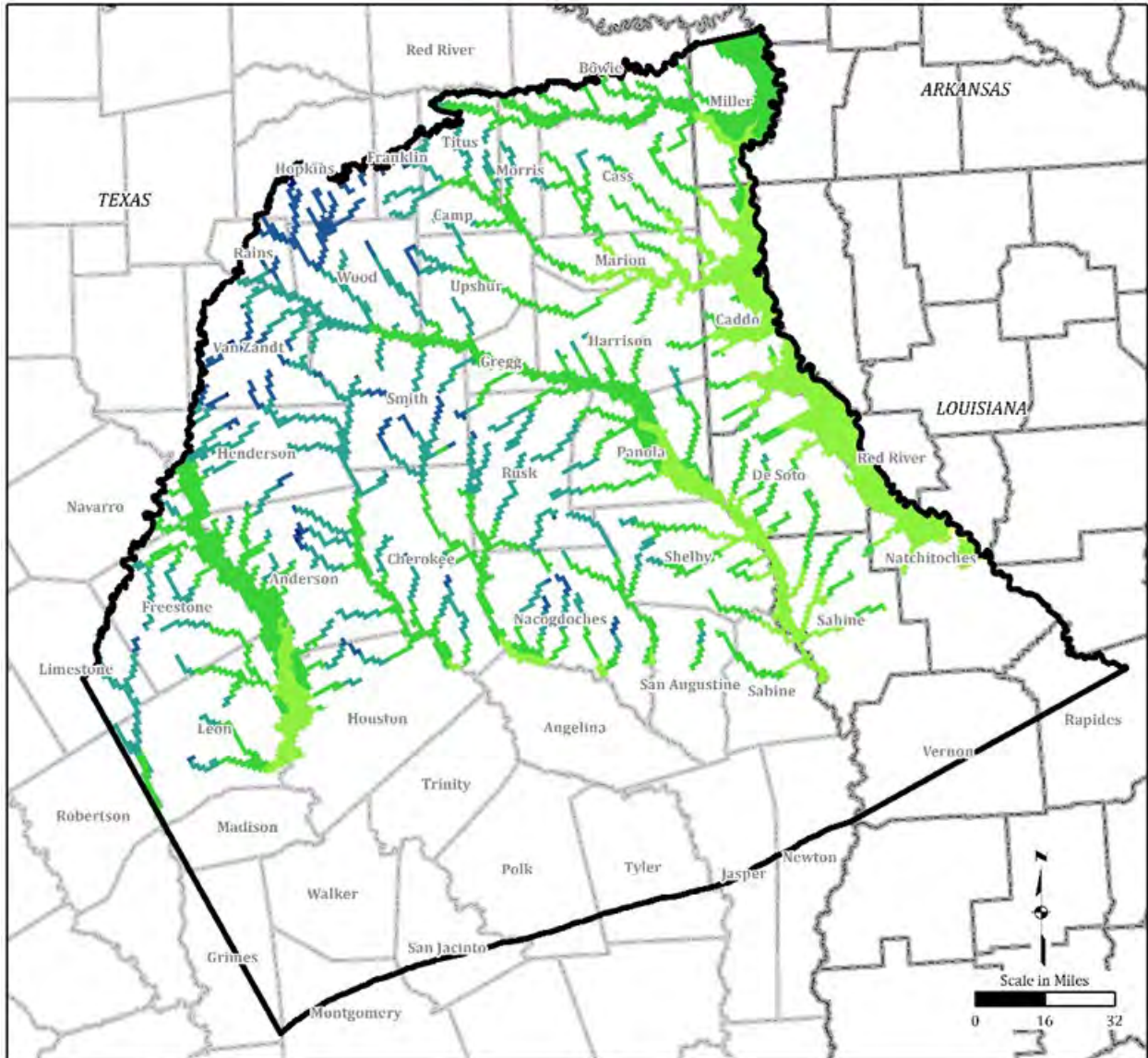


Figure 3.2-24. Measured and Simulated Water Level Elevation Hydrographs for Select Wells - Lower Wilcox (Layer 9)

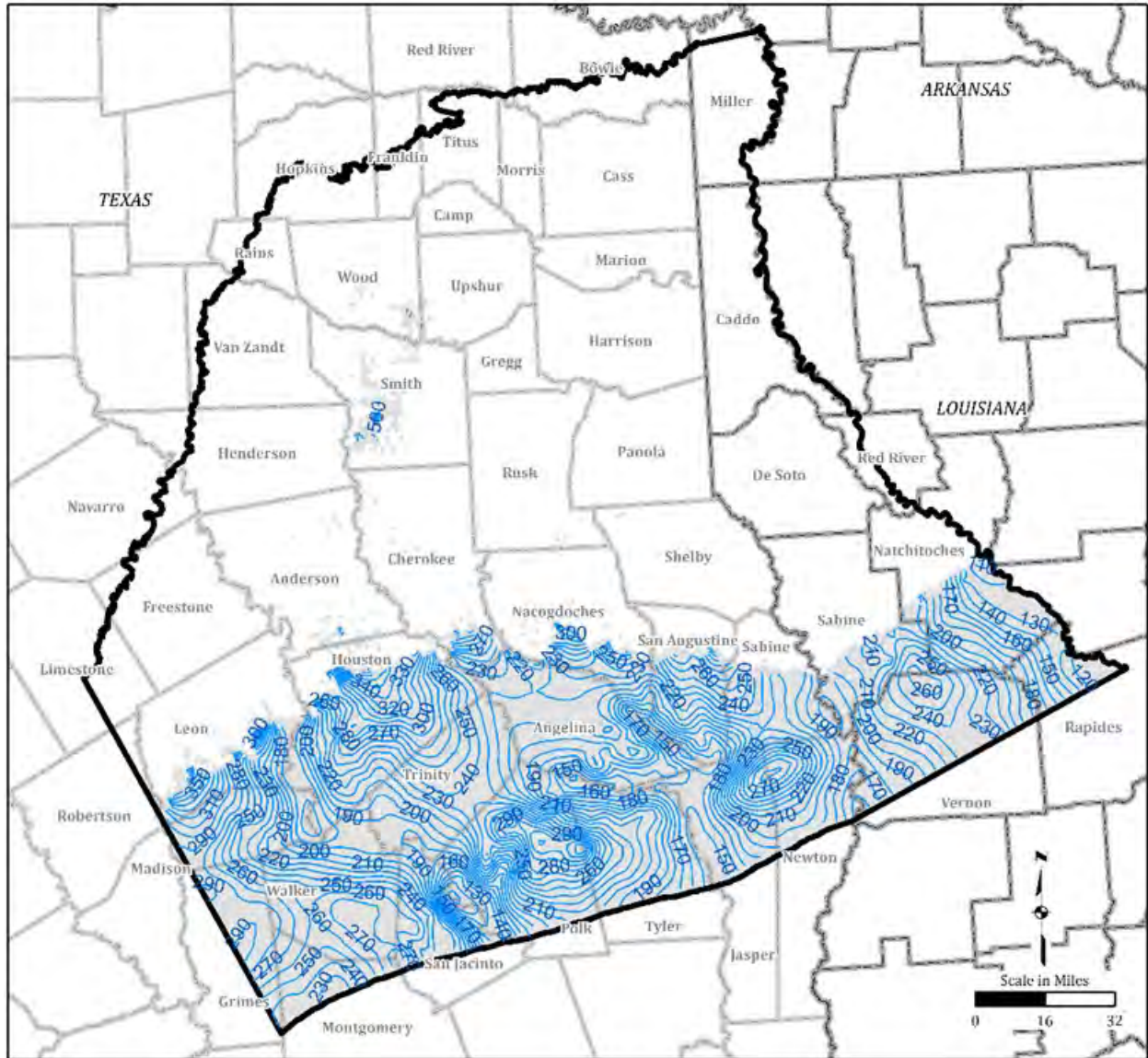


LEGEND





- Model Boundary
- County or Parish Boundary
- Simulated Water Level Elevations (feet above mean sea level)
- 85 to 100
- 100 to 200
- 200 to 300
- 300 to 400
- 400 to 500
- 500 to 525

Note:
 1. Projected Coordinate System
 Datum: GAM

Figure 3.2-25. Simulated Water Level Elevations in Quaternary Alluvium (Layer 1) for 2013



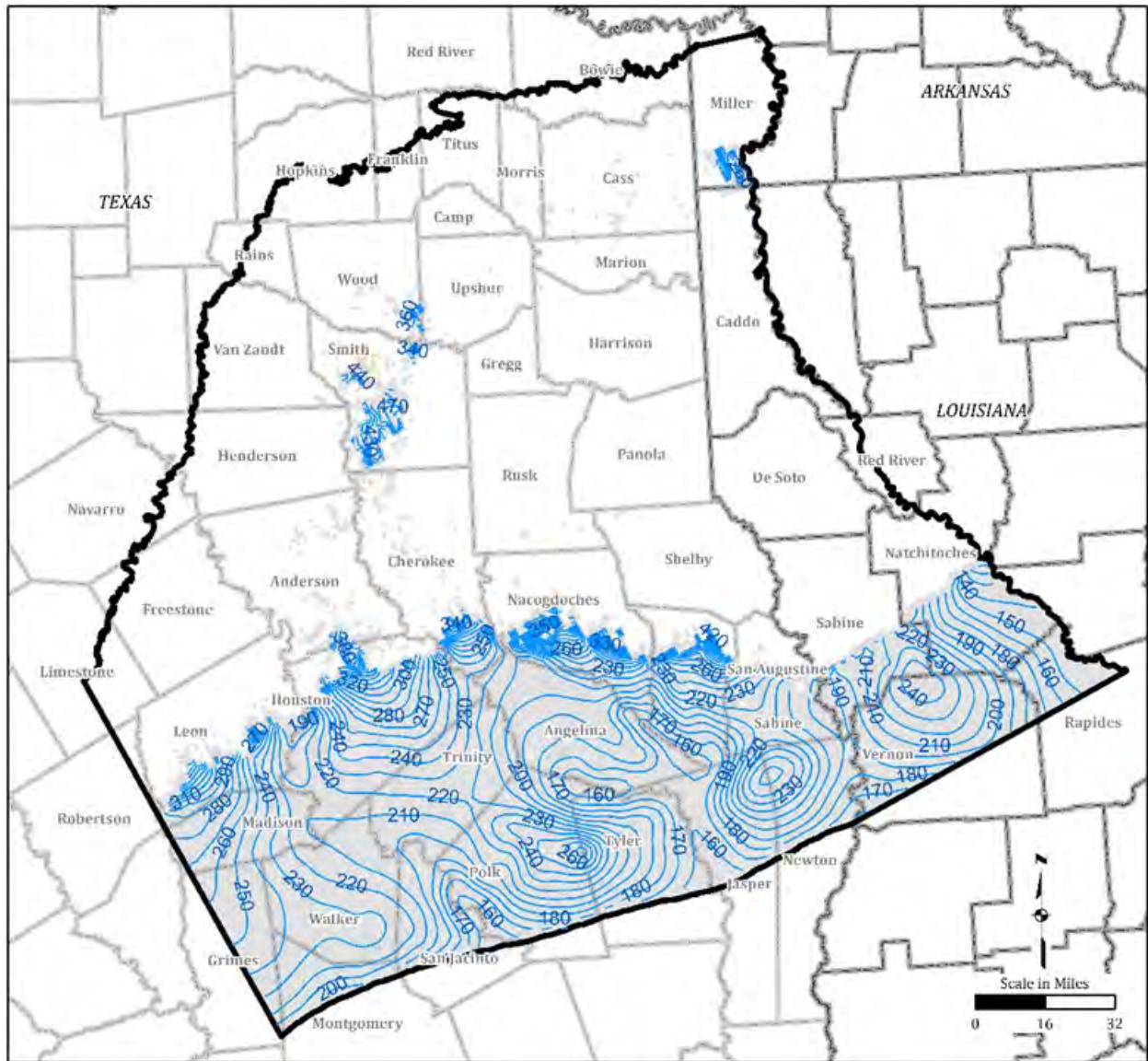
LEGEND

-  Simulated Water Level Elevations Contours (feet above mean sea level)
-  Model
-  County or Parish
-  Layer






Notes:

1. The layer contains discontinuous outcrops, consistent with the conceptual model (Section 2).
2. Projected Coordinate System Datum: GAM.

Figure 3.2-26. Simulated Water Level Elevation Contours in Sparta Aquifer (Layer 2) for 2013



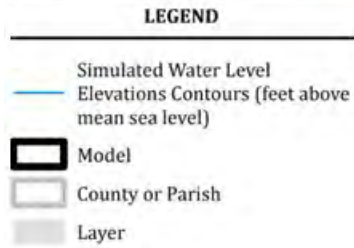
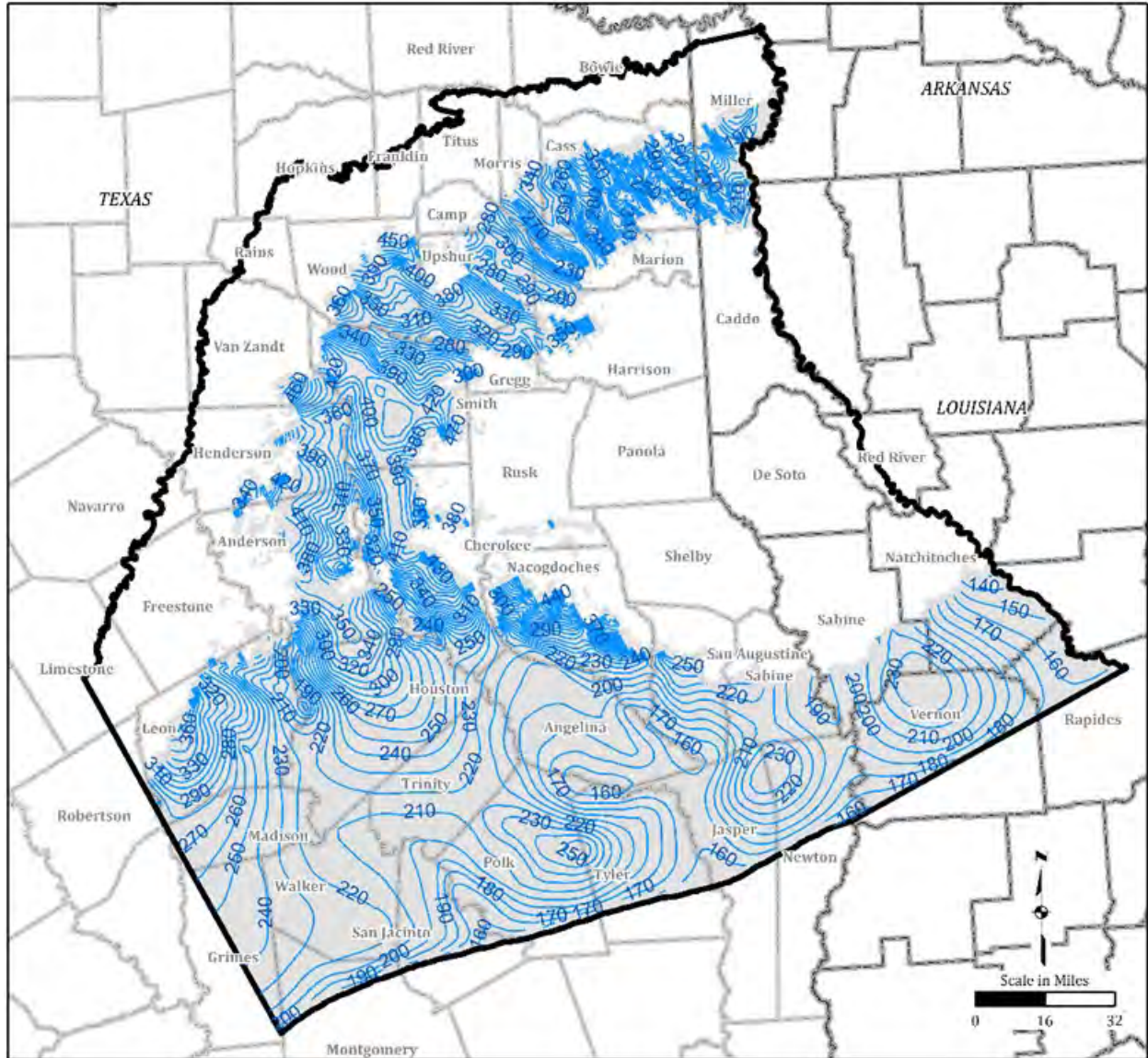
LEGEND

-  Simulated Water Level
-  Elevations Contours (feet above mean sea level)
-  Model
-  County or Parish
-  Layer

Notes:

1. The layer contains discontinuous outcrops, consistent with the conceptual model (Section 2).
2. Projected Coordinate System Datum: GAM.

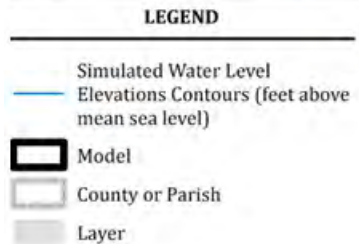
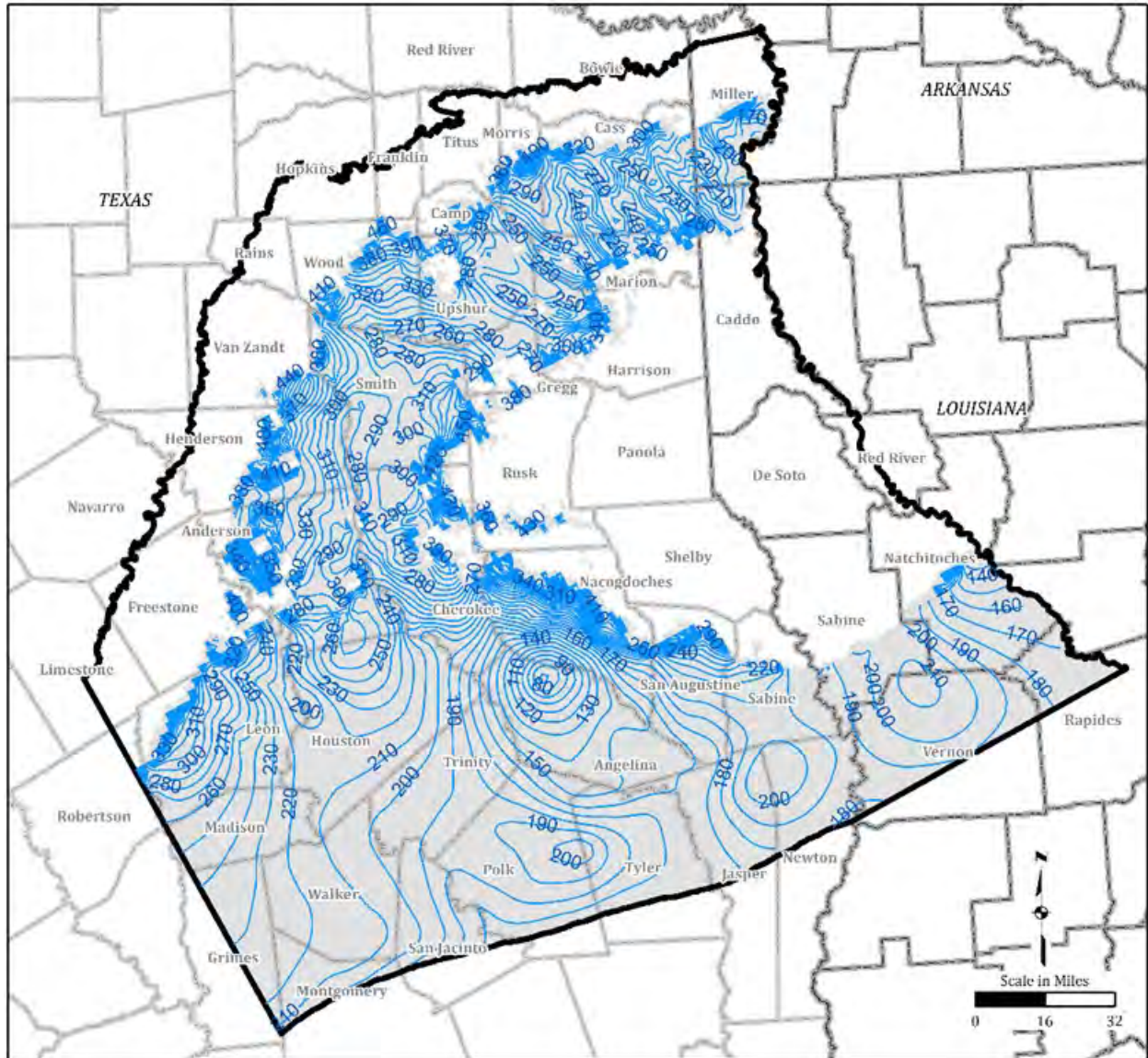
Figure 3.2-27. Simulated Water Level Elevation Contours in Weches Formation (Layer 3) for 2013



Notes:

1. The layer contains discontinuous outcrops, consistent with the conceptual model (Section 2).
2. Projected Coordinate System Datum: GAM.

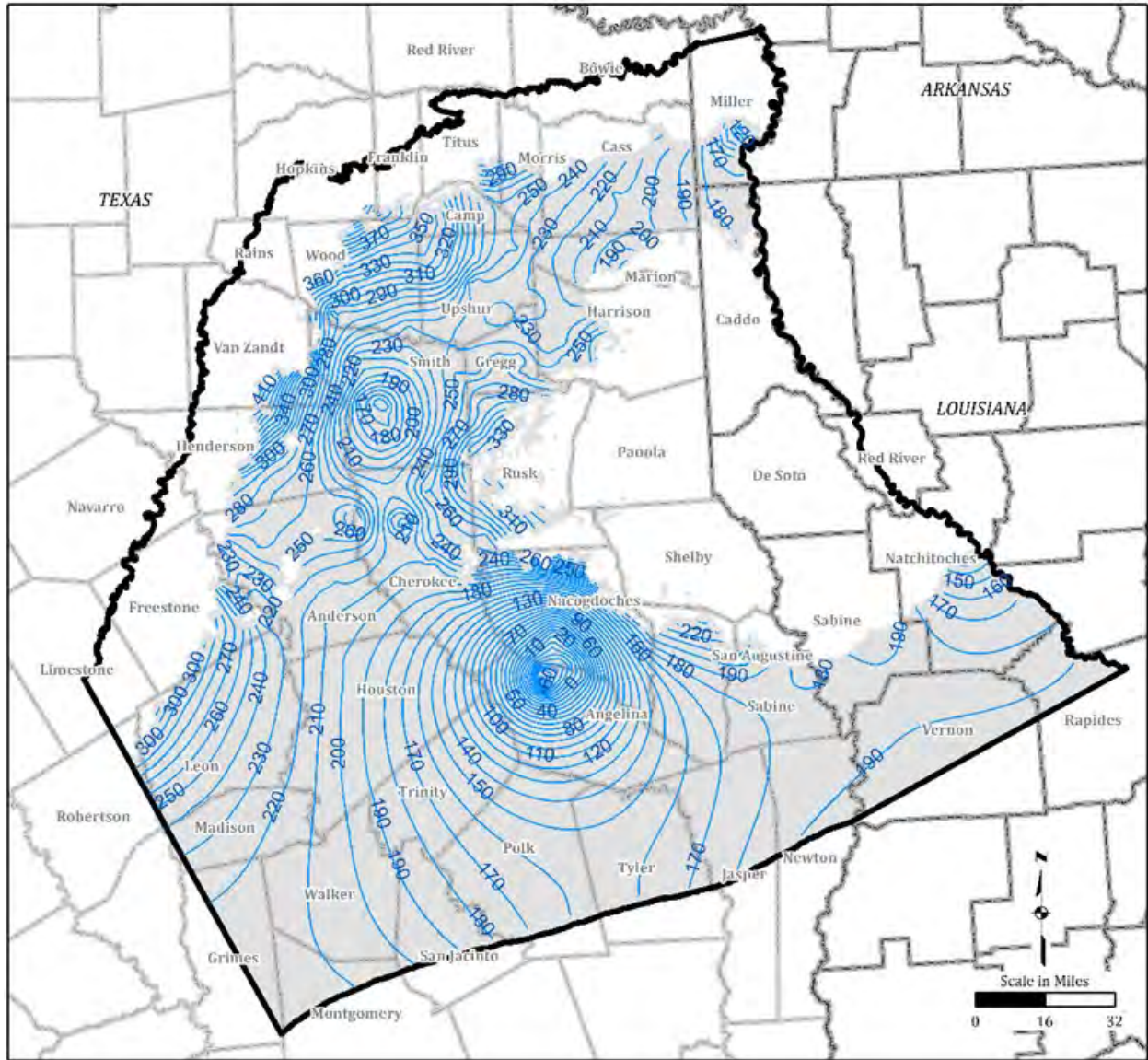
Figure 3.2-28. Simulated Water Level Elevation Contours in Queen City Aquifer (Layer 4) for 2013







Notes:

1. The layer contains discontinuous outcrops, consistent with the conceptual model (Section 2).
2. Projected Coordinate System Datum: GAM.

Figure 3.2-29. Simulated Water Level Elevation Contours in Reklaw Formation (Layer 5) for 2013



LEGEND

-  Simulated Water Level Elevations Contours (feet above mean sea level)
-  Model
-  County or Parish
-  Layer

Notes:

1. The layer contains discontinuous outcrops, consistent with the conceptual model (Section 2).
2. Projected Coordinate System Datum: GAM.

Figure 3.2-30. Simulated Water Level Elevation Contours in Carrizo Aquifer (Layer 6) for 2013

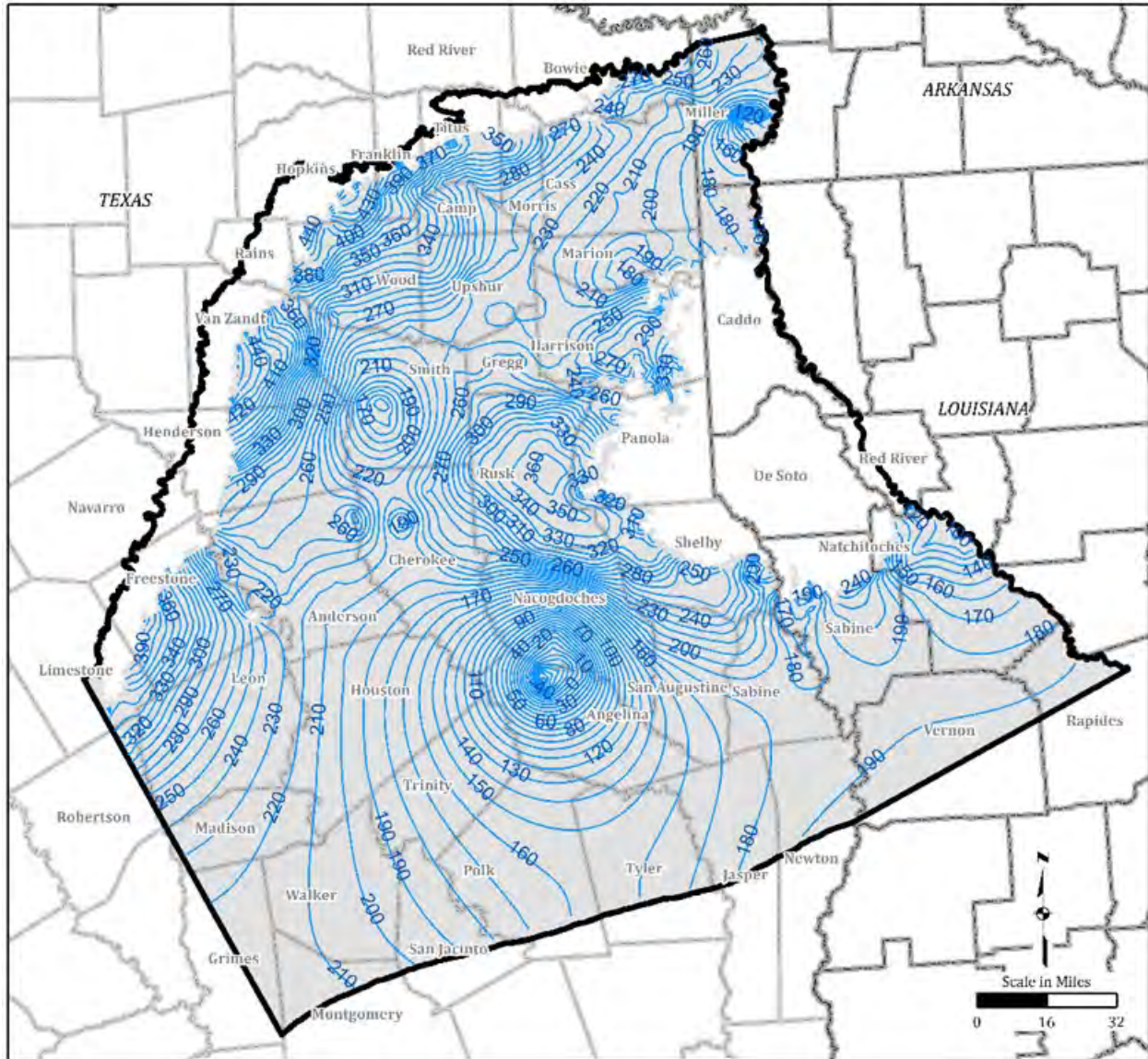
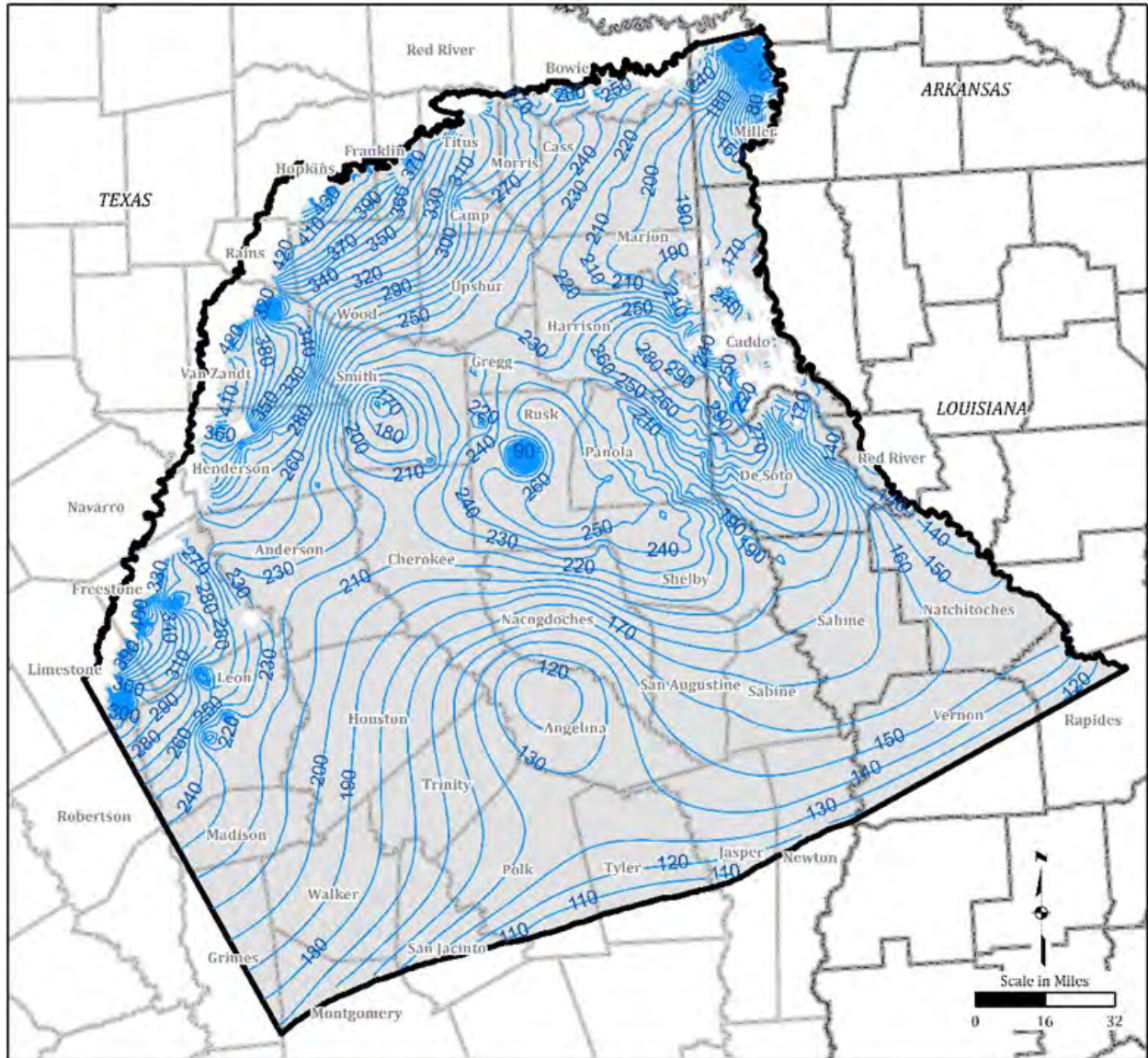


Figure 3.2-31. Simulated Water Level Elevation Contours in Upper Wilcox (Layer 7) for 2013



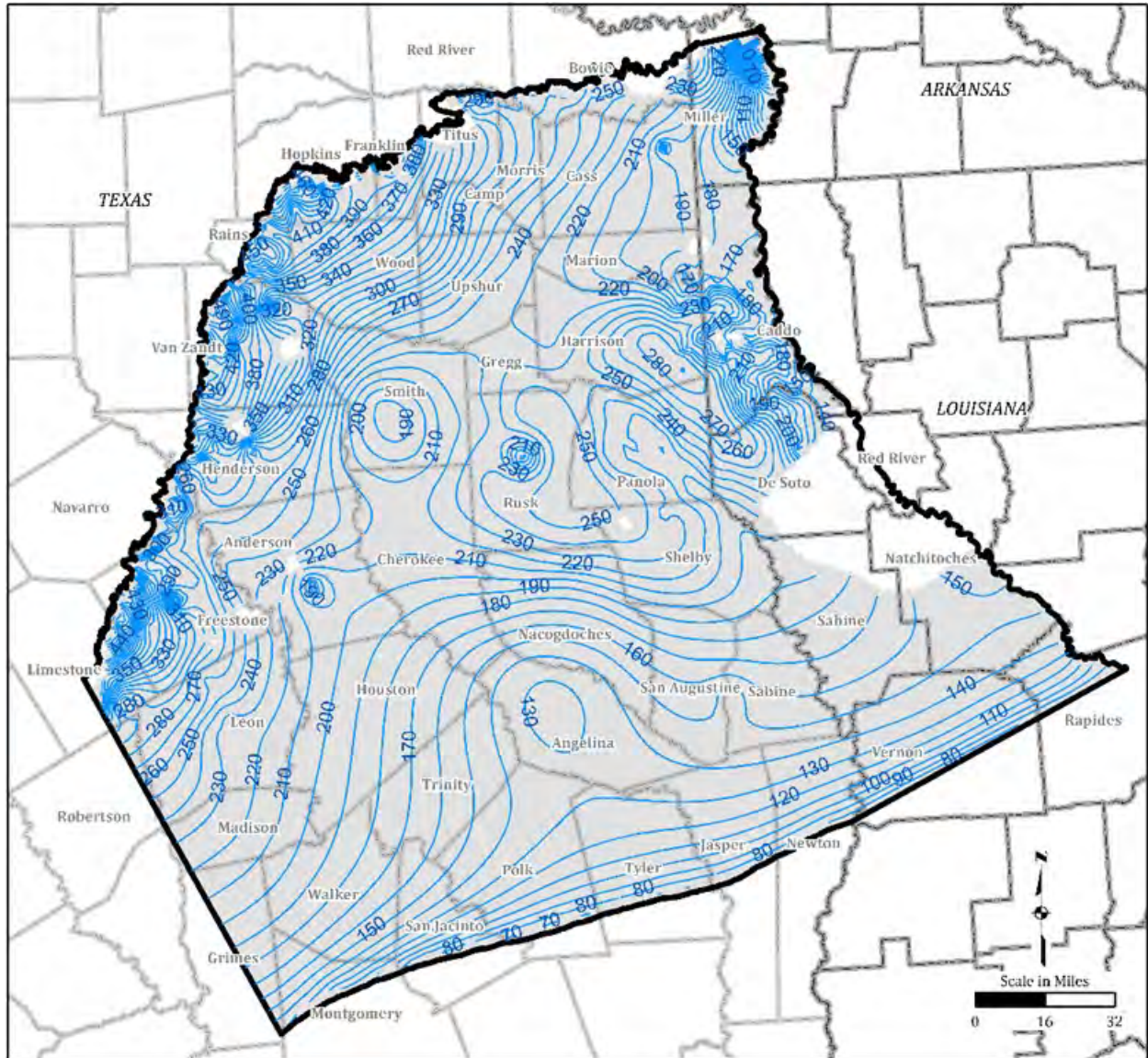
LEGEND

- Simulated Water Level
- Elevations Contours (feet above mean sea level)
- ▭ Model
- ▭ County or Parish
- ▭ Layer






Note:

1. Projected Coordinate System
Datum: GAM

Figure 3.2-32. Simulated Water Level Elevation Contours in Middle Wilcox (Layer 8) for 2013



LEGEND

-  Simulated Water Level
-  Elevations Contours (feet above mean sea level)
-  Model
-  County or Parish
-  Layer

Note:

1. Projected Coordinate System
Datum: GAM

Figure 3.2-33. Simulated Water Level Elevation Contours in Lower Wilcox (Layer 9) for 2013

Figure 3.2-25. Water level elevation contours in deeper units show drawdown cones at pumping wells. The northern portion of the Queen City Aquifer shows numerous water level elevation nonconformities (Figure 3.2-28). Within the Carrizo Aquifer and Wilcox Aquifers (layers 6 through 9), there is a large simulated cone of depression extending across Angelina and Nacogdoches counties (Figure 3.2-30 through 3.2-33). Slightly smaller drawdown cones are noted in Smith County within the Carrizo and Wilcox Aquifers (model layers 6 through 9).

Figures 3.2-34 through 3.2-42 show the change in water level elevations within each layer from 1980 to 2013. Water level elevation changes in the Quaternary Alluvium, Sparta Aquifer, and Weches Formation (model layers 1, 2, and 3) are small with most changes within 20 feet. Water level elevation changes in the lower layers (Queen City, Carrizo, and Wilcox Aquifers) show a large area in the northern portion of the model, centered about Smith County, showing groundwater level elevations decreasing up to 50 feet, as shown on Figures 3.2-37 through 3.2-42. In the Middle Wilcox (model layer 8), groundwater level elevations also decrease up to 500 feet in Miller County, Arkansas, located in the northernmost corner of the model (Figure 3.2-41).

Within the Reklaw Formation, Carrizo Aquifer, and Upper Wilcox (model layers 5, 6, and 7), there is an area of groundwater level elevation increase between 1980 and 2013 centered about Nacogdoches and Angelina counties (Figures 3.2-38 through 3.2-40). Mounding exceeds 50 feet in both the Carrizo Aquifer and Upper Wilcox (model layers 6 and 7). Otherwise, change in water level elevation figures for the Carrizo and Wilcox Aquifers (model layers 6 through 9) show the bulk of the model domain has groundwater elevations that fluctuate within 25 feet from 1980 to 2013 (Figures 3.2-39 through 3.2-42).

Figures 3.2-43 through 3.2-48 compare simulated groundwater level elevation contours from the end of the model simulation period, 2013, to the groundwater level elevation contours using 2015 data presented in the Conceptual Model Report (Montgomery and Associates, 2020). The Conceptual Model Report used observed data to interpolate the 2015 groundwater level elevation surface. Comparisons are provided for the Sparta Aquifer, Queen City Aquifer, Carrizo Aquifer, and Wilcox Aquifer (model layers 2, 4, 6, 7, 8, and 9). Even though comparisons are made between 2013 modeled conditions and 2015 observed conditions, there was minimal change in average water level conditions between the two years.

The Sparta Aquifer (model layer 2) conceptual contours are uncertain over much of the layer, as indicated on Figure 3.2-43 by dashed lines. Generally, 2013 simulated groundwater level elevations are consistent with the elevations of the observed 2015 water level elevation surface with similar gradients pointed in the southward direction. The Queen City Aquifer (model layer 4) 2013 simulated and 2015 observed groundwater contours are similar, and both show southward flow, as shown on Figure 3.2-44. The 2015 observed pumping centers near Wood and Cherokee counties are not clearly present in the 2013 simulated contours but the two-year time difference between the observed and simulated contours may account for some of these differences. The Carrizo Aquifer and Upper Wilcox (model layers 6 and 7) observed and simulated contours match more closely and both show pumping centers in Nacogdoches and Smith counties with elevations of similar values, showing flow to the south, as shown on Figures 3.2-45 and 3.2-46.

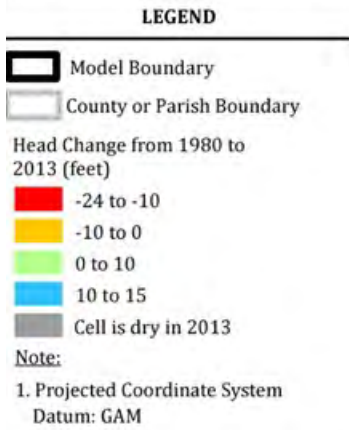
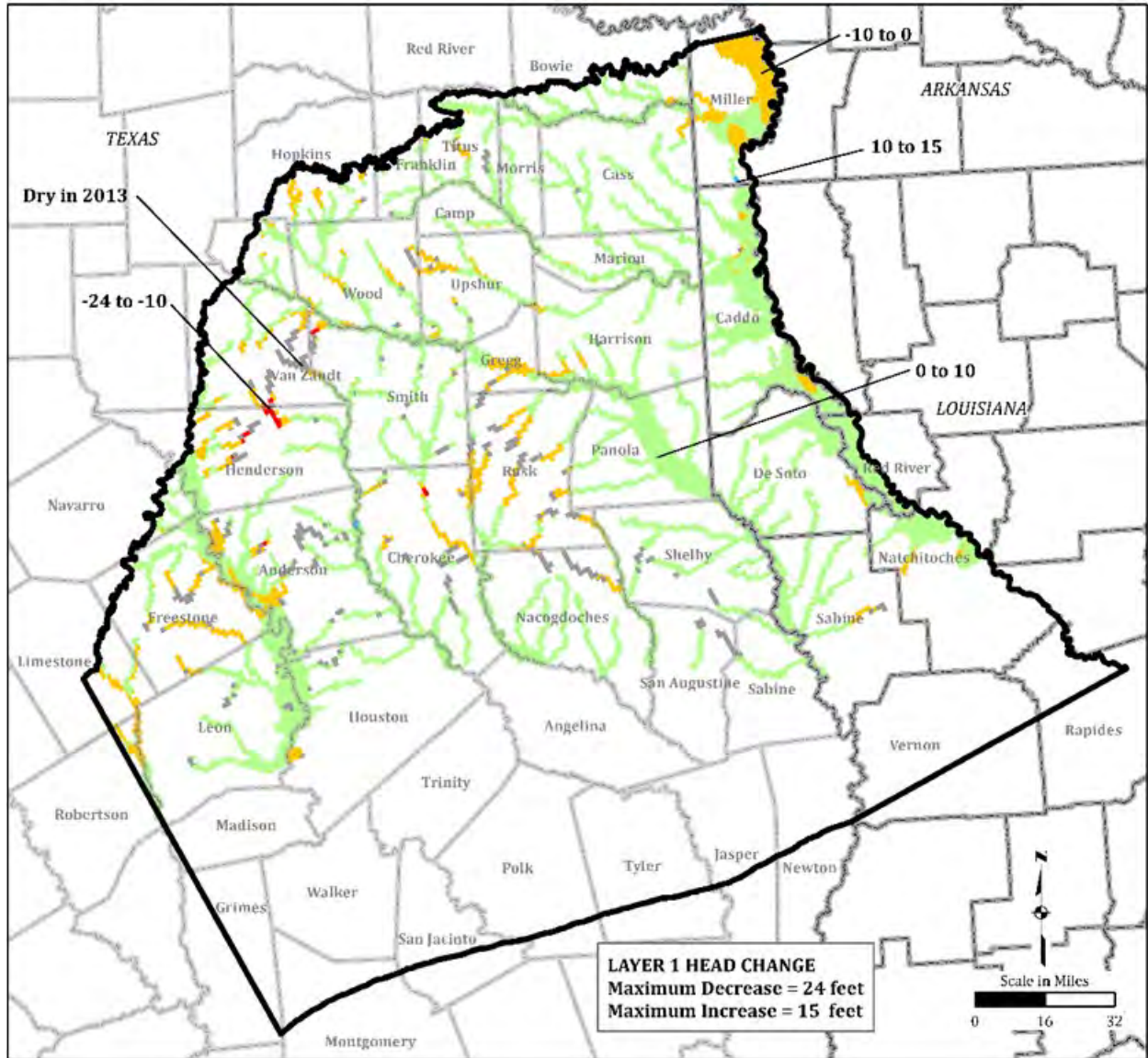
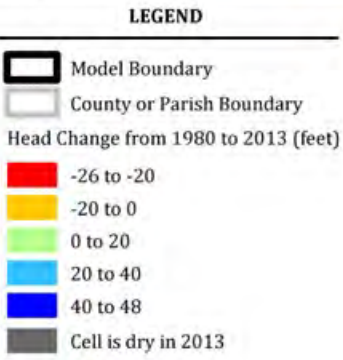
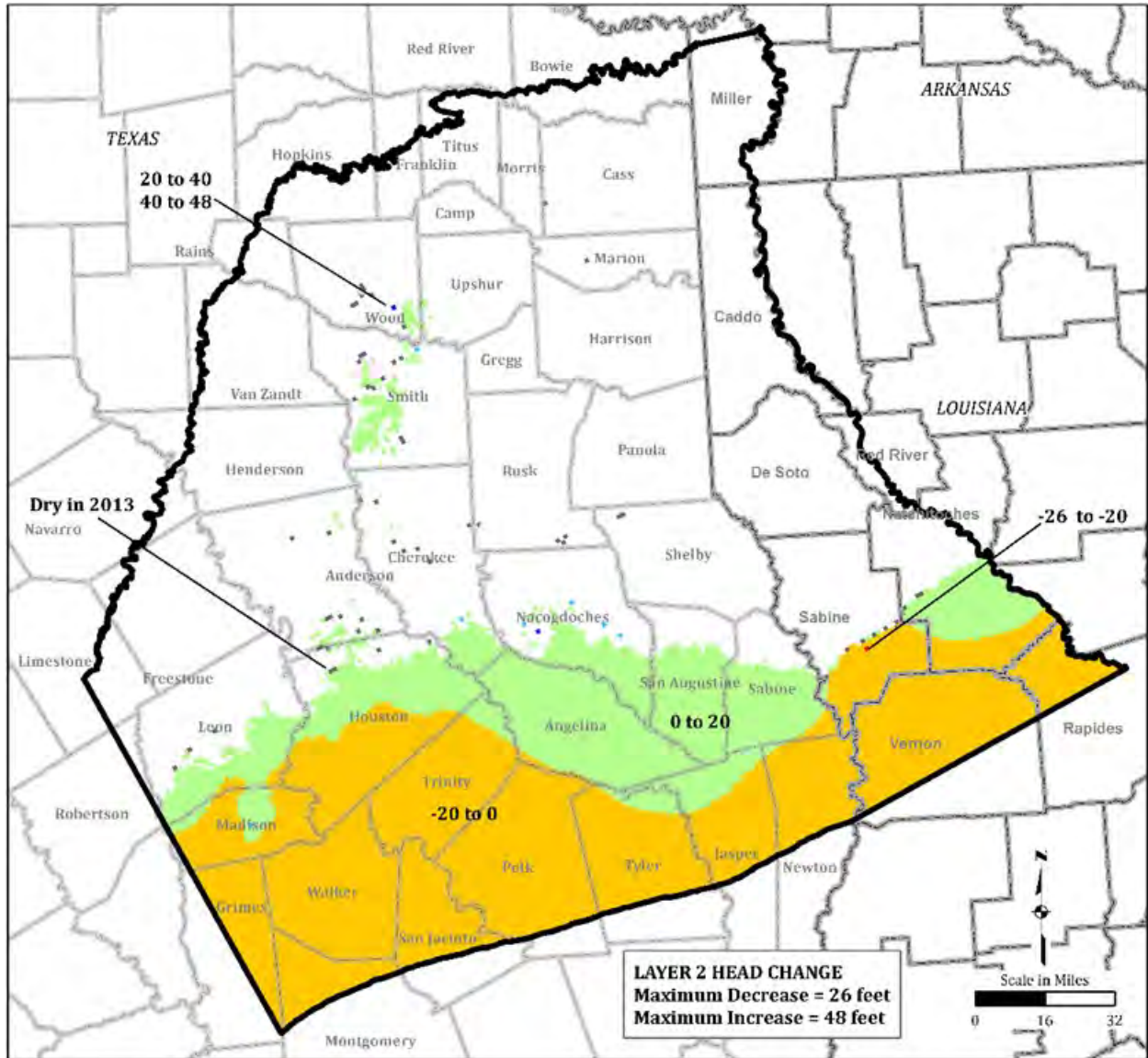


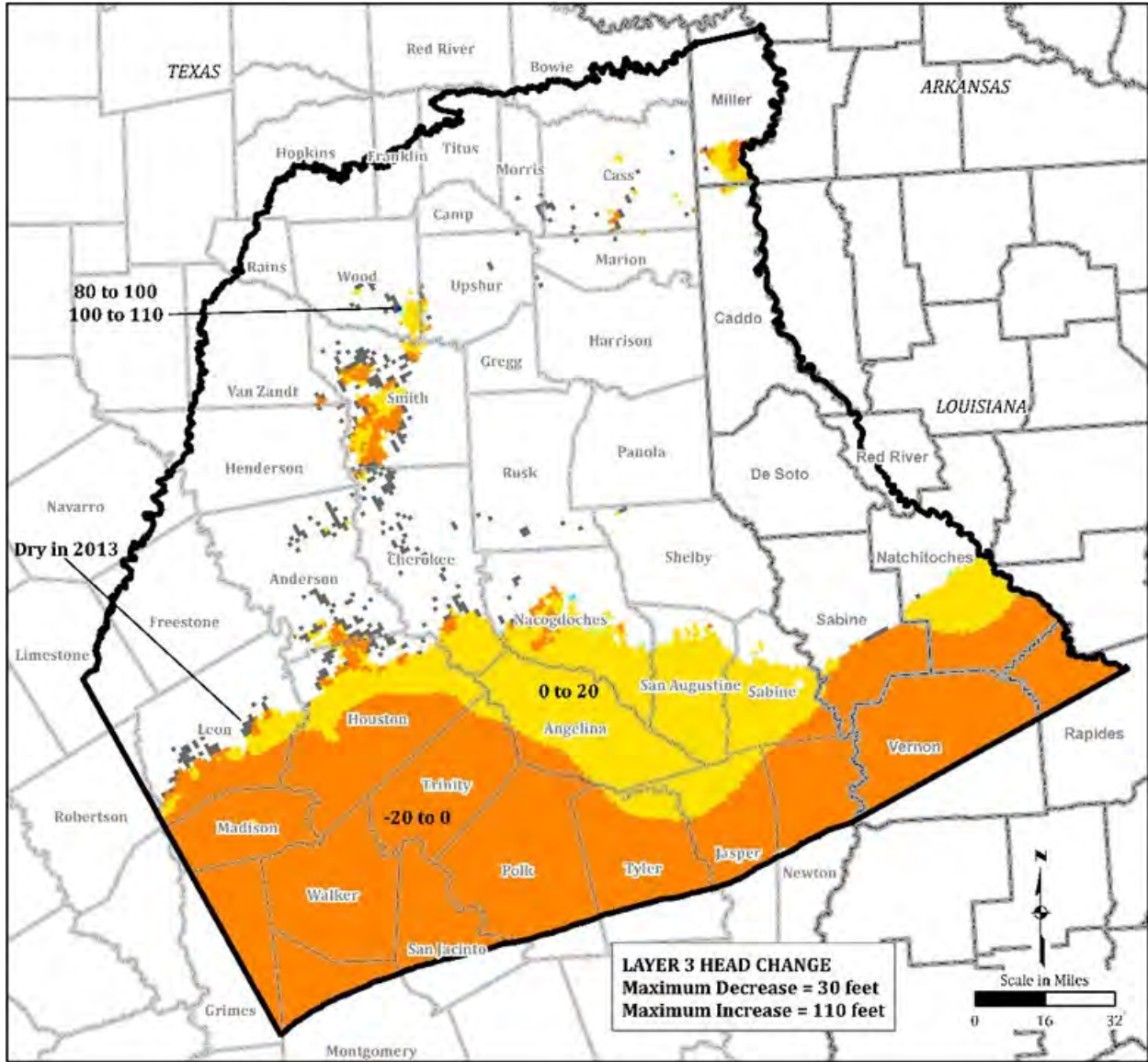
Figure 3.2-34. Change in Water Level Elevations Between 1980 and 2013 in Quaternary Alluvium (Layer 1)



Notes:

1. The layer contains discontinuous outcrops, consistent with the conceptual model (Section 2).
2. Projected Coordinate System Datum: GAM.

Figure 3.2-35. Change in Water Level Elevations Between 1980 and 2013 in Sparta Aquifer (Layer 2)



LEGEND

Head Change from 1980 to 2013 (feet)

- -30 to -20
- -20 to 0
- 0 to 20
- 20 to 40
- 40 to 60
- 60 to 80
- 80 to 100
- 100 to 110

- Model Boundary
- County or Parish Boundary
- Cell is dry in 2013

Notes:
 1. The layer contains discontinuous outcrops, consistent with the conceptual model (Section 2).
 2. Projected Coordinate System Datum: GAM.

Figure 3.2-36. Change in Water Level Elevations Between 1980 and 2013 in Weches Formation (Layer 3)

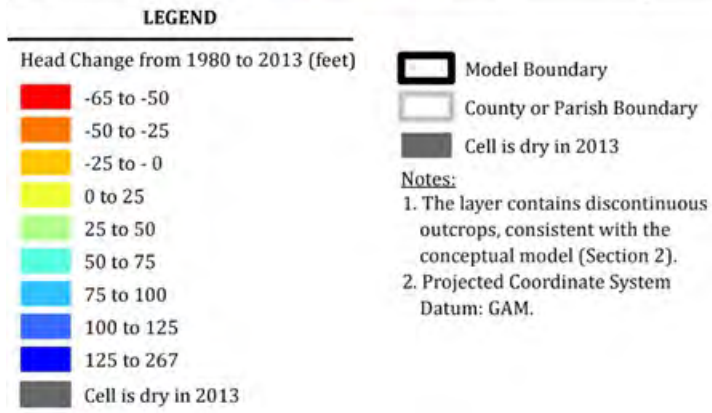
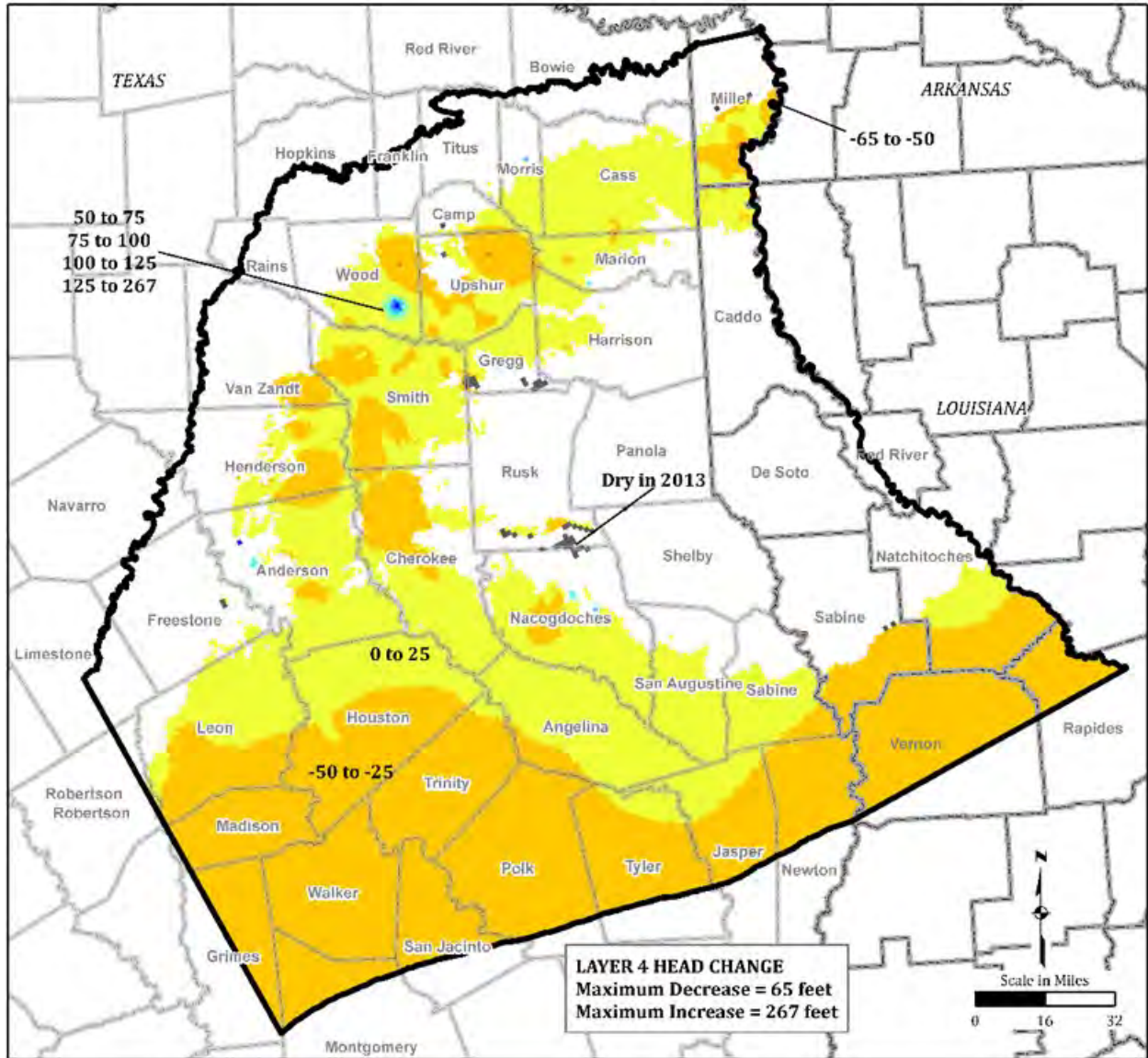


Figure 3.2-37. Change in Water Level Elevations Between 1980 and 2013 in Queen City Aquifer (Layer 4)

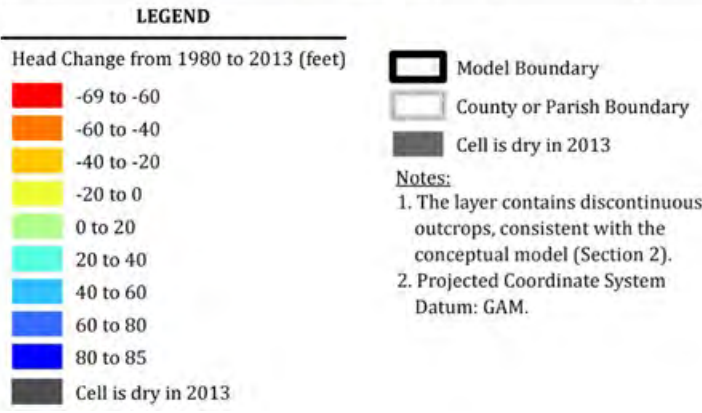
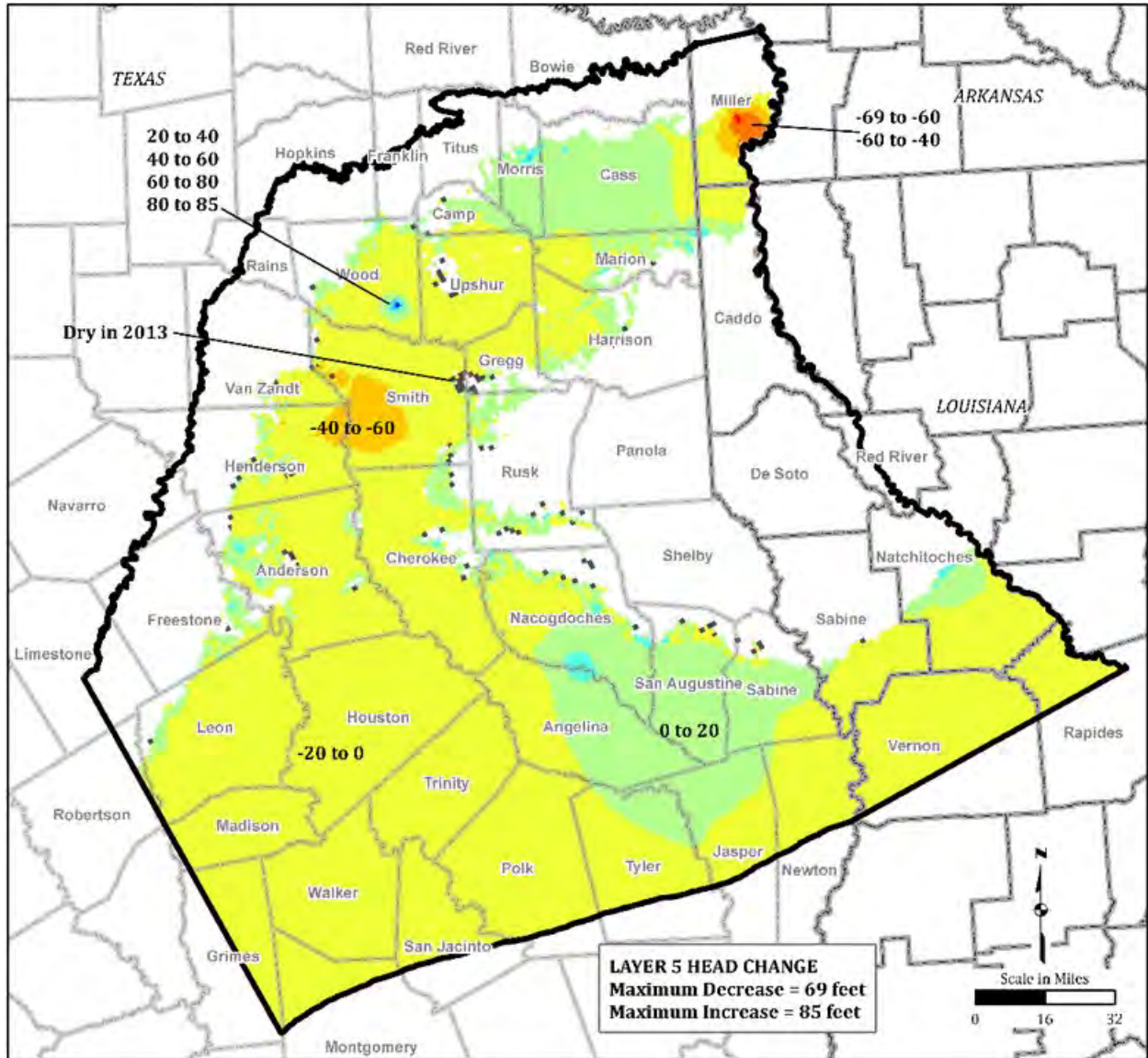


Figure 3.2-38. Change in Water Level Elevations Between 1980 and 2013 in Reklaw Formation (Layer 5)

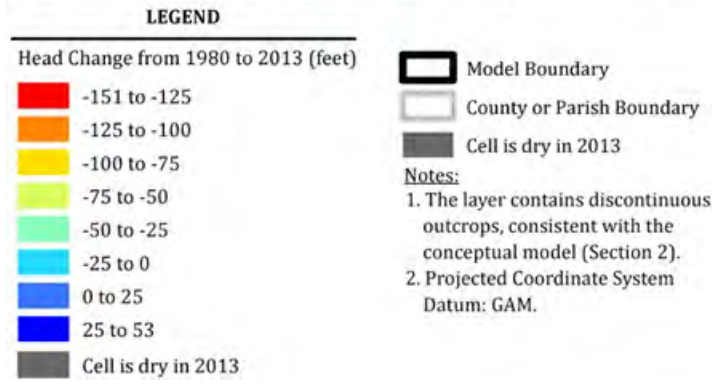
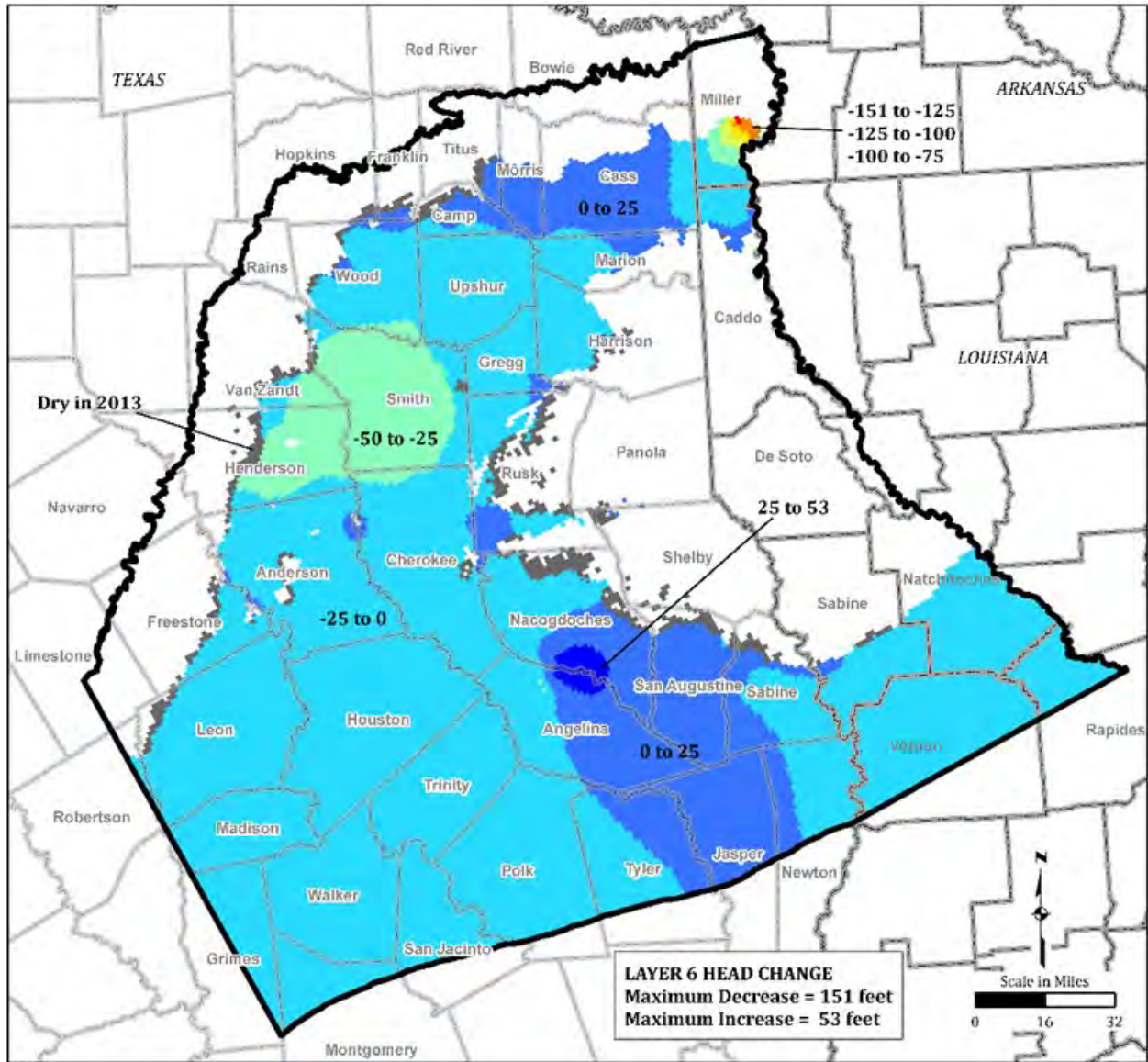


Figure 3.2-39. Change in Water Level Elevations Between 1980 and 2013 in Carrizo Aquifer (Layer 6)

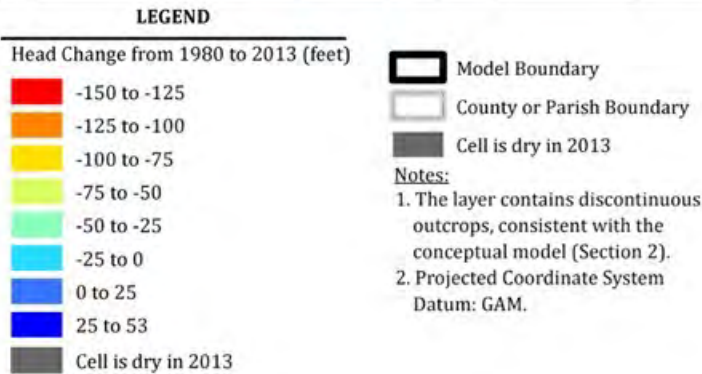
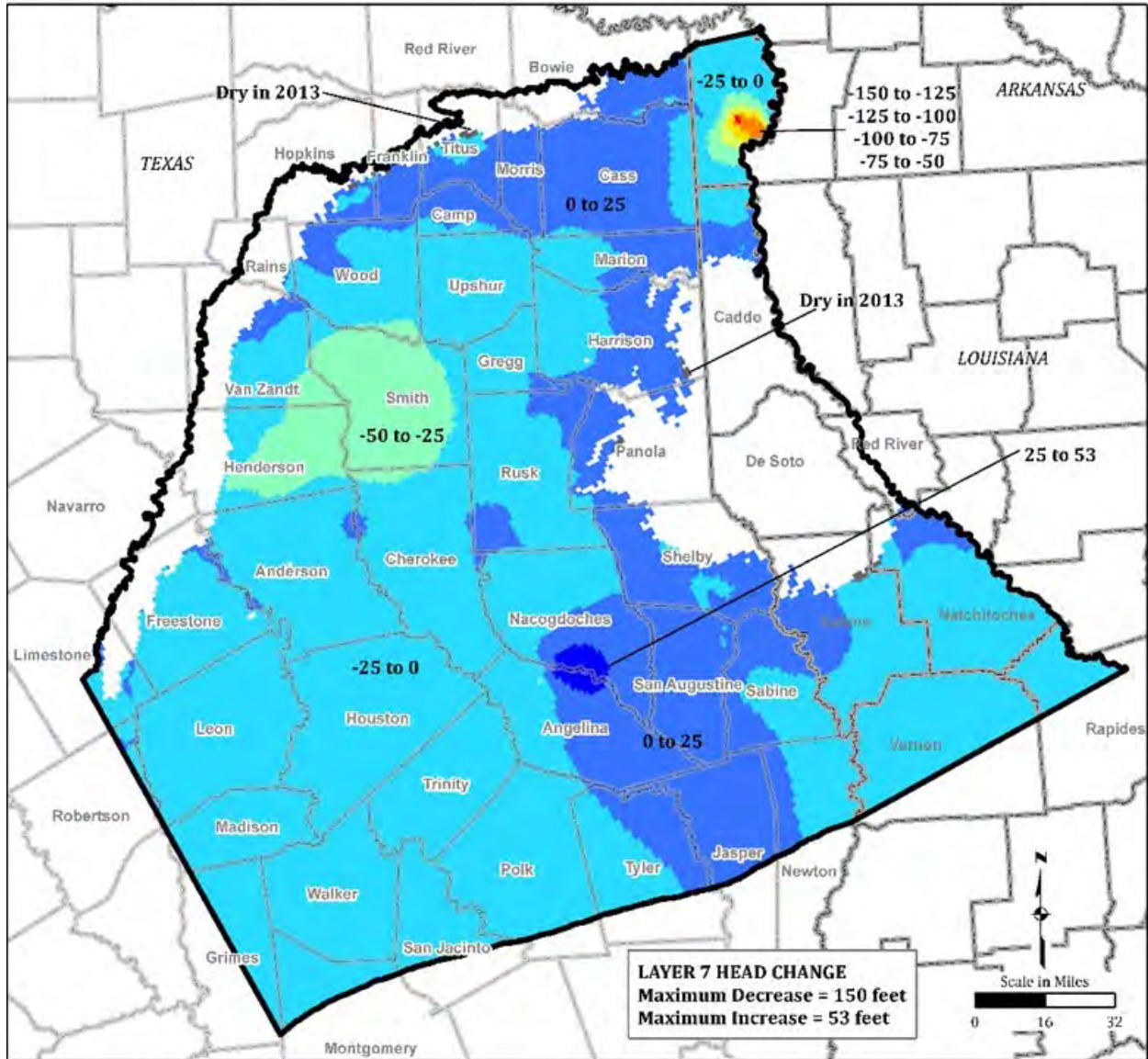


Figure 3.2-40. Change in Water Level Elevations Between 1980 and 2013 in Upper Wilcox (Layer 7)

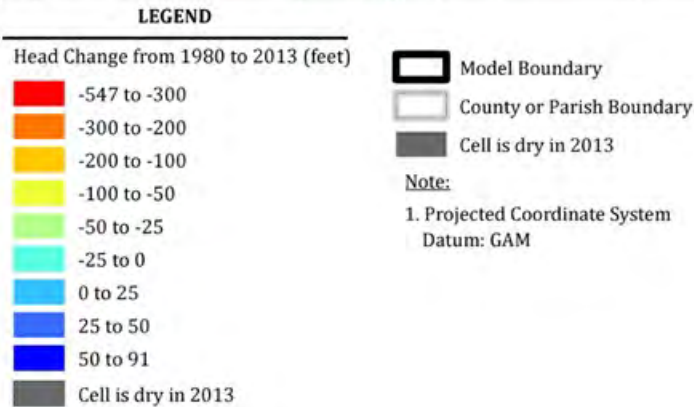
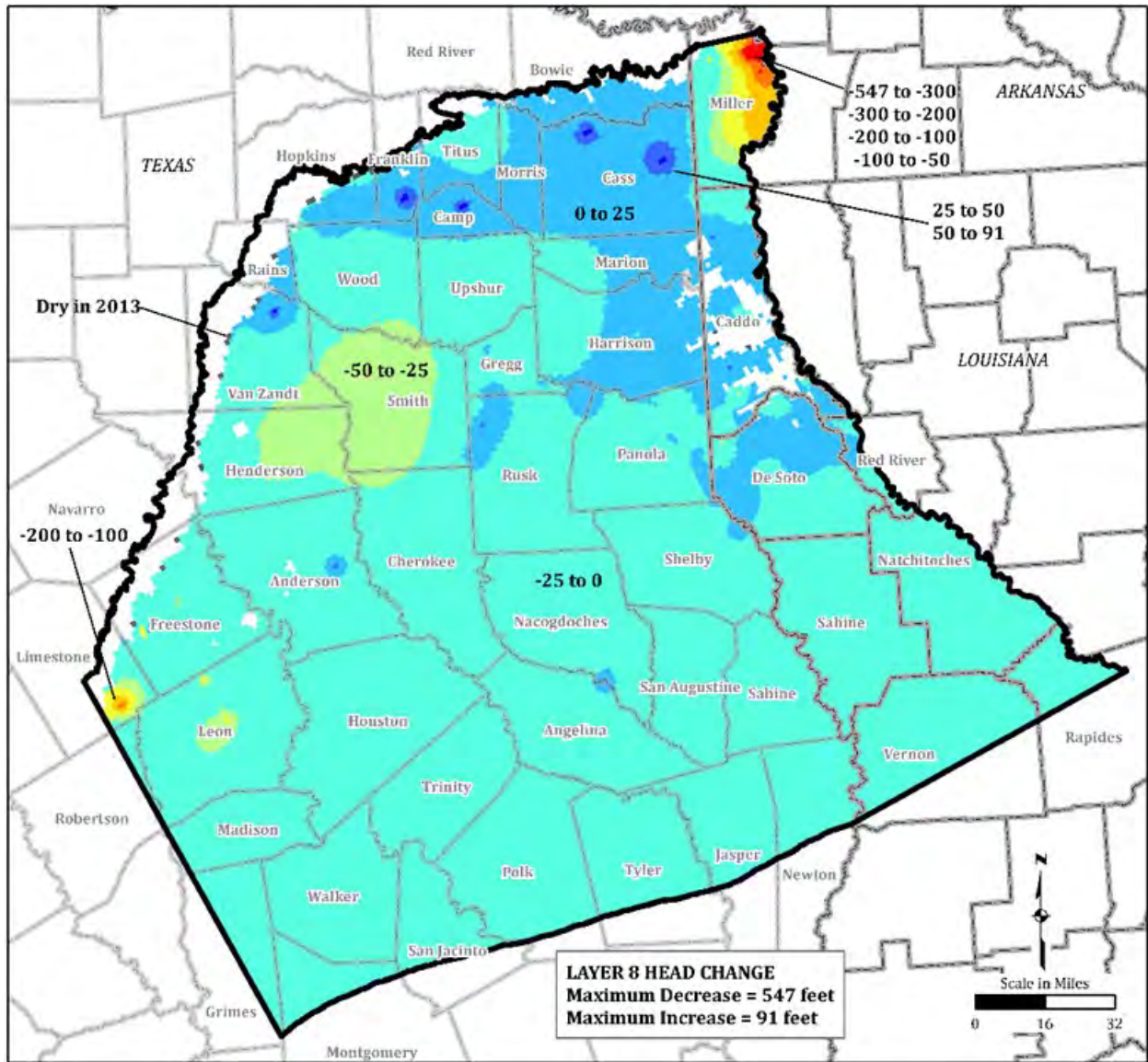


Figure 3.2-41. Change in Water Level Elevations Between 1980 and 2013 in Middle Wilcox (Layer 8)

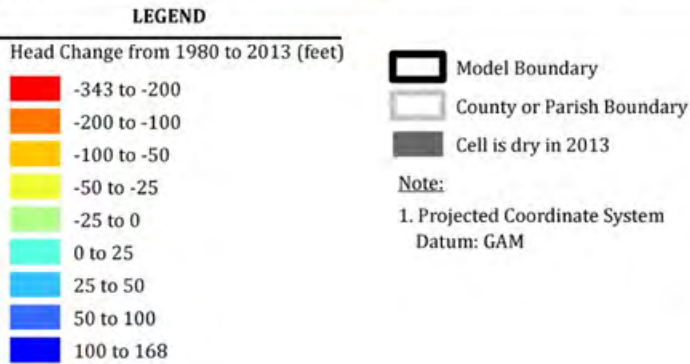
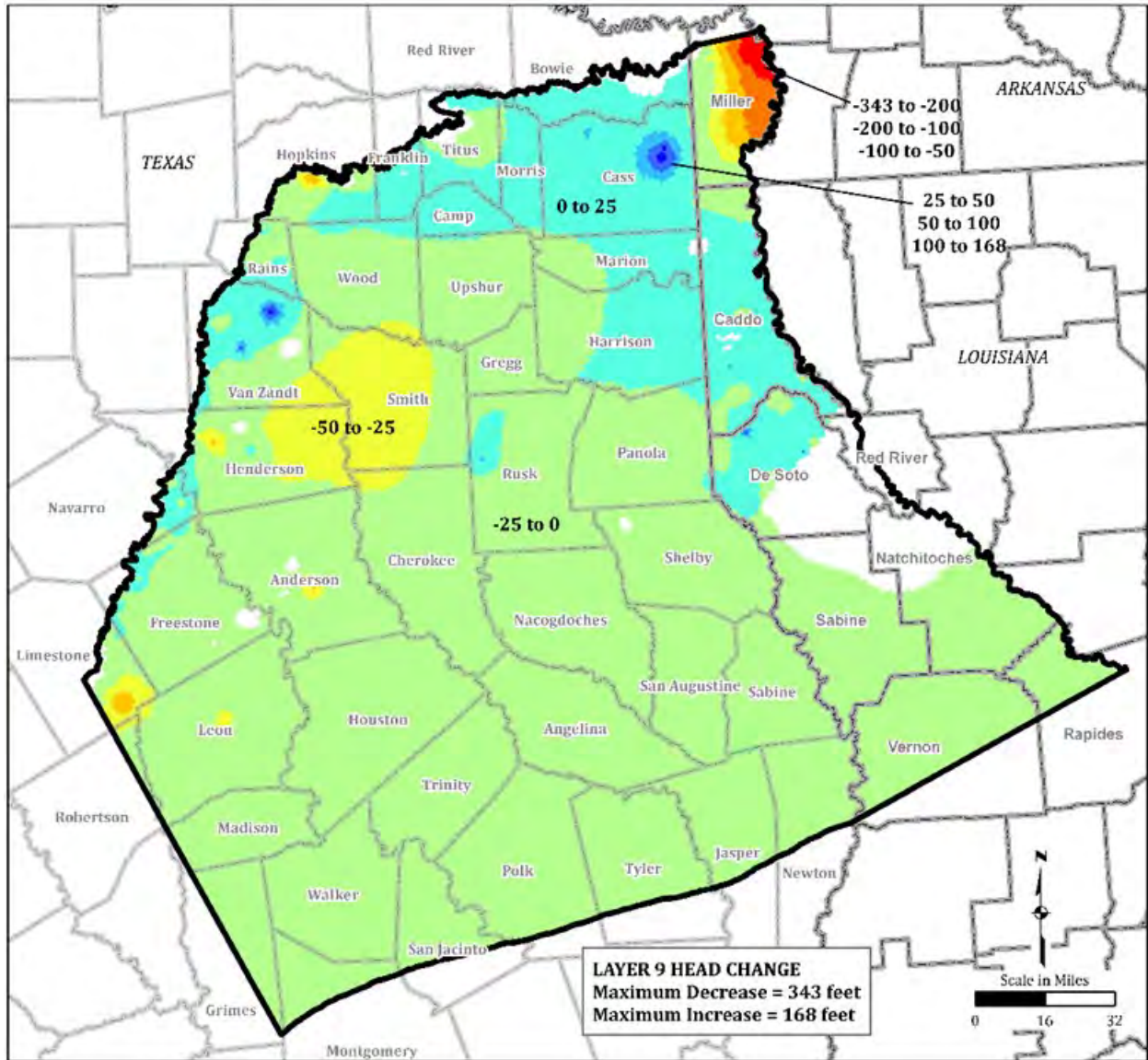


Figure 3.2-42. Change in Water Level Elevations Between 1980 and 2013 in Lower Wilcox (Layer 9)

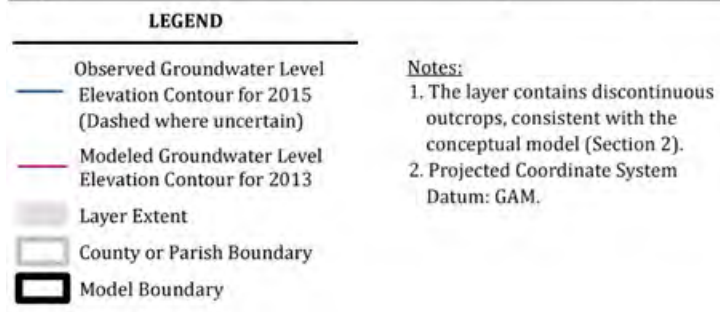
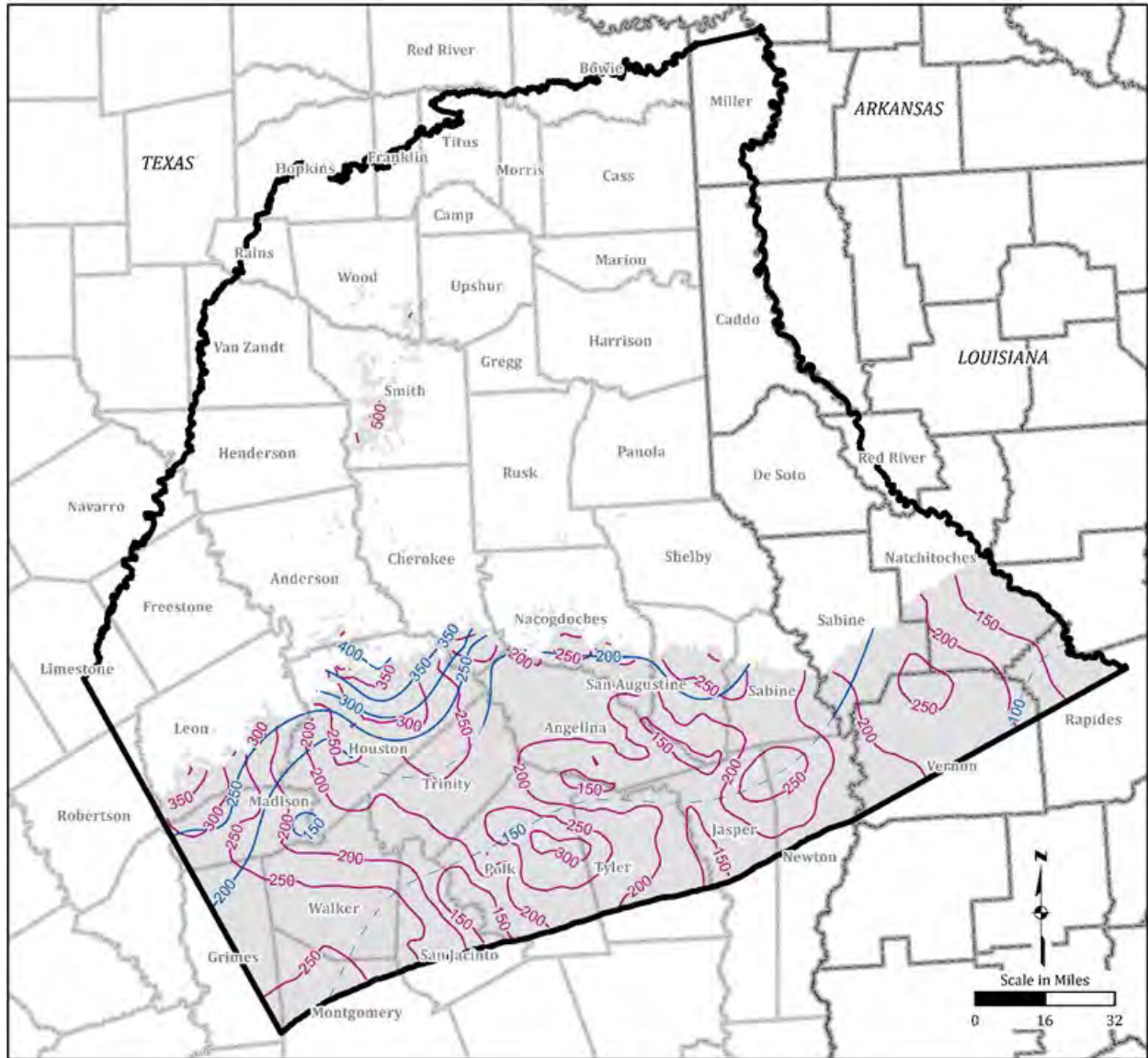
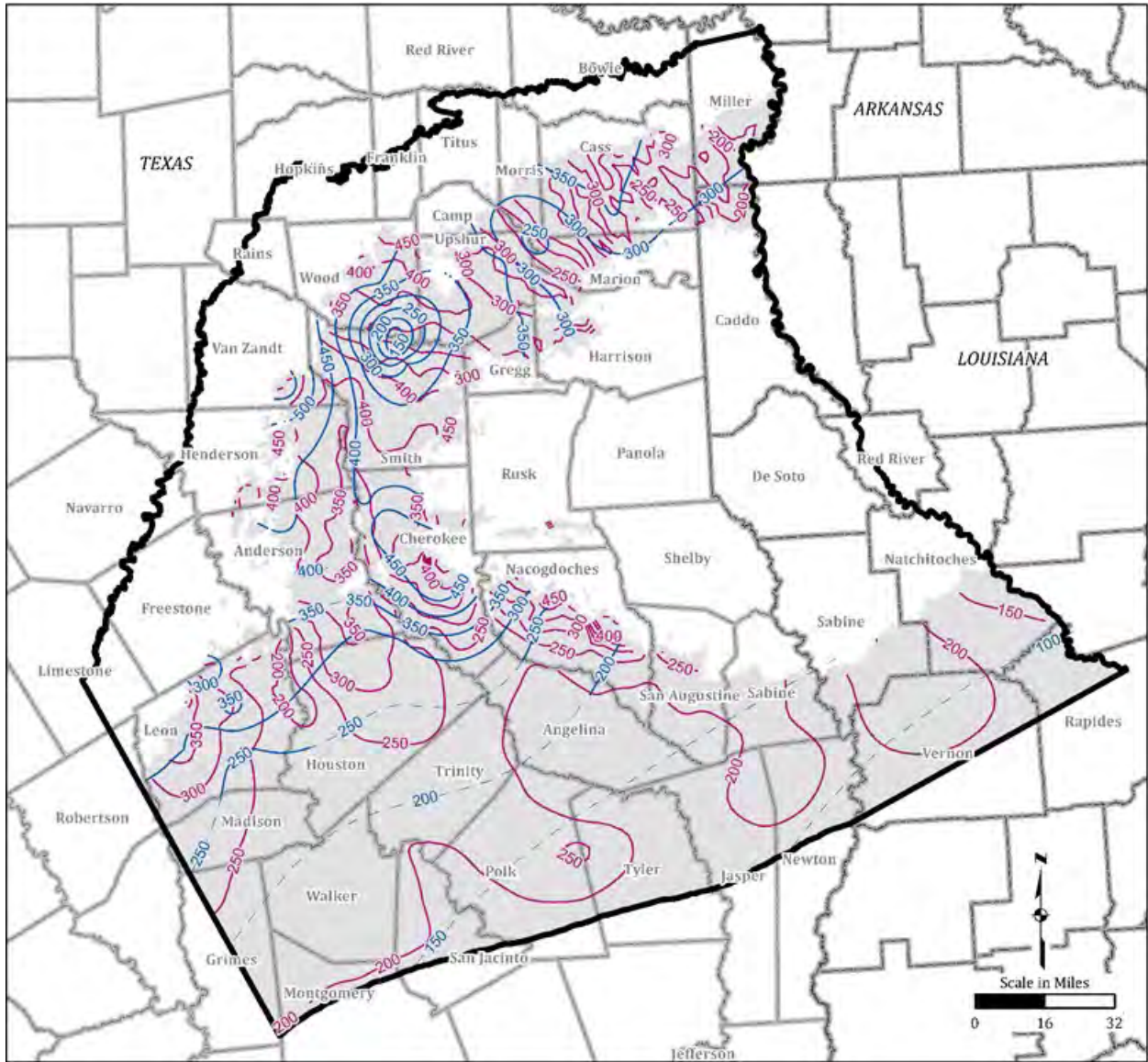


Figure 3.2-43. Observed and Modeled Groundwater Level Elevation Contours for Sparta Aquifer (Layer 2)



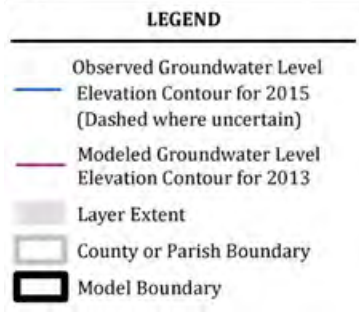
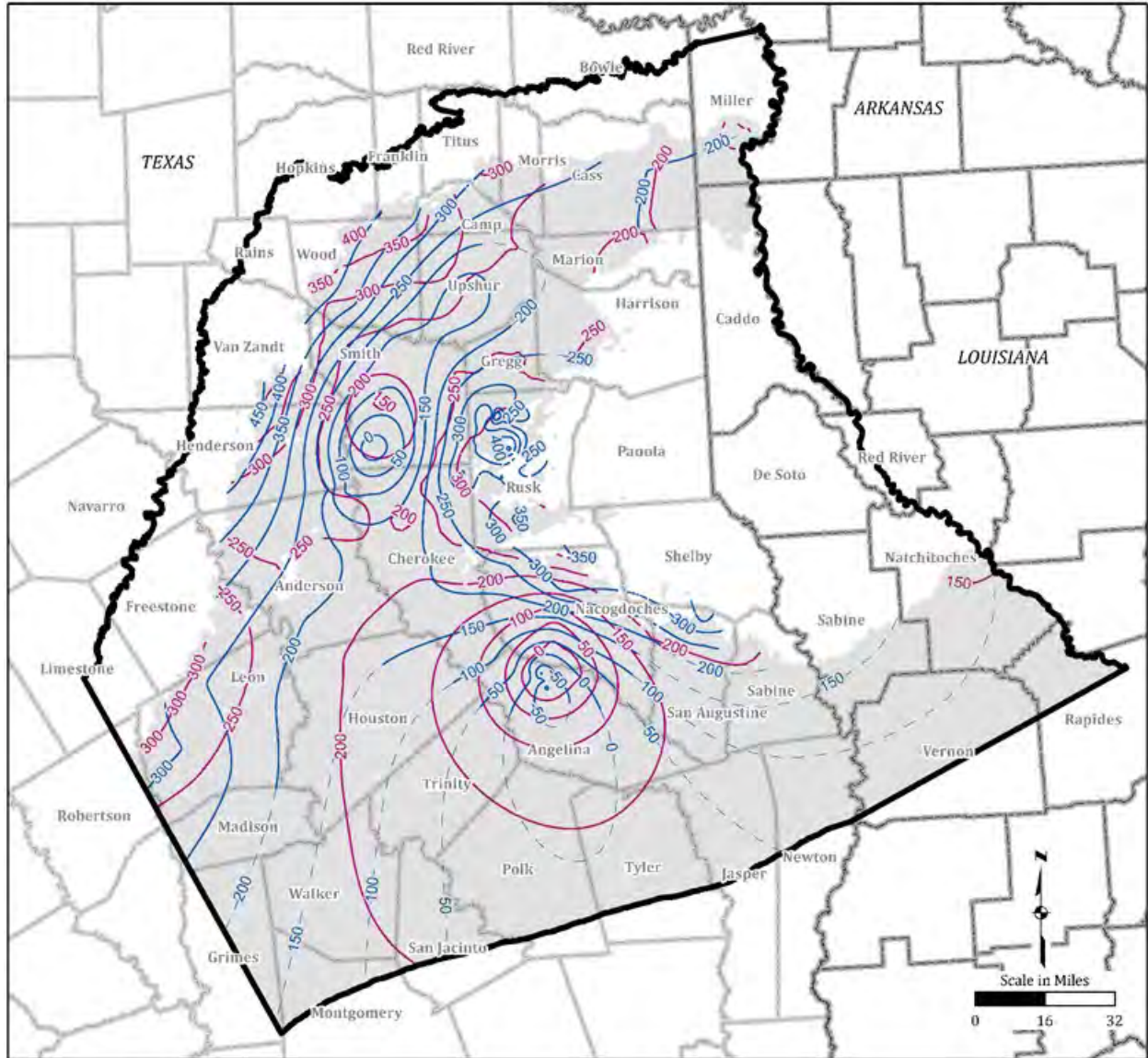
LEGEND

	Observed Groundwater Level
	Elevation Contour for 2015 (Dashed where uncertain)
	Modeled Groundwater Level
	Elevation Contour for 2013
	Layer Extent
	County or Parish Boundary
	Model Boundary

Notes:

1. The layer contains discontinuous outcrops, consistent with the conceptual model (Section 2).
2. Projected Coordinate System Datum: GAM.

Figure 3.2-44. Observed and Modeled Groundwater Level Elevation Contours for Queen City Aquifer (Layer 4)



Notes:

1. The layer contains discontinuous outcrops, consistent with the conceptual model (Section 2).
2. Projected Coordinate System Datum: GAM.

Figure 3.2-45. Observed and Modeled Groundwater Level Elevation Contours for Carrizo Aquifer (Layer 6)

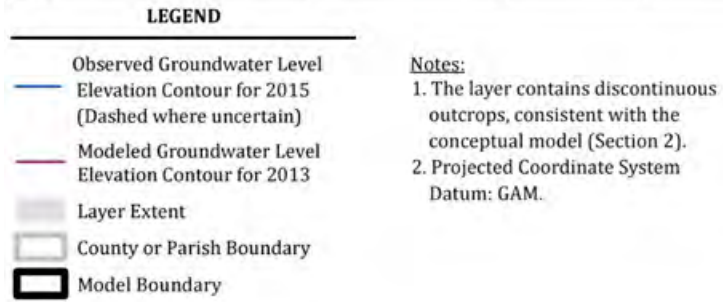
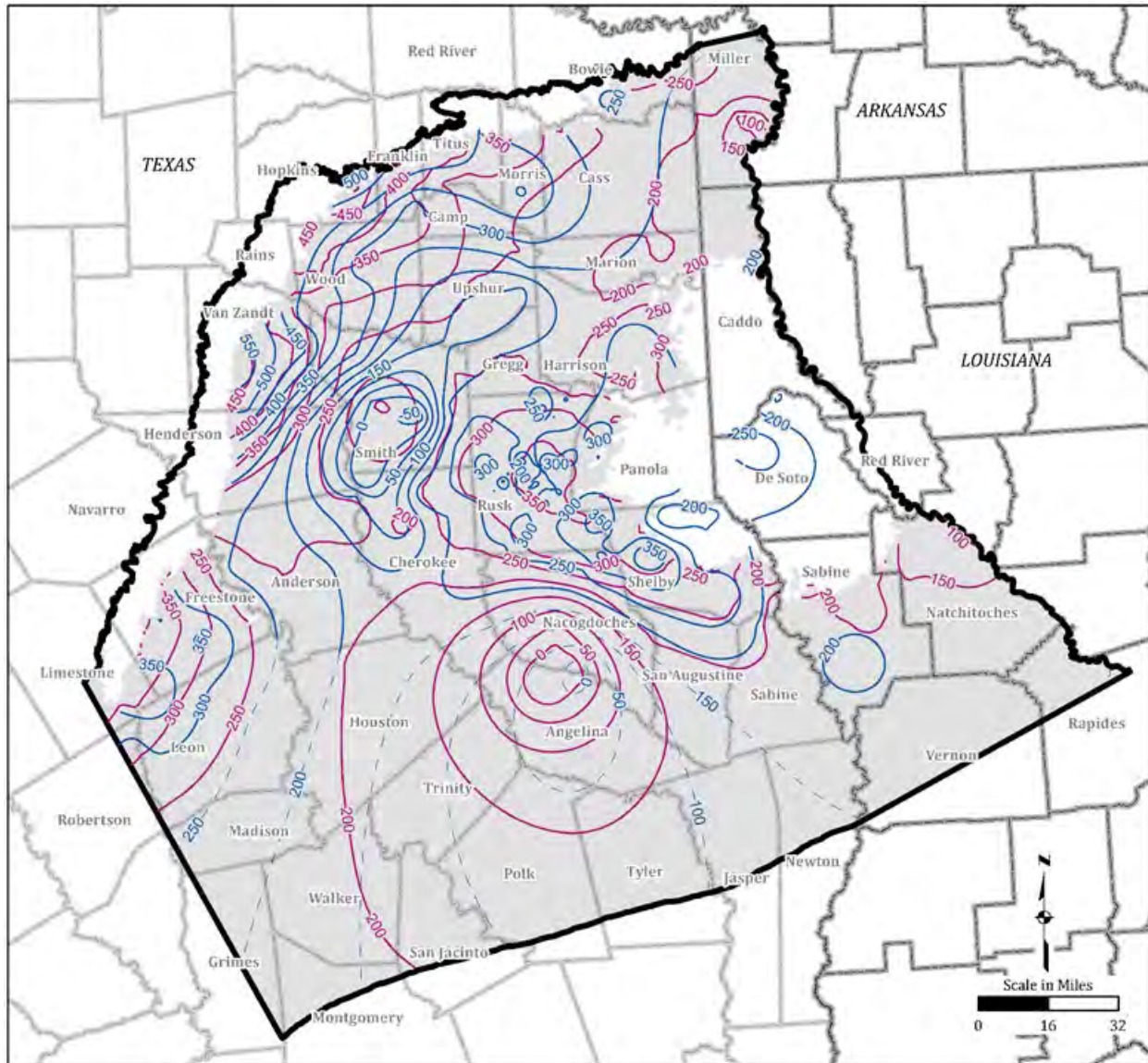
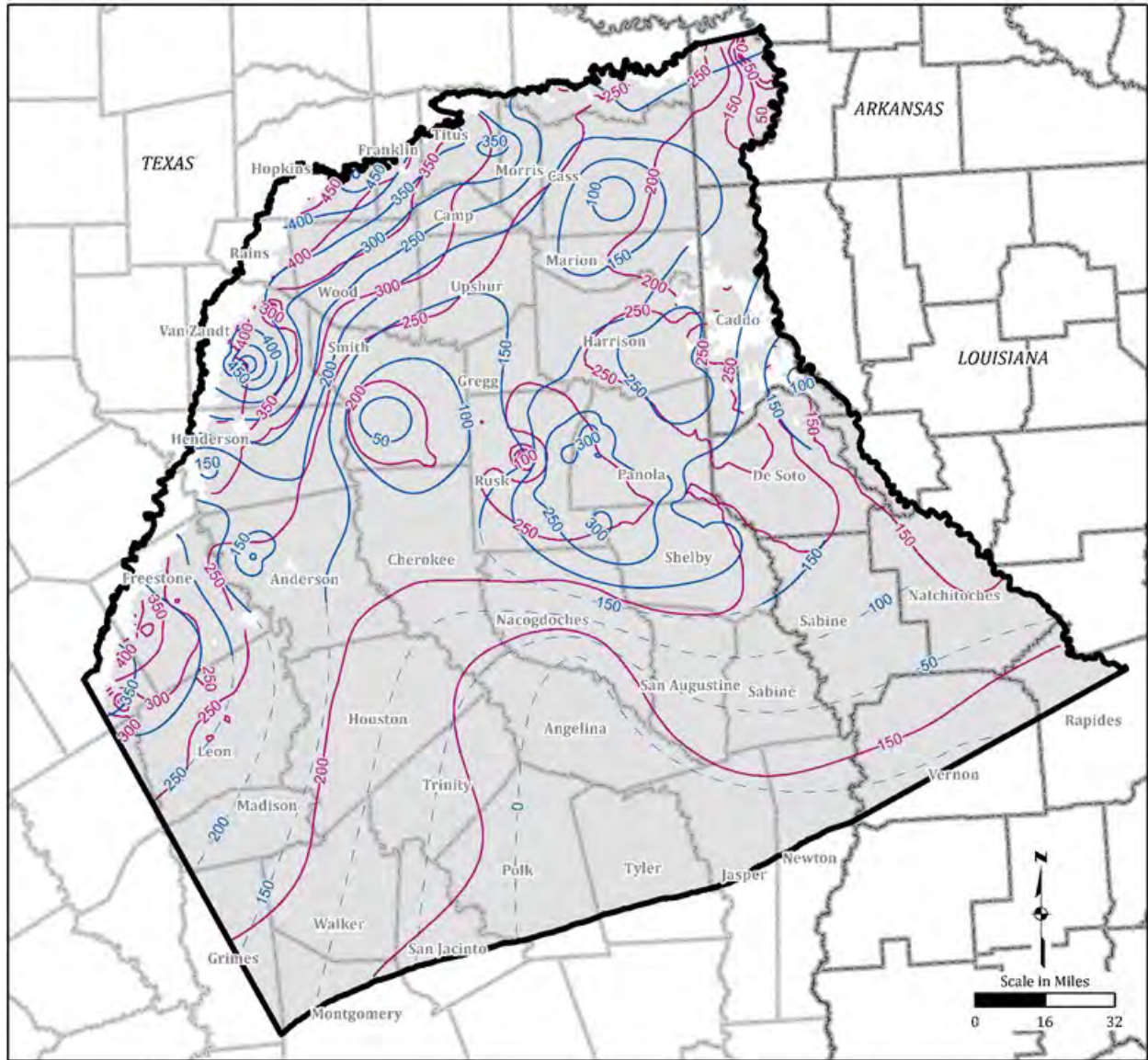


Figure 3.2-46. Observed and Modeled Groundwater Level Elevation Contours for Upper Wilcox (Layer 7)



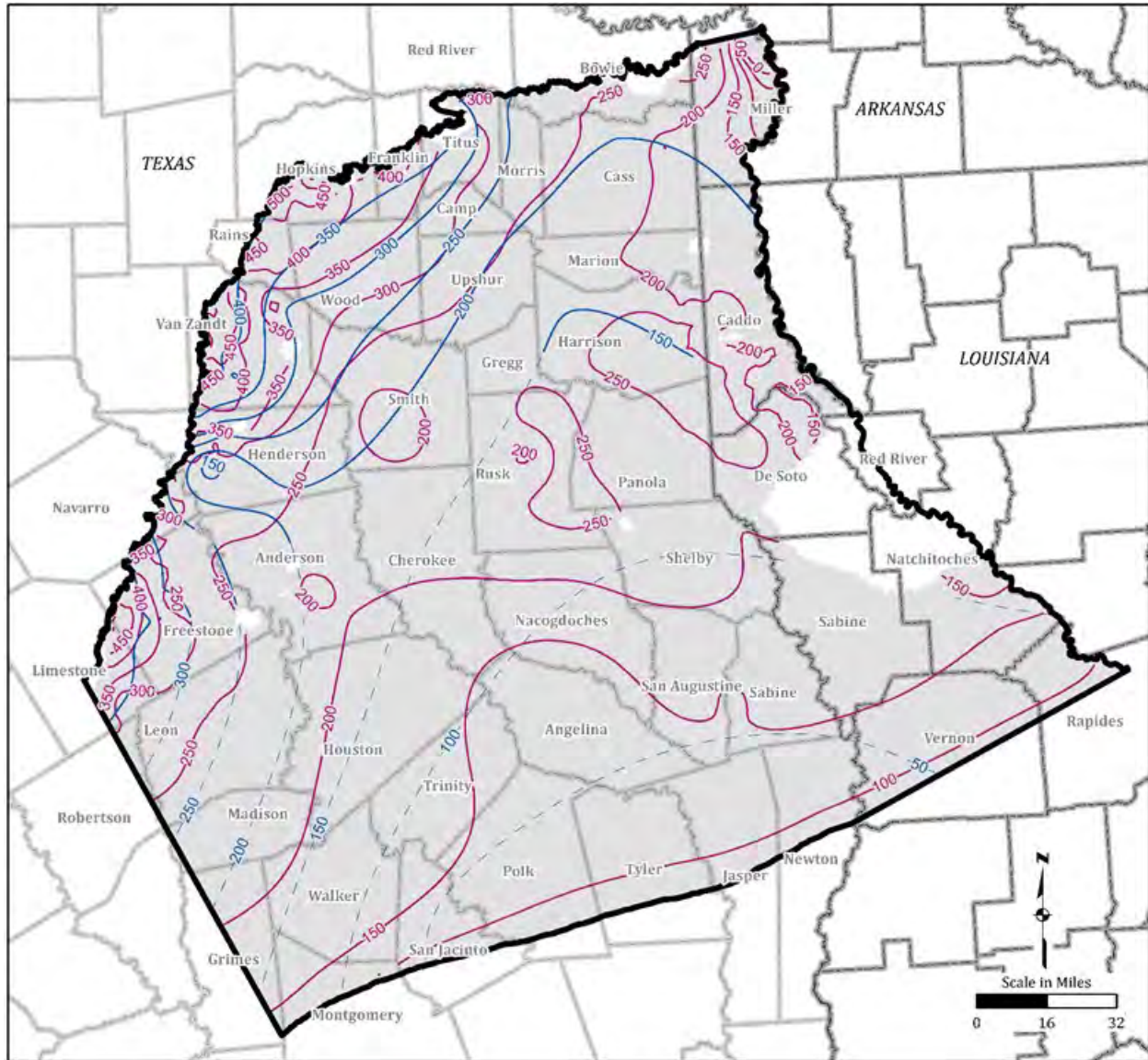
LEGEND

- Observed Groundwater Level
- Elevation Contour for 2015
(Dashed where uncertain)
- Modeled Groundwater Level
Elevation Contour for 2013
- Layer Extent
- County or Parish Boundary
- Model Boundary

Note:

1. Projected Coordinate System
Datum: GAM

Figure 3.2-47. Observed and Modeled Groundwater Level Elevation Contours for Middle Wilcox (Layer 8)



LEGEND

- Observed Groundwater Level
- Elevation Contour for 2015 (Dashed where uncertain)
- Modeled Groundwater Level
- Elevation Contour for 2013
- Layer Extent
- County or Parish Boundary
- ▭ Model Boundary

Note:
 1. Projected Coordinate System
 Datum: GAM

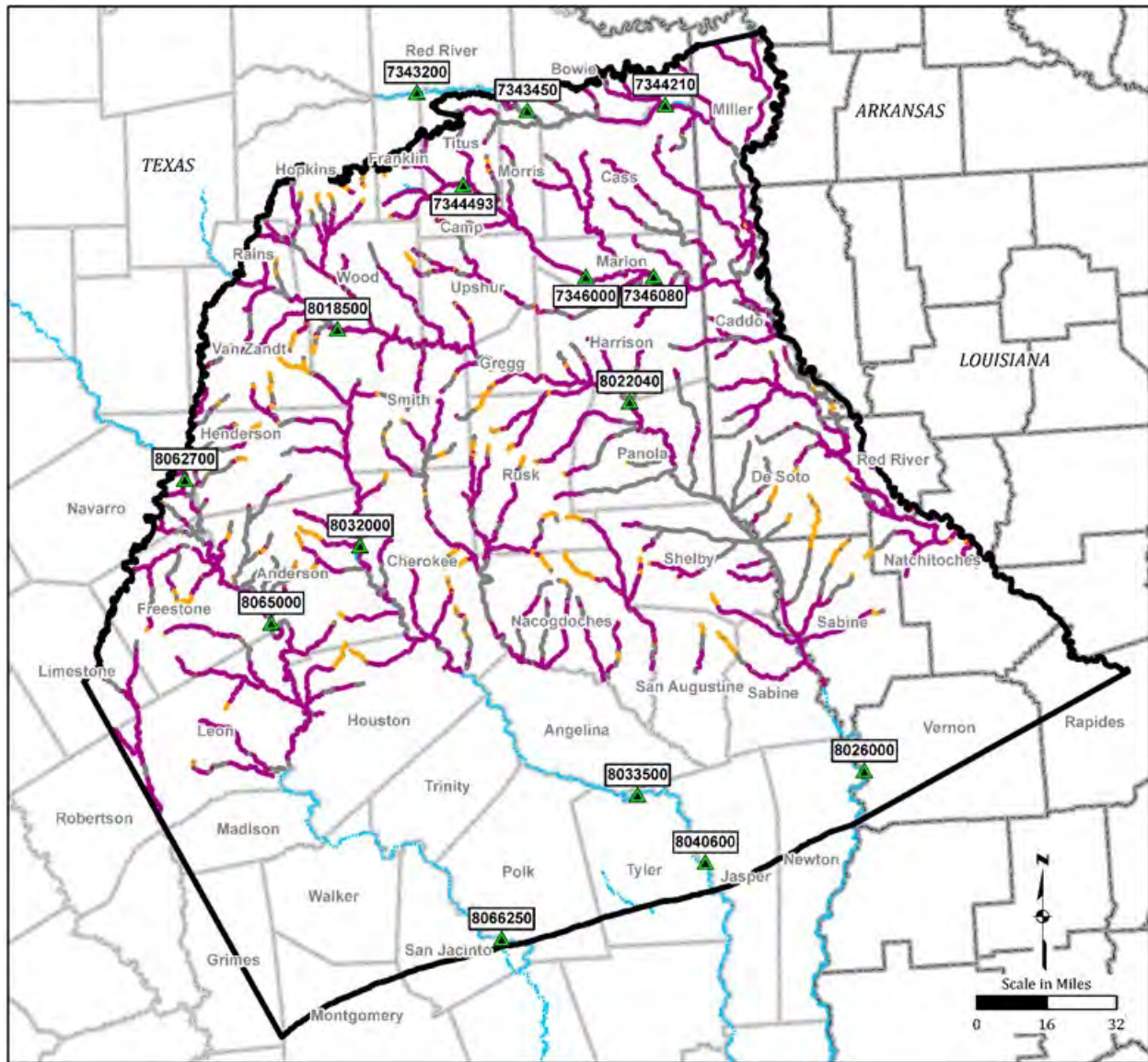
Figure 3.2-48. Observed and Modeled Groundwater Level Elevation Contours for Lower Wilcox (Layer 9)

The Middle and Lower Wilcox (model layers 8 and 9) 2015 observed contours are uncertain in the south portion of the model, as shown on Figures 3.2-47 and 3.2-48. In the Middle Wilcox (model layer 8), the 2013 simulated contours show similar features as the 2015 observed contours, including an elevation trough in the southern portion of the model, pumping in Smith County, and areas of groundwater mounding in Rusk and Harrison counties, shown on Figure 3.2-47, though a cone of depression indicated by data in Cass County was not simulated. The Lower Wilcox (model layer 9) 2013 simulated contours show details such as areas of pumping and areas of groundwater mounding not captured in the 2015 observed contours; most of the 2015 contours are uncertain in the Lower Wilcox within the model domain, as shown on Figure 3.2-48.

3.3 Model Simulated Versus Measured Baseflow

Surface-water to groundwater fluxes were used to constrain the model. The major rivers in the model domain were simulated with the RIV package as described in Section 2.9. Figures 2.9-1 through 2.9-5 show the annual flows at stream gages located on the major rivers in the model domain, the Trinity River, Neches River, Sabine River, Big Cypress Creek, and Sulphur River. The flow difference between stream gages was calculated at select river segments with unmanaged flows. A positive difference in flow signifies the river is gaining along the reach, and a negative difference in flow signifies the river is losing along the reach. The rivers simulated in the model are primarily gaining streams.

Measured stream gage data was used to evaluate simulated surface-water to groundwater fluxes. However, since the model does not simulate surface water flow, the flux between river and groundwater was evaluated qualitatively. Figure 3.3-1 shows the simulated flux between the simulated rivers and the groundwater in the model domain. A negative flux value indicates a gaining reach and a positive flux value indicates a losing reach. Most of the reaches shown on Figure 3.3-1 are gaining, which is consistent with measured gage data shown Figures 2.9-1 through 2.9-5. In addition, the simulated water budget for river inflow and outflow was evaluated. Figure 3.3-2 shows the inflow from the river boundary condition, outflow to the river boundary condition, and net river gain. The inflow from the river boundary condition, which represents water flowing from the river boundary condition into groundwater, is flat during the simulation period, with an average of approximately 38,000 acre-feet per year (acre-feet/year). The outflow from the river boundary, which represents water flowing from groundwater into the river boundary condition, varies during the simulation period with an average of approximately 260,000 acre-feet/year. The net flux from the groundwater to the river boundary condition average of approximately 222,000 acre-feet/year. Measured stream gage fluxes cannot be directly compared to simulated fluxes because measured stream gage data is not measuring only baseflow. However, the measured and simulated river flux both result in gaining stream conditions.



LEGEND

-  USGS Stream Gage
-  Model Boundary
-  County or Parish Boundary
-  River
- Model River Flux**
-  Gaining (Flux < 0)
-  Minimal Flux
-  Losing (Flux > 0)

Notes:
 1. USGS = United States Geological Survey
 2. Projected Coordinate System
 Datum: GAM

Figure 3.3-1. Simulated Groundwater Interaction Fluxes for 2013 Rivers

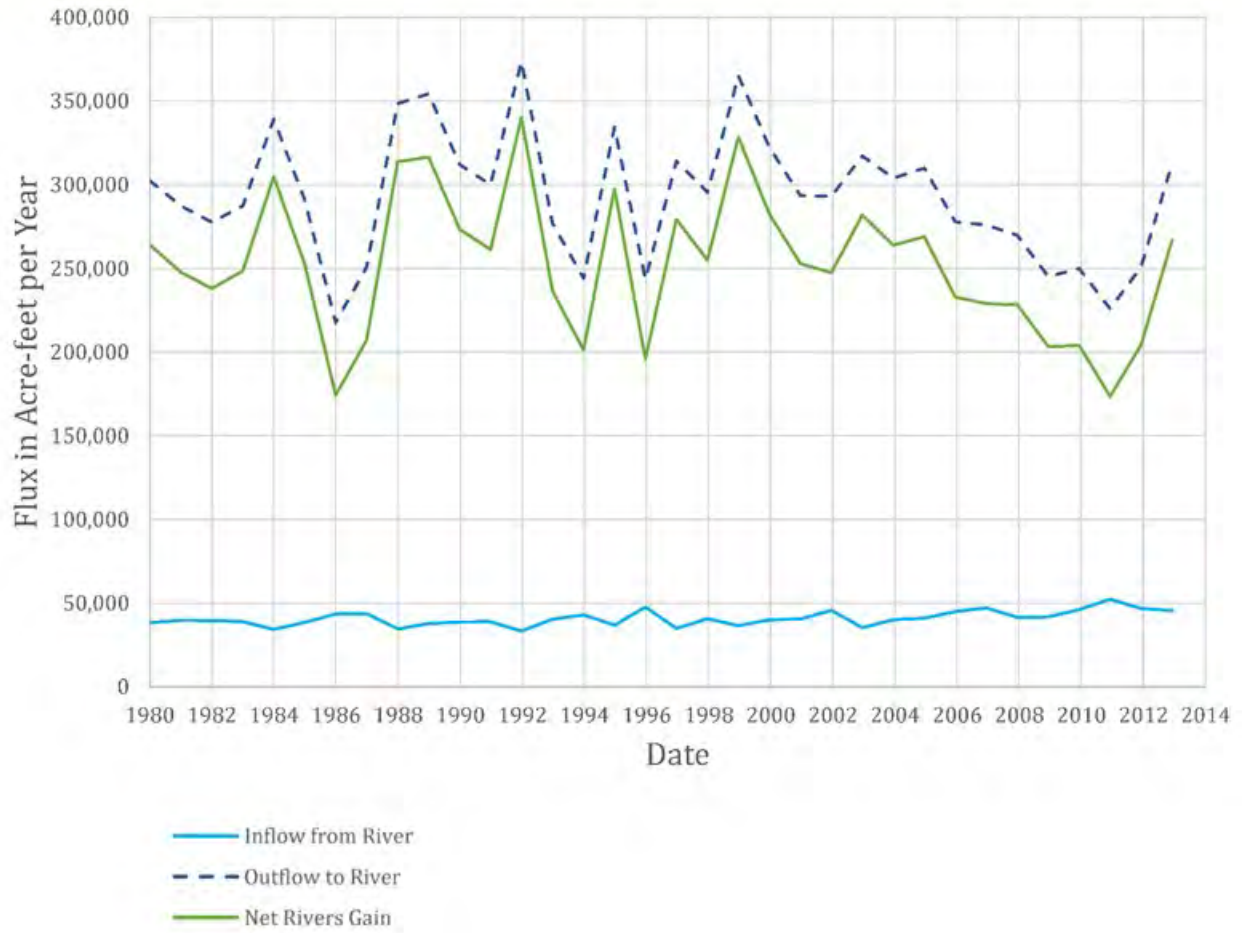


Figure 3.3-2. Groundwater Budget for River Flux for the 1980 to 2013 Calibration Simulation

3.4 Model Simulated Water Budgets

The water budget for steady-state 1980 simulation is shown in Table 3.4-1. The largest inflow in the model domain (besides internal flow between layers) is recharge contribution in all layers and especially within the Quaternary Alluvium (model layer 1). Simulated rivers contribute a minor amount of inflow into the Quaternary Alluvium (model layer 1) as does the GHB into the Sparta Aquifer and Carrizo Aquifer (model layers 2 and 6). Within the 1980 simulation, the largest total outflows (besides internal layer outflows) are to the simulated rivers in the Quaternary Alluvium (model layer 1), followed by evapotranspiration and groundwater pumping. Although total extraction of groundwater is not the largest outflow for the steady-state 1980 simulation period, it is the largest outflow in the Carrizo Aquifer and Wilcox Aquifers (model layers 6, 7, 8, and 9).

The water budget for the transient simulation from 1980 through 2013 is shown in Figure 3.4-1 and summarized in Table 3.4-2. Water budget values for each layer are exported from Groundwater Vistas. These values match the MODFLOW 6 output for mass balance, excepting a minor difference reflecting net values for model nodes with multiple river cells and for net storage from cells. However, the IN minus OUT term (the net flux to/from the river boundary) is preserved.

The largest model inflows and outflows are similar to those in the steady-state 1980 simulation. Inflow is dominated by recharge and outflow is dominated by rivers and evapotranspiration. Within individual layers, outflow was dominated by groundwater extraction in the Carrizo Aquifer and Wilcox Aquifers (model layers 6, 7, 8, and 9). Storage provided a negligible amount of inflow and outflow across the model.

A comparison of pumping outputs between the existing groundwater availability model (Kelley and others, 2004) and the updated groundwater availability model is presented in Appendix G. Pumping output in the previous groundwater availability model was reduced compared to the previous groundwater availability model pumping input due to dry cells in some areas of the model; dry cell conditions deactivate the cell's assigned pumping. The pumping output of the current groundwater availability model was slightly reduced compared to the current pumping input due to supply and demand conditions in some areas. Despite these differences, the comparison demonstrates that the output pumping from the previous groundwater availability model and current groundwater availability model are consistent.

Figure 3.4-1 shows water budget component fluctuations during the simulation period. Recharge (inflow) is the largest component in the model water budget and showed the greatest changes year to year. Recharge over time did not display a noticeable trend from 1980 to 2013 although recent drought conditions were reflected as an extended period of decreasing flux (2004 to 2012). River and evapotranspiration (outflows) showed some variability with time. Drought conditions were also reflected in the river and evapotranspiration water budget components with declining flows between 2004 and 2012. Groundwater extraction did not vary significantly year to year but showed an increasing trend from 1980 to 2013. Other inflow and outflow components were generally consistent across the model time interval and smaller in magnitude.

Table 3.4-1. Water Budget by Layer for the Steady-State 1980 Simulation

Mass Balance Components	Layer 1 Flow (Quaternary Alluvium)	Layer 2 Flow (Sparta Aquifer)	Layer 3 Flow (Weches Formation)	Layer 4 Flow (Queen City Aquifer)	Layer 5 Flow (Reklaw Formation)	Layer 6 Flow (Carrizo Aquifer)	Layer 7 Flow (Upper Wilcox)	Layer 8 Flow (Middle Wilcox)	Layer 9 Flow (Lower Wilcox)	Total Model Flow	
	(acre-feet per year)										
Inflows	Storage	--	--	--	--	--	--	--	--	--	
	Layer Top	--	515.9	19,600.6	213,722.5	20,523.9	80,698.1	407,459.5	29,069.8	19,534.6	
	Layer Bottom	604,524.2	2,932.6	2,834.4	2,760.1	536.3	110,610.5	7,009.3	2,743.8	--	
	Well	--	--	--	--	--	--	--	--	--	
	General Head Boundary	--	34,621.1	--	36.9	--	8,187.6	--	--	42,845.6	
	River	36,810.6	--	--	--	--	--	--	--	36,810.6	
	Recharge	337,212.0	42,892.9	13,945.0	94,048.0	29,915.8	21,247.2	61,181.7	32,082.6	7,148.2	
	Evapotranspiration	--	--	--	--	--	--	--	--	--	
Total Inflows	978,546.8	80,962.5	36,380.0	310,567.6	50,976.0	220,743.3	475,650.5	63,896.2	26,682.7	719,329.4	
Outflows	Storage	--	--	--	--	--	--	--	--	--	
	Layer Top	--	11,011.7	3,458.8	245,571.7	874.2	37,648.6	406,609.8	13,264.4	15,512.1	
	Layer Bottom	518,702.0	21,977.0	30,150.7	25,475.5	32,416.4	126,291.4	25,819.4	10,292.8	--	
	Well	--	3,868.2	--	10,050.9	--	55,631.9	33,037.1	24,959.6	7,978.6	
	General Head Boundary	--	26,874.5	--	1,153.3	--	1,853.7	840.9	144.7	373.1	
	River	302,065.0	--	--	--	--	--	--	--	302,065.0	
	Recharge	--	--	--	--	--	--	--	--	--	
	Evapotranspiration	158,123.6	17,235.8	2,773.4	27,556.6	17,418.6	163.0	9,173.0	15,234.7	2,819.3	
Total Outflows	978,890.5	80,967.1	36,383.0	309,808.1	50,709.3	221,588.5	475,480.2	63,896.2	26,683.1	719,329.4	
Net Flows	In-Out	-343.8	-4.6	-3.0	759.5	266.7	-845.2	170.3	0.0	-0.3	0.0
	Percent Discrepancy	-0.04%	-0.01%	-0.01%	0.24%	0.52%	-0.38%	0.04%	0.00%	0.00%	0.00%

Notes:

1. Mass balances per layer were obtained from Groundwater Vistas. Mass balance errors match those in the MODFLOW 1st file though there are averaging differences for river and storage terms.
2. Pumping was not simulated in model layers 1, 3, and 5 (Quaternary Alluvium, Weches Formation, and Reklaw Formation).

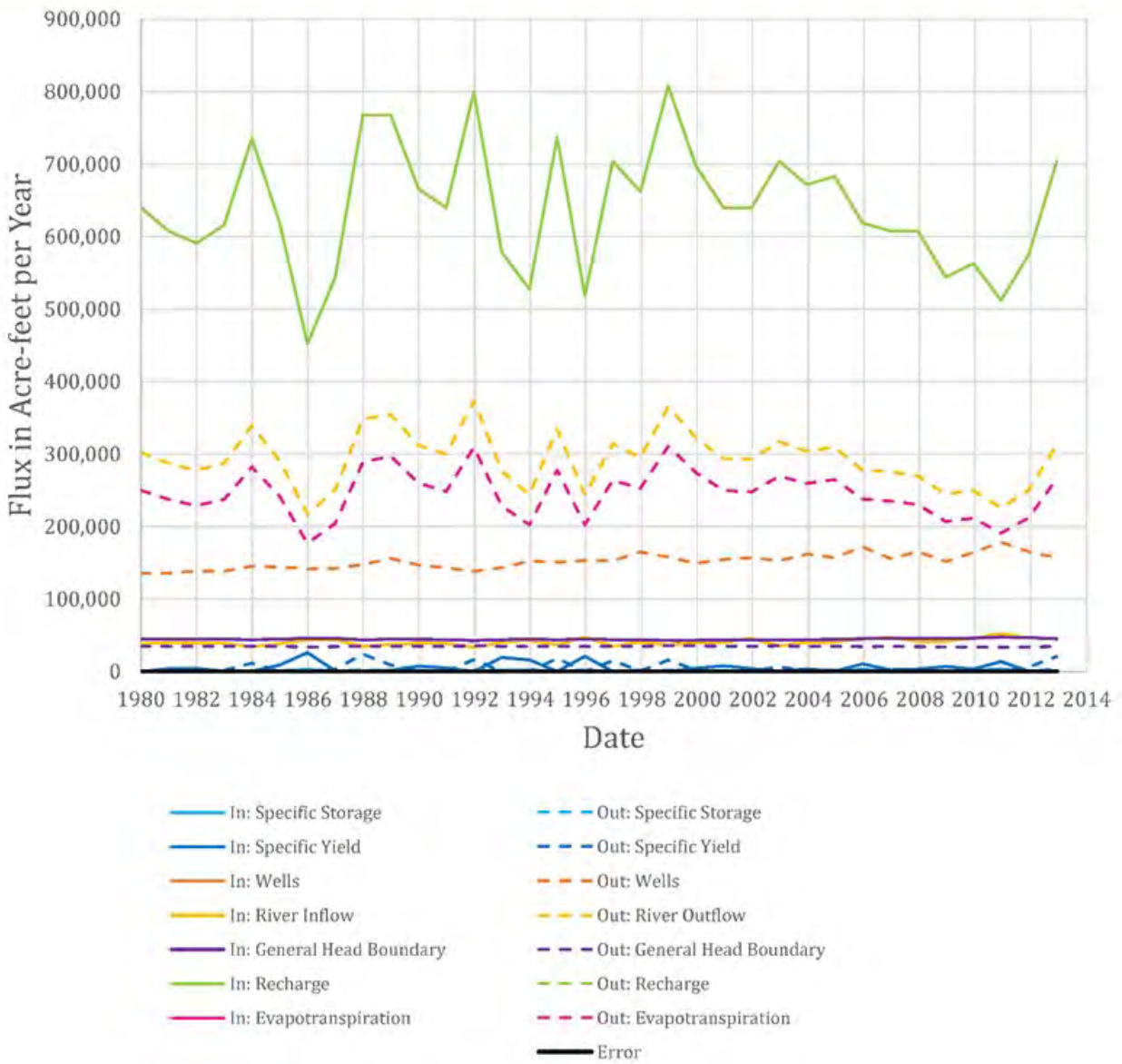


Figure 3.4-1. Water Budget for the 1980 to 2013 Calibration Simulation

Table 3.4-2. Water Budget by Layer at the End of the Transient 1980 to 2013 Simulation

	Mass Balance Components	Layer 1 Flow (Quaternary Alluvium)	Layer 2 Flow (Sparta Aquifer)	Layer 3 Flow (Weches Formation)	Layer 4 Flow (Queen City Aquifer)	Layer 5 Flow (Reklaw Formation)	Layer 6 Flow (Carrizo Aquifer)	Layer 7 Flow (Upper Wilcox)	Layer 8 Flow (Middle Wilcox)	Layer 9 Flow (Lower Wilcox)	Total Model Flows
		(acre-feet per year)									
Inflows	Storage	0.0	0.0	0.0	0.0	2.52	0.0	0.0	0.00	33.5	36.0
	Layer Top	0.0	471.6	20,661.0	222,376.3	23,680.5	88,425.3	421,970.7	39,094.2	21,928.7	0.0
	Layer Bottom	600,209.8	2,713.8	2,609.9	2,262.0	460.2	116,765.5	6,237.3	3,233.5	0.0	0.0
	Well	0.0	0.0	0.0	0.0	0.0	0.0	0.0	0.0	0.0	0.0
	General Head Boundary	0.0	34,950.5	0.0	60.3	0.0	10,153.9	0.0	0.0	0.0	45,164.8
	River	44,087.8	0.0	0.0	0.0	0.0	0.0	0.0	0.0	0.0	44,087.8
	Recharge	370,360.7	47,174.0	15,325.0	104,018.6	32,822.9	23,458.2	67,624.0	35,163.1	7,873.6	703,820.0
	Evapotranspiration	0.0	0.0	0.0	0.0	0.0	0.0	0.0	0.0	0.0	0.0
Total Inflows	1,014,658.3	85,310.0	38,595.9	328,717.3	56,966.1	238,803.1	495,832.0	77,490.8	29,835.7	793,108.6	
Outflows	Storage	1,042.7	390.9	650.0	4,999.8	654.4	3,472.3	7,758.4	4,089.9	1,186.5	24,244.9
	Layer Top	0.0	11,519.1	3,241.0	252,059.5	769.2	34,117.1	404,699.4	11,923.7	16,163.2	0.0
	Layer Bottom	536,901.2	23,313.6	31,595.7	30,017.4	35,998.0	132,982.7	35,538.5	12,262.0	0.0	0.0
	Well	0.0	3,941.4	0.0	9,094.0	0.0	68,521.2	36,173.9	31,968.8	7,419.9	157,119.2
	General Head Boundary	0.0	26,528.5	0.0	1,742.5	0.0	450.5	1,306.6	2,283.0	2,227.4	34,538.4
	River	311,011.2	0.0	0.0	0.0	0.0	0.0	0.0	0.0	0.0	311,011.2
	Recharge	0.0	0.0	0.0	0.0	0.0	0.0	0.0	0.0	0.0	0.0
	Evapotranspiration	166,051.5	19,619.8	3,113.5	29,995.2	19,268.4	160.8	10,182.8	14,963.4	2,839.5	266,194.9
Total Outflows	1,015,006.6	85,313.3	38,600.1	327,908.3	56,990.0	239,704.7	495,659.6	77,490.8	29,836.4	793,108.6	
Net Flows	In-Out	-348.3	-3.4	-4.2	809.0	276.1	-901.6	172.4	0.0	-0.7	0.0
	Percent Discrepancy	-0.03%	0.00%	-0.01%	0.25%	0.49%	-0.38%	0.03%	0.00%	0.00%	0.00%

Notes:

1. Mass balances per layer were obtained from Groundwater Vistas. Mass balance errors match those in the MODFLOW 1st file though there are averaging differences for river and storage terms.
2. Mass balance rates shown are for the end of the transient simulation at stress period 34, time step 5 (end of 2013).
3. Pumping was not simulated in model layers 1, 3, and 5 (Quaternary Alluvium, Weches Formation, and Reklaw Formation).

Detailed water budgets are provided in Appendix A for ten Texas Groundwater Conservation Districts present in the model domain (Tables A-1 through A-10). Texas counties not part of a conservation district were tabulated individually (Appendix A Tables A-11 through A-33). Water budgets were tabulated for each year of the model simulation (1980 through 2013) and for each model layer. Arkansas and Louisiana counties were grouped as areas outside Texas counties.

4.0 Sensitivity Analyses

A sensitivity analysis was conducted on the draft calibrated model presented in Appendix C to determine the impact of conceptual or parameter changes to the calibration results. The final model was adjusted from the draft model as per comments on the draft. The final and draft model calibration statistics, water level measurements, and water budgets were similar, with the only significant difference being calibration statistics in the Queen City Aquifer due to the reassignment of eight target wells to alternate hydrostratigraphic units. Because of this, the results of the sensitivity analyses conducted using the draft model were considered valid for both the final and draft models.

4.1 Procedure of Sensitivity Analysis

Sensitivity analyses were performed to evaluate the effects of hydraulic conductivity, pumping, recharge, evapotranspiration, and specific yield. Both transient and steady-state analyses were performed to evaluate parameters that have a high impact on calibration.

Evaluation of sensitivity was qualitative for the transient 1980 to 2013 model sensitivities. The parameters tested were evaluated by comparing water level hydrographs from the sensitivities to the calibrated model and observed values. The evaluated parameters/stresses consisted of: a no-pumping case, a simulation with constant recharge, and a sensitivity simulation on the specific yield value.

Evaluation of sensitivity was quantitative for the two-period steady-state model sensitivity analyses (representing 1980 and 2013 stress conditions). The parameters evaluated were: hydraulic conductivity, recharge, evapotranspiration, and pumping. For these sensitivities, the parameter values were raised and lowered by prescribed factors and the change in model calibration errors were evaluated for each case. These parameters were then categorized into high, medium, and low sensitivity groups based on the change in calibration statistics resulting from the change in the parameter value. The possible “sensitivity types” are defined by ASTM International (formerly the American Society for Testing and Materials) (ASTM, 1994, 2000) and are used for uncertainty evaluations of the predictive analyses. The sensitivity types categorize how parameters change the model calibration versus changing the model predictions and are as follows:

- Type I sensitivity is defined for parameters that cause insignificant changes to the calibration residuals as well as to model conclusions/predictions of interest. Type I sensitivity is of no concern because regardless of the value of the input, the prediction is also insensitive.
- Type II sensitivity is defined for parameters that cause significant changes to the calibration residuals but insignificant changes to model conclusions/predictions of

interest. Type II sensitivity is of no concern because the prediction is not sensitive to the calibration.

- Type III sensitivity is defined for parameters that cause significant changes to the calibration residuals as well as to the model conclusions/predictions. Type III sensitivity is of no concern because even though the model's predictions change as a result of variation of the input variable value, the calibration residuals are also sensitive, and the model becomes uncalibrated as a result. Thus, model calibration ensures that the predictions considered are appropriate for the modeled system.
- Type IV sensitivity is defined for parameters that cause insignificant changes to model calibration residuals but significant changes to the model predictions. Type IV sensitivity is of concern because, over the range of that parameter in which the model can be considered calibrated, the conclusions or predictions of the model can change. Additional data collection for such parameters can help narrow the band of uncertainty in the prediction.

Parameters evaluated were categorized based on the sensitivity statistics alone. Parameters with low residual mean, absolute residual mean head, or RMS error were categorized as possible Sensitivity Type I or IV. Future predictive model simulation results can differentiate between these types: if parameter changes result in large prediction changes, the parameter will be classified as Type IV; otherwise small prediction changes will classify the parameter as Type I. The Type IV sensitivity indicates that predictions would be more accurate for better estimates of the given parameter even though the parameter may not affect calibration.

Parameters with high residual mean, absolute residual mean head, or RMS error were categorized as possible Sensitivity Type II or III.

4.2 Results of Sensitivity Analysis

For parameters evaluated using the two-period steady-state model, the sensitivity model statistics (absolute residual mean head, residual mean head, and RMS head error) were compared to the draft steady-state model. The absolute residual mean head and residual mean head indicate whether the heads have overall increased or decreased as a result of the parameter change. The RMS head error indicates how the spread in observed versus modeled water level elevations has changed.

For parameters evaluated using the transient model, the evaluation of sensitivity utilized groundwater hydrographs. Detailed discussions of each parameter evaluation are provided below.

4.2.1 Sensitivity to Aquifer Hydraulic Conductivity Parameters

Sensitivity of the model calibration to hydraulic conductivity values of the various geologic units was evaluated for the two-period steady-state model. The parameter sensitivity study was conducted by using the automated sensitivity analysis option in Groundwater Vistas Version 7.24 (Rumbaugh and Rumbaugh, 2017). The automated sensitivity evaluated the steady-state model while adjusting hydraulic conductivity one layer at a time. The sand and clay hydraulic conductivities for each layer were evaluated individually as

separate simulations. For each layer, sand and clay hydraulic conductivity values were multiplied by factors of 0.3, 0.7, 1.3, and 1.7. The factors of 0.3 and 1.7 represent a 70 percent reduction and increase in the hydraulic conductivity, while the factors of 0.7 and 1.3 represent a 30 percent reduction and increase in the hydraulic conductivity. The automated sensitivity analysis calculated the calibration statistics for each parameter change and compiled the results in the autosens.out file.

Most model layers were not sensitivity to changes in sand or clay hydraulic conductivity; those that were showed various degrees of sensitivity. Figures 4.2-1 and 4.2-2 show the absolute residual mean for the hydraulic conductivity sensitivity and Figures 4.2-3 and 4.2-4 show the RMS head error for the hydraulic conductivity sensitivity.

For the sand sensitivities (where sand hydraulic conductivity generally controls horizontal hydraulic conductivity), the Middle Wilcox (model layer 8) had the greatest sensitivity, followed by the Lower Wilcox (model layer 9), as shown on Figures 4.2-1 and 4.2-3. The Queen City Aquifer (model layer 4) showed a slight improvement in model calibration with a decrease in sand hydraulic conductivity. The remaining layers showed little to no sensitivity to increases or decreases in the sand hydraulic conductivity.

For the clay sensitivities (where clay hydraulic conductivity generally controls the vertical hydraulic conductivity), the Upper Wilcox (model layer 7) had the highest sensitivity, followed by the Middle Wilcox (model layer 8) and Reklaw Formation (model layer 5), as shown on Figure 4.2-2 and 4.2-4. The remaining layers showed little to no sensitivity to increases or decreases in the clay hydraulic conductivity.

Table 4.2-1 categorizes the sensitivity simulations into low, medium, and high sensitivity values based on sensitivity statistics. Parameters with low, medium, or high sensitivity to calibration based on the absolute residual mean head and RMS error were categorized as possible Sensitivity Type II or III. These included the sand hydraulic conductivities for the Queen City Aquifer, the Middle Wilcox, and the Lower Wilcox (model layers 4, 8, and 9), and the clay hydraulic conductivities for the Reklaw Formation, the Upper Wilcox, and the Middle Wilcox (model layers 5, 7, and 8). The remaining layers showing little to no sensitivity to increases or decreases in the sand or clay hydraulic conductivity values were categorized as possible Sensitivity Type I or IV.

4.2.2 Sensitivity to Model Stresses Using the Two-Period Steady-State Model

The sensitivity of the model calibration to recharge, evapotranspiration, and groundwater pumping was evaluated. These sensitivity analyses were conducted using the two-period 1980 and 2013 steady-state model. For each steady-state sensitivity analysis, the stress values were multiplied by factors of 0.3, 0.7, 1.3 and 1.7 to note the impact on calibration errors. The factors of 0.3 and 1.7 represent a 70 percent reduction and increase in the respective flux values, while the factors of 0.7 and 1.3 represent a 30 percent reduction and increase in the respective flux values.

The mean head residual and the RMS head error were evaluated to establish model behavior. The mean head residual indicates whether the heads have overall increased or decreased as a result of the parameter change. The RMS head error indicates how the spread in observed versus modeled water level elevation has changed.

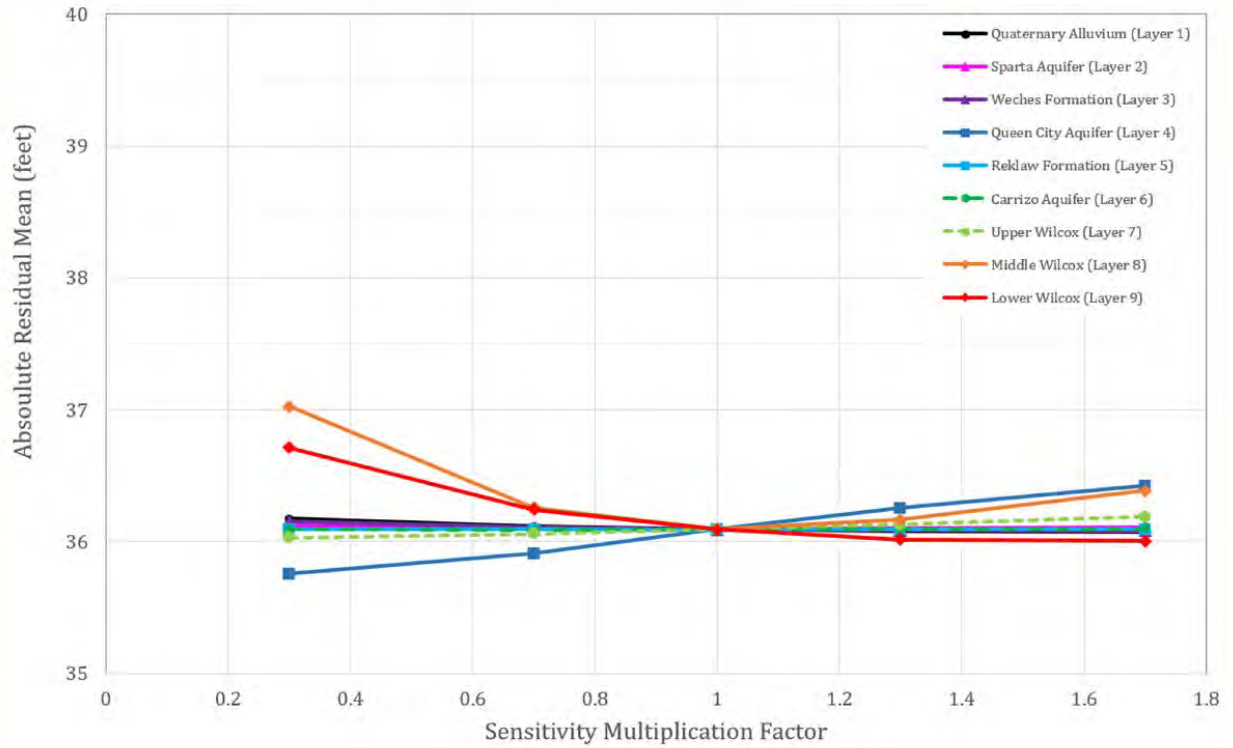


Figure 4.2-1. Sensitivity of Weighted Mean Head Error to the Sand Hydraulic Conductivity Value for the Various Geologic Units

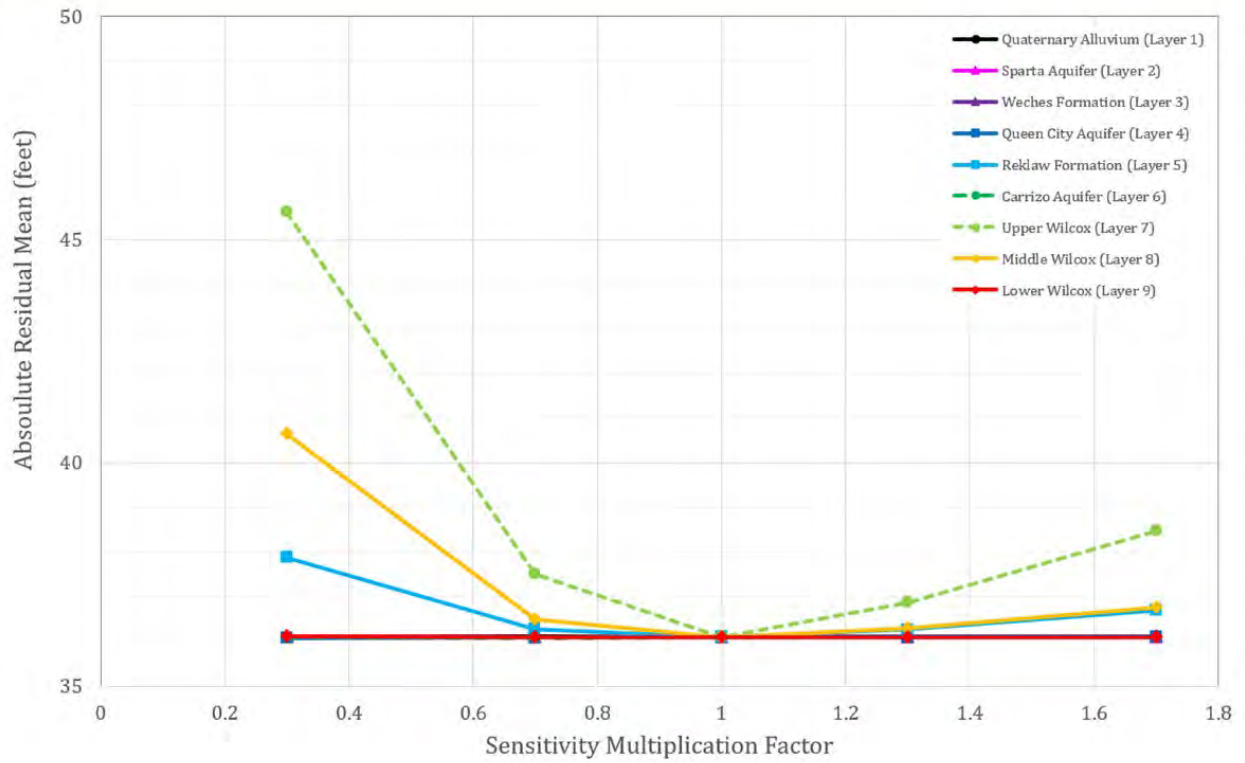
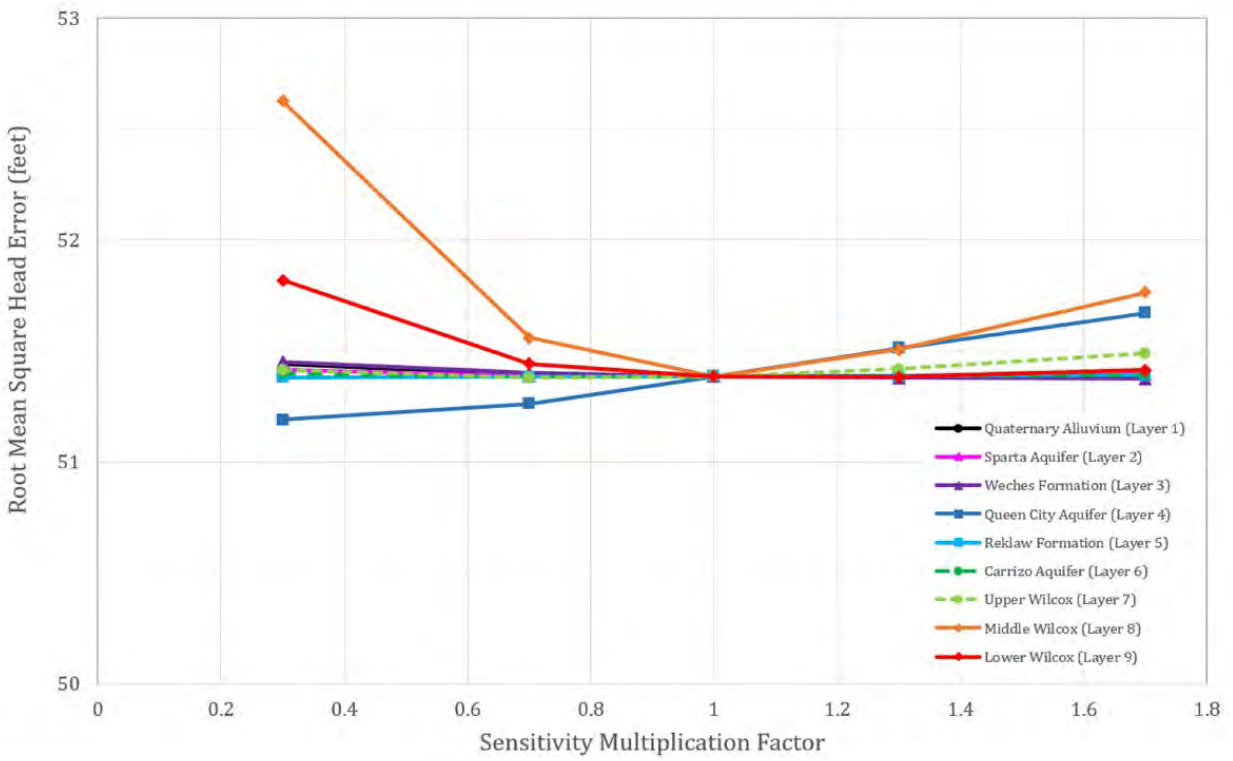
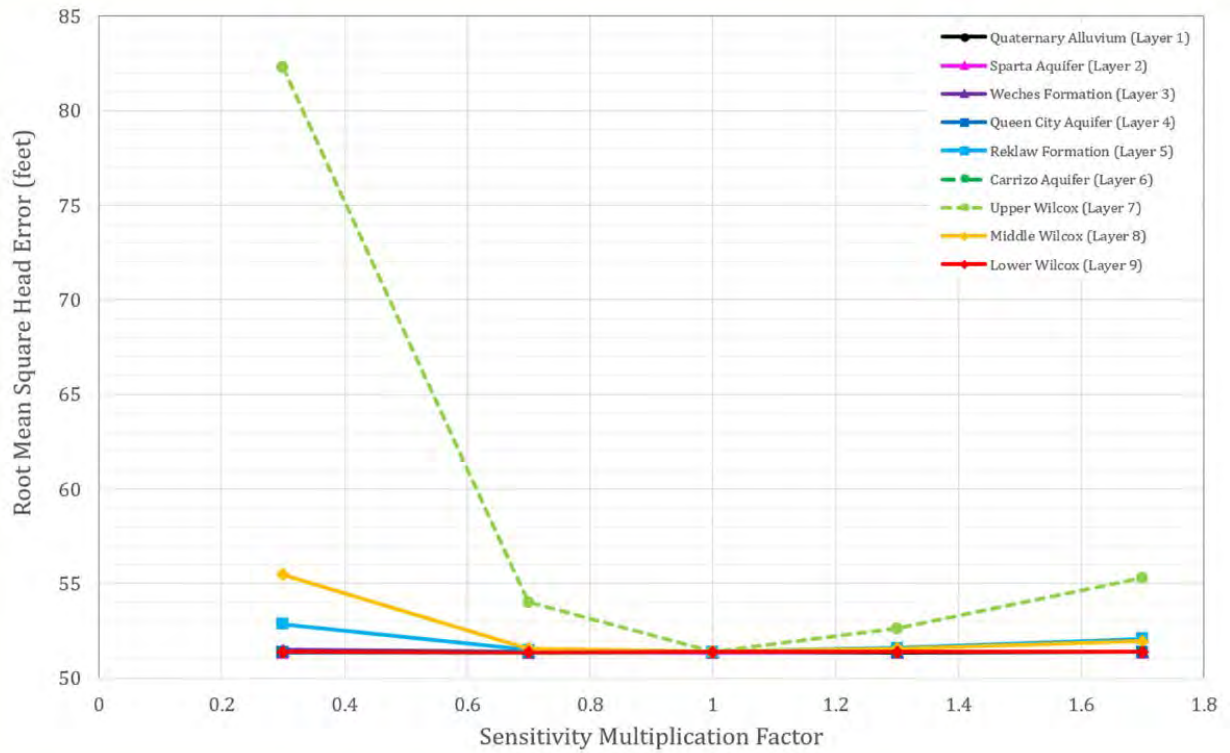


Figure 4.2-2. Sensitivity of Weighted Mean Head Error to the Clay Hydraulic Conductivity Value for the Various Geologic Units



Note: RMS = root mean square

Figure 4.2-3. Sensitivity of Weighted RMS Head Error to the Sand Hydraulic Conductivity Value for the Various Geologic Units



Note: RMS = root mean square

Figure 4.2-4. Sensitivity of Weighted RMS Head Error to the Clay Hydraulic Conductivity Value for the Various Geologic Units

Table 4.2-1. Model Parameter Sensitivity Type

Model Parameter	Residual Mean Sensitivity	Root mean square (RMS) Head Error Sensitivity	Possible ASTM Sensitivity Type
Horizontal Hydraulic Conductivity (Sand)			
Quaternary Alluvium (Layer 1)	No sensitivity	No sensitivity	Type I or IV
Sparta Aquifer (Layer 2)	No sensitivity	No sensitivity	Type I or IV
Weches Formation (Layer 3)	No sensitivity	No sensitivity	Type I or IV
Queen City Aquifer (Layer 4)	Low	Low	Type II or III
Reklaw Formation (Layer 5)	No sensitivity	No sensitivity	Type I or IV
Carrizo Aquifer (Layer 6)	No sensitivity	No sensitivity	Type I or IV
Upper Wilcox (Layer 7)	No sensitivity	No sensitivity	Type I or IV
Middle Wilcox (Layer 8)	Medium	Medium	Type II or III
Lower Wilcox (Layer 9)	Low	Low	Type II or III
Vertical Hydraulic Conductivity (Clay)			
Quaternary Alluvium (Layer 1)	No sensitivity	No sensitivity	Type I or IV
Sparta Aquifer (Layer 2)	No sensitivity	No sensitivity	Type I or IV
Weches Formation (Layer 3)	No sensitivity	No sensitivity	Type I or IV
Queen City Aquifer (Layer 4)	No sensitivity	No sensitivity	Type I or IV
Reklaw Formation (Layer 5)	Low	Low	Type II or III
Carrizo Aquifer (Layer 6)	No sensitivity	No sensitivity	Type I or IV
Upper Wilcox (Layer 7)	High	High	Type II or III
Middle Wilcox (Layer 8)	Medium	Low	Type II or III
Lower Wilcox (Layer 9)	No sensitivity	No sensitivity	Type I or IV
Recharge	High	High	Type II or III
Pumping	Medium	Medium	Type II or III
Evapotranspiration	No sensitivity	No sensitivity	Type I or IV

Notes:

1. The specific yield model sensitivity was evaluated for change in head fluctuations and is not categorized by ASTM sensitivity type.
2. ASTM sensitivity types are from ASTM D 5611-94 dated 1994, reapproved 2000.

Figure 4.2-5 shows the steady-state sensitivity of the mean head residual to recharge, evapotranspiration rate, and groundwater pumping. Recharge has the largest impact on the mean head value computed at the target groundwater cells, while the evapotranspiration rate had the smallest impact.

Figure 4.2-6 shows the steady-state sensitivity of the RMS head error to recharge, evapotranspiration rate, and groundwater pumping. The largest sensitivity, again, was to recharge. Evapotranspiration did not appreciably affect the RMS head error.

Pumping was categorized a possible Sensitivity Types II or III (Table 4.2-1) since the model showed medium sensitivity to pumping, as reflected in the residual mean and RMS error.

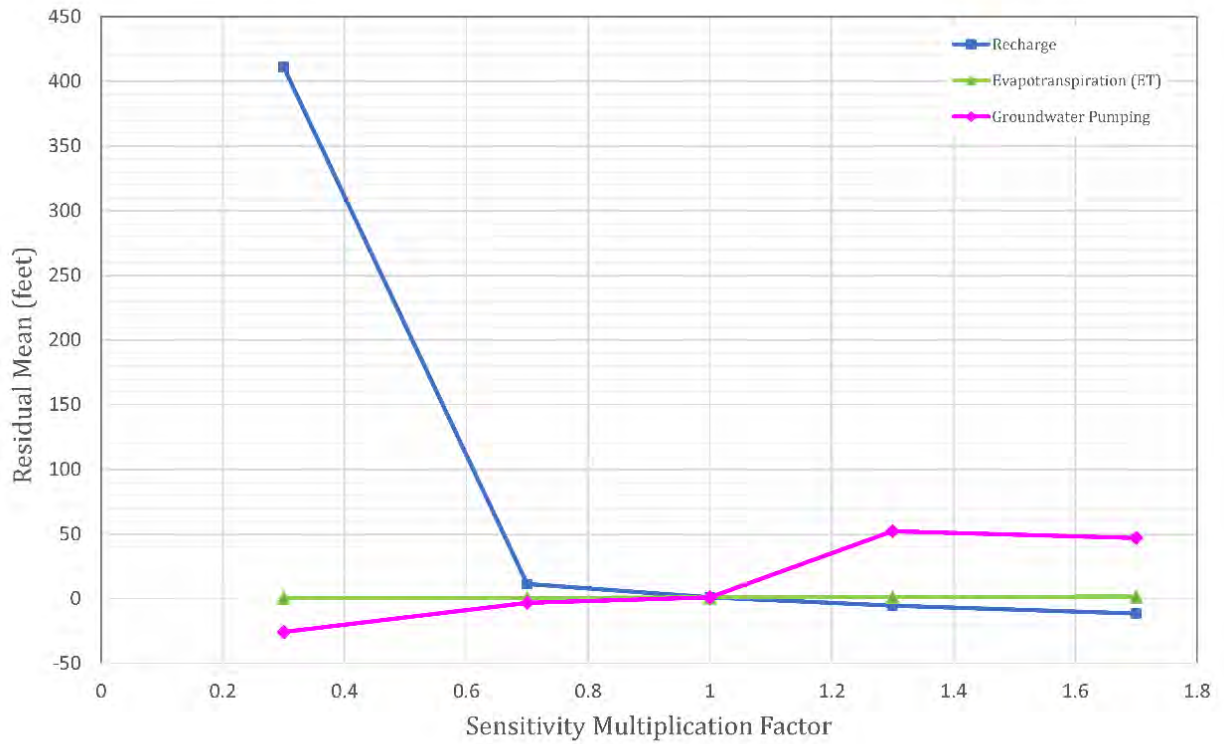
Recharge was categorized a possible Sensitivity Type II or III (Table 4.2-1). The model showed high sensitivity to decreases in recharge, as reflected in the residual mean and RMS error, even though the model was insensitive to increases in recharge. This is because increased recharge also increases baseflow and evapotranspiration fluxes, resulting in only small increases in water level elevations.

Evapotranspiration was categorized a possible Sensitivity Type I or IV parameter (Table 4.2-1). The model was not sensitive to evapotranspiration, as reflected in the residual mean and RMS error. If future predictive simulations for evapotranspiration indicate large prediction changes, evapotranspiration can be classified as Sensitivity Type IV, indicating that predictions would be more accurate for better estimates of this parameter even though it may not affect the calibration.

4.2.3 Sensitivity to Model Stresses Using the Transient Model

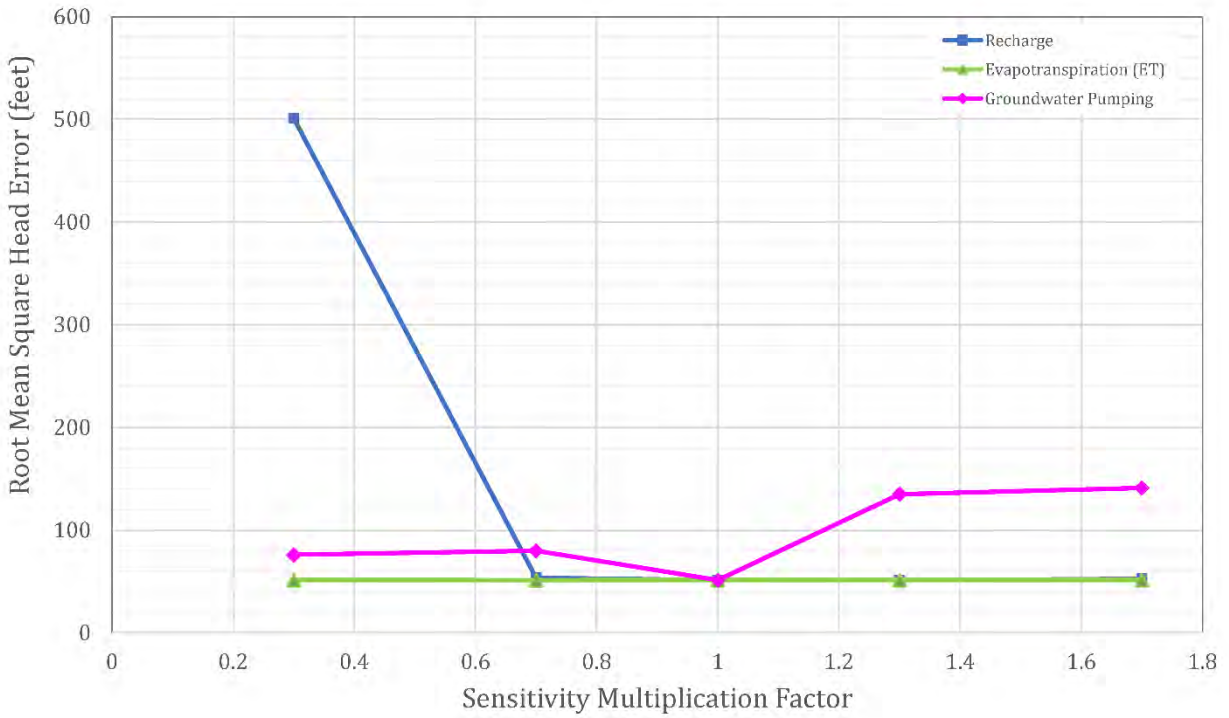
The transient model was used to evaluate the effects of no pumping and constant recharge. The no pumping model, in comparison to the calibration simulation, demonstrates the impact of pumping on water level elevation fluctuations. The constant recharge model demonstrates the impact of recharge fluctuations on water level elevations. Figures 4.2-7 through 4.2-13 show the hydrographs at select wells for these sensitivity studies.

The transient model with no pumping generally results in increased water level elevations, which at a few observation wells, improved calibration, as shown on Figures 4.2-7 through 4.2-13. This could be indicative of pumping within the wrong layer at those locations. In addition, the no pumping sensitivity resulted in dampened water level fluctuations at some of the observation wells. The transient model with a constant recharge rate generally resulted in the same magnitude of water level elevations as the calibrated model, but with dampened water level fluctuations at most of the observation wells and some showing no water level fluctuations. These sensitivities reveal both pumping and recharge stresses contribute to water level fluctuations. In general, unconfined aquifer water level fluctuations are primarily controlled by variations in recharge; and confined aquifer water level fluctuations are primarily controlled by variations in pumping rates, as shown on Figures 4.2-7 through 4.2-13.



Note: The 1.3 factor pumping sensitivity used 1,079 instead of 1,081 observation points due to boundary effects at 1 well.

Figure 4.2-5. Weighted Mean Error Sensitivity Graph for Model Parameters



Note: The 1.3 factor pumping sensitivity used 1,079 instead of 1,081 observation points due to boundary effects at 1 well.

Figure 4.2-6. Weighted Root Mean Squared Head Error Sensitivity Graph for Model Parameters

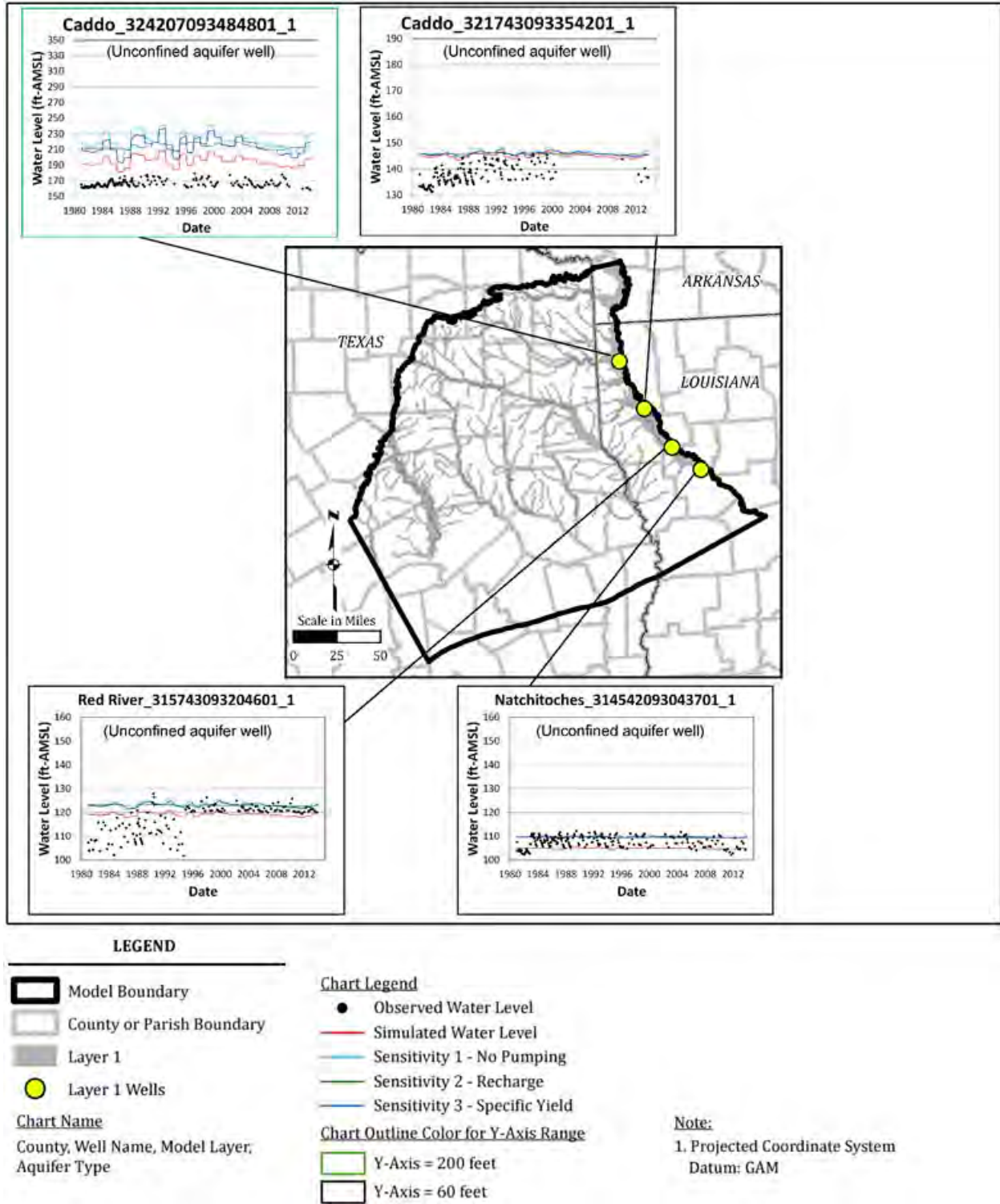
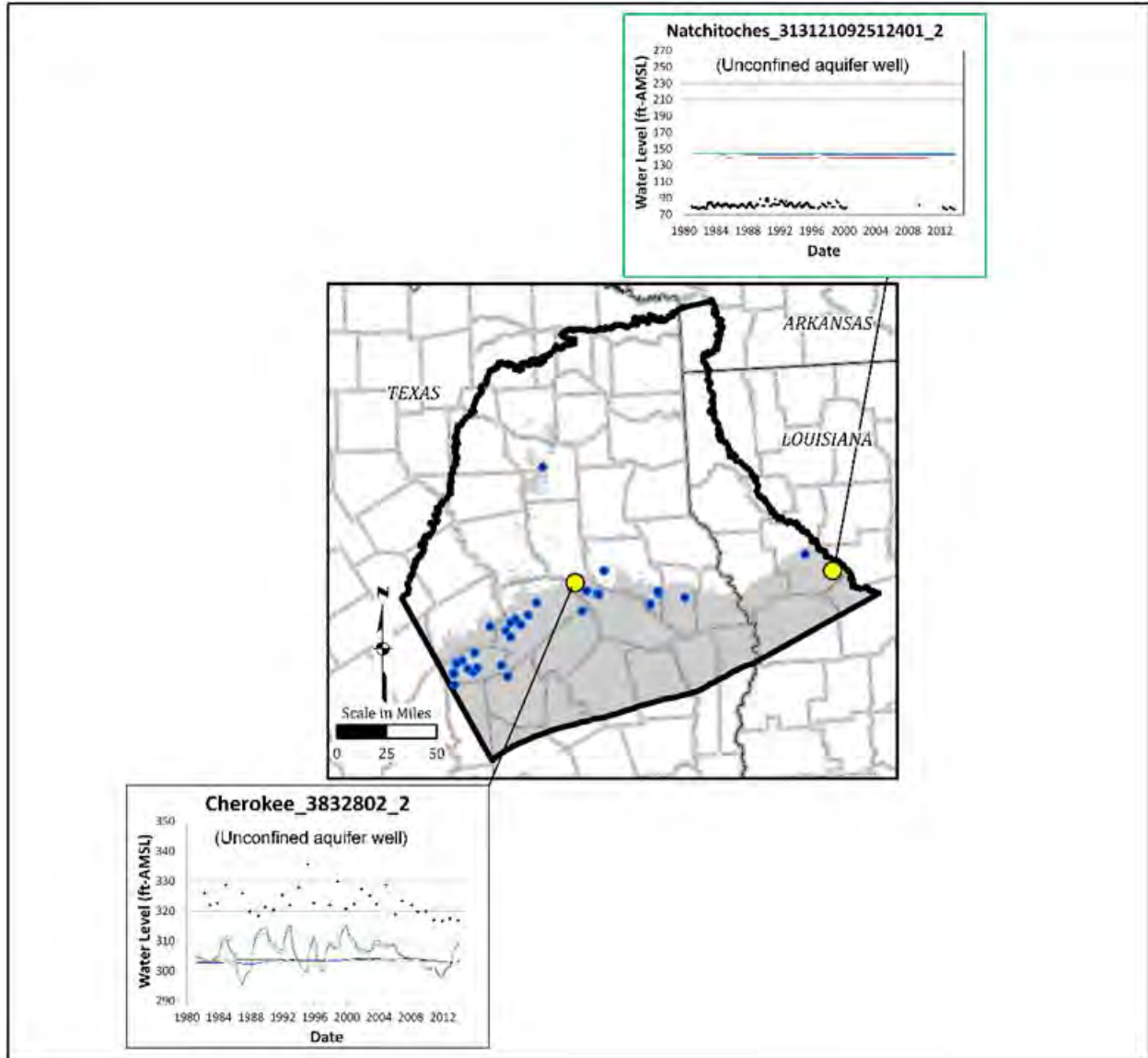


Figure 4.2-7. Measured and Simulated Hydrographs at Select Wells Showing Model Sensitivity - Quaternary Alluvium (Layer 1)



LEGEND

- Model
 - County or Parish Boundary
 - Layer 2
 - Select Layer 2
 - Layer 2
- Chart Name**
County, Well Name, Model Layer, Aquifer Type

- Chart Legend**
- Observed Water Level
 - Simulated Water Level
 - Sensitivity 1 - No Pumping
 - Sensitivity 2 - Recharge
 - Sensitivity 3 - Specific Yield
- Chart Outline Color for Y-Axis Range**
- Y-Axis = 200 feet
 - Y-Axis = 60 feet

- Notes:**
1. The layer contains discontinuous outcrops, consistent with the conceptual model (Section 2).
 2. Projected Coordinate System Datum: GAM.

Figure 4.2-8. Measured and Simulated Hydrographs at Select Wells Showing Model Sensitivity - Sparta Aquifer (Layer 2)

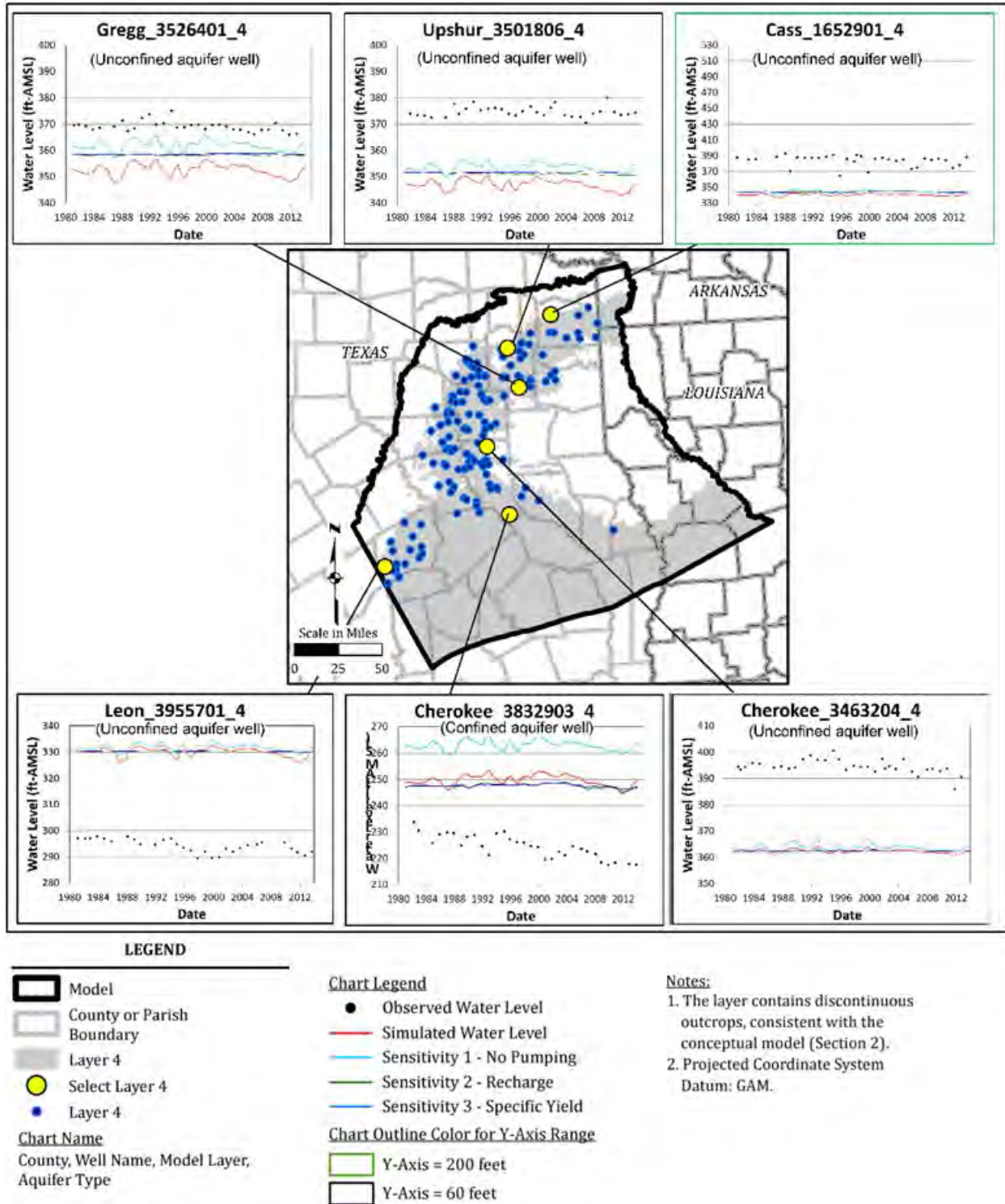


Figure 4.2-9. Measured and Simulated Hydrographs at Select Wells Showing Model Sensitivity - Queen City Aquifer (Layer 4)

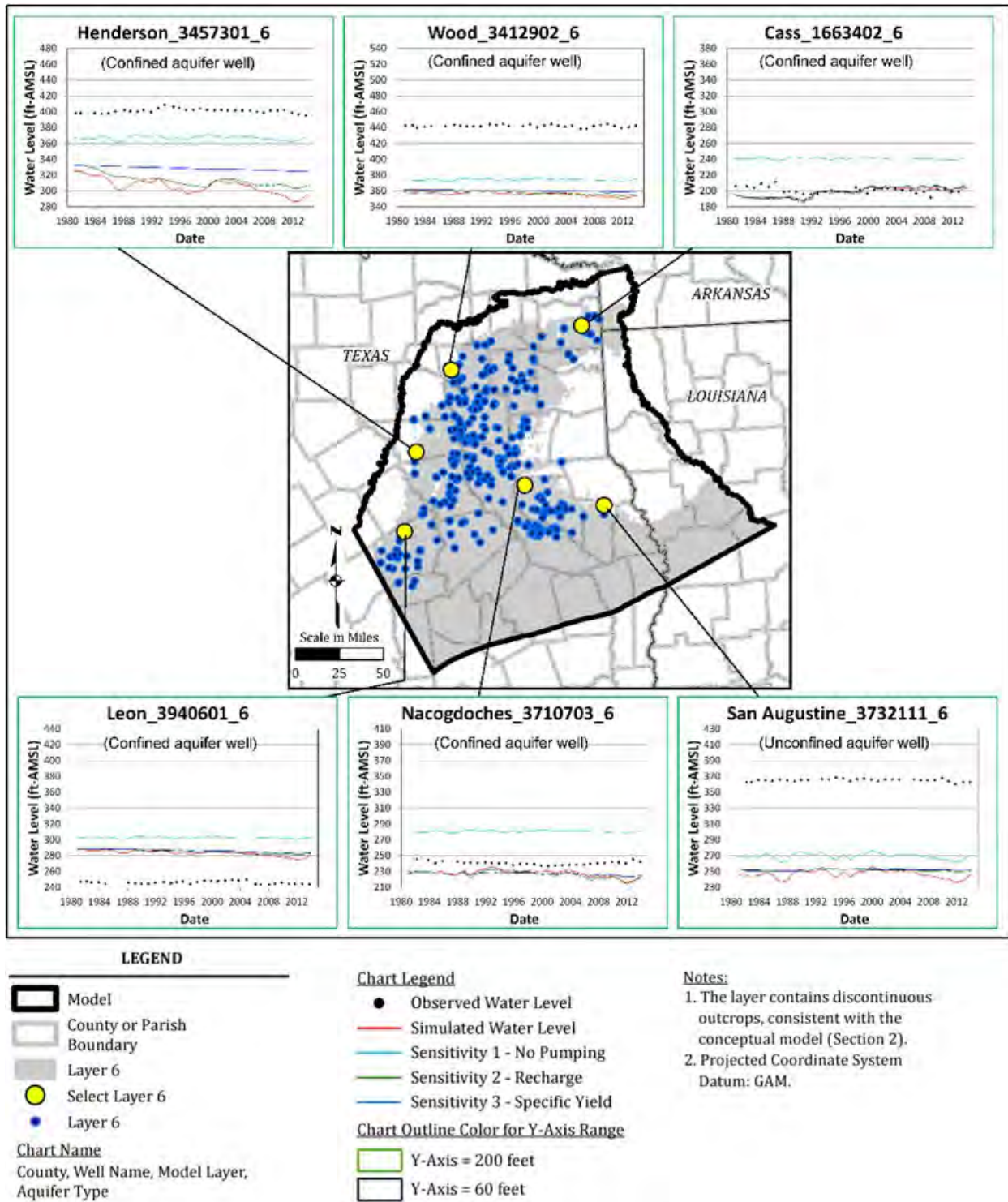


Figure 4.2-10. Measured and Simulated Hydrographs at Select Wells Showing Model Sensitivity - Carrizo Aquifer (Layer 6)

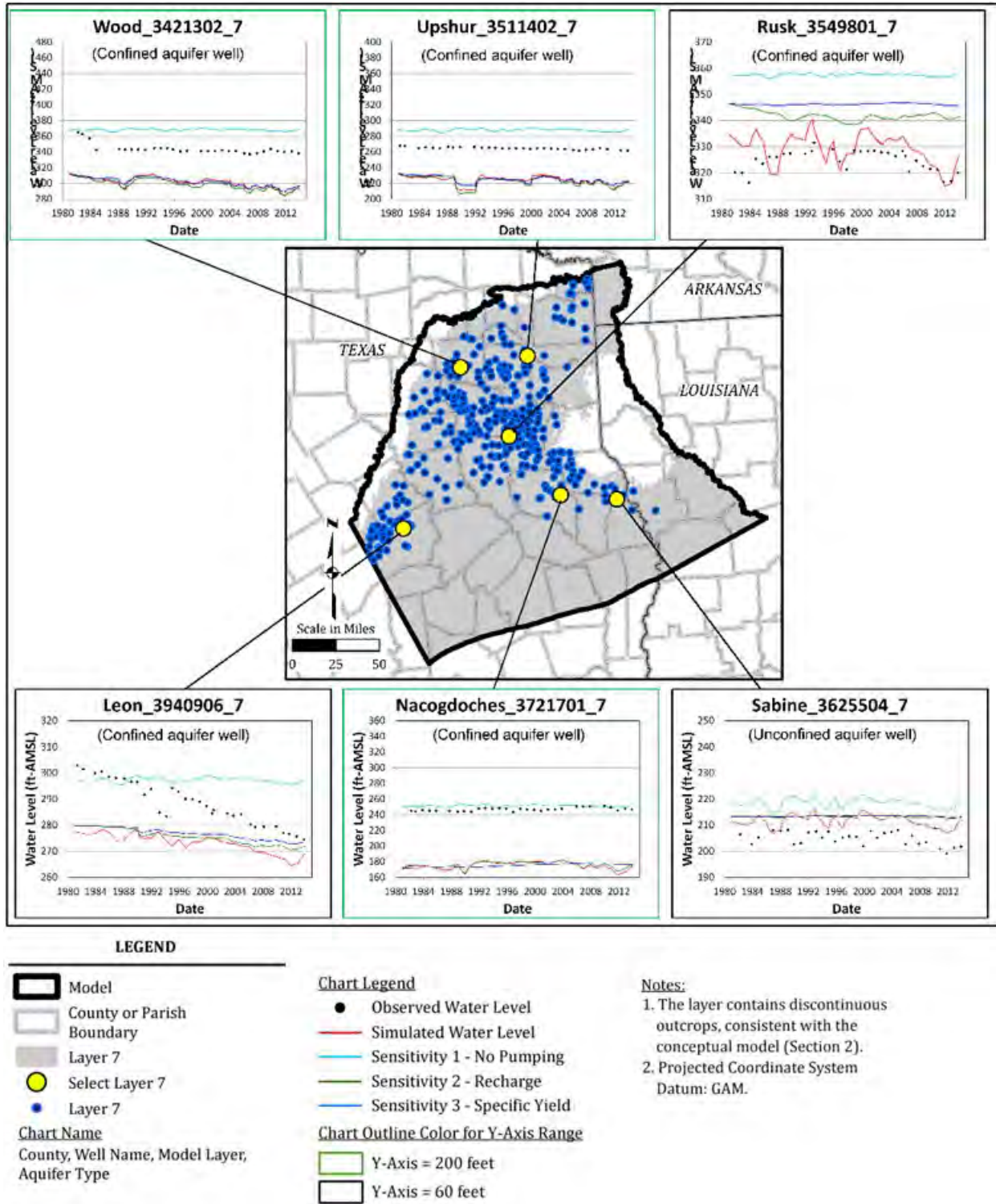


Figure 4.2-11. Measured and Simulated Hydrographs at Select Wells Showing Model Sensitivity - Upper Wilcox (Layer 7)

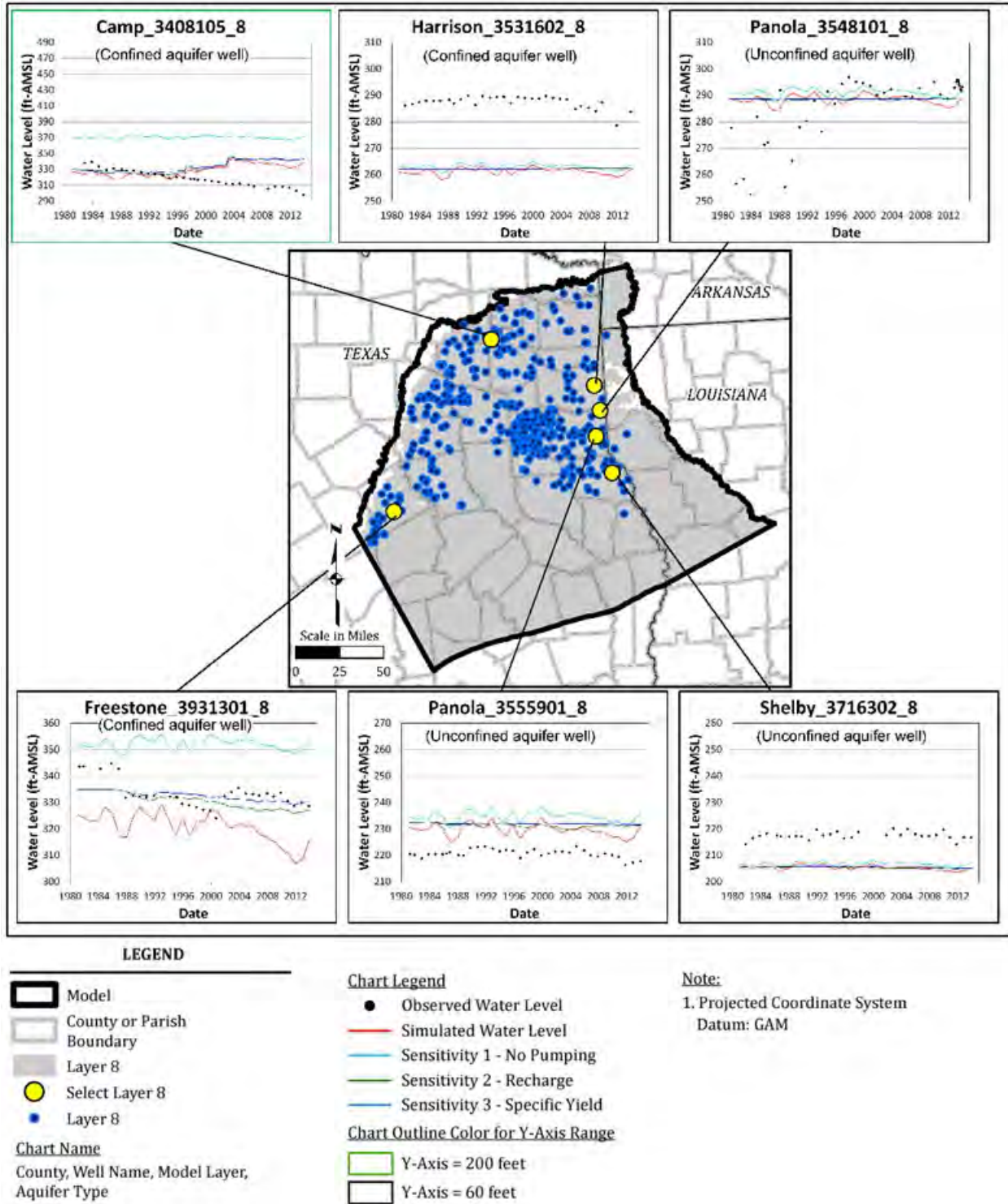
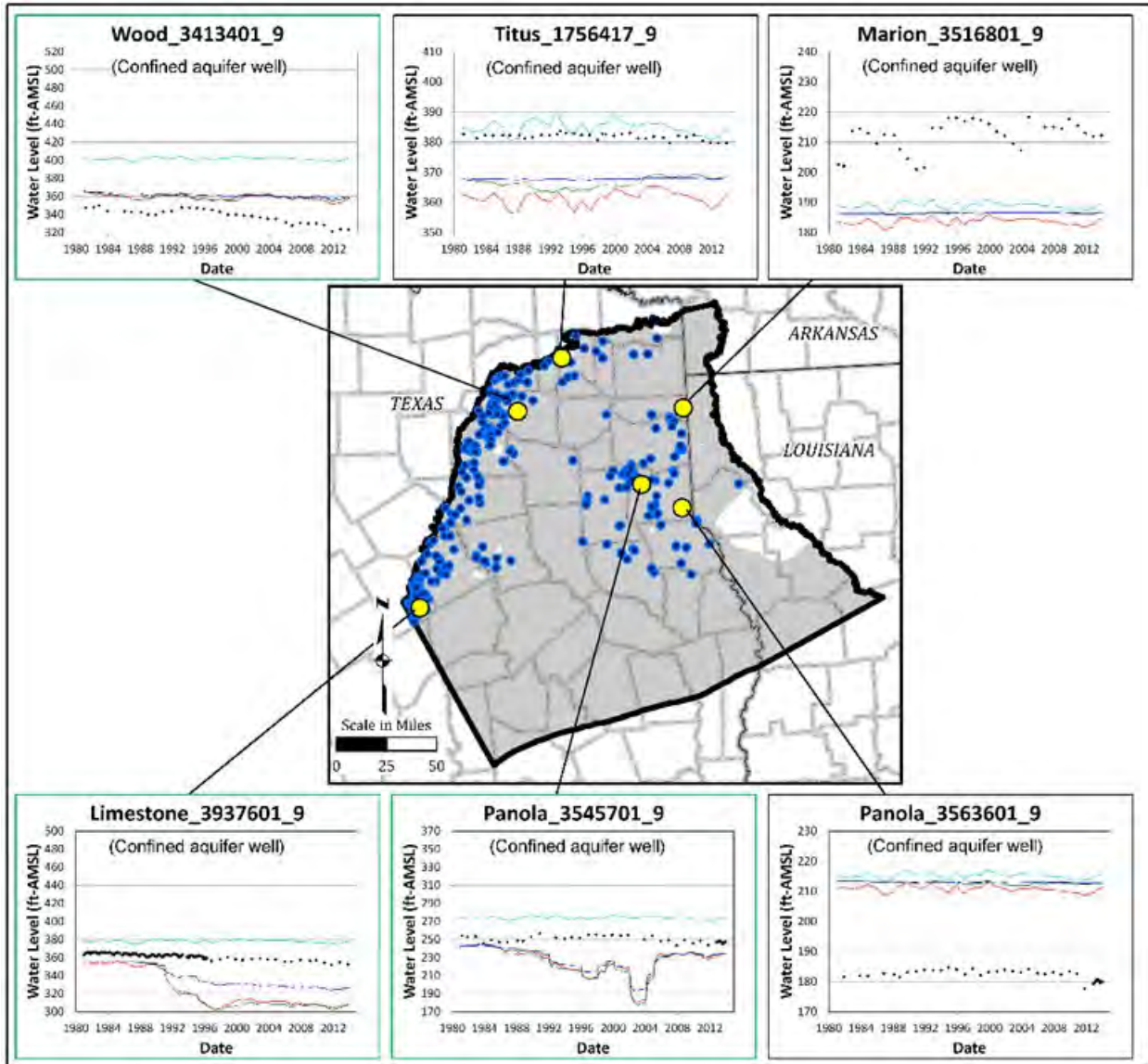


Figure 4.2-12. Measured and Simulated Hydrographs at Select Wells Showing Model Sensitivity - Middle Wilcox (Layer 8)



LEGEND

- Model
 - County or Parish Boundary
 - Layer 9
 - Select Layer 9
 - Layer 9
- Chart Name**
County, Well Name, Model Layer, Aquifer Type

- Chart Legend**
- Observed Water Level
 - Simulated Water Level
 - Sensitivity 1 - No Pumping
 - Sensitivity 2 - Recharge
 - Sensitivity 3 - Specific Yield
- Chart Outline Color for Y-Axis Range**
- Y-Axis = 200 feet
 - Y-Axis = 60 feet

Note:
1. Projected Coordinate System
Datum: GAM

Figure 4.2-13. Measured and Simulated Hydrographs at Select Wells Showing Model Sensitivity - Lower Wilcox (Layer 9)

4.2.4 Sensitivity to Aquifer Storage Properties

A sensitivity analysis was conducted to evaluate aquifer storage properties on water level fluctuations in the domain. Since the focus of this sensitivity was to evaluate water fluctuations and not calibration, the transient model was used, and the results were not categorized as ASTM sensitivity types. To evaluate the effect of the specific yield, specific yield was increased from 0.0007 to 0.05 for the transient model.

Figures 4.2-7 through 4.2-13 show the hydrographs at select wells for this sensitivity study. Water level fluctuations were generally dampened for the sensitivity simulation with increased specific yield compared to the calibrated simulation. Hydrographs show that simulated water level elevations at unconfined and confined monitoring well locations exhibit this flattened response. However, the general trends in the hydrographs for the calibration and specific yield simulations are similar and indicate the storage parameters are not very significant to the calibrated simulation.

5.0 Modeling Limitations

Several simplifications, assumptions, and approximations have been made in developing the groundwater availability model for the northern portion of the Queen City, Sparta, and Carrizo-Wilcox aquifers. Representation of the domain by discrete finite-volumes, approximation of groundwater flow by the continuity equation and Darcy's Law, and approximation of the various boundary conditions and stresses by steady-state or annual average conditions create an idealized representation of the flow system. This enables regional evaluations at long time-scales (of years to decades), but such an idealized system contains inherent divergence from actual conditions though the effect of these differences can be assessed. Errors are also associated with mesh design, aquifer or boundary geometry or areal extent, and the configuration of hydrologic components (conceptualization errors). These errors were minimized during model development and further evaluated and reduced during model calibration and sensitivity analysis as described below.

Data that is incorporated into a model may be incomplete, may contain errors, or may be incompatible with the modeled spatial and temporal scale. Possible measurement errors in the water level elevations were accounted for in this model by using a lower calibration weighting when these errors were discernable. A limitation of the model is that water level elevations measured instantly were compared to simulated water levels that result from annual stress periods.

Limitations in simulating pumping consisted of difficulty simulating recent pumping (after 1999) and simulating pumping using coarse spatial resolution. Pumping information from the conceptual model derived from TWDB databases was incomplete. Though the calibrated model used pumping values from the previous groundwater availability model (Kelley and others, 2004), values had to be extrapolated for 2000 through 2013. Additionally, using the previous model pumping had the effect of combining all pumping within a large model cell and simulating that flow in the center of the cell. Sensitivity analysis and automatic calibration methods showed that the model has low to moderate sensitivity to pumping. While sensitivity analysis suggested pumping may be more

accurately assigned to hydrostratigraphic units, the moderate sensitivity hindered efforts to calibrate pumping and resolve data issues. Better transient pumping information can provide a better transient calibrated model.

A groundwater flow model requires that the entire domain be appropriately parameterized. Although information exists on general aquifer characteristics, and more detailed sand fraction distributions were available for the geologic units, detailed hydrologic characterization is not possible except by extrapolating information from areas where data is available. This lack of hydrogeologic information can introduce uncertainty and errors in model results, especially in complex systems such as the groundwater availability model for the northern portion of the Queen City, Sparta, and Carrizo-Wilcox aquifers. Also, the hydraulic averaging formulas applied to determine horizontal and vertical hydraulic conductivities from sand and clay fractions may contain errors causing further limitations to the model. Sensitivity analyses helped to quantify the impact of these sand and clay fraction data and hydrogeologic averaging approaches.

The spatial resolution of the model was set to provide a regional evaluation of groundwater flow with refined discretization around surface-water features to capture the groundwater to surface-water interaction in a detailed manner. The temporal resolution of the model was set to annual stress periods for recharge, pumping, and boundary flows for long-term planning purposes. Annually-averaged stresses were calibrated to available water level elevation records and therefore it is assumed that the calibration is representative despite the different time scales of water level data and simulated stresses.

The model limitations further include uncertainty in predictions. Predictive sensitivity analyses should also be conducted with predictions of significance, to evaluate the impact of parameter variations on the prediction. Categorizing the predictive sensitivities along with calibration sensitivities as per ASTM (1994, 2000) would provide further information on the significance of data to the predictions.

6.0 Summary and Conclusions

The groundwater availability model for the northern portion of the Queen City, Sparta, and Carrizo-Wilcox aquifers has been updated to simulate impacts of groundwater pumping on groundwater resources in northeast Texas. The large model domain, complex geology, fine resolution, inconsistent pumping data, water level elevation quality control issues, and the 34-year time frame proved challenging and contributed to the considerable computational effort and model uncertainty.

Modeling challenges were addressed by selecting a robust and flexible software to best alleviate the computational burdens and still provide results at the scale of the modeling objectives. The MODFLOW 6 groundwater flow model was used for the simulations with the Groundwater Vistas graphic user interface. The numerical model was built in accordance with the conceptual model and consisted of 9 model layers to represent the 9 hydrostratigraphic units of interest: the Quaternary Alluvium, Sparta Aquifer, Weches Formation, Queen City Aquifer, Reklaw Formation, Carrizo Aquifer, and Wilcox Aquifer (Upper, Middle, and Lower).

The model simulation consisted of a steady-state period representing 1980 conditions followed by transient conditions from 1981 through 2013 using annual stress periods for recharge and pumping. The steady-state 1980 period was simulated using average aquifer conditions.

The model calibration was guided by available data. Quantitative and qualitative metrics were implemented in evaluating representativeness of the model. Observed water level elevations in wells and groundwater to surface water flow estimates were used to constrain the model. Calibration statistics show the model was well calibrated for the spatial and temporal scales of investigation. Mass balance errors were negligible and water fluxes at the various boundaries into and out of the domain were reasonable and consistent with the conceptual model. Qualitative comparison of estimated conceptual groundwater elevation contours to simulated contours confirm that the calibration matched observed conditions across the model domain.

Sensitivity analyses were conducted on the draft model to evaluate impact of parameter uncertainties and variations in boundary fluxes. Parameters evaluated were storage, hydraulic conductivity, recharge, evapotranspiration, and groundwater pumping. The model was moderately sensitive to pumping. A better estimation of pumping changes through time would have provided better transient calibration to water level elevation changes. As data collection continues and the conceptual model is improved, the uncertainties associated with the model can be reduced.

A predictive model was developed from the draft model for the period 2014 through 2080. Predictive simulations are summarized in Appendices D, E, and F. Predictive simulations were conducted to evaluate the impact of future pumping and recharge on the aquifers. The predictive simulations found that the groundwater model does not show unrealistic increases in water level elevations as the previous groundwater availability model had done. Since pumping and recharge values were held constant across the model for all counties, local variabilities in pumping were not accounted for, nor variability in other model parameters which were held constant through 2080. Predictive modeling from 2014 to 2080 using these various conditions showed that drawdown at Groundwater Management Area 11 counties may be significantly affected by baseline pumping rates or average recharge conditions. Despite the constant parameters used, the predictive drawdown charts for counties by aquifer may still be useful in guiding the Joint Planning Process and development of desired future conditions.

7.0 Future Improvements

A groundwater flow and transport model for the groundwater availability model for the northern portion of the Queen City, Sparta, and Carrizo-Wilcox aquifers was developed in this project using the MODFLOW 6 software. Use of oct-patch grids facilitated providing finer resolution to the numerical discretization near surface-water features to accurately capture the interactions. Pinch-outs and outcrops were handled in a geologically consistent manner. The Groundwater Vistas graphic user interface was used to develop the model. Multiple calibration metrics were used to constrain the model. The groundwater flow model generally depicts conditions within the domain during the 1980 to 2013 simulation period for annually averaged stress conditions.

There were several challenges overcome by this study. A regional domain was simulated with sufficient resolution of the solution near surface-water features by use of oct-patch grid refinement which provides fine resolution horizontally as well as vertically near to the river.

Further research suggested by this work includes:

- Evaluate sand fraction distributions along with hydraulic conductivity data for the Quaternary Alluvium, Carrizo Aquifer, Weches Formation, and Reklaw Formation would improve calibration as there were no sand fraction data for these units and a uniform sand fraction was used.
- Incorporate approximately 3,000 hydraulic conductivity values from specific capacity and pump testing within the study area identified in the Conceptual Model Report. These hydraulic conductivity values, supplemented with sand fraction data, could further improve model calibration.
- Improve pumping estimates, as there were clear data errors in the provided pumping estimates and calibrating the pumping rates proved to be impractical.
- Compile well construction data to better correlate observed water level elevation data to the hydrostratigraphic units these data represent.
- Process, perform quality assurance, and refine the water level elevation data using data science techniques to associate water level fluctuations among different wells (evaluate clustering) to identify proximity, a common dominant aquifer unit, or other connections between well locations such as conduits or displaced geologic layering across fractures.
- Process data using data science techniques to associate pumping stresses and their associated hydrogeologic units to water level elevation drawdowns for more reliable data, such that pumping data gaps can be filled where the data is inadequate.

8.0 Acknowledgements

This work was the combined effort of GSI Environmental, ESI (Jim Rumbaugh), Bill Hutchison, and Montgomery and Associates. All the efforts of personnel from these companies is greatly appreciated. Review and suggestions for the work were also provided by TWDB modeling staff (Appendix G). Their input has greatly assisted us with this work and has improved the model development, parameterization, and calibration efforts and is also greatly appreciated.

9.0 References

- ASTM, 1994 (reapproved 2000). Standard Guide for Conducting a Sensitivity Analysis for a Ground-Water Flow Model Application, ASTM D 5611-94. ASTM International, West Conshohocken, PA 19428-2959.
- Doherty, J., 2010, PEST, Model-independent parameter estimation—User manual (5th ed., with slight additions): Brisbane, Australia, Watermark Numerical Computing.
- Fryar, D.G., Senger, R., Deeds, N.E., Pickens, J., and Jones, T., 2003, Groundwater Availability Model for the Northern Carrizo-Wilcox Aquifer: Prepared for the Texas Water Development Board, January 31, 2003, 529 p.
- Harbaugh, A.W., 2005, Modflow-2005, The U.S. Geological Survey Modular Ground-Water Model – the Ground-Water Flow Process, U.S. Geological Survey Techniques and Methods 6-A16.
- Kelley, V.A., Deeds, N.E., Fryar, D.G., and Nicot, J.P., 2004, Groundwater Availability Models for the Queen City and Sparta Aquifers: Prepared for the Texas Water Development Board, October 2004, 867 p.
- Langevin, C.D., Hughes, J.D., Banta, E.R., Niswonger, R.G., Panday, Sorab, and Provost, A.M., 2017, Documentation for the MODFLOW 6 Groundwater Flow (GWF) Model: U.S. Geological Survey Techniques and Methods, book 6, chap. A55, 197 p., accessed August 4, 2017, at <https://doi.org/10.3133/tm6A55>
- Mehl, S.W. and Hill, M.C., 2005, MODFLOW-2005, the U.S. Geological Survey modular ground-water model -- documentation of shared node local grid refinement (LGR) and the Boundary Flow and Head (BFH) Package: U.S. Geological Survey Techniques and Methods 6-A12, 68 p.
- Montgomery and Associates, 2020, Conceptual Model Report: Groundwater Availability Model for the Northern Portion of the Queen City, Sparta, and Carrizo-Wilcox Aquifers, Prepared for the Texas Water Development Board, November 2020.
- Niswonger, R.G., Panday, S., and Ibaraki, M., 2011, MODFLOW-NWT, A Newton formulation for MODFLOW-2005: U.S. Geological Survey Techniques and Methods 6-A37, 44 p.
- Panday, S., Langevin, C.D., Niswonger, R.G., Ibaraki, M., and Hughes, J.D., 2013, MODFLOW-USG version 1: An unstructured grid version of MODFLOW for simulating groundwater flow and tightly coupled processes using a control volume finite-difference formulation: U.S. Geological Survey Techniques and Methods, book 6, chap. A45, 66 p.
- Rumbaugh, J.O., and Rumbaugh, D.B., 2017, Groundwater Vistas Version 7, www.groundwatermodels.com.

APPENDICES

Appendix A	Simulated Water Budget and Model Pumping
Appendix B	Model Targets and Residuals
Appendix C	Draft Groundwater Model
Appendix D	Technical Memorandum 1: Pumping Sensitivity
Appendix E	Technical Memorandum 2: Recharge Sensitivity
Appendix F	Technical Memorandum 3: Calculation of Drawdown from Existing Modeled Available Groundwater Using Updated Groundwater Availability Model
Appendix G	Technical Memorandum 4: Comparison of Input and Output Pumping: Previous Groundwater Availability Model and Updated Groundwater Availability Model
Appendix H	Response to Comments